THÈSE DE DOCTORAT EN COTUTELLE

ÉTUDE PHYTOCHIMIQUE ET PHARMACOLOGIQUE DE DEUX ESPÈCES D'AMARYLLIDACEAE DE LA FLORE SÉNÉGALAISE : *PANCRATIUM TRIANTHUM* ET *CRINUM JAGUS*

THÈSE PRÉSENTÉE À
L'UNIVERSITÉ DU QUÉBEC À TROIS-RIVIÈRES
ET À
L'UNIVERSITÉ CHEIKH ANTA DIOP DE DAKAR

COMME EXIGENCE PARTIELLE DU
DOCTORAT EN BIOLOGIE CELLULAIRE ET MOLÉCULAIRE

PAR
SEYDOU KA

JUIN 2021

UNIVERSITÉ DU QUÉBEC À TROIS-RIVIÈRES

DOCTORAT EN BIOLOGIE CELLULAIRE ET MOLÉCULAIRE (PH. D.)

Direction de recherche :

Isabel Desgagné-Penix	Directrice de recherche
Matar Seck	Codirecteur de recherche

Jury d'évaluation de la thèse :

Isabel Desgagné-Penix	Directrice de recherche
Matar Seck	Codirecteur de recherche
Tagnon Missihoun	Président de jury
Norman Voyer	Évaluateur externe
Djibril Fall	Évaluateur externe

Thèse soutenue le 25 Mai 2021

REMERCIEMENTS

Je dédie ce travail :

À mon père,

L'occasion m'est enfin offerte pour te témoigner toute ma reconnaissance, toute mon estime envers toi pour la bonne éducation que tu as su nous donner. Tu peux être fier de toi papa, toi qui t'es toujours soucié de l'éducation, du bien-être et par-dessus tout, de l'avenir de tes enfants. Nous prions pour qu'ALLAH te laisse encore parmi nous afin que tu puisses bénéficier de la réussite de tes enfants.

À ma mère,

Les mots ne seront jamais suffisants pour t'exprimer tout l'amour, toute l'estime que je ressens à ton égard. Tu as toujours su être une mère exemplaire. Ce travail n'est qu'une goutte d'eau de l'océan de bonheur que je souhaite t'offrir. Prions qu'ALLAH nous laisse le temps de réaliser nos rêves.

À mes frères et sœurs,

Omar, Assane, Amadou, Boubacar, Aby et Dieynaba : merci pour vos prières et pour le respect que vous me vouez. Que le bon Dieu vous mène sur le chemin du succès et fructifie vos efforts. Longue vie à vous.

Et aux personnes qui me sont chères :

Dre Aminata Diagne, Talla Wade, Moussa Ka et Alyssonko Diaw.

Pour les remerciements

J’exprime ma gratitude à ma directrice de thèse, la professeure Isabel Desgagné-Penix. Professeure, permettez-moi de vous adresser mes sincères

remerciements pour l'honneur que vous m'avez fait en acceptant de diriger ce travail avec toute la rigueur scientifique requise. J'ose espérer être digne de la confiance que vous m'avez accordée.

À mon directeur de thèse, le professeur Matar SECK, je voudrais vous exprimer mes profonds remerciements pour l'aide précieuse que vous m'avez apportée, pour votre patience et vos encouragements. Veuillez trouver dans ce travail qui vous est particulièrement dédié, l'expression de ma profonde gratitude et très grande estime.

Je remercie ensuite l'ensemble des membres du jury, qui ont accepté d'examiner avec attention mon travail à savoir : les professeurs Tagnon Missihoun, Normand Voyer et Djibril Fall.

Mes remerciements vont également à l'endroit du professeur Antonio Evidente et du Dr Marco Masi pour leur accueil chaleureux au sein du « *Dipartimento di Scienze Chimiche, Università degli Studi di Napoli Federico II* ».

Je tiens en outre à adresser mes vifs remerciements aux professeurs Lionel Berthoux, Laurent Chatel-Chaix, Geneviève Pépin, Benoit Daoust, Hugo Germain et Dr Simon Ricard pour leur collaboration et la mise à disposition d'instruments lors de la réalisation de mes expériences.

Je remercie en outre mes collègues de laboratoire, Dre Manel Ghribi, Nikunj Sharma, Andrew Diamond, Manoj, Bharat Majhi, Dr Saifur Rahman, Serge Basil Nouemsi, Dr Insa Seck, Dr Samba Fama Ndoye, Dr Mbaye Diaw Dioum, Abda Ba et Ismailla Ciss.

Je tiens à adresser mes vifs remerciements à nos braves assistantes de recherche Dre Fatma Meddeb, Mélodie B. Plourde et particulièrement à la Dre Natacha Merindol pour son appui dans mes recherches, ses précieux échanges, l'écriture et la relecture de mes manuscrits.

AVANT-PROPOS

Cette thèse fait l'objet d'une collaboration entre le Laboratoire de recherche sur le métabolisme spécialisé végétal de l'Université du Québec à Trois-Rivières (UQTR) et le Laboratoire de Chimie Organique et Thérapeutique de la Faculté de Médecine, de Pharmacie et d'Odontologie de l'Université Cheikh Anta Diop de Dakar (UCAD) du Sénégal pour étudier les alcaloïdes des Amaryllidaceae de la flore sénégalaise. Ces travaux ont été financés par la Chaire de recherche du Canada sur le métabolisme spécialisé des plantes (Subvention n° 950 232164) de la professeure Isabel Desgagné-Penix et une bourse de cotutelle du gouvernement du Sénégal. Les travaux de recherche ont été menés dans le cadre du projet de valorisation des plantes médicinales de la flore sénégalaise et de découvrir de nouveaux alcaloïdes d'Amaryllidaceae bioactifs.

Dans le premier chapitre, nous avons fait une revue de littérature qui présente d'abord l'intérêt des Amaryllidaceae dans la médecine traditionnelle dans le monde et en particulier au Sénégal. Ensuite, les alcaloïdes des Amaryllidaceae et les méthodes spectroscopiques utilisées pour élucider leur structure. Enfin, leurs effets biologiques remarquables notamment leurs activités antiacétylchoninestérase, cytotoxiques/tumorales et antivirales. Cette entrée en matière nous a permis de cerner les enjeux de notre démarche.

Dans le deuxième chapitre, nous avons démontré les activités anti-AChE, antibactériennes, cytotoxiques et anti-Dengue de l'extrait alcaloïde issu des bulbes de *Pancatium trianthum* (article en préparation).

Dans le troisième chapitre, nous avons isolé neuf alcaloïdes à partir des bulbes de *Crinum jagus* parmi lesquels trois sont nouveaux. Les activités cytotoxiques et anti-AChE de ces alcaloïdes ont par la suite été évaluées (article publié dans la revue *Phytochemistry*).

Dans le quatrième chapitre, nous avons démontré l'activité anti- Dengue et Zika des alcaloïdes isolés (article soumise dans la revue *Antimicrobial Agents and Chemotherapy AAC00398-21)*.

Dans le cinquième et dernier chapitre, nous avons tiré des conclusions sur l'ensemble des résultats et émis des perspectives en termes d'utilisations possibles de ces plantes dans la pharmacopée au Sénégal.

RÉSUMÉ

Les alcaloïdes constituent un groupe important de métabolites spécialisés azotés dotés d'un large éventail d'effets biochimiques et pharmacologiques. Les plantes de la famille des Amaryllidaceae sont connues en tant que productrices d'un groupe exclusif d'alcaloïdes. Ces alcaloïdes sont exploités pour leurs propriétés biologiques diverses à l'image de la galanthamine utilisée pour le traitement des symptômes de la maladie d'Alzheimer. Les alcaloïdes des Amaryllidaceae de la flore sénégalaise n'ont pas encore fait l'objet d'étude.

En portant une attention particulière aux plantes de la médecine traditionnelle sénégalaise, deux espèces notamment le *Pancratium trianthum* et le *Crinum jagus* ont été récoltées et les alcaloïdes y ont été ainsi extraits. L'extrait de *P. trianthum* a montré des activités anti-tumorales/cytotoxiques, anti-AChE et antibactériennes dépendamment de la dose. De plus, les extraits de *P. trianthum* et *C. jagus* ont fortement inhibé la réplication du **V**DEN$_{GFP}$ à des concentrations non cytotoxiques. La purification de l'extrait *C. jagus* a conduit à l'isolement de neuf AAs dont trois nouveaux notamment la gigantelline, la gigantellinine et la gigancrinine. L'activité antivirale de ces alcaloïdes purs a ensuite été testée contre le VDEN et le VZIK. Les résultats ont montré que les alcaloïdes inhibent la réplication des deux virus avec différentes efficacités. Parmi eux, la cherylline inhibe efficacement la réplication du VDEN (EC_{50} = 8,8 μM) et du ZIKV (EC_{50} = 20,3 μM). Des expériences de temps d'addition et d'élimination ont montré que la cherylline ciblait les premières étapes de la réplication virale. En utilisant des réplicons sous-génomiques exprimant la luciférase, nous avons confirmé que la libération de virion n'était pas affectée par la présence de la cherylline. La traduction des protéines de l'ARN du VDEN n'était pas inhibée non plus, alors que la réplication de l'ARN viral l'était. En conclusion, notre étude a d'une part, confirmé l'intérêt scientifique des résultats ethnopharmacologiques de ces deux plantes pour traiter des plaies et des infections et d'autre part servi à identifier la cherylline comme étant un inhibiteur efficace du VDEN et du VZIK qui pourrait être optimisé pour conduire au développement d'une nouvelle stratégie thérapeutique contre ces virus.

Mots-clés : Amaryllidaceae, alcaloïde, *Pancratium trianthum, Crinum jagus*, Dengue, Zika, acétylcholinestérase, cytotoxique

TABLE DES MATIÈRES

LISTE DES TABLEAUX

LISTE DES FIGURES

Figure **Page**

Chapitre IV

LISTE DES ABRÉVIATIONS ET ACRONYMES

MT	Médecine traditionnelle
APG	Angiosperm phylogeny group
PCR	Réaction en chaine de la polymérase
ADN	Acide désoxyribonucléique
DHBA	Dihydroxybenzaldéhyde
L-Phe	L-Phenylalanine
PAL	Phénylalanine ammonialyase
TYDC	Tyrosine decarboxylase
C3H	Coumarate-3-hydroxylase
C4H	Cinnamate-4-hydroxylase
AAs	Amaryllidaceae alkaloids
AChE	Acétylcholinestérase
RMN	Résonance magnétique nucléaire
COSY	Homonuclear COrrelated SpectroscopY
NOESY	Nuclear Over hauser Effect spectroscopY
HMBC	Heteronuclear Multiple Bond Correlation Spectroscopy
HMQC	Heteronuclear multiple Quantum Coherence
TLC	Thin layer chromatography
HPLC	High-performance liquid chromatography
GC-MS	Gas chromatography mass spectrum
ADI	Alzheimer’s Disease Interntional
VDEN	Virus de le Dengue

DENV	Dengue Virus
VZIK	Virus du Zika
ZIKV	Zika virus
DMSO	Dimethylsulfoxide
DMEM	Dulbecco's Modified Eagle's Medium
RPMI	Roswell Park Memorial Institute Medium
NITD008	Adenosine analog
HIV-1	Human Immunodeficiency Virus -1
PFU	Plaque forming unit
MOI	Multiplicity of infection
GFP	Green fluorescent protein
CC_{50}	Half cytotoxic concentration
EC_{50}	Half effective concentration
IFN	Interferon
WT	Wild type
STING	Stimulator of interferon gene
DMXAA	5,6-dimethylxanthenone-4-acetic acid

LISTE DES SYMBOLES

µL	Microlitre
µM	Micromolaire
mL	Millilitre
mg	Milligramme
µg	Microgramme
δ	Déplacement chimique
λ	Longueur d'onde

CHAPITRE I

INTRODUCTION

1.1 Médecine traditionnelle

1.1.1 Définition

La médecine traditionnelle (MT) est définie par l'Organisation mondiale de la santé (OMS) comme étant la somme globale des savoirs, des compétences et des pratiques qui se basent, raisonnablement ou non, sur les théories et les expériences propres à une culture et qui sont utilisées pour garder les êtres humains en bonne santé, ainsi que pour prévenir, diagnostiquer, traiter et soigner des patients physiques et mentaux. Dans certains pays, la MT est appelée médecine parallèle, alternative ou douce [1].

1.1.2 Utilisation de la médecine traditionnelle dans le monde

Les MTs utilisent des produits naturels (plantes ou animaux) pour prévenir et soigner les malades. Il existe plusieurs MTs dans le monde, notamment la médecine traditionnelle chinoise, le Kampo (médecine traditionnelle japonaise), l'Ayurveda (celle de l'Inde), la médecine traditionnelle africaine, etc. Ces MTs sont pratiquées dans le monde entier depuis des centaines, voire des milliers d'années, et elles se sont épanouies en systèmes de médecine réglementés [2, 3]. Cependant, la médecine traditionnelle africaine (MTA) exploite des connaissances transmises oralement de génération en génération à certaines personnes notamment les tradipraticiens et les herboristes. De nos jours, on estime que 80 % de la population africaine utilise la MT de premiers recours pour se soigner [4]. Ainsi, au Nigéria plusieurs plantes sont utilisées dans la MT. Parmi ces plantes, on peut citer l'Amaryllidaceae *Crinum jagus* (*C. jagus)* pour l'utilisation de ses bulbes et feuilles à des fins anthelminthiques et purgatifs [5].

1.1.3 Médecine traditionnelle sénégalaise

Comme dans le reste de l'Afrique, 80 % de la population sénégalaise ont eu recours à la MT et aux plantes médicinales pour se soigner. Cette utilisation de la MT et des plantes médicinales est due d'une part, par le fait que la majeure partie de la population sénégalaise est agricole et rurale. D'autre part, peu de personnes peuvent accéder aux services sanitaires du fait du manque de moyens ou de l'inexistence de centres de santé dans les coins les plus reculés du Sénégal [6, 7]. Cependant, au Sénégal 20 000 espèces sont recensées par l'OMS dont 600 utilisées dans la MT. Ces espèces sont accessibles dans la pharmacopée, chez les herboristes et dans les forêts, et elles sont utilisées en part entières ou en parties [6]. La capacité des plantes médicinales à soigner ou soulager les maladies est due aux principes actifs qu'elles renferment. Dépendamment des principes actifs, les plantes médicinales sont utilisées sous plusieurs formes notamment la décoction, l'infusion, la macération, la poudre entre autres. Au Sénégal, des médicaments traditionnels améliorés sont vendus dans les officines à moindre coût sous forme de tisanes notamment les feuilles de *Guiera senegalensis* contre la toux, et les feuilles d'*Euphorbia Hirta* contre les diarrhées [8]. Récemment, une enquête sur l'utilisation des plantes médicinales chez les peuls, au Nord du Sénégal, a permis de répertorier 74 espèces réparties en 32 familles botaniques. Ces espèces sont utilisées dans le traitement de 75 pathologies notamment dermatoses, virales, cancers, etc. Les Leguminoseae et les Combretaceae étaient les plus utilisés [9]. Une autre étude sur l'utilisation des plantes médicinales contre les dermatoses dans la région de Ziguinchor a permis de répertorier 36 espèces réparties en 25 familles. Parmi ces familles les Apocynaceae, Papilionaceae et les Rubiaceae étaient les plus utilisés et le macérât des feuilles était plus utilisé pour le traitement [10]. Ainsi, aucune plante appartenant à la famille des Amaryllidaceae n'a été répertoriée dans ces dernières études. En réalité, les Amaryllidaceae sont considérées comme des plantes toxiques au Sénégal. Peu d'ethnies les utilisent qu'à usage externe pour le traitement des dermatoses et plaies [11]. Fort de ce constat, dans ce travail, nous nous sommes intéressés aux Amaryllidaceae de la flore sénégalaise.

1.2 Généralités sur la famille des Amaryllidaceae

1.2.1 Définition

Le nom Amaryllidaceae vient du nom *Amaryllis*, genre endémique d'Afrique du Sud qui est largement cultivé comme plante ornementale. Les plantes appartenant à la famille des Amaryllidaceae sont des monocotylédones herbacées, à fleurs et à bulbes. Cette famille de plantes comprend environ 85 genres répartis en 1100 espèces qui sont largement distribuées dans les régions tropicales et subtropicales du globe [12].

1.2.2 Utilisation des Amaryllidaceae dans la MT

Depuis des siècles, les plantes de la famille des Amaryllidaceae sont utilisées dans la médecine traditionnelle pour traiter plusieurs maladies. On sait par exemple que l'huile extraite de la jonquille *Narcissus poeticus* était utilisée pour traiter les tumeurs utérines [13, 14]. En effet, plusieurs espèces du genre *Crinum* ont été utilisées dans différentes parties du monde pour traiter divers troubles. Les bulbes de *C. asiaticum* L. ont été utilisés en Inde comme toniques, laxatifs et expectorants, et dans les troubles urinaires. Ses racines fraîches provoquent des nausées et des vomissements. De plus, les graines ont été utilisées comme purgatifs, diurétiques et toniques, tandis que les feuilles ont été utilisées comme expectorants, contre les maladies de la peau et les processus d'inflammation [15].

En Afrique, les racines de certaines espèces du genre *Crinum* ont été utilisées pour traiter les infections urinaires, la toux, le rhume, les infections rénales et hépatiques, et les plaies [16]. Parmi ces espèces le *C. pupurascens* Herb. a été utilisé au Cameroun pour traiter l'asthénie sexuelle et les troubles de la rate [17]. De plus, le *Pancratium maritimum* a été utilisé comme un agent émétique [18]. Au Sénégal, les Amaryllidaceae sont peu utilisés dans la MT, car ils sont considérés comme des plantes toxiques. Toutefois, les bulbes de *Crinum ornatum* ont été utilisés à usage externe par les Socés (une ethnie) pour traiter les plaies et les infections, tandis que les bulbes et les feuilles de *Pancratium trianthum* (*P. trianthum)* étaient aussi utilisés à usage externe pour traiter les

dermatoses, les plaies et les troubles épileptiques [7, 19, 20]. Dans ce travail, nous allons étudier les propriétés pharmacologiques des Amaryllidaceae de la flore sénégalaise.

1.2.3 Répartition géographique des Amaryllidaceae

La famille des Amaryllidaceae est cosmopolite et sa composition en genre est diverse d'une région à l'autre (Figure 1.1). Les régions les plus riches en termes de diversité sont l'Amérique du Sud avec plus de 28 genres et l'Afrique du Sud avec plus de 19 genres. L'Australie possède 4 genres alors que la région méditerranéenne en comporte 8 [21]. La flore sénégalaise comprend 3 genres regroupant 13 espèces [22]. Le genre *Crinum* comprend 9 espèces, 2 espèces pour le genre *Pancratium* alors que les genres *Scadoxus* et *Hymenocallis* comportent chacune une seule espèce (Tableau 1.1 et Figure 1.2).

Figure 1.1 Distribution endogène des Amaryllidaceae dans le monde [21].

Tableau 1.1

Tableau récapitulatif des Amaryllidaceae du Sénégal et leurs localisations

Famille	Genres	Espèces	Localités
Amaryllidaceae	***Crinum***	*Distichum*	Ziguinchor, Kédougou, Sine-Saloum
		Zeylanicum	Dakar, Ziguinchor, Tambacounda
		Glaucum	Dans toute l'Afrique soudanienne
		Purpurascens	Ziguinchor, Haute Gambie
		Jagus	Thiès
		Sandérianum	Podor, Matam, Saint Louis, Richard Toll
		Broussanetii	Thiès
		Pauciflorum	Tambacounda, Bakel
		*sp**	Sabadola
	Pancratium	*Trianthum*	Dakar, Saint Louis
		Tenuifolium	Ziguinchor
	Scadoxus	*Multiflorus*	Dakar, Thiès, Ziguinchor
	Hymenocallis	*Littoralis*	Dakar, Thiès

* Espèce non identifiée.

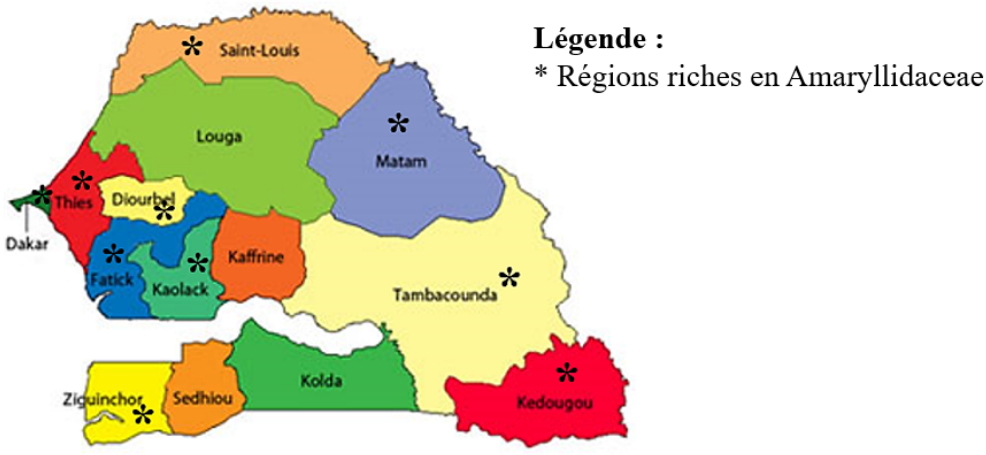

Figure 1.2 Régions Sénégalaises riches en Amaryllydaceae [141].

1.2.4 Description botanique et systématique des Amaryllidaceae

1.2.4.1 Description botanique

Les plantes de la famille des Amaryllidaceae ont des feuilles insérées à la base de la plante sous forme d'une pseudo-tige. Le limbe est simple, entier, parfois pétiolé, linéaire, pouvant aussi être plus ou moins ovale, et à nervures principales parallèles. Il y'a entre les feuilles une inflorescence, portée par une hampe nue, en forme d'ombelle et potentiellement contractée en un capitule ou réduite à une fleur, sous-tendue par un involucre généralement à deux bractées libres entre elles ou parfois soudées en une gaine. Les fleurs sont hermaphrodites, habituellement à plusieurs plans de symétrie : périgone à six tépales pétaloïdes disposés en 2 verticilles, libres entre eux ou soudés à la base en un tube. Elles ont presque toujours 6 étamines, disposées en 2 verticilles, opposées aux tépales. Les filets sont libres ou soudés entre eux à la base et ont 3 carpelles soudés entre eux. L'ovaire infère comporte 3 loges à fossés occasionnellement plus ou moins résorbées, et chacune des loges contient généralement de nombreux ovules. La placentation est axile et le style surmonté d'un stigmate capité ou de 3 lobes plus ou moins distincts. Le fruit est une gousse ou une baie tandis que la graine est un albumen charnu (Figure 1.3) [22].

1.2.4.2 Classification

Le tableau ci-dessous résume la classification des Amaryllidaceae selon la classification APG III de 2009.

Tableau 1.2

Classification des Amaryllidaceae selon APG III de 2009

Classe	Angiosperme
Sous-classe	Monocotylédones
Ordre	Asparagales
Famille	Amaryllidaceae

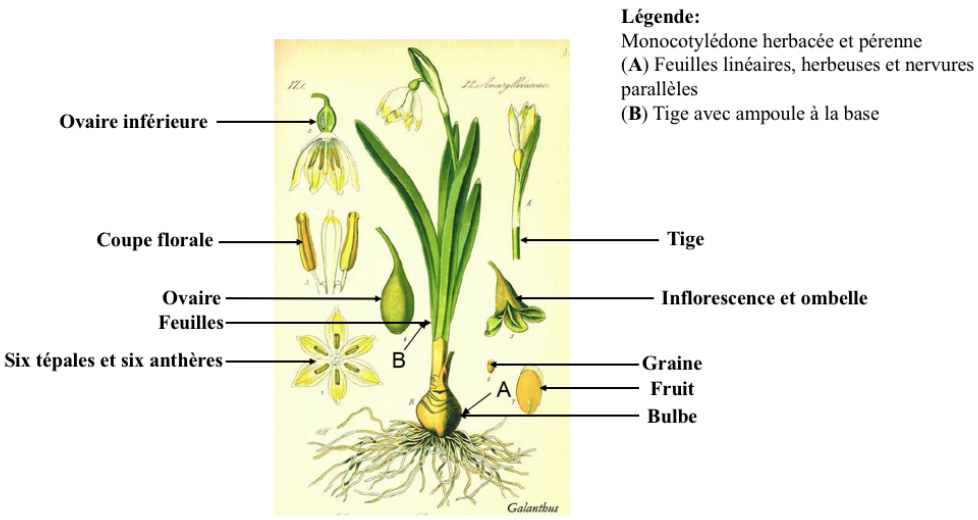

Figure 1.3 Description botanique des Amaryllidaceae [23].

1.2.4.3 Systématique des Amaryllidaceae

Les Amaryllidaceae appartiennent à la classe des Angiospermes et l'ordre des Asparagales (Tableau 1.3). Les botanistes ont proposé plusieurs systèmes de classifications des Angiospermes depuis la naissance de la botanique. Le terme « Angiosperme » provient du mot grec *aggeion* qui signifie « capsule » et *sperma* qui signifie « semence ». Ce sont des plantes à fleurs et à graines faisant partie des spermaphytes. Actuellement, le système *d'Angiosperm Phylogeny Group* (APG) basé sur des relations de parentés ou phylogénie des Angiospermes est généralement utilisé par la plupart des botanistes. L'avènement d'outils modernes de biologie moléculaire tels que la

réaction en chaîne par la polymérase (PCR), le séquençage de l'ADN génomique, ont notamment permis de décomposer l'ordre des Asparagales et des Liliale. Conduisant ainsi à une révision importante des groupements des différentes familles et leur composition en espèces [24]. Une mise à jour de la classification des ordres et familles des Angiospermes en 2016 a permis de reconnaitre 64 ordres et 416 familles (Figure 1.4). Dans cette nouvelle classification, les Amaryllidoideae font partie de la famille des Amaryllidaceae et de l'ordre des Asparagales [25]. Il existe plusieurs genres dans la famille des Amaryllidaceae. Parmi ces genres, on peut citer le genre *Crinum* comprenant environ 180 espèces et le genre *Pancratium* dénombre plus de 21 espèces [12, 21, 26]. Dans le cadre de notre étude, nous nous sommes focalisés sur le genre *Crinum* et *Pancratium* car ils sont plus représentatifs dans la flore sénégalaise.

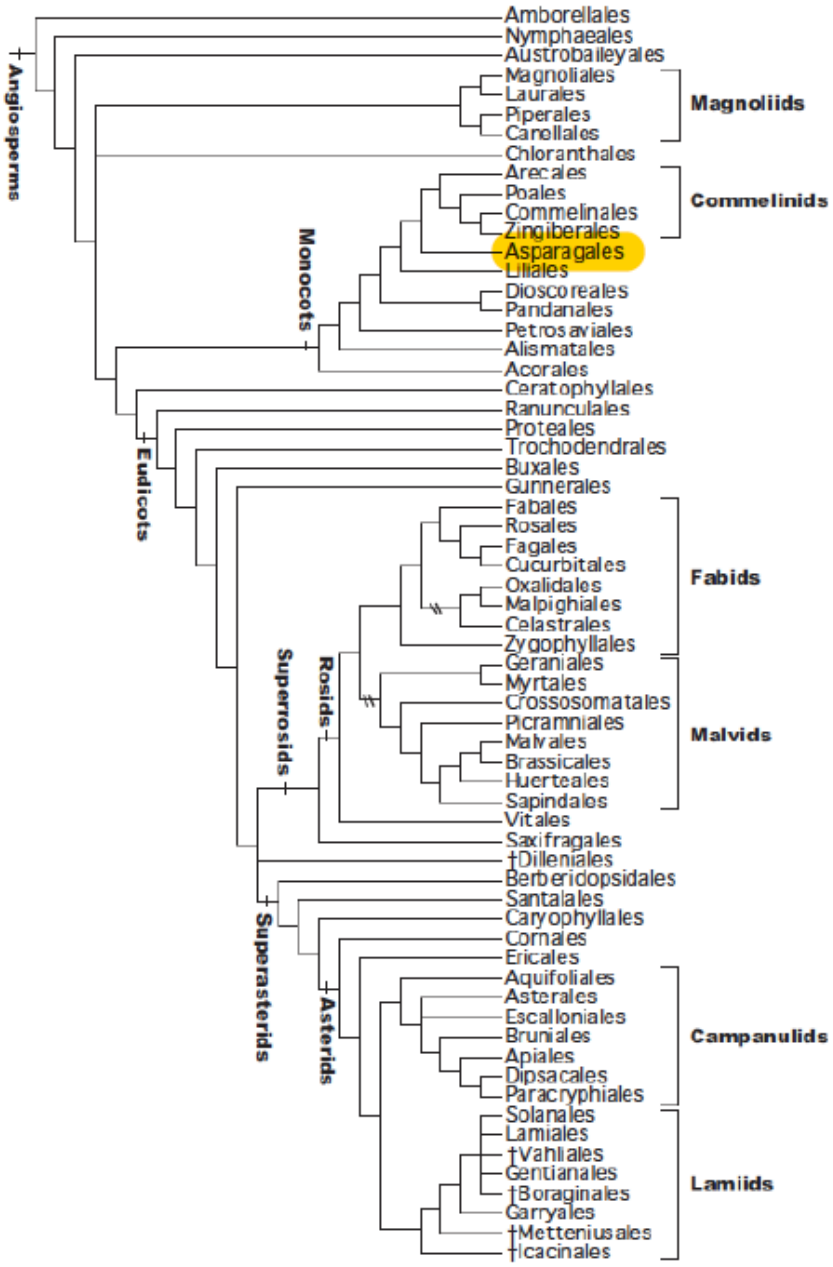

Figure 1.4 Phylogénie des Angiospermes. Les Amaryllydaceae à l'étude dans cette thèse font parti des Angiospermes, des monocotylédones et des Asparagales en jaune sur cette figure [25].

Le genre *Crinum*

Les feuilles à limbes non pétiolés et linéaires apparaissent en même temps que les fleurs. Les fleurs peuvent avoir des formes diverses à savoir : solitaire ou avec une ombelle de 8 à 10 fleurs ou subsessiles, à tépales blancs ou rose pâle, striés à la face supérieure d'une bande médiane-longitudinale rougeâtre ou verdâtre [22]. Le genre *Crinum* est très représentatif au Sénégal avec 9 espèces et peu utilisé dans la MT sénégalaise, mais très utilisé dans la MT hindou. Beaucoup sont sauvages et sont rencontrés dans les régions tropicales et subtropicales comme le *Crinum jagus* (Figure 1.5a). Dans le cadre de notre étude, nous avons récolté le *Crinum jagus* et procédé à son étude, car cette espèce est abondante dans la flore sénégalaise et elle est utilisée dans la MT nigériane, en Afrique de l'Ouest.

Le genre *Pancratium*

Le genre *Pancratium* se distingue des autres par des filets des étamines libres entre eux ou deux filets des étamines considérablement élargis et soudés entre eux à la base formant une espèce de coupe. Les fleurs sont blanches et parfumées tandis que les graines sont grosses et noires [22, 27]. Le genre *Pancratium* est moins utilisé que le genre *Crinum* dans la MT. On en dénombre 2 espèces dans la flore sénégalaise. Dans le cadre de notre étude, nous avons aussi récolté le *Pancratium trianthum* (Figure 1.5b) car cette espèce est abondante dans la flore sénégalaise et elle est utilisée dans la MT sénégalaise à usage externe pour soigner des dermatoses, des plaies et des crises épileptiques.

Figure 1.5 a) *Crinum jagus* et b) *Pancratium trianthum*.

1.2.5 Composition chimique de *Crinum jagus* et *Pancratium trianthum*

Composition chimique de *Crinum jagus*

Une étude phytotochimique a conduit l'isolement de 4 alcaloïdes notamment la lycorine, l'hamayne, la crinamine et la 6-hydroxycrinamine à partir de l'extrait méthanolique des bulbes frais de *C. jagus*, tandis qu'une autre étude sur les bulbes avait montré la présence de la lycorine, pseudolycorine et crinamine. Seule la crinamine a montré une forte activité antibactérienne [28]. Dans ce travail, nous allons procéder à l'étude des effets biologiques des alcaloïdes extraits des bulbes de *C. jagus* récoltés dans la flore sénégalaise.

Composition chimique de *Pancratium trianthum*

En 1983, une étude sur le profilage en alcaloïdes des parties épigées et hypogées de *P. trianthum*, a permis l'identification des alcaloïdes notamment la trisphaeridine, l'hippeastrine, l'hordenine, la pancratine, la tazettine, la lycorine, la galanthamine et la trianthine [29]. La lycorine est connue pour ses propriétés anticancéreuse alors que la galanthamine est utilisée dans le traitement des symptômes de la maladie d'Alzheimer grâce à son action inhibitrice de l'acétylcholinestérase [12]. Dans

ce travail, nous allons procéder à l'étude phytochimique et criblage biologique des alcaloïdes bruts extraits à partir des bulbes de *P. trianthum*.

1.3 Généralités sur les alcaloïdes

1.3.1 Définition

Le terme alcaloïde fut introduit par W. Meisner au début du XIX^{e} siècle pour désigner les substances naturelles réagissant comme des bases, c'est-à-dire comme des alcalis (de l'arabe « alcaly » qui signifie soude). Il n'existe pas de définition simple et précise des alcaloïdes, et il est parfois difficile de distinguer la frontière entre les alcaloïdes et les autres composés naturels contenant de l'azote. Ainsi, selon le phytochimiste Jean Bruneton, un alcaloïde est un composé organique d'origine naturelle, azoté, plus ou moins basique, de distribution restreinte et doué à faible dose de propriétés pharmacologiques marquées [30].

1.3.2 Applications thérapeutiques des alcaloïdes

Les composés d'origine végétale ont toujours été une source inépuisable de principes actifs médicamenteux du fait de leur diversité structurale. Parmi ces composés, les alcaloïdes occupent une place importante avec plus de 54 molécules utilisées dans la médecine à entité unique [31]. Parmi les alcaloïdes incitant le développement de médicaments, on peut citer la morphine. Cette dernière est extraite de *Papaver somniferum* utilisée dans le traitement des douleurs grâce à ses propriétés antalgiques [32]. On note aussi la vincristine extraite de *Catharanthus roseus* utilisée dans la lutte contre les cancers grâce à son action antimitotique sur la prolifération des cellules cancéreuses [33]. Enfin, la galanthamine extraite de plusieurs espèces Amaryllidaceae utilisée dans le traitement des symptômes de la maladie d'Alzheimer (MA) grâce à son action inhibitrice de l'acétylcholinestérase [27, 34]. Dans ce travail, nous nous sommes intéressés spécifiquement aux effets biologiques des alcaloïdes des Amaryllidaceae (AAs) de la flore sénégalaise.

1.3.3 Alcaloïdes des Amaryllidaceae

Les AAs représentent un groupe important et sont principalement de type isoquinoléine. Un isoquinoléine est un composé organique aromatique hétérocylique, analogue de la quinoléine pour lequel l'atome d'azote est en position 2. Depuis l'isolement de la lycorine en 1877 (initialement appelée narcissia) issue de *Narcissus pseudonarcissus* puis de *Lycoris radiata* en 1897 [35-37], près de 650 AAs ont été isolés et leurs structures élucidées [12]. Ces alcaloïdes sont principalement classés en 9 groupes dépendamment de leurs structures chimiques. Les plus représentatifs sont : la norbelladine, la cherylline, la galanthamine, la lycorine, l'homolycorine, la crinine, la narciclasine, la pretazettine et la montanine (Figure 1.6) [12].

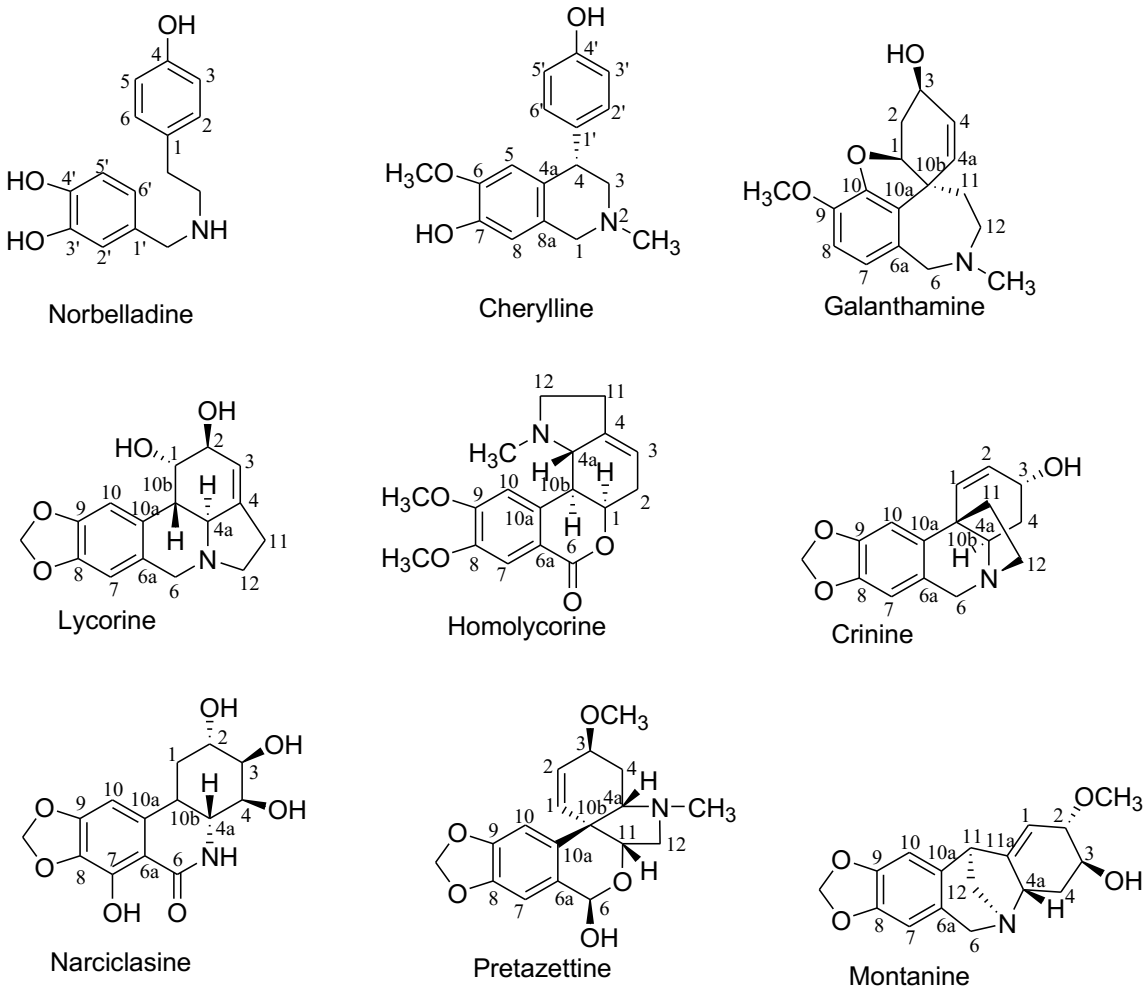

Figure 1.6 Types d'alcaloïdes des Amaryllidaceae les plus représentatifs.

1.3.4 Biosynthèse des alcaloïdes des Amaryllidaceae

La voie de biosynthèse des AAs implique une série de réactions biochimiques telles que l'oxydation, la réduction, l'hydroxylation, la méthylation, le couplage phénol-phénol et la formation de ponts d'oxyde à cause de leurs squelettes carbonés divers et complexes. Cependant, cette voie de biosynthèse n'est pas complètement élucidée même si plusieurs enzymes catalysant diverses étapes réactionnelles ont pu être identifiées [38, 39]. De nombreuses études de radiomarquage ont montré que les AAs ont une voie commune de biosynthèse. Elle peut être divisée en 3 étapes notamment la formation du précurseur clé la norbelladine, suivie de sa méthylation et la cyclisation pour donner les divers squelettes de base des AAs (Figure 1.7) [40-43]. La norbelladine provient de la dégradation de deux aminoacides à savoir le L-phénylalanine (L-Phe) et la L-tyrosine (L-Tyr) qui sont respectivement convertis en 3,4-dihydroxybenzaldéhyde (3,4-DHBA) et en tyramine. Par ailleurs, dans la biosynthèse des AAs il a été démontré que l'acide *trans*-cinnamique, l'acide *p*-coumarique et l'acide caféique sont les produits intermédiaires conduisant à la 3,4-DHBA. En particulier, la conversion de L-Phe en l'acide *trans*-cinnamique, implique la participation de l'enzyme phénylalanine ammonialyase (PAL) [44, 45]. De plus, la L-Tyr subit une décarboxylation par l'intermédiaire de l'enzyme tyrosine décarboxylase (TYDC) pour donner la tyramine [34]. La condensation de 3,4-DHBA et la tyramine conduisent à la formation de la norbelladine qui va subir à son tour une réduction, puis une *O*-méthylation pour former le *O*-méthylnorbelladine. Le *O*-méthylnorbelladine possède deux cycles phénoliques liés par un azote. Ces deux cycles subissent des couplages oxydatifs par régiosélectivité ortho-para', para-para' ou para-ortho' conduisant ainsi à la structure finale de l'alcaloïde. Par exemple, un couplage para-ortho' entraîne la formation des AAs de la famille des galanthamines, celui ortho-para' aboutit à la famille des lycorines alors que les familles des crinines, narciclasines, tazettines et montanines sont issues du couplage para-para (Figure 1.7) [12].

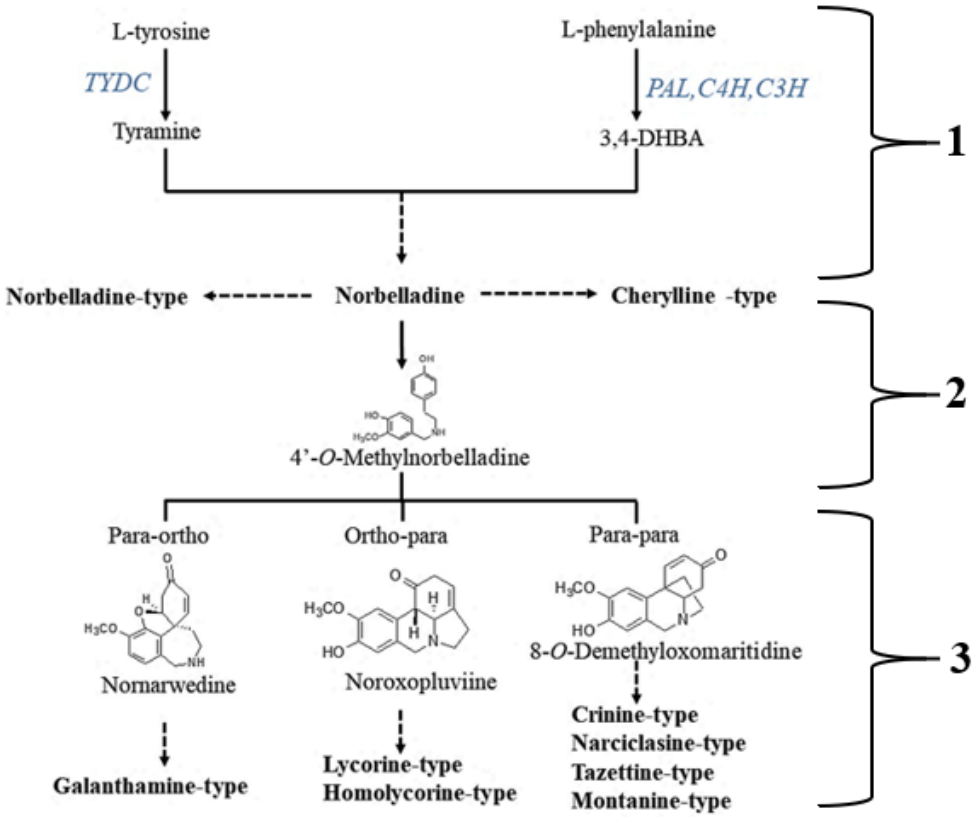

Figure 1.7 Schéma de biosynthèse des AAs modifié de Ka et al. [12]. **1 :** formation de la norbelladine, **2 :** formation d'*O*-méthylnorbelladine et **3 :** cyclisation pour donner les divers squelettes de base des AAs.

1.3.5 Avancés dans la synthèse des alcaloïdes des Amaryllidaceae

La synthèse totale des AAs naturels reste un domaine de recherche très convoité et actif. Cette recherche est motivée par les diverses et puissantes activités biologiques des AAs notamment leurs activités antibactériennes, anti-acétylcholinestérases (anti-AChE), cytotoxiques et antivirales [46, 47], ainsi que leur potentiel en tant qu'agents thérapeutiques. En outre, les nombreuses études sur la carence basée sur l'hémisynthèse des AAs de même que la synthèse totale d'analogues non naturels ont permis de comprendre la relation structure-activité de ces molécules et également conduit à de nouveaux analogues biologiquement plus actifs [48]. Ces dernières années, des progrès

ont été réalisés dans la synthèse de ces remarquables molécules de même que leurs analogues comme en témoignent par exemple la synthèse en 9 étapes de la (+)-*trans*-dihydrolycoricidine (type-narciclasine) [49], ainsi que la synthèse totale stéréosélective de la 3-*épi*-(+)-lycoricidine, la (+)-lycoricidine, la (+)*trans*-dihydronarciclasine, la (+)-pancratistatine, la (+)-α-lycorane, la (-)-α-Lycorane, la (+)-crinane, la (-)-galanthamine et la (-)-lycoramine [50].

Ainsi, pour élucider la structure d'un alcaloïde purifié ou synthétisé on fait recours à la spectroscopie résonance magnétique nucléaire (RMN).

1.3.6 Résonance magnétique nucléaire (RMN) des alcaloïdes des Amaryllidaceae

1.3.6.1 Définition de la RMN

La RMN est une technique spectroscopique pour l'élucidation des structures des molécules et des conformations moléculaires. Elle donne des informations magnétiques (constantes de couplages) et permet de déterminer des structures chimiques des molécules. Grâce aux progrès abondants accomplis dans la méthodologie de cette technique au cours des deux dernières décennies, la RMN est devenue un outil absolu pour l'analyse des extraits de plantes, y compris les Amaryllidaceae [51, 52].

L'élucidation structurale d'un produit naturel pur exige dans un premier temps l'analyse RMN 1D (^{1}H et ^{13}C) dans les meilleures conditions. Les spectres obtenus au cours de cette analyse 1D permettent d'obtenir des informations sur les déplacements chimiques exprimés en partie par million (ppm) et les constantes de couplages exprimées en hertz (Hz). Autrement, des expériences d'irradiations sélectives et de couplages sont exécutées pour identifier des signaux complexes d'un système de spin. Parfois il peut y avoir dans le cas des produits naturels notamment les extraits de plantes des recouvrements de signaux. Ces recouvrements peuvent rendre les informations sur les déplacements chimiques et constantes de couplages inaccessibles ou non interprétables. Dans ce contexte, la RMN à 2 dimensions (RMN 2D) permet d'obtenir des spectres avec de très bonnes résolutions pour l'élucidation de la structure.

Dans ce travail, nous nous intéresserons seulement aux techniques de RMN 2D COSY (homonuclear COrrelation SpectroscopY), HSQC (Heteronuclear Single Quantum Coherence), NOESY (Nuclear Over hauser Effect spectroscopY), et HMBC (Heteronuclear Multiple Bond Correlation Spectroscopy) pour l'élucidation des structures nos alcaloïdes purifiés.

La COSY (^{1}H-^{1}H) est une technique utile pour déterminer quels signaux proviennent de protons voisins (habituellement jusqu'à 4 liaisons). Lorsqu'il y'a un couplage spin-spin, des corrélations apparaissent, mais lorsqu'il n'y a pas de couplage aucune corrélation ne devrait apparaître. Les spectres COSY montrent les déplacements chimiques du proton en deux dimensions. Les pics de la diagonale observés dans un spectre COSY correspondent au spectre original du proton obtenu lors de l'analyse 1D. Les signaux hors de la diagonale représentent l'existence d'un couplage scalaire entre protons (J_{H-H}). Ces tâches surgissent de façon concordante par rapport à la diagonale et sont centrées aux coordonnées correspondant aux déplacements chimiques des deux noyaux couplés. Lorsqu'il y'a un carbone quaternaire, la corrélation s'arrête.

La NOESY par rapport à la COSY a l'avantage de prouver des interactions de longue distance entre deux protons décodant ainsi leur proximité spatiale.

Dans le cas des molécules complexes, l'attribution des signaux peut être difficile, voire même impossible à l'aide des spectres hononucléaires grâce aux signaux en RMN proton superposé. Dans ce cas, nous avons recours à la RMN hétéronucléaire notamment HSQC et HMBC. Pour régler ce problème, la RMN hétéronucléaire met en évidence le couplage carbone proton (J_{C-H}) qui transfert la polarisation du noyau du proton (H) vers le noyau du carbone (C). Cela permet de corréler d'une part, les signaux d'un proton à celui du carbone auquel il est lié dans le cas de HSQC, d'autre part de déterminer les couplages lointains jusqu'à 4 liaisons covalentes comme dans le cas de HMBC [53].

Étant donné que seuls des alcaloïdes de type lycorine, crinine, galanthamine et cherylline ont été isolés dans ce travail, seuls ces types de structures seront discutés en détail.

1.3.6.2 Résonance magnétique nucléaire des protons (1H) des alcaloïdes des Amaryllidaceae

La spectroscopie RMN ^{1}H permet d'obtenir suffisamment d'informations sur les différents types de structures des AAs. Généralement les spectres RMN ^{1}H des AAs montrent des signaux caractéristiques significatifs permettant leur identification [13]. Par exemple, on note la présence de signaux entre 6,5-8,5 ppm correspondant à un noyau aromatique. On peut observer sur ce dernier un ou plusieurs signaux méthoxyles autour de 3,6-4,0 ppm ou la présence du signal typique du méthylènedioxy autour de 6,0 ppm. Dans plusieurs structures des AAs la position C-6 benzylique est saturée comme dans le cas de la lycorine, galanthamine et crinine. Ainsi, ces protons sont caractéristiques du système AB. Il est intéressant de noter que le déplacement chimique peut être influencé par le doublet libre de l'atome d'azote et qu'il y'a des particularités pour chaque type d'alcaloïde [54].

Type-lycorine

Le spectre RMN ^{1}H de la lycorine et de ses dérivés est caractérisé principalement par la présence de deux singulets correspondant aux protons aromatiques *para*-orientés; un seul proton oléfinique et deux doublets correspondant à la position C-6 benzylique du système AB (Figure 1.6). Le déblindage observé dans les positions C-6 et C-12 du proton β, par rapport à leurs homologues, est dû à l'effet inductif attracteur de l'atome d'azote [13].

Type-crinine

Les AAs de types-crinine et -haemanthamine sont très similaires. Leurs différences est au niveau du pont 5, 10b-éthano, et ne peuvent être distinguées que par des analyses au dichroïsme circulaire en raison de leur configuration absolue [55]. Dans certains cas, on les appelle les crinanes [56]. On note quelques signaux remarquables dans leurs RMN ^{1}H à savoir l'amplitude des constantes de couplage entre chaque proton oléfinique (H-1 et

H-2) et H-3 qui donne des informations sur la configuration du substituant C-3. Ainsi, pour les AAs où le pont 5, 10b-éthano des carbones C-11 et C-12 est en position cis vers le substituant à C-3, le proton H-1 présente un couplage allylique avec H-3 ($J_{1,3}$~1-2 Hz), tandis que le proton H-2 présente un couplage plus faible avec H-3 ($J_{2,3}$~ 0-1,5 Hz), comme c'est le cas dans de la crinamine (Figure 1.6). Par ailleurs, dans un mélange épimérique, le carbone C-3 de l'haemanthamine montre un couplage plus important entre H-2 et H-3 ($J_{2,3}$ ~5 Hz), tandis que le couplage entre H-1 et H-3 est indétectable. De plus, on observe fréquemment un long couplage entre le proton H-2 et le proton H-4 en position équatoriale, tandis que le proton en position axiale H-4 présente un couplage important avec H-4a ($J_{4a,4a}$ ~13 Hz) en raison de leur disposition *trans*-diaxiale [13].

Type-galanthamine

Parmi tous les AAs, seul le type galanthamine présente une constante de couplage de type *ortho* (~ 8 Hz) entre les deux protons aromatiques du cycle A. L'attribution de la stéréochimie du substituant du carbone C-3 se fait en relation avec les constantes de couplage des protons oléfiniques H-4 et H-4a. En revanche, lorsque la constante de couplage $J_{3,4}$ est d'environ 5 Hz, le substituant est pseudo-axial, tandis que si elle est de ~ 0 Hz, le substituant du carbone C-3 devient pseudo-équatorial. Le déblindage du poton H-1 est dû à la présence de l'anneau furanique (Figure 1.6) [54].

Type-cherylline

Le spectre RMN ^{1}H de la cherylline et de ses dérivés est caractérisé par la présence de deux signaux qui correspondent à des doublets (6,91 et 6,64 ppm). Ces doublets sont caractéristiques d'un cycle aromatique 1,4-disubstitué. À cela, s'ajoute la présence de deux singulets à un proton (6,49 et 6,23 ppm) correspondant aux protons aromatiques *para*-orientés et deux singlets à trois protons à 3,51 et 2,24 ppm correspondant respectivement aux groupements OCH_3 et NCH_3 (Figure 1.6) [57].

1.3.6.3 Résonance magnétique nucléaire des carbones (13C) des alcaloïdes des Amaryllidaceae

Le RMN ^{13}C est généralement utilisée pour identifier les atomes de carbones dans une molécule. En général, les spectres RMN ^{13}C des AAs peuvent être divisés en deux zones. La zone de bas champ (> 90 ppm) contient les signaux du groupe carbonyle, des carbones oléfiniques et aromatiques, ainsi que celui du groupe méthylènedioxy, tandis que dans la zone à haut champ correspond aux carbones saturés. Ainsi, le *N*-CH_3 est le seul groupement caractéristique, facilement reconnaissable par un signal de quartet entre 40 et 46 ppm. Il importe de noter que la présence des substituants tels que OH, OCH_3 et OAc sur les résonances du carbone est d'une importance considérable pour localiser la position des groupements fonctionnels [54].

1.4 Effets biologiques des alcaloïdes des Amaryllidaceae

Depuis l'isolement de la lycorine en 1877, une centaine d'AAs ont été isolés et leurs structures élucidées [35-37, 58]. Ces AAs sont exploités pour leurs propriétés biologiques diverses notamment leurs propriétés anti-acétylcholinestérases (anti-AChE), cytotoxiques et antivirales [46, 47].

1.4.1 Activité anti-AChE

Les maladies neurodégénératives, telles que la maladie d'Alzheimer, sont parmi les maux du siècle qui ne trouvent pas de solution véritable à ce jour. La maladie d'Alzheimer est une maladie neurodégénérative complexe qui touche uniquement l'espèce humaine. Elle se caractérise par une perte progressive et irréversible des fonctions mentales, de la mémoire, des fonctions de mémorisation de nouvelles informations suivies d'une détérioration des fonctions de la pensée et de la manière de parler ainsi qu'un changement du comportement [59]. C'est la principale cause de démence chez les personnes âgées. En 2015, la démence a touché plus de 47 millions de personnes dans le monde, et ce nombre devrait atteindre 75 millions en 2030, puis 132 millions à l'horizon 2050 [60]. Au Sénégal en 2012, une étude portant sur la prévalence du déficit cognitif auprès de 872 personnes âgées de 55 ans a montré une prévalence de 10,8 % de déficit cognitif [61]. Selon ADI (Alzheimer's Disease Interntional), parmi les personnes atteintes de la démence 60 à 70 % sont atteintes de la maladie d'Alzheimer [60]. La maladie d'Alzheimer constitue donc un important problème de santé publique. Il n'existe aujourd'hui aucun traitement curatif de la maladie d'Alzheimer. Les seuls traitements existants sont symptomatiques. Ainsi certains médicaments permettent d'agir sur les troubles cognitifs et d'autres comportements spécifiques dus à la maladie d'Alzheimer. De plus, aucun des traitements existants ne permet de bloquer ou de ralentir l'évolution de la maladie. Les lésions provoquées par la maladie s'accompagnent de la diminution de l'acétylcholine, neurotransmetteur permettant aux neurones de la mémoire de communiquer. Les anticholinestérasiques permettent d'empêcher la destruction de l'acétylcholine par l'acétylcholinestérase. Parmi les traitements proposés pour la maladie d'Alzheimer, les inhibiteurs de l'acétylcholinestérase sont des médicaments approuvés pour le traitement d'un nombre limité de patients souffrant de la maladie d'Alzheimer, principalement ceux présentant une dégénérescence légère et modérée de la mémoire et des fonctions cognitives [62]. Actuellement, seule la galanthamine, un AA isolé des bulbes et fleurs des *Galanthus caucasicus* et d'autres Amaryllidacées telles que la *Lycoris radiata* a été approuvée comme un inhibiteur de l'AChE par la *Food and Drug Administration* aux États-Unis pour traiter les symptômes de la maladie d'Alzheimer [63]. Un des objectifs de ce travail est d'explorer les Amaryllidacées du Sénégal notamment le

P. trianthum et *C. jagus* afin de pouvoir proposer un ou des AAs, à l'image de la galanthamine capable de permettre une meilleure prise en charge de la maladie d'Alzheimer.

1.4.2 Activité cytotoxique/antitumorale

Le cancer est provoqué par des changements sous-jacents de l'information génétique. Ces changements se traduisent soit par des modifications des comportements cellulaires, soit par un comportement anormal de cellules souches. Ces cellules échapent aux actions normales de différentiation, de régulation de leur prolifération et résistent à la mort cellulaire programmée. Ces dysfonctionnements conduisent à la formation d'une masse tissulaire appelée tumeur. Ces tumeurs peuvent être malignes (cancéreuses) ou bénignes (non cancéreuses) [64]. Le cancer est l'une des principales causes de décès dans les pays développés et en développement. D'après les données des statistiques mondiales sur le cancer, on observe une tendance à la hausse de l'incidence et de la mortalité par cancer. On note environ 18,1 millions le nombre de nouveaux cas de cancer dans le monde en 2018, contre 14,1 millions en 2012 [65-67]. Bien que l'augmentation soit mondiale, les types de cancer sont différents entre les pays en développement et les pays développés, selon les diverses conditions liées à la démographie. Parmi ces types de cancers, le cancer du poumon représente 11,58 %, suivi du sein 11,55 % et du colorectum 10,23 % des cas de cancers. Le cancer du poumon est plus mortel avec un taux de 18,43 %, suivi de celui du foie et du canal biliaire avec 9,91 %, et de l'estomac avec 8,19 % [66]. Au Sénégal, une récente étude a permis de recenser 3157 cas de cancers. Parmi ces cas, 1107 sont confirmés histologiquement. À travers les cas recensés, 47 % étaient des hommes et 53 % des femmes [68]. De plus, selon une étude antérieure, 1197 femmes sénégalaises sont diagnostiquées chaque année avec un cancer du col de l'utérus, et 795 de ces cas sont mortels [69]. Donc le cancer pose un problème majeur de santé publique dans le monde et en particulier au Sénégal. Au Sénégal, le diagnostic du cancer est souvent tardif et la prise en charge est coûteuse et difficile. Il existe plusieurs types de traitement du cancer. Parmi ces traitements on note la chimiothérapie. Cette dernière se définit par l'usage de molécules chimiques pour traiter

une maladie notamment le cancer. Les agents chimiothérapeutiques sont qualifiés de cytotoxiques ou antiprolifératifs.

La lycorine est l'AA le plus abondant. Elle est isolée presque de tous les Amaryllidaceae. Les effets biologiques de la lycorine sont connus depuis de nombreuses années et elle est toujours à l'étude pour diverses applications thérapeutiques en particulier comme un agent cytotoxique ou anticancéreux [12]. Cependant, une étude a révélé que la lycorine exerçait une puissante activité antitumorale avec de faibles niveaux de toxicité *in vivo* [70]. De plus, une autre étude a montré que la lycorine avait la capacité d'inhiber la prolifération et la migration de la tumeur chez les souris sans toxicité [71]. Outre la lycorine, plusieurs autres AAs, dont l'hémanthamine et la narciclasine, ont été utilisées comme molécules phares pour la recherche anticancéreuse [72]. Dans le cas de notre travail, nous allons évaluer *in vitro* le potentiel cytotoxique de l'extrait brut alcaloïdique de *P. trianthum* et des AAs isolés de *C. jagus* récoltés dans la flore sénégalaise.

1.4.3 Activité antivirale (Dengue et Zika)

La dengue est une maladie virale causée par le virus de la dengue (VDEN), un flavivirus apparenté au virus Zika (VZIK) appartenant tous deux à la famille des *Flaviviridae*. Ces derniers sont transmis à leur hôte par des moustiques du genre *Aedes* [73]. Le génome des VDEN et VZIK est sous forme d'un ARN simple brin de sens positif, long d'environ 11 kb codant une polyprotéine unique. Cette dernière est clivée pendant et après sa traduction en 7 protéines non structurales (NS1, NS2A, NS2B, NS3, NS4A, NS4B et NS5) et 3 protéines structurales la capside (C), l'enveloppe (E), et la membrane (prM) [74-76]. Actuellement, il existe 4 sérotypes différents du virus de la Dengue notamment VDEN-1, VDEN-2, VDEN-3 et VDEN-4. Ces 4 sérotypes peuvent être en cause dans la Dengue hémorragique et la Dengue avec syndrome de choc pouvant tous entrainer la mort [77, 78].

L'infection par le VZIK est le plus souvent asymptomatique ou associée à des symptômes légers chez l'adulte, mais elle peut provoquer le syndrome de Guillain-Barré et la microcéphalie chez les enfants. L'infection fœtale par le ZIKV provoque des

affections plus graves, telles que le syndrome congénital de Zika, et d'autres malformations congénitales graves [79, 80].

En effet, la maladie de la Dengue est répandue dans toutes les zones tropicales et subtropicales du globe. Selon l'OMS, 3,9 milliards de personnes dans 128 pays dans le monde sont exposées à l'infection à la Dengue. Chaque année on dénombre 390 millions de cas de dengue dont 96 millions présentent des manifestations cliniques. La maladie de la Dengue occasionne chaque année entre 20 à 25 000 décès principalement des enfants dans les pays en développement [81]. En 2015, lors de l'épidémie de ZIKV au Brésil 4300 enfants sont nés avec une microcéphalie [79].

Entre 2017 et 2018, le Sénégal a connu deux épidémies de la Dengue principalement VDEN-1. Dans la première vague, 131 cas ont été confirmés dans la région de Louga [82]. Dans la deuxième vague, 1740 cas ont été suspectés. Parmi ces cas, 145 ont été confirmés et plus tard d'autres cas ont été ensuite détectés dans la région de Diourbel, de Louga et de Saint-Louis [82].

À ce jour, il n'existe aucun traitement antiviral approuvé contre le VDEN ou le VZIK, et aucun vaccin contre le VZIK [83]. Dans le cas du VDEN, l'efficacité du vaccin n'est pas optimale pour tous les sérotypes et son utilisation n'est pas recommandée chez les personnes séronégatives pour le VDEN [84, 85]. Donc la maladie de la Dengue constitue un véritable problème de santé publique dans les zones tropicales et subtropicales dans le monde.
Ainsi l'urgence de trouver des molécules antivirales efficaces contre ces flavivirus s'impose.

Les plantes médicinales constituent une alternative, car elles sont source de molécules bioactives. Parmi ces plantes médicinales, on note les Amaryllidaceae. Ces Amaryllidaceae contiennent des alcaloïdes ayant diverses activités biologiques, notamment une activité contre les moustiques tel que *Aedes aegypti* et des propriétés antivirales [38, 86-89]. L'extrait méthanolique du *C. macawonii* inhibe *in vitro* l'infection de deux flavivirus notamment le virus de la fièvre jaune (VYF) et le virus de l'encéphalite japonaise (VJE) [90]. Antérieurement, il a été démontré que la lycorine inhibe les

flavivirus notamment VDEN, VZIK, VYF, VJE et de nombreuses autres familles de virus, y compris le rétrovirus HIV-1, les coronavirus, ainsi que les virus à l'ADN [91-98].

Forts de ce constat, dans le cadre de notre travail nous allons évaluer les activités antiflavivirales des extraits alcaloïdes bruts de *P. trianthum* et alcaloïdes purs de *C. jagus* afin de trouver des molécules capables de permettre une meilleure prise en charge des malades de la Dengue et du Zika.

Plusieurs autres AAs ont révélé d'importantes activités biologiques (Tableau 1.3).

Tableau 1.3

AAs à structures diverses isolés entre janvier 2015 et août 2020 et leurs effets biologiques

No	Alcaloïde	Activité	Formule	Organe	Ref.
		TYPE-NORBELLADINE			
1	6-*O*-Demethylbelladine	SNC	$C_{18}H_{23}NO_3$	B	[99]
2	4′-*O*-Demethylbelladine	SNC	$C_{18}H_{23}NO_3$	B	[99]
3	4′-*O,N*-dimethylnorbelladine *N*-oxide	Tum	$C_{17}H_{22}NO_4$	B	[100]
4	Carltonine A	SNC	$C_{27}H_{32}N_2O_3$	B	[101]
5	Carltonine B	SNC	$C_{26}H_{28}N_2O_3$	B	[101]
6	Carltonine C	SNC	$C_{44}H_{49}N_3O_5$	B	[101]
		TYPE-CHERYLLINE			
7	Gigantelline	SNC, Tum	$C_{18}H_{21}NO_3$	B	[102]
8	Gigantellinine	SNC, Tum	$C_{18}H_{21}NO_4$	B	[102]
		TYPE-GALANTAMINE			
9	Lycoranine C	Tum	$C_{16}H_{21}NO_3$	B	[103]
10	Crijaponine B	SNC, Tum	$C_{19}H_{23}NO_5$	R, F	[104]
11	11β-Hydroxylycoramine	Inf	$C_{17}H_{23}NO_4$	B, L, F	[105]
12	9-De-*O*-methyl-11β-hydroxylycoramine	Inf	$C_{16}H_{21}NO_4$	B, L, F	[105]
13	9-De-*O*-methyl-11β-hydroxygalantamine	SNC, Inf	$C_{16}H_{19}NO_4$	B, L, F	[105]
14	11β-Hydroxylycoramine *N*-oxide	Inf	$C_{17}H_{23}NO_5$	B, L, F	[105]
15	11β-Hydroxygalantamine *N*-oxide	Inf	$C_{17}H_{21}NO_5$	B, L, F	[105]

No	Alcaloïde	Activité	Formule	Organe	Ref.
16	2β,11β-Dihydroxygalantamine	Inf	$C_{17}H_{21}NO_5$	B, L, F	[105]
	TYPE-LYCORINE				
17	(+)-1-Hydroxy-ungeremine	Inf, Tum	$C_{16}H_{12}NO_4^+$	B	[106]
18	Réticulinine	SNC	$C_{17}H_{21}NO_4$	B, L	[107]
19	Isoréticulinine	SNC	$C_{17}H_{21}NO_4$	B, L	[107]
20	Galanthine *N*-β-oxide	SNC	$C_{18}H_{23}NO_5$	B, L, F	[108]
21	Carinatine *N*-α-oxide	SNC	$C_{17}H_{21}NO_5$	B, L, F	[108]
22	Zéphycarinatine I	SNC	$C_{17}H_{15}NO_3$	B, L, F	[108]
23	Oxoincartine	SNC	$C_{18}H_{21}NO_6$	B, L, F	[109]
24	7-Oxonorpluviine	nm	$C_{16}H_{17}NO_4$	B	[110]
25	pseudolycorine *N*-oxide	Tum	$C_{16}H_{19}NO_5$	B, L, F	[111]
	TYPE-HOMOLYCORINE				
26	(+)-2-Hydroxy-8-demethyl-homolycorine-α-*N*-oxide	Inf, Tum	$C_{17}H_{19}NO_6$	B	[106]
27	Lycoranine E	Tum	$C_{17}H_{19}NO_6$	B	[103]
28	Lycoranine F	Tum	$C_{17}H_{19}NO_4$	B	[103]
29	2α-10bα-Dihydroxy-9-*O*-demethylhomolycorine	Tum	$C_{17}H_{19}NO_6$	B	[112]
30	7-Hydroxyclivonine	SNC	$C_{17}H_{19}NO_6$	B	[113]
	TYPE-CRININE				
31	(+)-6β-Acetyl-8-hydroxy-9-methoxy-crinamine	Inf, Tum	$C_{19}H_{23}NO_6$	B	[106]
32	Crijaponine A	SNC, Tum	$C_{16}H_{19}NO_4$	R, F	[104]
33	6α-Methoxyundulatine	Tum	$C_{19}H_{23}NO_6$	L	[114]
34	6α-Methoxycrinamidine	Tum	$C_{18}H_{21}NO_6$	L	[114]
35	Undulatine *N*-oxide	Tum	$C_{18}H_{21}NO_6$	L	[114]
36	1,4-Dihydroxy-3-methoxy powellan	Par, Tum	$C_{18}H_{23}NO_6$	B	[115]
37	Augustine *N*-oxide	SNC, Par	$C_{17}H_{19}NO_5$	B, L	[116]
38	Buphanisine *N*-oxide	SNC, Par	$C_{17}H_{19}NO_4$	B, L	[116]
39	6α-Hydroxymaritidine	SNC, Par	$C_{17}H_{21}NO_4$	B, L	[107]
40	6β-Hydroxymaritidine	SNC, Par	$C_{17}H_{21}NO_4$	B, L	[107]
41	3,11-*O*-Diacetyl-9-*O*-demethylmaritidine	SNC	$C_{20}H_{22}NO_6$	B, L, F	[109]
42	11-*O*-Acetyl-9-*O*-demethylmaritidine	SNC	$C_{18}H_{20}NO_5$	B, L, F	[109]
43	Crinsarnine	Ins, Lar	$C_{20}H_{25}NO_6$	B	[117]

No	Alcaloïde	Activité	Formule	Organe	Ref.
44	Gigancrinine	SNC, Tum	$C_{16}H_{17}NO_4$	B	[102]
45	Haemanthamine *N*-oxide	nm	$C_{17}H_{19}NO_5$	B, L	[118]
46	Crinasiaticine A	hCAII	$C_{18}H_{19}NO_5$	B	[119]
47	Crinasiaticine B	hCAII	$C_{18}H_{21}NO_5$	B	[119]
48	3-*O*-Acetylvittatine	Tum	$C_{18}H_{19}NO_4$	B	[100]
49	3-*O*-Methyl-*epi*-vittatine	Tum	$C_{17}H_{19}NO_3$	B	[120]
50	Crouchinine	nm	$C_{19}H_{23}NO_6$	B	[120]
	TYPE-NARCICLASINE				
51	Narciclasine-4-*O*-β-D-xylopyranoside	Tum	$C_{19}H_{21}NO_{11}$	B, L, F	[121]
	TYPE-TAZETTINE				
52	Jonquailine	Tum	$C_{19}H_{23}NO_5$	B	[122]
53	Scillitazettine	Par, Tum	$C_{19}H_{21}NO_6$	B	[100]
54	Scilli-*N*-desmethylpretazettine	Par, Tum	$C_{18}H_{19}NO_5$	B	[100]
	TYPE-MONTANINE				
55	4-*O*-Méthylnangustine	SNC	$C_{17}H_{19}NO_4$	B	[113]
	AUTRE-TYPES				
	PLICAMINE				
56	*N*-Isopentyl-5,6-dihydroplicane	Inf	$C_{23}H_{30}N_2O_4$	B, L, F	[105]
57	*N*-(*S*)-*s*-Pentyl-5,6-dihydroplicane	Inf	$C_{23}H_{30}N_2O_4$	B, L, F	[105]
58	*N*-Hexyl-5,6-dihydroplicane	Inf	$C_{24}H_{32}N_2O_4$	B, L, F	[105]
59	*N*-Hydroxycarbonylpropyl-5,6-dihydroplicane	Inf	$C_{22}H_{26}N_2O_6$	B, L, F	[105]
60	*N*-Phénethyl-5,6-dihydroplicane	Inf	$C_{26}H_{28}N_2O_4$	B, L, F	[105]
61	*N*-3-Indolylethyl-5,6-dihydroplicane	SNC, Inf	$C_{28}H_{29}N_3O_4$	B, L, F	[105]
62	*N*-Isopentyl-5,6-dihydroplicane *N*-oxide	Inf	$C_{23}H_{30}N_2O_5$	B, L, F	[105]
63	Bliquine *N*-oxide	SNC	$C_{26}H_{28}N_2O_6$	B, L, F	[105]
64	Zéphycarinatine C	Inf	$C_{23}H_{28}N_2O_5$	B, L, F	[108]
65	Zéphycarinatine D	Inf	$C_{19}H_{20}N_2O_5$	B, L, F	[108]
66	Zéphycarinatine E	Inf	$C_{23}H_{28}N_2O_5$	B, L, F	[108]
67	Zéphycarinatine F	SNC, Inf	$C_{20}H_{24}N_2O_6$	B, L, F	[108]

No	Alcaloïde	Activité	Formule	Organe	Ref.
		SECO-PLICAMINE			
68	*N*-Methyl-11,12-*seco*-5,6-dihydroplicane	Inf	$C_{19}H_{22}N_2O_5$	B, L, F	[105]
69	*N*-Isopentyl-11,12-*seco*-5,6-dihydroplicane	Inf	$C_{23}H_{30}N_2O_5$	B, L, F	[105]
70	Zephycarinatine H	SNC	$C_{23}H_{32}N_2O_4$	B, L, F	[108]
		CRIPOWELLINE			
71	4,8-Dimethoxy-cripowellin C	Inf, Mic, Oxy, Tum	$C_{26}H_{35}NO_{11}$	B	[123]
72	4,8-Dimethoxy-cripowellin D	Inf, Mic, Oxy, Tum	$C_{26}H_{37}NO_{10}$	B	[123]
73	9-Methoxy-cripowellin B	Inf, Mic, Oxy, Tum	$C_{26}H_{35}NO_{12}$	B	[123]
74	4-Methoxy-8-hydroxy-cripowellin B	Inf, Mic, Oxy, Tum	$C_{25}H_{35}NO_{11}$	B	[123]
75	Cripowellin C	Tum	$C_{25}H_{31}NO_{11}$	L	[124]
76	Cripowellin D	Tum	$C_{25}H_{33}NO_{10}$	L	[124]
		MESEMBRINE			
77	Sarniensinol	Ins, Lar	$C_{18}H_{23}NO_4$	B	[117]
78	Sarniensine	Ins, Lar	$C_{19}H_{25}NO_4$	B	[125]
		AUTRES			
79	(+)-*N*-Methoxylcarbonyl-2-demethyl-isocorydione	Inf, Tum	$C_{20}H_{17}NO_7$	B	[106]
80	Lycoranine D	Tum	$C_{15}H_{15}NO_3$	B	[103]
81	Zephycandidine A	Tum	$C_{16}H_{10}N_2O_2$	B, L, F	[126]
82	Hymenolitatine	Tum	$C_{17}H_{15}NO_4$	B	[127]
83	Zéphycandidine I	SNC	$C_{18}H_{25}NO_4$	B, L, F	[128]
84	Zéphycandidine II	SNC	$C_{15}H_{19}NO_2$	B, L, F	[128]
85	Zéphycandidine III	SNC	$C_{17}H_{19}NO_4$	B, L, F	[128]
86	Narcipavline	SNC	$C_{33}H_{34}N_2O_5$	B	[129]
87	Narcikachnine	nm	$C_{33}H_{36}N_2O_5$	B	[129]
88	Narcimatuline	SNC	$C_{33}H_{34}N_2O_5$	B	[130]
89	Zéphycarinatine A	SNC	$C_{25}H_{32}N_2O_5$	B, L, F	[108]
90	Zéphycarinatine B	SNC	$C_{22}H_{30}N_2O_4$	B, L, F	[108]
91	Zéphycarinatine G	SNC	$C_{23}H_{32}N_2O_3$	B, L, F	[108]

Les abréviations des activités biologiques sont : SNC : système nerveux central, hCAII : isozyme carbonique humain II, Inf : anti-inflammatoire, Ins : insecticide, Lar : larvicide, Mic : antimicrobien, Oxy : antioxydant, Par : antiparasitaire, Tum : antitumoral, et nm : non mesuré.

Les abréviations des organes sont :L : feuilles, B : bulbes, F : fleurs, et R : rhizomes.

1.5 Hypothèses et objectifs

1.5.1 Hypothèses

Dans cette thèse, nous testons l'hypothèse principale selon laquelle les Amaryllidaceae est une famille très répandue dans la flore sénégalaise dans laquelle le *P. trianthum* et le *C. jagus,* pourraient contenir des alcaloïdes anti-AChE, cytotoxiques et antiflavivirus.

Cela nous amène à formuler les hypothèses spécifiques suivantes :

Hypothèse 1 : Les AAs pourraient être la base scientifique de l'utilisation des bulbes de *P. trianthum* dans la médecine traditionnelle sénégalaise pour traiter les plaies et les infections.

Hypothèse 2 : Compte tenu des conditions environnementales et climatiques du Sénégal, le *C. jagus* pourrait contenir de nouveaux alcaloïdes.

Hypothèse 3 : Les AAs isolés de *C. jagus* ont des effets anti-AChE, cytotoxiques et antiflaviviraux.

1.5.2 Objectifs

1.5.2.1 Objectif général

L'objectif général de cette thèse est d'évaluer les activités antibactériennes, anti-AChE, cytotoxiques et anti-dengue de l'extrait alcaloïde de *P. trianthum*, de purifier l'extrait alcaloïde de *C. jagus* et d'enfin évaluer les activités anti-AChE, cytotoxiques et anti-dengue des alcaloïdes purifiés.

Pour atteindre cet objectif général, nous avons mis au point des objectifs spécifiques ci-dessous.

1.5.2.2 Objectifs spécifiques

Objectif spécifique 1

Le premier objectif spécifique concerne uniquement l'étude de l'espèce *P. trianthum* qui est utilisée dans la médecine traditionnelle au Sénégal. Dans cet objectif, nous visons d'abord à extraire les alcaloïdes à partir des bulbes de *P. trianthum*, les caractériser et les identifier par des techniques chromatographiques et spectrométriques (CCM, HPLC et GC-MS). Ensuite, nous comptons évaluer l'activité antibactérienne, anti-AChE, cytotoxique et anti-dengue de l'extrait alcaloïdique (voir chapitre II).

Objectif spécifique 2

Le deuxième objectif spécifique consiste à isoler et élucider les structures des alcaloïdes extraits des bulbes de *C. jagus* et évaluer leurs activités cytotoxiques et anti-AChE (voir chapitre III).

Objectif spécifique 3

Dans le troisième objectif spécifique, nous visons à évaluer les activités antivirales des alcaloïdes isolés des bulbes de *C. jagus* contre les virus de la Dengue et du Zika (voir chapitre IV).

Le chapitre II contient les activités antibactériennes, anti-AChE, cytotoxiques et anti-Dengue des alcaloïdes extraits à partir des bulbes de *P. trianthum*.

CHAPITRE II

BIOLOGICAL INVESTIGATION OF AMARYLLIDACEAE ALKALOID EXTRACTS FROM THE BULBS OF *PANCRATIUM TRIANTHUM* COLLECTED IN THE SENEGALESE FLORA

Seydou Ka, Natacha Merindol, Simon Ricard, Insa Seck, Amadou Diop, Cheikh Sadibou Boye, Benoit Daoust, Matar Seck, Isabel Desgagné-Penix

Le contenu de ce chapitre est sous forme d'un article en préparation pour soumission dans la revue *Journal of Ethnopharmacology*.

2.1 Contribution des auteurs

SK, NM, MS et IDP ont conçu les expériences, analysé les données, rédigé et révisé le manuscrit et la révision du manuscrit. SK, BD et SR ont mené et analysé les expériences sur le GC-MS. SK, AD, IS et CSB ont mené et interprétés les expériences en lien avec les activités antibactériennes.

2.2 Résumé de l'article (français)

P. trianthum est une espèce d'Amaryllidaceae qui est largement utilisée dans la médecine traditionnelle africaine pour traiter plusieurs maladies telles que les troubles du système nerveux central, les tumeurs, les infections microbiennes et des plaies. L'étude actuelle explore la cytotoxicité, les propriétés anti-AChE, antibactériennes, antivirales et pro-inflammatoires des extraits totaux d'alcaloïdes des bulbes de *P. trianthum* récoltés dans la flore sénégalaise. Les alcaloïdes extraits sont analysés et identifiés par CCM, HPLC-DAD et GC-MS. L'activité cytotoxique des extraits a été déterminée sur des cellules d'hépatocarcinome Huh7 et sur des cellules THP-1 de leucémie monocytaire aiguë. L'activité anti-AChE a été mesurée par la méthode colorimétrique d'Ellman, tandis

que des essais de microdilution et de diffusion sur gélose ont été utilisés pour évaluer l'activité antibactérienne contre *Staphylococcus aureus*, *Escherichia coli* et *Pseudomonas aeruginosa*. L'activité anti-dengue (DENV) de l'extrait a été mesurée par l'infection de cellules avec des vecteurs rapporteurs $DENV_{GFP}$. L'activité pro-inflammatoire a été évaluée à l'aide de lignées cellulaires LL171 exprimant l'élément de réponse stimulé par l'interféron (ISRE)-rapporteur de la luciférase. L'extrait alcaloïdique de *P. trianthum* a montré des activités anti-tumorales/cytotoxiques, anti-AChE, antibactériennes et antivirales en fonction de la dose. La cytotoxicité et l'activité antivirale étaient les propriétés biologiques les plus frappantes de l'extrait. Il est important de noter que les concentrations non cytotoxiques de l'extrait de *P. trianthum* ont été très efficaces pour inhiber la réplication du $DENV_{GFP}$. En conclusion, nos résultats ont montré que le *P. trianthum* est une source riche de composés pour la potentielle découverte de nouveaux traitements contre le cancer, les maladies neurodégénératives et les maladies virales. Nous avons démontré ainsi que l'extrait brut alcaloïde est antimicrobien et nous suggérons l'utilisation traditionnelle du *P. trianthum* pour le traitement des plaies, sous forme d'anti-dermatose et d'antiseptique.

2.3 Article complet (anglais): Biological investigation of Amaryllidaceae alkaloid extracts from the bulbs of *Pancratium trianth*um collected in the Senegalese flora

Abstract

Ethnopharmacological relevance: P. trianthum, belonging to the Amaryllidaceae family is widely used in African folk medicine to treat several diseases such as central nervous system disorders, tumors, microbial infections and to heal wounds.

Aim of the study: The current investigation explores the cytotoxicity, anti-AChE, antibacterial, antiviral and proinflammatory properties of alkaloid extracts from bulbs of *P. trianthum* collected in Senegalese flora.

Materials and methods: Alkaloid extracts were obtained by acid base method, analyzed and identified by TLC, HPLC-DAD and GC-MS. Cytotoxic activity of the extracts was determined on hepatocarcinoma Huh7 cells and on acute monocytic leukemia THP-1 cells. Anti-AChE activity was measured using Ellman's colorimetric method, while agar diffusion and microdilution assays were used to evaluate antibacterial activity against *Staphylococcus aureus*, *Escherichia coli* and *Pseudomonas aeruginosa*. Anti-dengue virus (DENV) activity of the extracts was measured by infection of extracts-pretreated cells with $DENV_{GFP}$ reporter vectors. Proinflammatory activity was assessed using LL171 cell lines expressing the interferon stimulated response element (ISRE)-luciferase reporter.

Results: Alkaloid extract of *P. trianthum* displayed anti-tumoral/cytotoxic, anti-AChE, antibacterial and antiviral activities in a dose dependent manner. Cytotoxicity and antiviral activity were the most striking biological properties of the extracts. Importantly, non-cytotoxic concentrations of *P. trianthum* alkaloid extracts were highly effective in inhibiting the replication of $DENV_{GFP}$.

Conclusions: Our results show that *P. trianthum* is a rich source of compounds for the potential discovery of new treatments against cancer, neurodegenerative diseases and viral

diseases. Herein, we demonstrate that alkaloid extract is antimicrobial and confirm traditional uses of *P. trianthum* for wound treatment, as anti-dermatosis and antiseptic.

Keywords: Amaryllidaceae; *Pancratium trianthum;* alkaloids; acetylcholinesterase; antibacterial; cytotoxicity, Dengue virus; GC-MS.

Introduction

Plants have been used in traditional medicine to treat human diseases since antiquity and are still the most important source of today's drugs. The Amaryllidaceae plant family encompasses over 1600 species scattered all around the globe, and is among the top 20 most widely considered medicinal plant families [1]. They are bulbous flowering plants that are also exploited for ornamental reason. Approximately, one third of known Amaryllidaceae species grow in South Africa, and they are largely used in folk medicine [2, 3]. Traditional usage of Amaryllidaceae ranges from simple health problems (headache, cough, boils) to complicated diseases (cancer, tuberculosis, diabetes). They are recognized for their anti-bacterial [4], anti-tumoral [5], anti-acetylcholinesterase (AChE) properties [6]. Some are also notoriously toxic [7, 8]. West-African Amaryllidaceae species have been relatively poorly studied. Their complete therapeutic potential is not known and could provide therapeutic alternatives to improve human health. *Pancratium* Amaryllidaceae species are collected for their medicinal properties in Senegal. The genus *Pancratium* contains approximately 20 species, extending from the Canary islands through the Mediterranean region to tropical Asia, and West Africa to Namibia [9]. The latin word '*pancrace*' refers to a violent combat sport and the Greek word 'pan' means all, while '*kratos*' meaning force, possibly referring to the strong toxicity of this plant. Some species belonging to the *Pancratium* genus, have been used around the world to treat cancer but they are generally poorly studied [10]. *P. trianthum* is characterized by white fragrant flowers, and plant extracts are used for their irritation-calming, wound-healing, anti-oedema, anti-dermatosis, anti-septic, anti-epileptic, psychotropic and fungicidal therapeutic properties [11, 12]. *P. trianthum* is

recognized to be toxic in Senegal and Sudan and thus used for external used only [7], but considered to be edible in Nigeria and Western Sahara [8, 13].

Phytochemical studies have shown that the therapeutic properties of Amaryllidaceae extracts originate from a specific class of specialized metabolites that they produced, called Amaryllidaceae alkaloids (AAs). Galanthamine, a widely occurring AA, is approved by the FDA as an AChE inhibitor to treat the symptoms of Alzheimer‘s disease [14], while AA lycorine is intensively studied for its anti-cancer and anti-viral properties [15, 16]. Pharmaceutical compounds of some *Pancratium sp.* have been studied, although scarcely, lycorine-, crinine- and haemanthamine-types are reported as the most abundant alkaloids in this genus [17]. In 1983, one report investigated the alkaloid content of epigeal and hypogeal parts of *P. trianthum* and identified AAs trisphaeridine, hippeastrine, hordenine, pancratine, tazettine, lycorine, galanthamine, and trianthine [18, 19].

Continuing our screening on biological activities of native and under-studied Amaryllidaceae from Senegal, we thus focused on *P. trianthum*. The current investigation explores the antibacterial, anti-AChE, cytotoxicity, antibacterial, antiviral and proinflammatory effects of alkaloid extracts from *P. trianthum* collected in Senegal to extend efforts towards the discovery of new phytomedicines.

Materials and Methods

Plant material and species identification

Bulbs of *P. trianthum* were collected in Senegal, in Saint Louis (16°3’19,35’’N and 16°25’42,25’’W) in December 2018. A senior scientist from the Herbarium of IFAN of University Cheikh Anta Diop of Dakar taxonomically identified the plant materials.

Genomic DNA was extracted from dried roots of *P. trianthum* using the DNeasy plant mini kit (QIAGEN) according to the manufacturer’s instructions. Yield and purity of total

extracted DNA was quantified with a Nanodrop (IMPLEN, QC, CA), and stored at -20 ºC for later use. Ribulose-bisphosphate carboxylase gene (*rbcL*) DNA barcode of *P. trianthum* was amplified by PCR using TaKaRa's PrimeSTAR GXL Premix kit, and primers (F-GGATTACCAGCCTTGATCG, and R-TTCACGAGCAAGATCACGTC) [20]. The PCR mixture (20 µL) contained 2 µL of genomic DNA, 10 µL Takara mix, 0.4 µL of each primer (10 µM, forward and reverse primers), and 7.2 µL of ultrapure-DNase free water. The thermocycler program consisted of initial denaturation at 98 °C for 2 min; followed by 30 cycles of 98 °C for 10 s, 55 °C for 15 s, and 68 °C for 75 s. After PCR, 5 µl of amplified product was loaded on a 1% agarose gel, and specific size amplicons (1044 pb) were sequenced using both forward and reverse primers.

Crude alkaloids extraction, and TLC analysis

Dried bulbs (50 g) of *P. trianthum* were crushed and extracted for 24 h with MeOH at room temperature, and the combined macerates were filtered and evaporated under reduced pressure. The crude extract of *P. trianthum* was acidified with sulphuric acid (2%) at pH = 2 and extracted with Et_2O (4 x 200 mL) and EtOAc (4 x 200 ml) to remove neutral material. The acidic aqueous solution was basified with ammonia (25%) up to pH = 10 and extracted with EtOAc (4 x 200 mL) to obtain 31,4 mg of crude alkaloids [21].

Crude alkaloid extract was then dissolved in extraction solvent (EtOAc) at a final concentration of 1 mg/mL and used for thin layer chromatography (TLC) analysis. Drops of alkaloid extract solutions were loaded onto the baseline of the layer of the plate and eluted with MeOH: EtOAc (25:75 v/v). Plates were dried, observed under UV light at 254 nm and 365 nm, and revealed with Dragendorff reagent [22].

HPLC-DAD and GC-MS analysis of alkaloid extracts

We followed the method by Singh *et al.* with some modification [23]. The alkaloid extract was dissolved in MeOH at a final concentration 0,5 mg/mL. Afterwards, 10 µL of each sample and 10 µL of each standard (galanthamine, lycorine and narciclasine) were

injected and analyzed on a Shimadzu Prominence-i LC-2030C with diode array detector (PDA). HPLC oven temperature was set at 40 °C using Kinetex C18 column (150 × 4.6 mm, 5 μm particle size; Phenomenex). The total run time was 23 minutes. A gradient elution with two solvents, 1% ammonium acetate buffer (solvent A) and 100% acetonitrile (solvent B) was used. The gradient elution started at 10% and progressively increased to 31% of solvent B for the first 11 minutes and then from 70% to 90% of solvent B at 4 and 3 minutes respectively, and then reduced to 10% again for the following 5 minutes.

For GC-MS analysis, 1 mg/mL of alkaloid extract in MeOH was directly injected into the GC-MS (Agilent Technologies 6890N GC coupled with 5973N inert MSD; Trois-Rivières, QC, CAN) in EI (Electron Ionization) mode at 70 eV. Program was set to 2 min at 100 °C, 100-180 °C at 15 °C min^{-1}, 180-300 °C at 5 °C min^{-1} and a 10 min hold at 300 °C. Injector and detector temperatures were 250 °C and 280 °C, respectively, and the flowrate of carrier gas (He) was 1 mL min^{-1}. A split ratio of 1:10 was applied and the injection volume was 1 μL [24]. Alkaloids were identified by comparison with the National Institute of Standards and Technology (NIST 05) database based on matching mass spectra, GC-MS spectra of authentic compounds previously isolated and identified by other spectroscopic methods in these species, or with data obtained from the literature. Total ion current (TIC) percentage provided in Table 1 was connotated with the proportion of each compound in the extract. The area of the GC-MS peaks depends both on the concentration of the related compounds and on the intensity of their mass spectrum.

In vitro Acetylcholinesterase (AChE) assay

In vitro AChE activity of the alkaloid extract of *P. trianthum* was assessed using the method described in [25].

Cell lines

Human hepatocarcinoma cell line Huh7 provided by Hugo Soudeyns, and murine LL171 reporter cells [26] were maintained in Dulbecco's Modified Eagle's Medium high glucose (DMEM), supplemented with 10% fetal bovine serum (FBS) and 1% penicillin-streptomycin (PS) solution. Human acute monocytic leukemia cell line THP-1 was kindly shared by Lionel Berthoux and grown in Roswell Park Memorial Institute medium (RPMI) containing 10% FBS and 1% PS. All cells were maintained at 37 °C and 5% CO_2.

Cytotoxicity assay

Cell viability was evaluated using the Cell-Titer GLO assay kit (Promega). Briefly, 50 µL of 7,5 x 10^3 Huh7 cells/well or 20 x 10^3 THP-1 cells/well were seeded in 96-well dark plates and cultured for 16 h. Then, they were treated with 50 µL of alkaloid extract at concentrations (< 0.5% DMSO) ranging from 0.019 to 2.5 µg/mL for 72 h. Afterwards, 100 µL of room temperature Cell-Titer GLO reagent was added in each well to room temperature-equilibrated plates. Plates were rocked for 2 min, and luminescence signal was measured 10 min later using a microplate spectrophotometer (Synergy H1, Biotek, Quebec, Canada). The percentage of viable cells was calculated at each concentration. All assays were performed in triplicate.

Bacteria and viruses

Three bacteria species including the Gram-positive strain *Staphylococcus aureus* ATCC 29213 and two Gram-negative strains: *Escherichia coli* ATCC 25922 and *Pseudomonas aeruginosa* ATCC 27253 were obtained from the American Type Culture Collection (ATCC) and from the Bacteriology-Virology Laboratory at Aristide Le Dantec Hospital (Senegal). The bacterial strains were cultured in Mueller Hinton (MH) agar media and incubated at 37 °C for 24 hours before use.

Dengue virus vectors expressing green fluorescent protein ($DENV_{GFP;}$ [27]) were kindly shared by Laurent Chatel-Chaix and Lionel Berthoux'lab, and used for the antiviral activity.

Agar Diffusion Assay

Antibacterial activity of the alkaloid extract was studied using the agar diffusion assay method. A suspension of each strain was prepared into sterile physiological water to obtain a final inoculum estimated at 1.5 x 10^8 CFU/mL, according to 0.5 McFarland turbidity. Alkaloid extract was dissolved in DMSO at 16 mg/mL. For the assay, a sterile cotton swab was immersed in the inoculum, then wrung on the wall of the tube. The swab was then spread over on the agar plate to obtain uniform inoculums. Wells were made on Mueller Hinton agar plates using a sterile cylinder of 6 mm diameter. Plates were dried for 5 minutes and 100 µL of alkaloid extracts were deposited. Plates were incubated at 37 °C for 18-24 h. Antimicrobial activity of the alkaloid extract was then measured as an inhibition zone surrounding the well [28].

Broth dilution method for determination of Minimal Inhibitory Concentration (MIC)

Microdilution of the alkaloid extracts of *P. trianthum* was performed using a modified method of Balouiri *et al* [29]. The microdilutions were started by dispensing 100 µL of alkaloid extract in the first column of a 96-well plate containing 100 µL of MH broth. Serial dilutions were then carried out in order to obtain a range of concentrations between 0.03 to 8 mg/mL. Then, 10 µL of bacterial suspension cultures were added into corresponding wells. Plates were incubated at 37 °C during 24 h. The MIC (minimal inhibitory concentration) was determined as the lowest concentration of the alkaloid extract that completely suppressed the growth of microorganism (which is determined by the wells showing no turbidity). Tested bacteria were exposed to broth without the alkaloid extract as a control. Erythromycin and tetracycline were used as positive controls.

In vitro antiviral activity

The antiviral assay of the alkaloid extract of *P. trianthum* was performed using $DENV_{GFP}$. Briefly, Huh7 were seeded at 15 x 10^3 cells per well in 48 well-plates, cultured for 16 h, and then pretreated with indicated concentration of alkaloid extract of *P. trianthum* ranging from 0.02 to 2.5 µg/mL, infected with $DENV_{GFP}$ 2 h later at a multiplicity of infection (MOI) of 0.1 PFU/cell cells and incubated at 37 ºC for 72 h. Green fluorescence signal of infected cells were visualized, and pictured on the Axio Observer microscope (Carl Zeiss, Inc., Toronto, ON, Canada). Cells were trypsinized and fixed in 4% formaldehyde to measure the percentage of infected cells on a FC500 MPL cytometer (Beckman Coulter, Inc., CA) and analyzed using FCS express 6 software (De novo software, CA). The adenosine analogue NITD008 (10 µM) was used as positive control. All assays were performed in triplicate at least twice.

In vitro proinflammatory assay

In vitro proinflammatory assay was performed using the Luciferase Assay Systems kit (Promega). Briefly, 200 µL LL171 cells were seeded at 15 x 10^3 cells/well in 96-well plates and cultured for 16 h. Then, medium was replaced with medium containing alkaloid extracts at concentration ranging from 0.0625 to 0.5 µg/mL for 24 h. The supernatant was removed, and cells were rinsed with PBS. Then, 30 µL of lysis buffer was added, and cells were scratched. Afterwards, 20 µL of each well was transferred into 96 wells opaque plates, 100 µL of LAR (Luciferase Assay Reagent, Promega) was added, and luminescence was measured at 480 nm using a microplate spectrophotometer (Synergy H1, Biotek, Quebec, Canada). 5,6-dimethylxanthenone-4-acetic acid (DMXAA, 20 µg/mL) was used as a positive control. All assays were performed in triplicate.

Results

Species phylogenetic analysis

To confirm the species of the bulbs collected and used herein, we amplified and sequenced DNA from the chloroplastic gene encoding the large subunit of *rbcL* [20]. *P. trianthum rbcL* sequence, (available in supplementary file 1), was blasted in the National Center for Biotechnology Information (NCBI) database using BLASTn. Top hits were related to *rbcL* sequences from *Pancratium* species with over 96% sequence identity. Phylogenetic analysis was carried out using phylogeny.fr [30], with default values, including *rbcL* sequences from 10 *Pancratium* species, and from 1 outgroup, the species *Lilium lancifolium*an, an Asparagales that belongs to the Liliaceae instead of the Amaryllidaceae family. Maximum likelihood analysis showed a monophyletic clade of the *rbcL* sequences from all *Pancratium* species, including *P. trianthum*. *Pancratium illyricum rbcL* sequence clustered outside this common node and the outgroup *Lilium lancifolium* was robustly separated from all Amaryllidacease species. *Pancratium trianthum* sequence grouped closely to the species *Pancratium canariense, Pancratium zeylanicum,* and *Pancratium hirtum* (Figure 1).

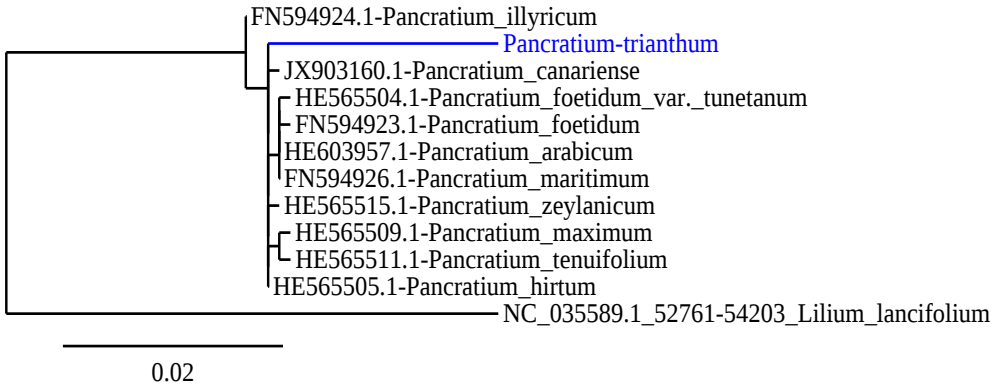

Figure 1 Phylogenetic analysis by maximum likelihood of ribulose-bisphosphate carboxylase gene (rbcL) DNA sequences from *P. trianthum* (blue) collected in Senegal.
Reference sequences are identified by GenBank accession number. *rbcL* sequence from *Lilium lancifolum*, an Asparagales belonging to Liliaceae but not Amaryllidaceae family was used as outgroup. The scale of branch length = 0.02 (2% of genetic variation is shown in the bottom of the tree).

Phytochemical analysis

Next, an acid-base extraction method was performed on bulbs of *P. trianthum* to extract alkaloids from other organic compounds based on their acid-base properties. The phytochemical properties of the alkaloid extracts were then analysed using chromatographic methods. TLC screening revealed with Dragendorff reagent showed the presence of different alkaloids with distinct R_f values 0.6, 0.4 and 0.2 (Figure 2A).

Next, an optimized high-performance liquid chromatography (HPLC) with photodiode array (PDA) detector was performed to better characterize alkaloids. Three alkaloid standards (*i.e.*, lycorine, galanthamine and narciclasine) were used. Identification of the alkaloids extracted from bulbs of *P. trianthum* was accomplished by a comparison of the retention time (RT) and absorption spectrum with these standards. Lycorine, galanthamine and narciclasine standards were measured at RT 7.19, 7.61 and 7.94 min, respectively. Peaks of lycorine and narciclasine, or their derivatives were detected in alkaloid extracts, although in some cases the absorption spectra were slightly different between the pure standards and the alkaloid or the derivative present in the crude extract. No peaks of galanthamine could be detected. Interestingly, abundant and unidentified compounds appeared at the retention times of 6.46, 7.48, 8.40, 8.86, 15.45 and 17.6 min (Figure 2B).

AAs were further identified by comparing their GC-MS spectra with those available in NIST 05 Database, and from literature data. Alkaloid extracts were subjected to GC-MS analysis, which resulted in the detection of eight alkaloids of types lycorine (**1** and **2**), crinine (**3**,**4** and **5**) and narciclasine (**6**), together with two unidentified alkaloids (**7** and **8**). Compounds (**2**) and (**6**) showed molecular ions at m/z 249, 248, 190, 163, 123 and 95, and at m/z 223, 193, 164, 138 and 111, respectively, which were not listed in NIST 05 database. However, identical fragmentations were reported in the literature, and corresponded to 11,12-dehydroanhydrolycorine (**2**) and trisphaeridine (**6**) [31]. Hamayne (**5**), also not available in NIST 05 database, showed molecular ions at m/z 287, 258, 242, 186 and 153 and was identified by similarity with the reported AA from *Rhodophiala pratensis* [32], while compound (**4**) displayed molecular ions at m/z 273,

201, 175, 157, 141 and 128, identically to 8-*O*-demethylmaritidine from *Amaryllis belladonna* L.[33].

The relative proportion of AAs was determined as a percentage of total ion current (TIC). The major compounds were hamayne (**5**, 39.126% of TIC), 8-*O*-Demethylmaritidine (**4**, 15.386% of TIC) and unidentified compound **8** (16.435% of TIC). Approximately 58% of identified alkaloids were crinine-type, 14% of lycorine-type and 5% of the narciclasine-type (Table 1 and Figure 2C).

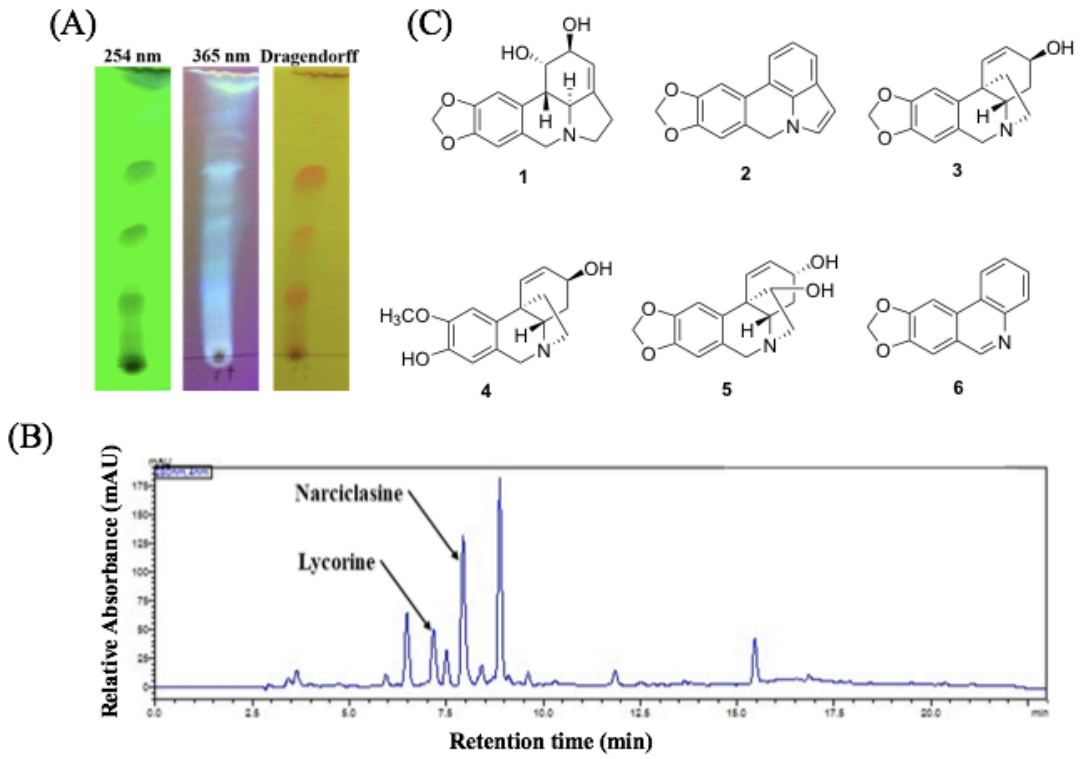

Figure 2 **Phytochemical analysis of *P. trianthum* alkaloid extract.**
(A) TLC revealed by UV at 254, 365 nm and Dragendorff. (B) HPLC-DAD chromatogram of *P. trianthum* alkaloid extract at 280 nm using lycorine, narciclasine and galanthamine as standards. Peaks corresponding to Lycorine and Narciclasine at retention time 7.19 and 7.94 min are indicated with arrows. (C) Structure of identified AAs by GC-MS. **1:** Lycorine, **2:** 11,12-Dehydroanhydrolycorine, **3:** Vittatine, **4:** 8-*O*-Demethylmaritidine, **5:** Hamayne, **6:** Trisphaeridine.

Table 1. Alkaloids identified by GC-MS in *P. trianthum* bulb extract. Values are expressed as percentages of total ion current (TIC) for the relative quantitative (PT).

Alkaloid	[M$^+$]	B.P.	R.T. (min)	PT (%)	Identification
Lycorine (**1**)	287	226	25.902	5.909	NIST 05 Database
11,12-Dehydroanhydrolycorine (**2**)	249	248	23.811	9.062	[31]
Vittatine (**3**)	271	271	21.886	3.828	NIST 05 Database
8-*O*-Demethylmaritidine (**4**)	273	273	22.275	15.386	[33]
Hamayne (**5**)	287	258	25.321	39.126	[32]
Trisphaeridine (**6**)	223	223	19.022	5.032	[31]
Unidentified (**7**)	287	223	23.547	5.221	n/a
Unidentified (**8**)	279	278	27.682	16.435	n/a

BP: base peak, RT: retention time (in minute), PT: *P. trianthum*, n/a: not applicable.

In vitro anti-AChE activity

P. trianthum extracts are used in folk medicine to treat central nervous system disorder, thus we tested the anti-AChE activity of our extract. Galanthamine was used at a concentration of 10 µM as a positive control, and extract dilutions-matching DMSO concentrations were used as negative controls. Galanthamine blocked 59% of acetylcholinesterase activity, whereas DMSO treatment had no apparent effect on the enzyme activity. Alkaloid extract dilutions inhibited the activity of AChE in a dose dependent manner at concentrations ranging from 3.9 to 500 µg/mL, with IC_{50} of 94 µg/mL (Figure 3).

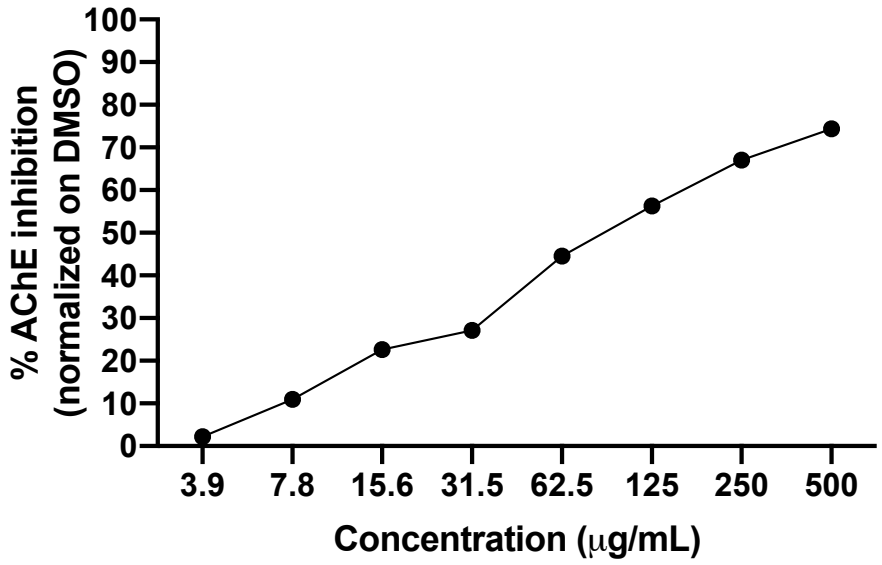

Figure 3 Anti-acetylcholinesterase activity of AAs bulb extracts from *Pancratium trianthum.*

Cytotoxicity activity

Pancratium species are toxic plants with anti-cancer properties and the AA lycorine detected in *P. trianthum* is notoriously cytotoxic. The cytotoxic activity of *P. trianthum* alkaloid extract was determined in THP-1 and Huh7 cell lines and half cytotoxic concentration (CC_{50}) was also calculated for each cell line. Cell viability measured with Cell-Titer GLO was strongly affected by alkaloid extract in a dose dependent manner at concentrations ranging from 0.02 to 2.5 μg/mL for both cell lines, with CC_{50} values 0.23 and 0.45 μg/mL, respectively for THP-1 and Huh7 cells (Figure 4). Alkaloid extract were cytotoxic until 0.078 μg/mL concentration in THP-1 and 0.156 μg/mL in Huh7.

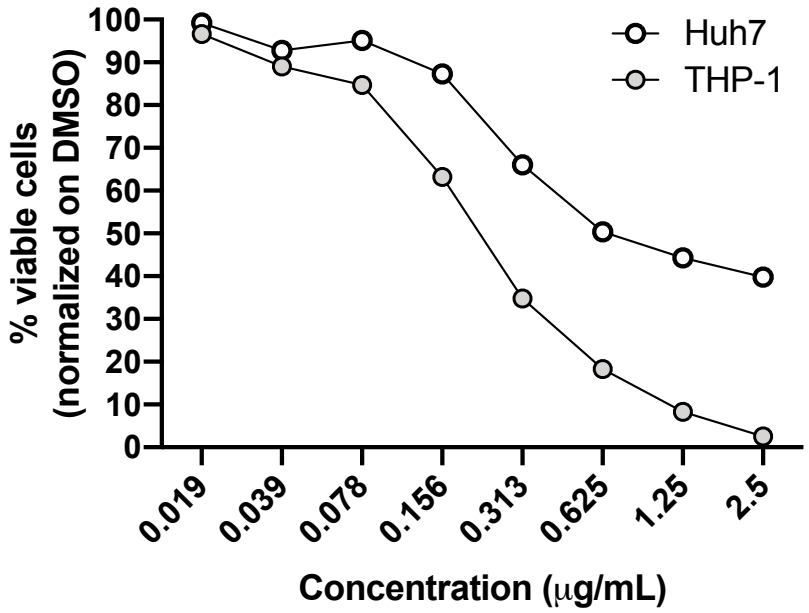

Figure 4 Cytotoxic activity of alkaloid extracts of *P. trianthum.*
The level of cellular ATP was measured in Huh7 and THP-1 cells to assess viability following 72 hours of incubation.

Antibacterial activity

P. trianthum extracts are used in folk medicine to treat wounds, irritation, oedema, dermatosis and as anti-septic. Agar diffusion assay was used to test *P. trianthum* alkaloid extract antibacterial effect. MICs were determined on different bacterial strains. Inhibition zones and MICs obtained are summarized in Table 2 and inhibition effects are shown in Figure 5. The highest antibacterial activity was observed against *S. aureus* with a 20 mm inhibition zone at 16 mg/mL of extract. Microdilution results confirmed that alkaloid extract was active against Gram-positive strain (*S. aureus*), and also against Gram-negative strains (*E. coli* and *P. aeruginosa*), albeit at lower levels, with MIC values ranging from 1 to 2 mg/mL, respectively (Table 2). Thus, alkaloid extract of *P. trianthum* holds anti-bacterial properties.

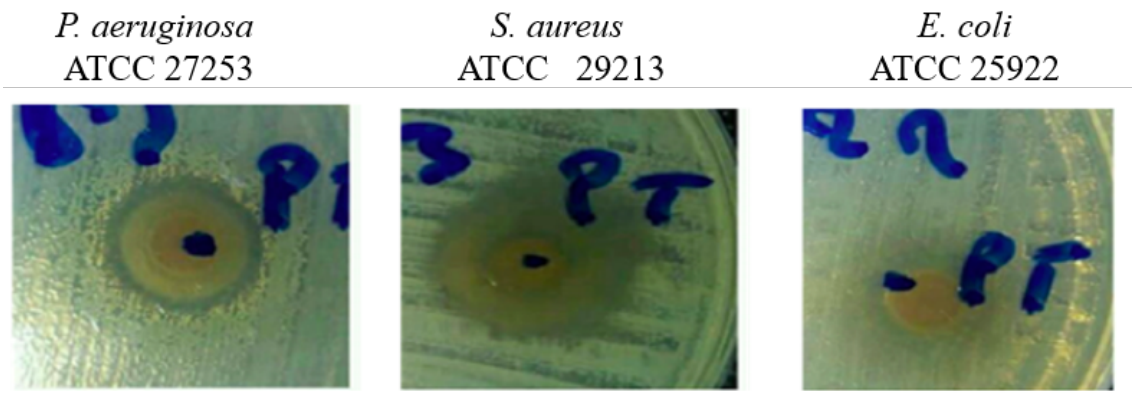

Figure 5 **Inhibition of growth of *Pseudomonas aeruginosa*, *Staphylococcus aureus* and *Escherichia coli* by the alkaloid extracts of *P. trianthum*.**
Inhibition zones surrounding wells containing 16 mg/mL were observed after 18-24 h incubation at 37 °C.

Table 2. Antibacterial activity of the alkaloid extract from the bulb of *P. trianthum* measured on the growth of *P. aeruginosa*, *S. aureus*, and *E. coli* using minimum inhibitory concentration (MIC) and inhibition zone following incubation at 37 °C for 18-24 h.

	P. aeruginosa	*S. aureus*	*E. coli*
Inhibition zone (mm)	16	20	15
MIC (mg/mL)	2	1	2

Antiviral activity

The antiviral activity of alkaloid extract of *P. trianthum* was measured specifically against the dengue flavivirus in Huh7 cells. Adenosine analog NITD008 was used as a positive control at 5 µM, whereas matching DMSO concentrations were used as negative controls for each dilution. Fluorescent infected cells were visualized on an inverted microscope and their frequency was measured on a flow cytometer. NITD008 blocked completely viral replication at the concentration used, whereas DMSO treatment had no apparent effect on viral replication. All tested concentrations ranging from 0.019 to 2.5 µg/mL significantly inhibited $DENV_{GFP}$ infection in a dose dependent manner (Figure 6A, B**)**. Infected cells could not be detected in presence of alkaloid extracts at concentration higher than 0.078 µg/mL with the microscope. Flow cytometry analysis showed that at the lowest concentration of extracts (0.019 µg/mL), there was already a 20% reduction of DENV

infectivity compared to controls. It also confirmed that DENV replication was nearly completely blocked at 0.078 µg/mL with only 3.3% of cells infected. These results further support that alkaloids extract of *P. trianthum* remained active at all non-cytotoxic concentration with a strikingly low EC_{50} of 0.029 µg/mL **(**Figure 6B**)**.

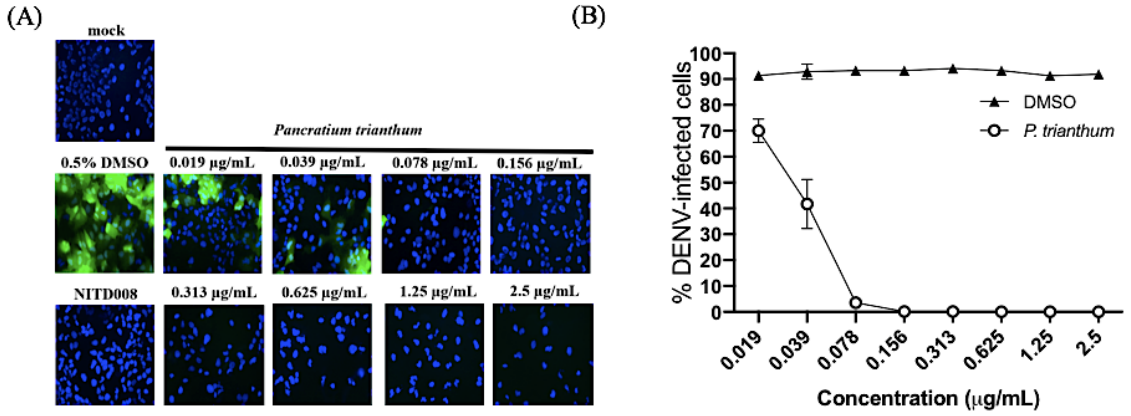

Figure 6 Anti-Dengue virus activity of *P. trianthum* alkaloid extracts. (A) Inhibition of $DENV_{GFP}$ infection in Huh7 cells pretreated with *P. trianthum* alkaloid extracts was observed by inverted microscopy. Representative images are shown with cell nuclei stained with Hoechst33342 (blue) and DENV-infected cells (green). (B) Inhibition of the % of $DENV_{GFP}$ infected Huh7 cells by increasing concentration of *P. trianthum* alkaloid extracts, as measured by flow cytometry.

Pro-inflammatory activity

Proinflammatory activity was assessed to investigate if interferon (IFN) activation was responsible for the antiviral effects *P. trianthum* alkaloid extract. IFN stimulation was measured in LL171 cell lines expressing the interferon stimulated response element (ISRE)-Luciferase reporter. DMXAA, a STING (stimulator of interferon genes) activator, was used as positive control, whereas DMSO was used as negative control. All tested concentrations ranging from 0.0625 to 0.5 µg/mL of alkaloid extract were unable to activate luciferase expression, and hence IFN induction was not the mechanism responsible for the antiviral effect of *P. trianthum* extract (Supplementary file 2).

Discussion

In this study, alkaloid contents of bulbs of *P. trianthum* collected in Senegalese flora were investigated for their biological properties. TLC analysis of the crude extract showed different types of AAs, while HPLC analysis detected lycorine and narciclasine or their derivatives. and of additional peaks suggesting that other AAs were present. In contradiction to a previous report, no galanthamine was detected [18, 19]. Alkaloid extract was subjected to GC-MS analysis, which resulted in the identification of lycorine (**1**) and vittatine (**3**) by comparison with their mass spectra available in NIST05 data base and of 11,12-dehydroanhydrolycorine (**2**), 8-*O*-demethylmaritidine (**4**), hamayne (**5**) and trisphaeridine (**6**) by comparing their mass spectra with those available in the literature. Hence, the narciclasine peak observed during HPLC analysis was indeed the narciclasine derivative trisphaeridine (**6**). We still could not detect galanthamine, consistently with the HPLC analysis. Its production could be affected by environmental and climatic conditions. Transcriptomic analysis will assess if the genes responsible for galanthamine bisoynthesis are expressed. Using the percentage of TIC as relative quantification, we show that crinine- and lycorine-type AAs are the most abundant AAs in *P. trianthum* bulb extract. Unidentified compounds represented approximately 21% of the crude extracts and will be isolated in future studies using chromatography technics.

In Senegal, leaves and bulbs of *P. trianthum* are used to treat central nervous system disorder, heal wound, and soothe irritations [11], suggesting potential anti-AChE, antibacterial and antiviral activity. In this work, we evaluated the properties of alkaloid extract from bulbs of *P. trianthum*. The AChE inhibitory activity is attributed mainly galanthamine and to the lycorine-types among the AAs [34, 35]. Hamayne (**5**) detected in the extract was also previously reported to have weak AChE inhibitory activity, [36]. In our study, alkaloid extract inhibited AChE activity in a dose dependent manner with concentrations ranging from 3.9 to 500 µg/mL. Although the observed inhibition is lower than what was observed in *Pancratium maritimum* [37, 38], it is consistent with the lack of detection of galanthamine-type AAs in our extract.

Alkaloid extract was highly cytotoxic from 0.156 µg/mL for hepatocarcinoma Huh7 cells and from 0.078 µg/mL for monocytic leukemia THP-1 cells. *P. trianthum* bulb alkaloid extract appeared to be more cytotoxic than reported for other *Pancratium* species such as *Pancratium Illyricum* L., although different cell lines were used [39]. Previous studies showed that lycorine (**1**), the main phenanthridine AA displayed a strong antitumor activity [40, 41], suggesting that the presence of this alkaloid in the crude extract contributes to the observed cytotoxicity.

Next, antibacterial assays using agar diffusion showed that, all strains were sensitive to the alkaloid extract. The Gram+ cocci *S. aureus* was more strongly inhibited than Gram-negative strains (*E. coli* and *P. aeruginosa*). These results are consistent with those of the microdilution assay with MIC values 1 mg/mL for *S. aureus* and 2 mg/mL for *E. coli* and *P. aeruginosa*. *Pancratium illyricum* alkaloid extract was described to be completely ineffective against both Gram-positive and Gram-negative bacteria [39], but we used higher concentrations. Previously it was demonstrated that crinine and lycorine-types AAs, exhibited antibacterial properties [42-44]. Thus, identified vittatine (**3**) and lycorine (**1**) might contribute to the antimicrobial effect of the alkaloid extract.

Several flaviviruses cocirculate in tropical and subtropical areas of the world and threaten the life of hundreds of millions of people, the development of broad spectrum anti-flaviviruses compounds is necessary. Several Amaryllidaceae possess antiviral activities but the antiviral effect of alkaloid extract of *P. trianthum* against dengue virus has not been previously investigated. In this study, we demonstrate that alkaloid extracts of *P. trianthum* block dengue virus infection. As the alkaloid extract is highly cytotoxic at concentrations above 0.313 µg/mL, the antiviral activity observed at these concentrations may be confounded by cell death. However, concentrations ranging from 0.019 to 0.078 µg/mL were not cytotoxic, and still displayed strong antiviral activity. Interestingly, this antiviral activity may be specific to dengue virus or flaviviruses infection, as the extracts did not display any IFN-inducing activity. Although some plant extracts have been studied for their anti-dengue potential, this is the first report on crude alkaloid extract of Amaryllidaceae against dengue virus [45]. Previous study showed that lycorine (**1**) potently inhibits flaviviruses in *in vitro* and *in vivo* models [46-48]. This suggests that

lycorine (**1**) and its derivatives in the crude extracts contribute to the observed antiviral activity. Purification of alkaloids from *P. trianthum* could potentially lead to the discovery of strong antiviral compounds.

Conclusions

In conclusion, this study has led the detection of eight AAs with six known identified by GC-MS in the alkaloid extracts of *P. trianthum* collected in Senegalese flora. Based on the traditional use of the *Pancratium* genus for wound-healing, central nervous system disorder, anticancer and antiviral, the alkaloid extract was screened for antibacterial, anti-AChE, cytotoxic and anti-flaviviral properties. Alkaloid extract displayed significant anti-AChE (IC_{50} = 94 µg/mL) and weak antibacterial with MIC values 1 mg/mL for *S. aureus* and 2 mg/mL for *E. coli* and *P. aeruginosa*. Interestingly, the alkaloid extracts also displayed strong antiviral activity against $DENV_{GFP}$ with an EC_{50} of 0.029 µg/mL. We conclude that the medicinal properties of *P. trianthum* may be attributed to its alkaloids content and provide the scientific basis for its traditional use to prevent infection and treat central nervous system disorder. Finally, this study supports the role of Amaryllidaceae species as a source compounds with potential therapeutical application.

Acknowledgments

The authors would like to thank Fatma Meddeb, Manel Ghribi and Karima Landelouci and all the lab members for their technical support and useful advices, Professors Hugo Germain, Céline Van Themsche, Carlos Reyes-Moreno, Geneviève Pepin, and Lionel Berthoux for kindly providing cells and cell cultures equipment. The authors wish to acknowledge Aïcha Aïssatou Sow and Laurent Chatel-Chaix for sharing $DENV_{GFP}$ vectors, and Sebastien Santini (CNRS/AMU IGS UMR7256) and the PACA Bioinfo platform (supported by IBISA) for the availability and management of the phylogeny.fr website used to confirm plant species. This work was funded by the Canada Research Chair on plant specialized metabolism Award No 950-232164 to I.D-P. Thanks are extended to the Canadian taxpayers and to the Canadian government for supporting the Canada Research Chairs Program.

References

1. Jin, Z.; Yao, G., Amaryllidaceae and Sceletium alkaloids. *Natural Product Reports* **2019**.

2. Nair, J. J.; Bastida, J.; Codina, C.; Viladomat, F.; van Staden, J., Alkaloids of the South African Amaryllidaceae: a review. *Natural product communications* **2013,** *8* (9), 1934578X1300800938.

3. Meerow, A.; Snijman, D., Amaryllidaceae. In *Flowering plants·monocotyledons*, Springer: 1998; pp 83-110.

4. Cheesman, L.; Nair, J. J.; van Staden, J., Antibacterial activity of crinane alkaloids from Boophone disticha (Amaryllidaceae). *Journal of Ethnopharmacology* **2012,** *140* (2), 405-8.

5. Kornienko, A.; Evidente, A., Chemistry, biology, and medicinal potential of narciclasine and its congeners. *Chemical Reviews* **2008,** *108* (6), 1982-2014.

6. Berkov, S.; Codina, C.; Viladomat, F.; Bastida, J., N-Alkylated galanthamine derivatives: Potent acetylcholinesterase inhibitors from Leucojum aestivum. *Bioorganic & Medicinal Chemistry Letters* **2008,** *18* (7), 2263-6.

7. Kerharo, J.; Adam, J.-G., La pharmacopée sénégalaise traditionnelle : plantes médicinales et toxiques. **1974**.

8. Kerharo, J.; Bouquet, A., Plantes médicinales et toxiques de la Côte d'Ivoire-Haute-Volta : mission d'étude de la pharmacopée indigène en AOF. **1950**.

9. Sanaa, A.; Boulila, A.; Bejaoui, A.; Boussaid, M.; Fadhel, N. B., Variation of the chemical composition of floral volatiles in the endangered Tunisian Pancratium maritimum L. populations (Amaryllidaceae). *Industrial Crops and Products* **2012,** *40*, 312-7.

10. Ioset, J.-R.; Marston, A.; Gupta, M. P.; Hostettmann, K., A methylflavan with free radical scavenging properties from Pancratium littorale. *Fitoterapia* **2001,** *72* (1), 35-9.

11. Ba, D. Le pancraium trianthum. http://seyilaabe-htkm.blogspot.com/2015/10/ (accessed 25 Novembre 2020).

12. Schultes E. R., *Atlas des Plantes hallucinogènes du monde*. Harward ed.; 1973.

13. Monteil, V., Contribution à l'étude de la flore du Sahara occidental II. Institut des Hautes Etudes Marocaines. *Notes et Documents VI Edit Larose* **1953**.

14. Heinrich, M., Galanthamine from Galanthus and other Amaryllidaceae–chemistry and biology based on traditional use. In *The Alkaloids: Chemistry and Biology*, Elsevier: 2010; Vol. 68, pp 157-65.

15. Berkov, S.; Osorio, E.; Viladomat, F.; Bastida, J., Chemodiversity, chemotaxonomy and chemoecology of Amaryllidaceae alkaloids. In *The Alkaloids: Chemistry and Biology*, Elsevier: 2020; Vol. 83, pp 113-85.

16. Cao, Z.; Yang, P.; Zhou, Q., Multiple biological functions and pharmacological effects of lycorine. *Science China Chemistry* **2013,** *56* (10), 1382-91.

17. Cedrón, J. C.; Del Arco-Aguilar, M.; Estévez-Braun, A.; Ravelo, Á. G., Chemistry and biology of Pancratium alkaloids. In *The Alkaloids: Chemistry and Biology*, Elsevier: 2010; Vol. 68, pp 1-37.

18. Frederik, D. M.; Murav'eva, D., Alkaloid composition of Pancratium trianthum. *Chemistry of Natural Compounds* **1983**.

19. lanata Tuss, A., CHAPTER! OCCURRENCE OF ALKALOIDS IN PLANT SPECIES. *Chemistry of Natural Compounds* **1996,** *32* (1).

20. De Castro, O.; Brullo, S.; Colombo, P.; Jury, S.; De Luca, P.; Di Maio, A., Phylogenetic and biogeographical inferences for Pancratium (Amaryllidaceae), with an emphasis on the Mediterranean species based on plastid sequence data. *Botanical Journal of the Linnean Society* **2012,** *170* (1), 12-28.

21. de Andrade, J. P.; Guo, Y.; Font-Bardia, M.; Calvet, T.; Dutilh, J.; Viladomat, F.; Codina, C.; Nair, J. J.; Zuanazzi, J. A. S.; Bastida, J., Crinine-type alkaloids from Hippeastrum aulicum and H. calyptratum. *Phytochemistry* **2014,** *103*, 188-95.

22. Sasidharan, S.; Chen, Y.; Saravanan, D.; Sundram, K.; Latha, L. Y., Extraction, isolation and characterization of bioactive compounds from plants' extracts. *African Journal of Traditional, Complementary and Alternative Medicines* **2011,** *8* (1).

23. Singh, A.; Desgagné-Penix, I., Transcriptome and metabolome profiling of Narcissus pseudonarcissus 'King Alfred'reveal components of Amaryllidaceae alkaloid metabolism. *Scientific Reports* **2017,** *7* (1), 1-14.

24. Tallini, L. R.; Torras-Claveria, L.; Borges, W. D. S.; Kaiser, M.; Viladomat, F.; Zuanazzi, J. A. S.; Bastida, J., N-oxide alkaloids from Crinum amabile (Amaryllidaceae). *Molecules* **2018,** *23* (6), 1277.

25. Ka, S.; Masi, M.; Merindol, N.; Di Lecce, R.; Plourde, M. B.; Seck, M.; Górecki, M.; Pescitelli, G.; Desgagne-Penix, I.; Evidente, A., Gigantelline, gigantellinine and gigancrinine, cherylline- and crinine-type alkaloids isolated from Crinum jagus with anti-acetylcholinesterase activity. *Phytochemistry* **2020,** *175*, 112390.

26. Uzé, G.; Di Marco, S.; Mouchel-Vielh, E.; Monneron, D.; Bandu, M.-T.; Horisberger, M. A.; Dorques, A.; Lutfalla, G.; Mogensen, K. E., Domains of interaction between alpha interferon and its receptor components. *Journal of molecular biology* **1994,** *243* (2), 245-57.

27. Fischl, W.; Bartenschlager, R., High-throughput screening using dengue virus reporter genomes. In *Antiviral Methods and Protocols*, Springer: 2013; pp 205-19.

28. Shawky, E., Phytochemical and biological Investigation of Clivia nobilis flowers Cultivated in Egypt. *Iranian journal of pharmaceutical research: IJPR* **2016,** *15* (3), 531.

29. Balouiri, M.; Sadiki, M.; Ibnsouda, S. K., Methods for in vitro evaluating antimicrobial activity: A review. *Journal of pharmaceutical analysis* **2016,** *6* (2), 71-9.

30. Dereeper, A.; Guignon, V.; Blanc, G.; Audic, S.; Buffet, S.; Chevenet, F.; Dufayard, J.-F.; Guindon, S.; Lefort, V.; Lescot, M., Phylogeny. fr: robust phylogenetic analysis for the non-specialist. *Nucleic acids research* **2008,** *36* (suppl_2), W465-W9.

31. Al Shammari, L.; Al Mamun, A.; Koutová, D.; Majorošová, M.; Hulcová, D.; Šafratová, M.; Breiterová, K.; Maříková, J.; Havelek, R.; Cahlíková, L., Alkaloid profiling of Hippeastrum cultivars by GC-MS, isolation of Amaryllidaceae alkaloids and evaluation of their cytotoxicity. *Rec Nat Prod* **2020,** *14*, 154-9.

32. Trujillo-Chacón, L. M.; Pastene-Navarrete, E. R.; Bustamante, L.; Baeza, M.; Alarcón-Enos, J. E.; Cespedes-Acuña, C. L., In vitro micropropagation and alkaloids analysis by GC–MS of Chilean Amaryllidaceae plants: Rhodophiala pratensis. *Phytochemical Analysis* **2020,** *31* (1), 46-56.

33. Tallini, L. R.; Andrade, J. P. d.; Kaiser, M.; Viladomat, F.; Nair, J. J.; Zuanazzi, J. A. S.; Bastida, J., Alkaloid constituents of the Amaryllidaceae plant Amaryllis belladonna L. *Molecules* **2017,** *22* (9), 1437.

34. López, S.; Bastida, J.; Viladomat, F.; Codina, C., Acetylcholinesterase inhibitory activity of some Amaryllidaceae alkaloids and Narcissus extracts. *Life Sciences* **2002,** *71* (21), 2521-9.

35. Houghton, P. J.; Ren, Y.; Howes, M.-J., Acetylcholinesterase inhibitors from plants and fungi. *Natural Product Reports* **2006,** *23* (2), 181-99.

36. Houghton, P. J.; Agbedahunsi, J. M.; Adegbulugbe, A., Choline esterase inhibitory properties of alkaloids from two Nigerian Crinum species. *Phytochemistry* **2004,** *65* (21), 2893-6.

37. Orhan, I.; Sener, B., Bioactivity-directed fractionation of alkaloids from some Amaryllidaceae plants and their anticholinesterase activity. *Chemistry of Natural Compounds* **2003,** *39* (4), 383-6.

38. Soltan, M. M.; Hamed, A. R.; Hetta, M. H.; Hussein, A. A., Egyptian Pancratium maritimum L. flowers as a source of anti-Alzheimer's agents. *Bulletin of Faculty of Pharmacy, Cairo University* **2015,** *53* (1), 19-22.

39. Bonvicini, F.; Antognoni, F.; Iannello, C.; Maxia, A.; Poli, F.; Gentilomi, G. A., Relevant and selective activity of Pancratium illyricum L. against Candida albicans clinical isolates: a combined effect on yeast growth and virulence. *BMC complementary and alternative medicine* **2014,** *14* (1), 1-8.

40. Lamoral-Theys, D.; Andolfi, A.; Van Goietsenoven, G.; Cimmino, A.; Le Calvé, B.; Wauthoz, N.; Mégalizzi, V.; Gras, T.; Bruyère, C.; Dubois, J., Lycorine, the main phenanthridine Amaryllidaceae alkaloid, exhibits significant antitumor activity in cancer cells that display resistance to proapoptotic stimuli: an investigation of structure− activity relationship and mechanistic insight. *Journal of medicinal chemistry* **2009,** *52* (20), 6244-56.

41. Lamoral-Theys, D.; Decaestecker, C.; Mathieu, V.; Dubois, J.; Kornienko, A.; Kiss, R.; Evidente, A.; Pottier, L., Lycorine and its derivatives for anticancer drug design. *Mini reviews in medicinal chemistry* **2010,** *10* (1), 41-50.

42. Adesanya, S.; Olugbade, T.; Odebiyl, O.; Aladesanmi, J., Antibacterial alkaloids in Crinum jagus. *International Journal of Pharmacognosy* **1992,** *30* (4), 303-7.

43. Tan, C.-X.; Schrader, K. K.; Mizuno, C. S.; Rimando, A. M., Activity of lycorine analogues against the fish bacterial pathogen Flavobacterium columnare. *Journal of agricultural and food chemistry* **2011,** *59* (11), 5977-85.

44. Evidente, A.; Andolfi, A.; Abou-Donia, A. H.; Touema, S. M.; Hammoda, H. M.; Shawky, E.; Motta, A., (−)-Amarbellisine, a lycorine-type alkaloid from Amaryllis belladonna L. growing in Egypt. *Phytochemistry* **2004,** *65* (14), 2113-8.

45. Abd Kadir, S. L.; Yaakob, H.; Zulkifli, R. M., Potential anti-dengue medicinal plants: a review. *Journal of natural medicines* **2013,** *67* (4), 677-89.

46. Wang, P.; Li, L. F.; Wang, Q. Y.; Shang, L. Q.; Shi, P. Y.; Yin, Z., Anti-dengue-virus activity and structure–activity relationship studies of lycorine derivatives. *ChemMedChem* **2014,** *9* (7), 1522-33.

47. Chen, H.; Lao, Z.; Xu, J.; Li, Z.; Long, H.; Li, D.; Lin, L.; Liu, X.; Yu, L.; Liu, W., Antiviral activity of lycorine against Zika virus in vivo and in vitro. *J Virol* **2020**.

48. Zou, G.; Puig-Basagoiti, F.; Zhang, B.; Qing, M.; Chen, L.; Pankiewicz, K. W.; Felczak, K.; Yuan, Z.; Shi, P.-Y., A single-amino acid substitution in West Nile virus 2K peptide between NS4A and NS4B confers resistance to lycorine, a flavivirus inhibitor. *Virology* **2009,** *384* (1), 242-52.

Supplementary Materials

Supplementary file 1: sequences used for phylogeny analysis

>*Pancratium-trianthum*

GNNNTCGGCNCATTGAGGCCGTTGTTGGGGAGAAATCAATATATTGCTTATG
TAGCTTATCCTTTAGACCNTTTTGAAGAAGGTTCTGTTACTAACATGTTTACT
TCCATTGTGGGTAATGTATTTGGTTTCAAAGCCCTACGAGCTCTACGTCTGG
AGGATCTGCGAATTCCCCCTGCTTATTCCAAAACTTTCCAAGGCCCGCCCCA
TGGCATCCAATCTGAAAGAGATAAATTGAACAAGTATGGTCGTCCCCTATTG
GGATGTACTATTAAACCAAAATTGGGATTATCCGCAAAAAACTACGGTAGA
GCGGTTTATGAATGTCTACGCGGTGGGCTTGATTTTACCAAGGATGACGAAA
ACGTGAACTCCCAACCTTTTATGCGTTGGAGAGACCGTTTCTTATTTTGTGCT
GAAGCAATTTATAAAGCGCAAGCCGAAACAGGTGAAATCAAAGGACATTAC
TTGAATGCAACTGCGGGTACATGTGAAGAAATGATCAAAAGGGCCGTATTT
GCCAGAGAATTGGGAGTTCCTATCGTAATGCATGACTACTTAACTGGGGGAT
TCACTGCAAATACTAGTTTGGCTTTTTATTGCCGCGACAACGGTCTACTTCTT
CACATCCACCGCGCAATGCATGCAGTTATTGATAGACAGAAAAATCATGGT
ATGCATTTTCGTGTACTAGCTAAAGCATTACGTATGTCTGGTGGAGATCATA
TTCACGCTGGTACAGTGTAAGGTAAACTGGAAGGAAGAGATGACTTTAGGT
TTTGTTGATTTATTACGTGATGATTATATTGAAAAAGACCGAAGTCGTGGTA
TTTTTTTCACTCAAGATTGGGTTTCTATGCCAGGTGATCTGCGTATTGCCTAT
GGGGGTATTCATGTTTGGCATATGCCGCCCTACGGAATCTTTGGGATGATTC
CGTACTACAGTTCGGTGGAGGAACTTNAGGACACCCTTGGGGAAATGCNCC
TGGTGCGTAGCTAATCGGGTAGCTTAGAAGCGATATAGANCC

>HE565505.1-*Pancratium hirtum*

CATTGAGGCCGTTGTTGGGGAAGAAAATCAATATATTGCTTATGTAGCTTAT
CCTTTAGACCTTTTTGAAGAAGGTTCTGTTACTAACATGTTTACTTCCATTGT
GGGTAATGTATTTGGTTTCAAAGCCCTACGAGCTCTACGTCTGGAGGATCTG
CGAATTCCCCCTGCTTATTCCAAAACTTTCCAAGGCCCGCCCCATGGCATCC

AATCTGAAAGAGATAAATTGAACAAGTATGGTCGTCCCCTATTGGGATGTAC
TATTAAACCAAAATTGGGATTATCCGCAAAAAACTACGGTAGAGCGGTTTAT
GAATGTCTACGCGGTGGGCTTGATTTTACCAAGGATGACGAAAACGTGAACT
CCCAACCTTTTATGCGTTGGAGAGACCGTTTCTTATTTTGTGCTGAAGCAATT
TATAAAGCGCAAGCCGAAACAGGTGAAATCAAAGGACATTACTTGAATGCA
ACTGCGGGTACATGTGAAGAAATGATCAAAAGGGCCGTATTTGCCAGAGAA
TTGGGAGTTCCTATCGTAATGCATGACTACTTAACTGGGGGATTCACTGCAA
ATACTAGTTTGGCTTTTTATTGCCGCGACAACGGTCTACTTCTTCACATCCAC
CGCGCATGCATGCAGTTATTGATAGACAGAAAAATCATGGTATGCATTTTCG
TGTACTAGCTAAAGCATTACGTATGTCTGGTGGAGATCATATTCACGCTGGT
ACAGTAGTAGGTAAACTGGAAGGGGAACGTGAGATGACTTTAGGTTTTGTT
GATTTATTACGTGATGATTTTATTGAAAAAGACCGAAGTCGCGGTATTTTTTT
CACTCAAGATTGGGTTTCTATGCCAGGTGTTATTCCCGTAGCTTCCGGGGGT
ATTCATGTTTGGCATATGCCCGCCCTAACCGAAATCTTTGGAGATGATTCCG
TACTACAGTTCGGTGGAGGAACTTTAGGACACCCTTGGGGAAATGCACCTGG
TGCGGTAGCTAATCGGGTAGCTTTAGAAG

>JX903160.1-*Pancratium canariense*

CATTGAGGCCGTTGTTGGGGAAGAAAATCAATATATTGCTTATGTAGCTTAT
CCTTTAGACCTTTTTGAAGAAGGTTCTGTTACTAACATGTTTACTTCCATTGT
GGGTAATGTATTTGGTTTCAAAGCCCTACGAGCTCTACGTCTGGAGGATCTG
CGAATTCCCCCTGCTTATTCCAAAACTTTCCAAGGCCCGCCCCATGGCATCC
AATCTGAAAGAGATAAATTGAACAAGTATGGTCGTCCCCTATTGGGATGTAC
TATTAAACCAAAATTGGGATTATCCGCAAAAAACTACGGTAGAGCGGTTTAT
GAATGTCTACGCGGTGGGCTTGATTTTACCAAGGATGACGAAAACGTGAACT
CCCAACCTTTTATGCGTTGGAGAGACCGTTTCTTATTTTGTGCTGAAGCACTT
TATAAAGCGCAAGCCGAAACAGGTGAAATCAAAGGACATTACTTGAATGCA
ACTGCGGGTACATGTGAAGAAATGATCAAAAGGGCCGTATTTGCCAGAGAA
TTGGGAGTTCCTATCGTAATGCATGACTACTTAACTGGGGGATTCACTGCAA
ATACTAGTTTGGCTTTTTATTGCCGCGACAACGGTCTACTTCTTCACATCCAC

CGCGCAATGCATGCAGTTATTGATAGACAGAAAAATCATGGTATGCATTTTC
GTGTACTAGCTAAAGCATTACGTATGTCTGGTGGAGATCATATTCACGCTGG
TACAGTAGTAGGTAAACTGGAAGGGGAACGTGAGATGACTTTAGGTTTTGTT
GATTTATTACGTGATGATTTTATTGAAAAAGACCGAAGTCGCGGTATTTTTTT
CACTCAAGATTGGGTTTCTATGCCAGGTGTTATTCCCGTAGCTTCCGGGGGT
ATTCATGTTTGGCATATGCCCGCCCTAACCGAAATCTTTGGAGATGATTCCG
TACTACAGTTCGGTGGAGGAACTTTAGGACACCCTTGGGGAAATGCACCTGG
TGCGGTAGCTAATCGGGTAGCTTTAGAAGCG

>HE603957.1-*Pancratium arabicum*

CATTGAGGCCGTTGTTGGGGAAGAAAATCAATATATTGCTTATGTAGCTTAT
CTTTAGACCTTTTTGAAGAAGGTTCTGTTACTAACATGTTTACTTCCATTGTG
GGTAATGTATTTGGTTTCAAAGCCCTACGAGCTCTACGTCTGGAGGATCTGC
GAATTCCCCCTGCTTATTCCAAAACTTTCCAAGGCCCGCCCCATGGCATCCA
ATCTGAAAGAGATAAATTGAACAAGTATGGTCGTCCCCTATTGGGATGTACT
ATTAAACCAAAATTGGGATTATCCGCAAAAAACTACGGTAGAGCGGTTTAT
GAATGTCTACGCGGTGGGCTTGATTTTACCAAGGATGACGAAAACGTGAACT
CCCAACCTTTTATGCGTTGGAGAGACCGTTTCTTATTTTGTGCTGAAGCAATT
TATAAAGCGCAAGCCGAAACAGGTGAAATCAAAGGACATTACTTGAATGCA
ACTGCGGGTACATGTGAAGAAATGATCAAAAGGGCCGTATTTGCCAGAGAA
TTGGGAGTTCCTATCGTAATGCATGACTACTTAACTGGGGGATTCACTGCAA
ATACTAGTTTGGCTTTTTATTGCCGCGACAACGGTCTACTTCTTCACATCCAC
CGCGCAATGCATGCAGTTATTGATAGACAGAAAAATCATGGTATGCATTTTC
GTGTACTAGCTAAAGCATTACGTATGTCTGGTGGAGATCATATTCACGCTGG
TACAGTAGTAGGTAAACTGGAAGGGGAACGTGAGATGACTTTAGGTTTTGTT
GATTTATTACGTGATGATTTTATTGAAAAAGACCGAAGTCGCGGTATTTTTTT
CACTCAAGATTGGGTTTCTATGCCAGGTGTTATTCCCGTAGCTTCCGGGGGT
ATTCATGTTTGGCATATGCCCGCCCTAACCGAAATCTTTGGAGATGATTCCG
TACTACAGTTCGGTGGAGGAACTATAGGACACCCTTGGGGAAATGCACCTG
GTGCGGTAGCTAATCGGGTAGCTTTAGAAG

>HE565515.1-*Pancratium zeylanicum*

CATTGAGGCCGTTGTTGGGGAAGAAAATCAATATATTGCTTATGTAGCTTAT
CCTTTAGACCTTTTTGAAGAAGGTTCTGTTACTAACATGTTTACTTCCATTGT
GGGTAATGTATTTGGTTTCAAAGCCCTACGAGCTCTACGTCTGGAGGATCTG
CGAATTCCCCCTGCTTATTCCAAAACTTTCCAAGGCCCGCCCCATGGCATCC
AATCTGAAAGAGATAAATTGAACAAGTATGGTCGTCCCCTATTGGGATGTAC
TATTAAACCAAAATTGGGATTATCCGCAAAAAACTACGGTAGAGCGGTTTAT
GAATGTCTACGCGGTGGGCTTGATTTTACCAAGGATGACGAAAACGTGAACT
CCCAACCTTTTATGCGTTGGAGAGACCGTTTCTTATTTTGTGCTGAAGCAATT
TATAAAGCGCAAGCCGAAACAGGTGAAATCAAAGGACATTACTTGAATGCA
ACTGCGGGTACATGTGAAGAAATGATCAAAAGGGCCGTATTTGCCAGAGAA
TTGGGAGCTCCTATCGTAATGCATGACTACTTAACTGGGGGATTCACTGCAA
ATACTAGTTTGGCTTTTTATTGCCGCGACAACGGTCTACTTCTTCACATCCAC
CGCGCAATGCATGCAGTTATTGATAGACAGAAAAATCATGGTATGCATTTTC
GTGTACTAGCTAAAGCATTACGTATGTCTGGTGGAGATCATATTCACGCTGG
TACAGTAGTAGGTAAACTGGAAGGGGAACGTGAGATGACTTTAGGTTTTGTT
GATTTATTACGTGATGATTTTATTGAAAAAGACCGAAGTCGCGGTATTTTTTT
CACTCAAGATTGGGTTTCTATGCCAGGTGTTATTCCCGTAGCTTCCGGGGGT
ATTCATGTTTGGCATATGCCCGCCCTAACCGAAATCTTTGGAGATGATTCCG
TACTACAGTTCGGTGGAGGAACTTTAGGACACCCTTGGGGAAATGCACCTGG
TGCGGTAGCTAATCGGGTAGCTTTAGAAG

>FN594926.1-*Pancratium maritimum*

CATTGAGGCCGTTGTTGGGGAAGAAAATCAATATATTGCTTATGTAGCTTAT
CCTTTAGACCTTTTTGAAGAAGGTTCTGTTACTAACATGTTTACTTCCATTGT
GGGTAATGTATTTGGTTTCAAAGCCCTACGAGCTCTACGTCTGGAGGATCTG
CGAATTCCCCCTGCTTATTCCAAAACTTTCCAAGGCCCGCCCCATGGCATCC
AATCTGAAAGAGATAAATTGAACAAGTATGGTCGTCCCCTATTGGGATGTAC
TATTAAACCAAAATTGGGATTATCCGCAAAAAACTACGGTAGAGCGGTTTAT
GAATGTCTACGCGGTGGGCTTGATTTTACCAAGGATGACGAAAACGTGAACT

CCCAACCTTTTATGCGTTGGAGAGACCGTTTCTTATTTTGTGCTGAAGCAATT
TATAAAGCGCAAGCCGAAACAGGTGAAATCAAAGGACATTACTTGAATGCA
ACTGCGGGTACATGTGAAGAAATGATCAAAAGGGCCGTATTTGCCAGAGAA
TTGGGAGTTCCTATCGTAATGCATGACTACTTAACTGGGGGATTCACTGCAA
ATACTAGTTTGGCTTTTTATTGCCGCGACAACGGTCTACTTCTTCACATCCAC
CGCGCAATGCATGCAGTTATTGATAGACAGAAAAATCATGGTATGCATTTTC
GTGTACTAGCTAAAGCATTACGTATGTCTGGTGGAGATCATATTCACGCTGG
TACAGTAGTAGGTAAACTGGAAGGGGAACGTGAGATGACTTTAGGTTTTGTT
GATTTATTACGTGATGATTTTATTGAAAAAGACCGAAGTCGCGGTATTTTTTT
CACTCAAGATTGGGTTTCTATGCCAGGTGTTATTCCCGTAGCTTCCGGGGGT
ATTCATGTTTGGCATATGCCCGCCCTAACCGAAATCTTTGGAGATGATTCCG
TACTACAGTTCGGTGGAGGAACTATAGGACACCCTTGGGGAAATGCACCTG
GTGCGGTAGCTAATCGGGTAGCTTTAGAAG

>HE565511.1-*Pancratium tenuifolium*

CATTGAGGCCGTTGTTGGGGAAGAAAATCAATATATTGCTTATGTAGCTTAT
CCTTTAGACCTTTTTGAAGAAGGTTCTGTTACTAACATGTTTACTTCCATTGT
GGGTAATGTATTTGGTTTCAAAGCCCTACGAGCTCTACGTCTGGAGGATCTG
CGAATTCCCCCTGCTTATTCCAAAACTTTCCAAGGCCCGCCCCATGGCATTC
AATCTGAAAGAGATAAATTGAACAAGTATGGTCGTCCCCTATTGGGATGTAC
TATTAAGCCAAAATTGGGATTATCCGCAAAAAACTACGGTAGAGCGGTTTAT
GAATGTCTACGCGGTGGGCTTGATTTTACCAAGGATGACGAAAACGTGAACT
CCCAACCTTTTATGCGTTGGAGAGACCGTTTCTTATTTTGTGCTGAAGCAATT
TATAAAGCGCAAGCCGAAACAGGTGAAATCAAAGGACATTACTTGAATGCA
ACTGCGGGTACATGTGAAGAAATGATCAAAAGGGCCGTATTTGCCAGAGAA
TTGGGAGTTCCTATCGTAATGCATGACTACTTAACTGGGGGATTCACTGCAA
ATACTAGTTTGGCTTTTTATTGCCGCGACAACGGTCTACTTCTTCACATCCAC
CGCGCAATGCATGCAGTTATTGATAGACAGAAAAATCATGGTATGCATTTTC
GTGTACTAGCTAAAGCATTACGTATGTCTGGTGGAGATCATATTCACGCTGG
TACAGTAGTAGGTAAACTGGAAGGGGAACGTGAGATGACTTTAGGTTTTGTT
GATTTATTACGTGATGATTTTATTGAAAAAGACCGAAGTCGCGGTATTTTTTT

CACTCAAGATTGGGTTTCTATGCCAGGTGTTATTCCCGTAGCTTCCGGGGGT
ATTCATGTTTGGCATATGCCCGCCCTAACCGAAATCTTTGGAGATGATTCCG
TACTACAGTTCGGTGGAGGAACTTTAGGACACCCTTGGGGAAATGCACCTGG
TGCGGTAGCTAATCGGGTAGCTTTAGAAG

>HE565509.1-*Pancratium maximum*

CATTGAGGCCGTTGTTGGGGAAGAAAATCAATATATTGCTTATGTAGCTTAT
CCTTTAGACCTTTTTGAAGAAGGTTCTGTTACTAACATGTTTACTTCCATTGT
GGGTAATGTATTTGGTTTCAAAGCCCTACGAGCTCTACGTCTGGAGGATCTG
CGAATTCCCCCTGCTTATTCCAAAACTTTCCAAGGCCCGCCCCATGGCATCC
AATCTGAAAGAGATAAATTGAACAAGTATGGTCGTCCCCTATTGGGATGTAC
TATTAAGCCAAAATTGGGATTATCCGCAAAAAACTACGGTAGAGCGGTTTAT
GAATGTCTACGCGGTGGGCTTGATTTTACCAAGGATGACGAAAACGTGAACT
CCCAACCTTTTATGCGTTGGAGAGACCGTTTCTTATTTTGTGCTGAAGCAATT
TATAAAGCGCAAGCCGAAACAGGTGAAATCAAAGGACATTACTTGAATGCA
ACTGCGGGTACATGTGAAGAAATGATCAAAAGGGCCGTATTTGCCAGAGAA
TTGGGAGTTCCTATCGTAATGCATGACTACTTAACTGGGGGATTCACTGCAA
ATACTAGTTTGGCTTTTTATTGCCGCGACAACGGTCTACTTCTTCACATCCAC
CGCGCAATGCATGCAGTTATTGATAGACAGAAAAATCATGGTATGCATTTTC
GTGTACTAGCTAAAGCATTACGTATGTCTGGCGGAGATCATATTCACGCTGG
TACAGTAGTAGGTAAACTGGAAGGGGAACGTGAGATGACTTTAGGTTTTGTT
GATTTATTACGTGATGATTTTATTGAAAAAGACCGAAGTCGCGGTATTTTTTT
CACTCAAGATTGGGTTTCTATGCCAGGTGTTATTCCCGTAGCTTCCGGGGGT
ATTCATGTTTGGCATATGCCCGCCCTAACCGAAATCTTTGGAGATGATTCCG
TACTACAGTTCGGTGGAGGAACTTTAGGACACCCTTGGGGAAATGCACCTGG
TGCGGTAGCTAATCGGGTAGCTTTAGAAG

>HE565504.1-*Pancratium foetidum* var. *tunetanum*

CATTGAGGCCGTTGTTGGGGAAGAAAATCAATATATTGCTTATGTAGCTTAT
CCTTTAGACCTTTTTGAAGAAGGTTCTGTTACTAACATGTTTACTTCCATTGT

GGGTAATGTATTTGGTTTCAAAGCCCTACGAGCTCTACGTCTGGAGGATCTG
CGAATTCCCCCTGCTTATTCCAAAACTTTCCAAGGCCCGCCCCATGGCATCC
AATCTGAAAGAGATAAATTGAACAAGTATGGTCGTCCCCTATTGGGATGTAC
TATTAAACCAAAATTGGGATTATCCGCAAAAAACTACGGTAGAGCGGTTTAT
GAATGTCTACGCGGTGGGCTTGATTTTACCAAGGATGACGAAAACGTGAACT
CCCAACCTTTTATGCGTTGGAGAGACCGTTTCTTATTTTGTGCTGAAGCAATT
TATAAAGCGCAAGCCGAAACAGGTGAAATCAAAGGACATTACTTGAATGCA
ACTGCGGGTACATGTGAAGAAATGATCAAAAGGGCCGTATTTGCCAGAGAA
TTGGGAGTTCCTATTGTAATGCATGACTACTTAACTGGGGGATTCACTGCAA
ATACTAGTTTGGCTTTTTATTGCCGCGACAACGGTCTACTTCTTCACATCCAC
CGCGCAATGCATGCAGTTATTGATAGACAGAAAAATCATGGTATGCATTTTC
GTGTACTAGCTAAAGCATTACGTATGTCTGGTGGAGATCATATTCACGCTGG
TACAGTAGTAGGTAAACTGGAAGGGGAACGTGAGATGACTTTAGGTTTTGTT
GATTTATTACGTGATGATTTTATTGAAAAAGACCGAAGTCGCGGTATTTTTTT
CACTCAAGATTGGGTTTCTATGCCAGGTGTTATTCCCGTAGCTTCCGGGGGT
ATTCATGTTTGGCATATGCCCGCCCTAACCGAAATCTTTGGAGATGATTCCG
TACTACAGTTCGGTGGAGGAACTATAGGACACCCTTGGGGAAATGCACCTG
GTGCGGTAGCTAATCGGGTAGCTTTAGAAG

>FN594924.1-*Pancratium illyricum*

CATTGAGGCCGTTGTTGGGGAAGAAAATCAATATATTGCTTATGTAGCTTAT
CCTTTAGACCTTTTTGAAGAAGGTTCTGTTACTAACATGTTTACTTCCATTGT
GGGTAATGTATTTGGTTTCAAAGCCCTACGAGCTCTACGTCTGGAGGATCTG
CGAATTCCCCCTGCTTATTCCAAAACTTTCCAAGGCCCGCCCCATGGCATCC
AATCTGAAAGAGATAAATTGAACAAGTATGGTCGTCCCCTATTGGGATGTAC
TATTAAACCAAAATTGGGATTATCCGCAAAAAACTACGGTAGAGCGGTTTAT
GAATGTCTACGCGGTGGGCTTGATTTTACCAAGGATGACGAAAACGTGAACT
CCCAACCTTTTATGCGTTGGAGAGACCGTTTCTTATTTTGTGCTGAAGCAATT
TATAAAGCGCAAGCCGAAACAGGTGAAATCAAAGGACATTACTTGAATGCA
ACTGCGGGTACATGTGAAGAAATGATCAAAAGGGCCGTATTTGCCAGAGAA
TTGGGAGTTCCTATCGTAATGCATGACTACTTAACCGGGGGATTCACTGCAA

ATACTAGTTTGGCTTATTATTGCCGCGACAACGGTCTACTTCTTCACATCCAC
CGCGCAATGCATGCAGTTATTGATAGACAGAAAAATCATGGTATGCATTTTC
GTGTACTAGCTAAAGCATTACGTATGTCTGGTGGAGATCATATTCACGCTGG
TACAGTAGTAGGTAAACTGGAAGGGGAACGTGAGATGACTTTAGGTTTTGTT
GATTTATTACGTGATGATTTTATTGAAAAAGACCGAAGTCGCGGTATTTTTTT
CACTCAAGATTGGGTTTCTATGCCAGGTGTTATTCCCGTAGCTTCCGGGGGT
ATTCATGTTTGGCATATGCCCGCCCTAACCGAAATCTTTGGAGATGATTCCG
TACTACAGTTCGGTGGAGGAACTTTAGGACACCCTTGGGGAAATGCACCTGG
TGCGGTAGCTAATCGGGTAGCTTTAGAAG

>FN594923.1-*Pancratium foetidum*

CATTGAGGCCGTTGTTGGGGAAGAAAATCAATATATTGCTTATGTAGCTTAT
CCTTTAGACCTTTTTGAAGAAGGTTCTGTTACTAACATGTTTACTTCCATTGT
GGGTAATGTATTTGGTTTCAAAGCCCTACGAGCTCTACGTCTGGAGGATCTG
CGAATTCCCCCTGCTTATTCCAAAACTTTCCAAGGCCCGCCCCATGGCATCC
AATCTGAAAGAGATAAATTGAACAAGTATGGTCGTCCTCTATTGGGATGTAC
TATTAAACCAAAATTGGGATTATCCGCAAAAAACTACGGTAGAGCGGTTTAT
GAATGTCTACGCGGTGGGCTTGATTTTACCAAGGATGACGAAAACGTGAACT
CCCAACCTTTTATGCGTTGGAGAGACCGTTTCTTATTTTGTGCTGAAGCAATT
TATAAAGCGCAAGCCGAAACAGGTGAAATCAAAGGACATTACTTGAATGCA
ACTGCGGGTACATGTGAAGAAATGATCAAAAGGGCCGTATTTGCCAGAGAA
TTGGGAGTTCCTATCGTAATGCATGACTACTTAACTGGGGGATTCACTGCAA
ATACTAGTTTGGCTTTTTATTGCCGCGACAACGGTCTACTTCTTCACATCCAC
CGCGCAATGCATGCAGTTATTGATAGACAGAAAAATCATGGTATGCATTTTC
GTGTACTAGCTAAAGCATTACGTATGTCTGGTGGAGATCATATTCACGCTGG
TACAGTAGTAGGTAAACTGGAAGGGGAACGTGAGATGACTTTAGGTTTTGTT
GATTTATTACGTGATGATTTTATTGAAAAAGACCGAAGTCGCGGTATTTTTTT
CACTCAAGATTGGGTTTCTATGCCAGGTGTTATTCCCGTAGCTTCCGGGGGT
ATTCATGTTTGGCATATGCCCGCCCTAACCGAAATCTTTGGAGATGATTCCG
TACTACAGTTCGGTGGAGGAACTATAGGACACCCTTGGGGAAATGCACCTG
GTGCGGTAGCTAATCGGGTAGCTTTAGAAG

>NC_035589.1:52761-54203 *Lilium lancifolium*

ATGTCACCACAAACAGAGACTAAAGCAAGTGTTGGATTCAAAGCTGGTGTT
AAAGATTACAAATTGACTTATTATACTCCTGACTATGAAACCAAAGATACTG
ATATTTTGGCAGCATTCCGAGTAACTCCTCAACCCGGAGTTCCACCTGAAGA
GGCAGGGGCAGCGGTAGCCGCCGAATCTTCCACTGGTACATGGACAACTGT
GTGGACTGATGGACTTACCAGTCTTGATCGTTACAAAGGGCGATGCTACCAC
ATCGAGAGCGTTGTTGGGGAGGAAAATCAATATATTGCTTATGTAGCTTATC
CTTTAGACCTTTTTGAAGAAGGTTCTGTTACTAACATGTTCACTTCCATTGTG
GGTAATGTATTTGGTTTCAAAGCCCTACGAGCTCTACGTCTGGAGGATCTGC
GAATTCCTACTTCTTATTCCAAAACTTTTCAAGGCCCGCCTCATGGCATCCAA
GTTGAAAGGGATAAATTGAACAAGTATGGTCGTCCCCTATTAGGATGTACCA
TTAAACCAAAATTGGGATTATCTGCAAAGAACTATGGTAGAGCGGTTTATGA
ATGTCTGCGCGGTGGACTTGATTTTACCAAGGATGATGAAAACGTGAACTCA
CAACCATTTATGCGTTGGAGAGACCGTTTCTTATTTTGTGCCGAAGCACTTTA
TAAAGCGCAAGCCGAAACGGGTGAAATCAAAGGACATTACTTGAATGCTAC
TGCGGGTACATGTGAAGAAATGATAAAAAGGGCCGTATTTGCTAGAGAATT
GGGAGTTCCTATCGTAATGCATGACTACTTAACGGGGGGATTCACTGCAAAT
ACTAGCTTGGCTCATTATTGCCGAGACAACGGCCTACTTCTTCACATTCATCG
TGCAATGCATGCAGTTATTGATAGACAGAAAAATCATGGTATGCATTTTCGC
GTACTAGCTAAAGCATTACGTATGTCCGGTGGCGATCATATTCACGCTGGTA
CAGTAGTAGGTAAACTGGAAGGAGAACGCGAGATGACTTTAGGTTTTGTTG
ATTTACTGCGCGATGATTTTATTGAAAAAGACCGAAGTCGTGGTATTTTTTTC
ACTCAAGATTGGGTCTCTATGCCAGGTGTTCTGCCCGTGGCTTCGGGGGGTA
TTCATGTTTGGCATATGCCTGCTCTAACCGAAATCTTTGGGGATGATTCTGTA
CTACAGTTCGGTGGAGGAACTTTAGGGCACCCTTGGGGAAATGCACCTGGTG
CAGTAGCTAATCGAGTGGCTTTAGAAGCGTGTGTACAAGCTCGTAATGAAG
GGCGTGATCTTGCTCGTGAGGGTAATGAAATTATCCGTGAAGCTTGCAAATG
GAGTCCTGAACTAGCTGCTGCTTGTGAAGTATGGAAGGCGATCAAATTCGAG
TTCGAACCAGTAGATAAGCTAGATAAAGAGAAGAAATAA

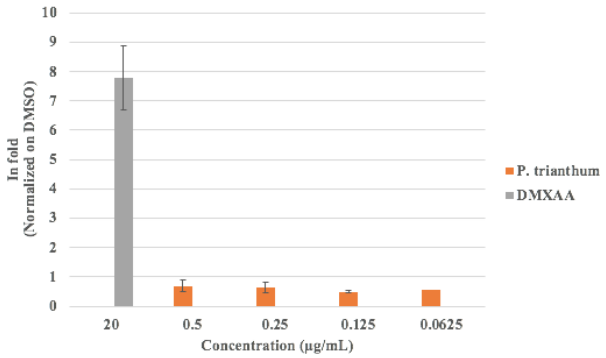

Supplementary file 2: *Pancratium trianthum* alkaloid extract do not trigger the transcription of inferferon-stimulated genes. (A). LL71 cells were treated with concentrations ranging from 0.0625 to 0.5 µg/mL of *P. trianthum* bubs extract. Matched concentrations of DMSO, and 20 µg/mL DMXAA (a STING activator) were used as negative and positive control, respectively. Luciferase expression under the promoter of IFN-sensitive response element (ISRE) was measured by luminescence 24 hours after treatment.

Mass spectrum of the identified alkaloids

Lycorine (**1**)

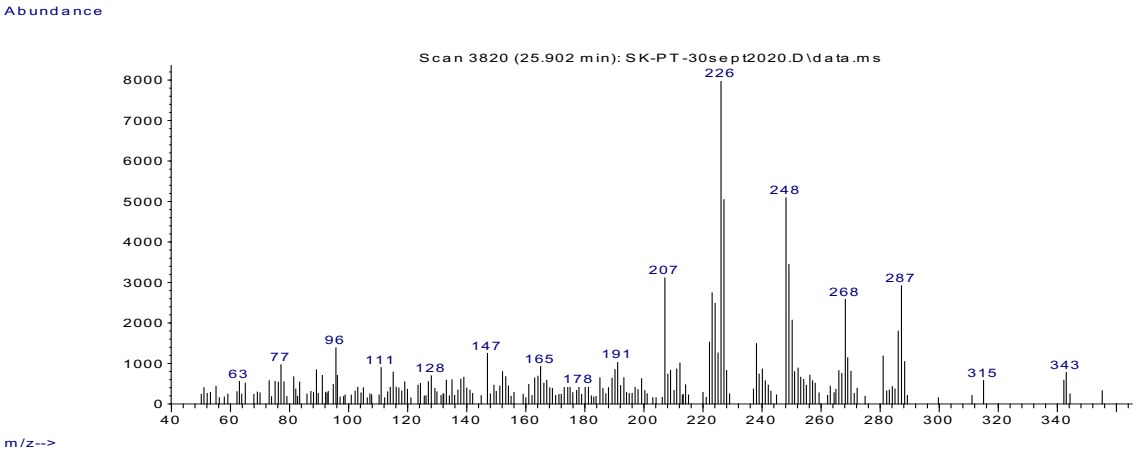

11,12-Dehydroanhydrolycorine (**2**)

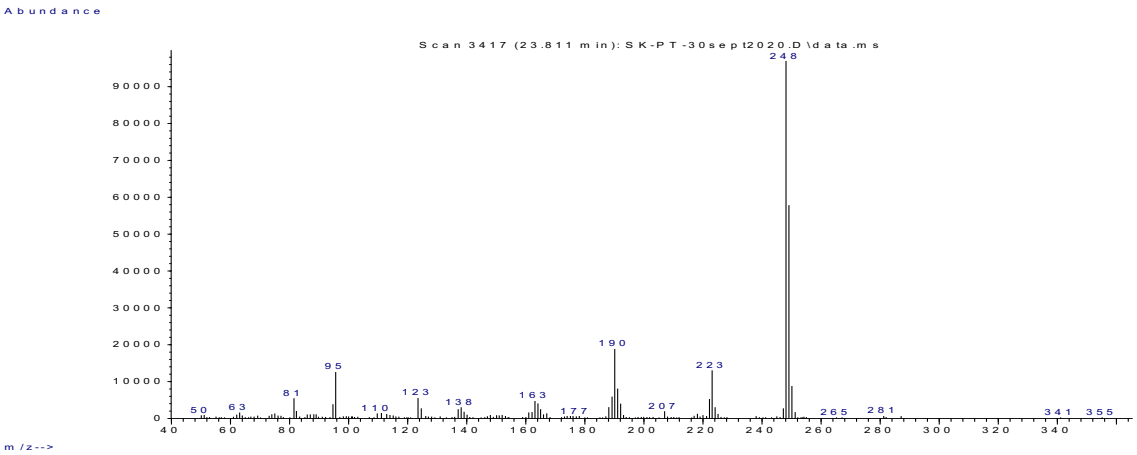

Vittatine (**3**)

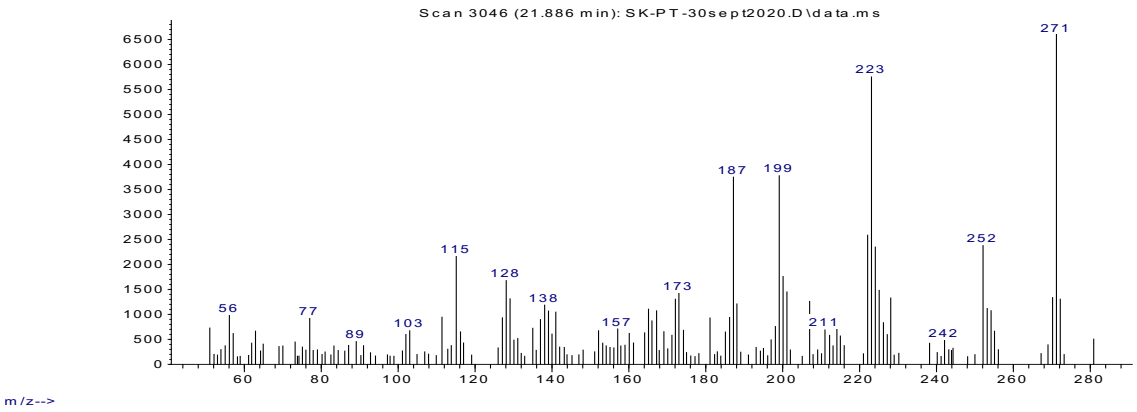

8-*O*-Demethylmaritidine (**4**)

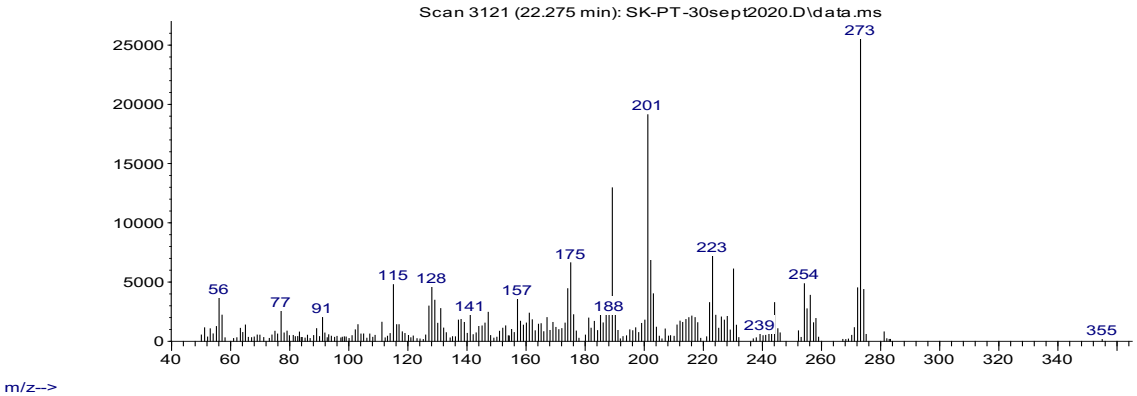

Hamayne (**5**)

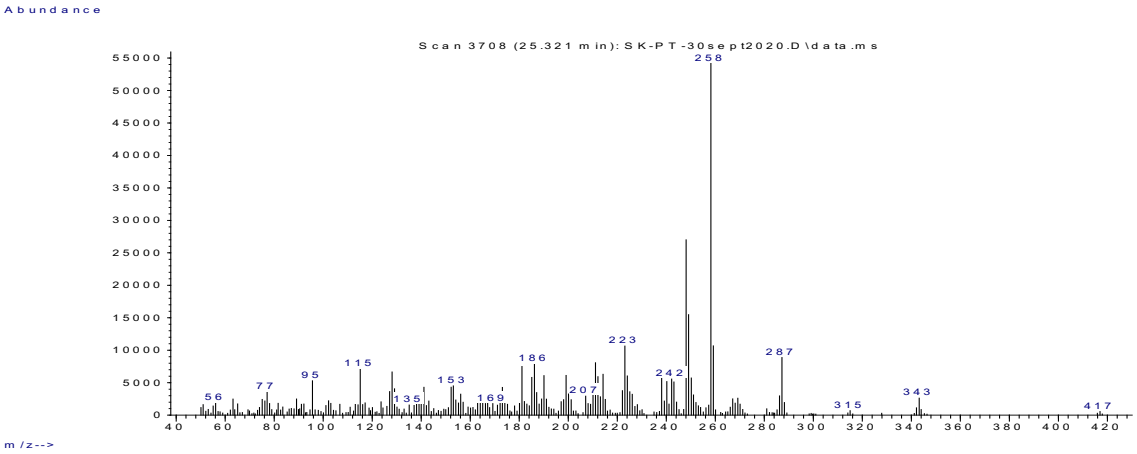

Trisphaeridine (**6**)

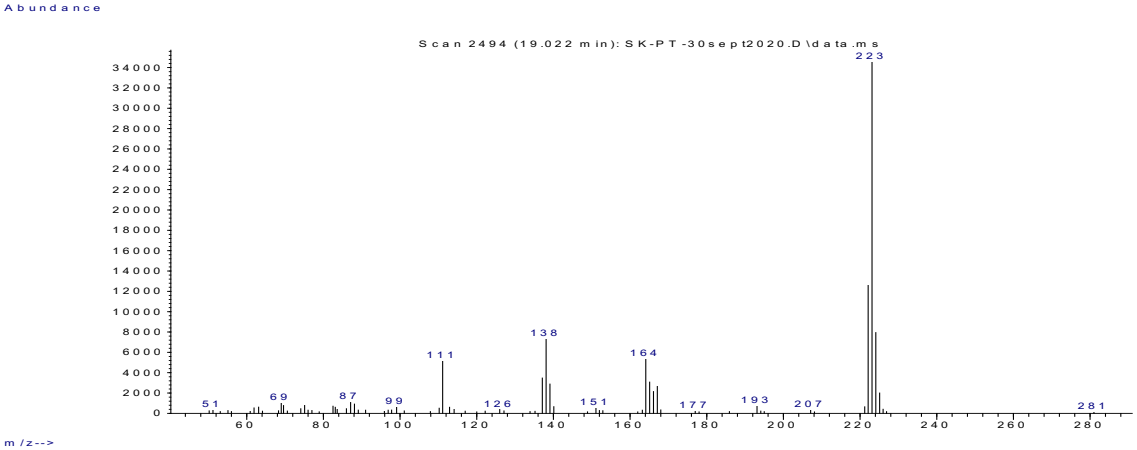

Unidentified **(7)**

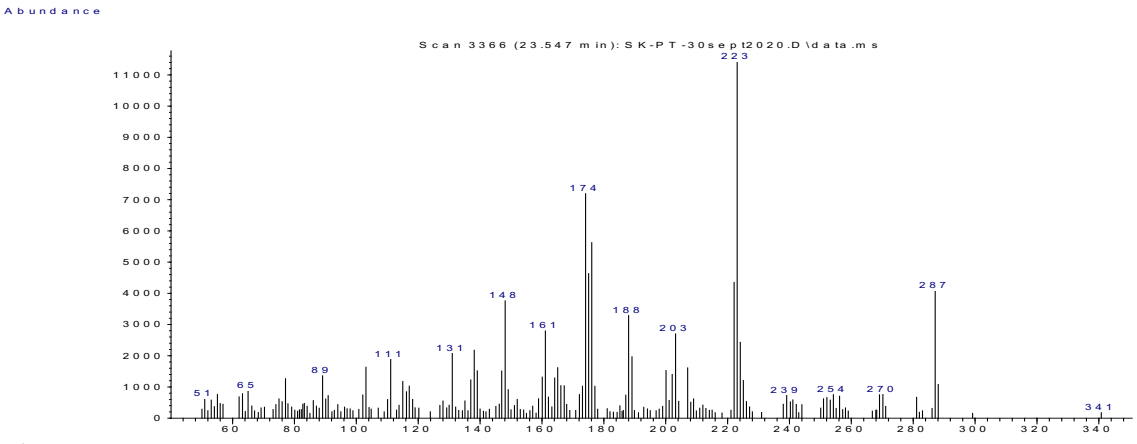

Unidentified **(8)**

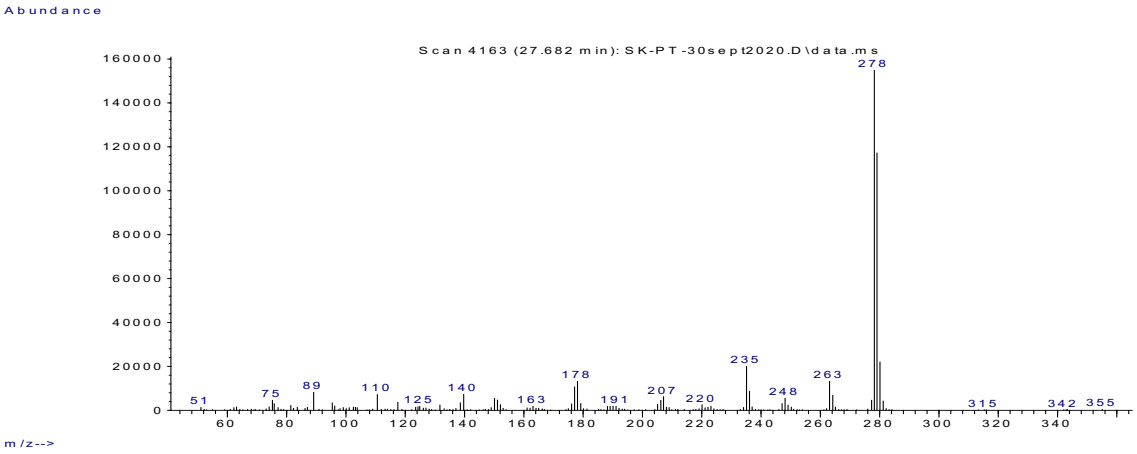

Le chapitre III contient l'isolement des alcaloïdes à partir des bulbes de *Crinum jagus* ainsi que leurs activités anti-AChE et cytotoxiques.

CHAPITRE III

GIGANTELLINE, GIGANTELLININE AND GIGANCRININE, CHERYLLINE AND CRININE-TYPE ALKALOIDS ISOLATED FROM *CRINUM JAGUS* WITH ANTI-ACETYLCHOLINESTERASE ACTIVITY

Seydou Ka, Marco Masi, Natacha Merindol, Roberta Di Lecce,
Mélodie B. Plourde, Matar Seck, Marcin Górecki, Gennaro Pescitelli,
Isabel Desgagne-Penix, Antonio Evidente

Le contenu de ce chapitre a fait l'objet d'une publication en anglais dans la revue *Phytochemistry*, 2020.

3.1 Contribution des auteurs

SK, IDP et MS ont planifié les expériences. SK, RDL, MM et AE ont isolé les AAs et élucidé les structures. MG et GP ont particpé à l'élucidation de l'une des structures. SK, NM, MBP et IDP ont planifié les expériences sur les effets bilogiques des composés isolés. SK, IDP, NM, AE, MM, MG et GP ont écrit et édité le manusrit.

3.2 Résumé de l'article (français)

Trois nouveaux alcaloïdes nommés la gigantelline, la gigantellinine et la gigancrinine ont été isolés à partir du *C. jagus* (syn. = *C. giganteum*) récolté au Sénégal, ainsi que la sanguine, la cherylline, la lycorine, la crinine, la flexinine et le dérivé d'isoquinolinone hippadine qui sont des alcaloïdes d'Amaryllidaceae déjà connus. La gigantelline, la gigantellinine et la gigancrinine ont été caractérisées par des techniques spectroscopiques (1D et 2D, ^{1}H et ^{13}C, RMN et HRESIMS) et chimiques comme étant le 4-(6,7-diméthoxy-2-méthyl-1,2,3,4-tétrahydro isoquinolin-4-yl)-phénol, son dérivé 7-O-déméthyl-5'-hydroxy-4'-méthoxy et 5,6a,7,7a,8a,9-hexahydro-6,9a

éthano[1,3]dioxolo[4,5-j]oxireno[2,3-b]phénanthridine 9-ol respectivement. La configuration relative de chaque alcaloïde a été déterminée par la NOESY et la chimie computationnelle, tandis que les configurations absolues ont été déterminées par des techniques de dichroïsme circulaire. La sanguinine, la cherylline, la crinine, la flexinine et l'isoquinolinone hippadine ont été isolées pour la première fois du *C. jagus*. La cherylline, la gigantellinine, la crinine, la flexinine et la sanguinine ont inhibé l'activité de l'AChE de manière dose-dépendante, et l'inhibition de l'AChE par la sanguinine a été remarquablement efficace (CI_{50} = 1,83 ± 0,01 μM). La cherylline et l'hippadine ont montré une faible cytotoxicité à 100 μM.

3.3 Article complet (anglais): Gigantelline, gigantellinine and gigancrinine, cherylline and crinine-type alkaloids isolated from Crinum jagus with anti-acetylcholinesterase activity

Abstract

Three undescribed Amarylidaceae alkaloids, named gigantelline, gigantellinine and gigancrinine, were isolated from *Crinum jagus* (syn. = *Crinum giganteum*) collected in Senegal, together with the already known sanguinine, cherylline, lycorine, crinine, flexinine and the isoquinolinone derivative hippadine. Gigantelline, gigantellinine and gigancrinine were characterized as 4-(6,7-dimethoxy-2-methyl-1,2,3,4-tetrahydro-isoquinolin-4-yl)-phenol, its 7-*O*-demethyl-5'-hydroxy-4'-methoxy derivative and 5,6a,7,7a,8a,9-hexahydro-6,9a-ethano[1,3]dioxolo[4,5-*j*]oxireno[2,3-*b*]phenanthridin-9-ol, respectively, by using spectroscopic (1D and 2D ^{1}H and ^{13}C NMR and HRESIMS) and chemical methods. Their relative configuration was assigned by NOESY NMR spectra and NMR calculations, while the absolute configuration was assigned using electronic circular dichroism (ECD) experiments and calculations. Sanguinine, cherylline, crinine, flexinine, and the isoquinolinone hippadine, were isolated for the first time from *C. jagus*. Cherylline, gigantellinine, crinine, flexinine and sanguinine inhibited the activity of AChE in a dose-dependent manner, and inhibition by sanguinine was remarkably effective (IC_{50} = 1.83 ± 0.01 mM). Cherylline and hippadine showed weak cytotoxicity at 100 μM.

Keywords: *Crinum jagus*; Amaryllidaceae; Alkaloids; Tetrahydroisoquinoline-type; Acetylcholinesterase; Cytotoxicity; Alzeihmer's disease

Introduction

Plants and microorganisms are an important reservoir of bioactive specialized metabolites. Among them, the plants of the Amaryllidaceae species are a demonstrated rich source of alkaloids and related isocarbostyryl compounds, with a broad spectrum of biological activity [1-3].

Amaryllidaceae plants are found in tropical and subtropical regions of the world, but essentially in Andean South America, in the Mediterranean basin, and in Southern Africa [2]. These bulbous flowering plants, including ca. 1600 species, are classified into about 75 genera [4]. Approximately one third of the known Amaryllidaceae species grow in South Africa [2], and they are largely utilized in folk medicine [5].

The Amaryllidaceae alkaloids (AAs) are grouped into 12 ring types [6]. Many studies have been carried out on AAs since their structures provide a viable platform for phytochemical-based drug discovery [7]. Hundreds of structurally diverse alkaloids have been found [3, 6, 7], and many have shown promising anticancer activity. Among them there are lycorine- and its related isocarbostyryl narciclasine-type, crinine-type, pretazettine-type, and the montanine-type alkaloids [7]. Galanthamine is the most promising for the treatment of the symptoms of Alzheimer's disease and it is currently being used as a cholinesterase inhibitor drug for this disease [8]. Recently, from *Narcissus tazetta* subsp. *tazetta* L., collected in Turkey, lycorine, pseudolycorine, galanthamine and 11-hydroxygalanthamine were isolated [9]. In addition, sarniensine, sarniesinol and crinsarnine, showing significant insecticidal activity against *Aedes aegypti,* the mosquito responsible of yellow and dengue fevers and Zika, were isolated together with several known AAs from *Nerine sarniensis* collected in South Africa [10, 11]. Coccinine, montanine, albomaculine and incartine, belonging to the isoquinoline-, homolycorine- and lycorine-type alkaloids, were isolated from *Haemanthus humilis*, collected in the same country, with only coccinine and montanine exhibiting anticancer activity at low micromolar concentrations [12]. *Crinum buphanoides*, *Crinum graminicola*, *Cyrtanthus mackenii*, *Brunsvigia grandiflora*, native species of South Africa, produced lycorine as the main alkaloid [13].

Continuing our screening on biologically active undescribed alkaloids from native and unstudied Amaryllidaceae from Africa, our interest was focused on *Crinum jagus* (syn. = *Crinum giganteum*) collected in Senegal, belonging to a genus which showed to be very rich in crinine-type alkaloids [14]. The aqueous and organic extracts of this plant were previously investigated in different studies and showed to contain biologically active

metabolites. In fact, these compounds have the potential for the treatment of inflammatory processes [15] and possesses several other important activities such as antibacterial [16], sedative [17], inhibition of cholinesterases [18], antiviral [19] etc. However, only few reports are available on the alkaloids produced by this species [16, 18, 20].

This study reports on the isolation and the chemical and biological characterization of three undescribed alkaloids, named gigantelline, gigantellinine and gigancrinine from *Crinum jagus*, together with five known AAs and the isoquinolinone derivative hippadine. The results of their acetylcholinesterase (AChE) inhibitory and cytotoxic activity on breast cancer cells are also discussed.

Materials and Methods

General experimental procedures

A Perkin-Elmer Spectrum 100 Fourier transform infrared (FTIR) spectrometer was employed to record infrared (IR) spectra on a glassy film. UV spectra were measured in CH_3OH on a JASCO V-530 spectrophotometer. ECD spectra of **1**, **2**, **4**, **5**, **7** and **8** were recorded on a JASCO J-815 spectrometer in CH_3OH (C 0.3). The ECD spectra of **3** were recorded with a JASCO J-715 spectropolarimeter, on CH_3CN solutions and using a quartz cell with 0.01 cm path-length. ECD measurement parameters were the following: scan speed 100 nm/min; time-constant 0.5 s; bandwidth 1 nm; 4 accumulations. ^{1}H and ^{13}C NMR spectra were recorded at 500/125 MHz in CD_3OD on Varian spectrometers. The same solvent was used as internal standard. Carbon multiplicities were determined by DEPT spectra [21] DEPT, COSY-45, HSQC, HMBC, [21] were performed using Varian microprograms. HRESI mass spectra and liquid chromatography (LC)/MS analyses were performed using the LC/MS TOF system AGILENT 6230B, HPLC 1260 Infinity. The HPLC separations were performed with a Phenomenex LUNA (C18 (2) 5u 150×4.6 mm). The ESI MS/MS were recorded on Alliance waters 2695 HPLC-MS/MS QQQ. Analytical and preparative TLC were performed on silica gel (Kieselgel 60, F_{254}, 0.25 and 0.5 mm respectively, Merck) plates. The spots were visualized by exposure to

UV radiation (253), or iodine vapour. Colum chromatography (CC) was performed using silica gel (Kieselgel 60, 0.063-0.200 mm, Merck).

Plant material

Bulbs of *Crinum jagus* (syn. = *Crinum giganteum*) were collected in Senegal, in Montrolland district (14°55'56,22''N and 16°59'38,62''W), in December 2018 (Figure S1). A senior scientist from the Herbarium of IFAN of University Cheikh Anta Diop of Dakar taxonomically identified the plant materials.

Extraction and purification

Fresh bulbs of *C. jagus* were dried at room temperature and then finely powdered. The resultant powder (1.35 kg) was extracted with 1% H_2SO_4, (2 x 2L) overnight at room temperature. The suspension was filtered through cloth and successively centrifuged at 10 °C at 7000 rpm for 30 min. The acid extract was alkalinized to pH 9-10 with 12 N NaOH. The aqueous solution was extracted with EtOAc (3 x 1.2 L), and the organic extracts were combined, dried (Na_2SO_4) and evaporated under reduced pressure to give a brown oil residue (3.0 g). This latter was crystallized by EtOH obtaining lycorine (**6**, 600 mg) as white crystals. The mother liquors of crystallization were dried, and the residue (2.4 g) was fractionated by column chromatography eluted with $CHCl_3$-EtOAc-MeOH (2:2:1), affording eighteen groups of homogeneous fractions (F1-F18). The residue (134.8 mg) of fraction F2 was purified on silica gel chromatography and eluted with $CHCl_3$-*i*-PrOH (95:5), yielding eleven fractions. The residue (10.5 mg) of fraction 2 was further purified on preparative TLC and eluted with $CHCl_3$, yielding hippadine (**9**, 1.6 mg) as an amorphous solid. The residues (90.5 and 128.2 mg) of fractions F7 and F8 were combined and treated with hot EtOH, affording a homogeneous amorphous precipitate which being an undescribed compound, as below reported, was named gigantelline (**1**, 50.7 mg, R_f 0.55 in $CHCl_3$-EtOAc-MeOH (2:2:1)). The supernatant was purified by column chromatography, eluted with $CHCl_3$-CH_3OH (85:15) obtaining, cherylline (**5**, 15.4 mg) and an amorphous solid, which being

undescribed as below reported, was named gigantellinine (**2**, 17.72 mg, R_f 0.43) and further amount of gigantelline (20.8 mg for a total of 71.5 mg). The residue (98.5 mg) of fraction F17 of the initial column was purified on silica gel chromatography and eluted with $CHCl_3$-CH_3OH (8:2), yielding 6 fractions. The residue (27.5 mg) of fraction 2 was further purified by preparative TLC eluted with $CHCl_3$-CH_3OH (85:15), yielding flexinine (**8**, 16.0 mg), as crystals. The residue (230.6 mg) of fraction F18 of the initial column was purified by silica gel column, eluted with EtOAc-CH_3OH-H_2O (75:15:10), yielding 8 fractions. The residue of fraction 6 was an amorphous solid which was identified, as below reported, as crinine (**7**, 42.3 mg). The residue of fraction 8 was identified as sanguinine (**4**, 6.7 mg). The residue (23.9 mg) of fraction 4 was further purified on preparative TLC and eluted with CH_2Cl_2-CH_3OH (75:25), yielding an amorphous solid which being an undescribed compound, as below reported, was named gigancrinine (**3**, 5.5 mg, R_f 0.55).

*Gigantelline (**1**).* $[\alpha]_D^{25}$ +16.3 (c 2.9, CH_3OH); UV λ_{max} nm (log ε) 281 (3.35); IR λ_{max} 3291, 1588, 1512, 1465 cm^{-1}; ^1H and ^{13}C NMR, see Table 1; HR ESIMS (+) *m/z*: 300.1591 $[M + H]^+$ (calculated for $C_{18}H_{22}NO_3$ 300.1600).

*Gigantellinine (**2**).* $[\alpha]_D^{25}$ -39.1 (c 0.8, CH_3OH); UV λ_{max} nm (log ε) 283 (3.64); IR λ_{max} 3390, 1588, 1506, 1462 cm^{-1}; ^1H and ^{13}C NMR, see Table 1; HR ESIMS (+) *m/z*: 316.1539 $[M + H]^+$ (calculated for $C_{18}H_{22}NO_4$ 316.1549).

*Gigancrinine (**3**).* $[\alpha]_D^{25}$ -4.5 (c 0.3, CH_3OH); UV λ_{max} nm (log ε) 294 (2.59); IR λ_{max} 3456, 1505, 1487, 1288 cm^{-1}; ^1H and ^{13}C NMR, see Table 2; HR ESIMS (+) *m/z*: 288.1228 $[M + H]^+$ (calculated for $C_{16}H_{18}NO_4$ 288.1236).

*Sanguinine (**4**).* $[\alpha]_D^{25}$ -100.4 (c 0.6, EtOH) [[22], $[\alpha]_D^{25}$ -133.0 (c 0.2, EtOH)]; ^1H and ^{13}C NMR spectra are identical to those previously reported in [22]; ESIMS (+) *m/z*: 274 $[M + H]^+$.

*Cherylline (**5**)*. $[\alpha]_D^{25}$ -68.4 (c 0.1, CH_3OH) [[23]: $[\alpha]_D^{25}$ -70.6 (c 0.2, CH_3OH)]; ^1H and ^{13}C NMR spectra are identical to those previously reported in [23, 24] as well ECD [25]; ESIMS (+) *m/z*: 286 $[M + H]^+$.

*Lycorine (**6**)*. $[\alpha]_D^{25}$ -72.5 (c 0.1, CH_3OH) [[26]: $[\alpha]_D^{25}$ -71.2 (c 0.1, CH_3OH)]; ^1H and ^{13}C NMR spectra are identical to those previously reported in [27]. ESIMS (+) *m/z*: 288 $[M + H]^+$.

*Crinine (**7**)*. $[\alpha]_D^{25}$ -17.9 (c 0.6, EtOH) [[28]: $[\alpha]_D^{22}$ -9.0 (c 0.6, EtOH)]; ^1H and ^{13}C NMR and specific optical rotation are identical to those previously reported in [28]. ESIMS (+) *m/z*: 272 $[M + H]^+$.

*Flexinine (**8**)*. $[\alpha]_D^{25}$ -12.7 (c 0.1, CH_3OH) [[26]: $[\alpha]_D^{25}$ -12.5 (c 0.1, CH_3OH)]; ^1H and ^{13}C NMR and specific optical rotation are identical to those previously reported in [26]. ESIMS (+) *m/z*: 288 $[M + H]^+$.

*Hippadine (**9**)*. ^1H and ^{13}C NMR are identical to those previously reported in [10, 29]; ESIMS (+) *m/z*: 812 $[3M + Na]^+$, 549 $[2M + Na]^+$, 286 $[M + Na]^+$ and 264 $[M + H]^+$.

4'-O-*Acetylgigantelline (**10**)*. Gigantelline (**1**, 2.0 mg), was acetylated using a common method to obtain the corresponding acetyl derivative **10** as an amorphous solid (1.46 mg). **10** had: UV λ_{max} (log ε) 285 (3.15) nm; IR λ_{max} 1763, 1607, 1512, 1459, 1217 cm^{-1}; ^1H NMR, differed from that of **1** only for the following signals: δ, 7.23 (2H, d, *J* = 8.6 Hz, H-3′ and H-5′), 7.07 (2H, d, *J* = 8.6 Hz, H-2′ and H-6′), 2.29 (3H, s, OAc); ESIMS (+) *m/z*: 342 $[M + H]^+$ and 300 $[M + H - CH_2CO]^+$.

Computational methods

Molecular mechanics, Hartree-Fock (HF) and density functional theory (DFT) calculations were run with Spartan'18 (Wavefunction, Inc., Irvine CA, 2018), with standard parameters and convergence criteria. DFT and time-dependent (TD) DFT

calculations were run with Gaussian16 with default grids and convergence criteria. NMR calculations were run on four isomers of **3** with the configurations (1*R*,2*R*,3*R*,4a*R*,10b*S*), (1*S*,2*R*,3*R*,4a*R*,10b*S*), (1*R*,2*S*,3*S*,4a*R*,10b*S*) and (1*S*,2*S*,3*S*,4a*R*,10b*S*). The conformers obtained by a conformational search run with the Monte Carlo algorithm using Merck molecular force field (MMFF) were geometry-optimized at HF/3-21G level, screened by single-point calculations at ωB97X-D/6-31G(d) level, and geometry-optimized at the same level. Final energies and populations were estimated at the ωB97X-V/6-311+G(2df,2p) level, according to the procedure described by Hehre et al. 2019. The procedure afforded up to 3 energy minima for each isomer. ^{13}C-NMR chemical shifts were then calculated with the GIAO method at ωB97X-D/6-31G(d) level; an empirical correction was applied depending on the number of bonds to the carbon and on the bond lengths [37]. ^{1}H-^{1}H NMR spin-spin coupling constants were calculated at ωB97X-D/pcJ-0 level, including only the Fermi contact (FC) term. ECD calculations were run on the (1*R*,2*R*,3*R*,4a*R*,10b*S*)-**3** isomer. The sets of low-energy minima found as described above were re-optimized at the ωB97X-D/6-311+G(d,p)/PCM level including the IEF-PCM continuum solvent model for acetonitrile. TDDFT calculations were run at the B3LYP/def2-TZVP/PCM and CAM-B3LYP/def2-TZVP/PCM levels, yielding consistent results. They included 32 excited states (roots) in each case. Average ECD spectra were computed by weighting component ECD spectra with Boltzmann factors at 300 K estimated from DFT internal energies and were plotted using the program SpecDis using dipole-length rotational strengths; the difference with dipole-velocity values was negligible in all cases.

Cell culture

The human breast cancer cell line MCF-7 was kindly provided by the Celine Van Themsche and Carlos Reyes-Moreno laboratory's at the Université du Québec in Trois-Rivières (Trois-Rivières, Canada). Cells were grown in complete Dulbecco's modified Eagle medium (DMEM, Wisent) with 10% fetal bovine serum (FBS) and antibiotics (100 µg/mL penicillin and 100 µg/mL streptomycin and plasmocin, (Invivogen

Cedar Lane, Burlington, Ontario, Canada). Cells were maintained in a humidified atmosphere at 37 °C and 5% CO_2.

XTT cell viability assay

Cytotoxicity properties were evaluated using the XTT assay kit (Roche, sigma-aldrich.com). MCF-7 were seeded at $10x10^3$ cells per well in 96-well plates and cultured for 24 h. Then, they were treated with the compounds at concentrations ranging from 0.4 to 400 µM for 72 h. At that time, media was replaced by fresh phenol-free DMEM medium (Wisent) containing 0.3 mg/mL XTT. After 4 hours of incubation, the absorbance was measured at 450 nm using a microplate spectrophotometer (Synergy H1, Biotek, Québec, Canada). Experiments were performed in triplicate. Control assays were performed in the presence of compounds and in the absence of cells, as well as in the presence of cells and in the absence of compounds (with 0.1% DMSO) and were used to assess maximal cytotoxicity. The percentage of cells viability was calculated at each concentration for each compound.

In vitro Acetylcholinesterase (AChE) activity assay

In vitro AChE activity was assessed according to Ellman's colorimetric method, with some modifications using the Acetylcholinesterase Assay Kit (Abcam). Compounds were dissolved in DMSO at 100 mM. Galanthamine hydroxybromide (Tocris Bioscience, Bristol, UK, 2016) dissolved in H_2O at 50 mM was used as standard compound. Samples were diluted in Assay Buffer to a final concentration ranging from 0.001 to 1000 µM. The AChE stock solution was prepared by resuspension in 0.1% bovine serum albumin/double distilled (dd) H_2O at 50 U/mL first and then dissolved in Assay Buffer at 0.25 U/mL, right before the assay. The substrates acetylthiocholine iodide and 5,5'-dithiobis-2-nitrobenzoic acid (DTNB) were dissolved in ddH_2O and assay buffer, respectively. For the enzymatic reaction in 96-well plates, samples (50 µL) were mixed with AChE solution (45 µL) and the reaction was started by the addition of 5 µL of Ellman's mixture (acetylthiocholine and DNTB). Following an incubation of 5 minutes at

room temperature, the absorbance was measured at 412 nm using a microplate spectrophotometer every 2 minutes for 10 min (Synergy H1, Biotek, Québec, Canada). Negative control was performed in the absence of enzyme, whereas positive control was assayed in the absence of compound (with 0.1% DMSO). All experiments were performed in triplicates, and the percentage of anti-AChE activity was calculated according to the following formula: ((E - S)/E) × 100, where E is the activity of enzyme without test sample and S is the activity of the enzyme with the test sample.

Statistical analysis

Results are presented as bar plots or curves with dots showing the mean with error bars +/- standard deviation of the mean. Statistical analyses were performed using the GraphPad Prism 8 software. The means of 2 variables (e.g. inhibition or cytotoxicity and concentration) were compared between groups using a two-way ANOVA with Dunnet's multiple comparisons test. Results were considered significant when the *p*-value (p) < 0.05.

Results and discussion

The acid organic extract of powdered bulbs of *C. jagus* was purified by a combination of column and TLC chromatography to yield three undescribed alkaloids (**1-3**, Figure 1) together with the well-known AAs sanguinine, cherylline, lycorine, crinine and flexinine, and the isoquinolinone hippadine (**4-9**, Figure 1). These latter compounds were identified by comparison of their spectroscopic (essentially ^{1}H and ^{13}C NMR and ECD) and physical (specific optical rotation) data with those previously reported for **4** [22] , **5** [22, 24, 25], **6** [26, 27], **7** [28], **8** [26] and **9** [10, 29], respectively.

The previously undescribed alkaloids **1-3**, were named gigantelline, gigantellinine and gigancrinine, respectively.

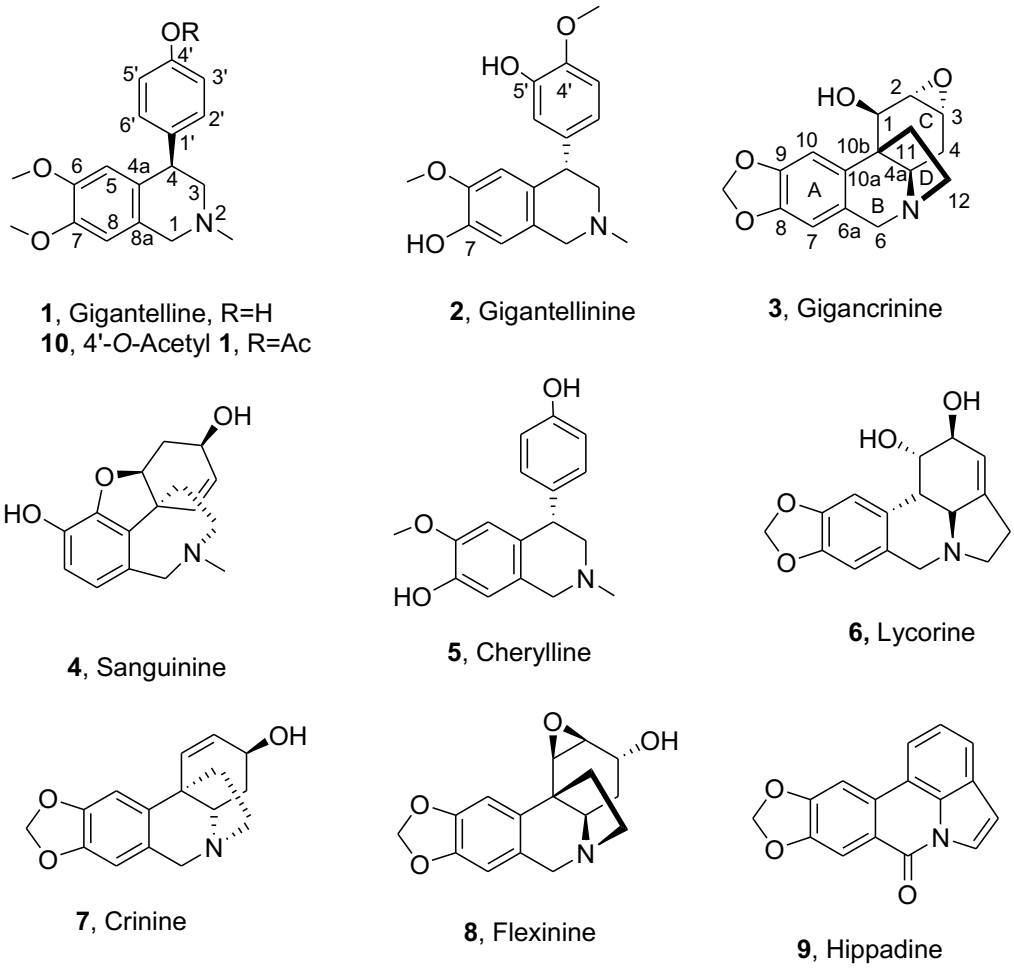

Figure 1 Structures of the isolated compounds (**1**-**9**).

Gingantelline (**1**) has a molecular formula of $C_{18}H_{21}NO_3$ consistent with nine hydrogen deficiencies. Its ^1H and COSY spectra [21] (Table 1) showed the signal patterns of a tetra-substituted-tetrahydroisochinoline and a *para*-substituted phenol ring. In particular, the singlets of two methoxy groups were observed at δ 3.83 and 3.59 while that of a N-methyl resonated at δ 2.44 [30]. C-4 represents the carbon bridging the tetrasubstituted tetrahydroisoquinoline and the *para*-substituted phenol rings, as evidenced by the long-range couplings observed in the HMBC spectrum [21] (Table 1, Figure 2). The methoxy group at δ 3.83 was located at C-6 as demonstrated by the long-range coupling with H-5 observed in the HMBC spectrum (Table 1, Figure 2) and the coupling between MeO-C6 with both C-5 and C-6 (Table 1 and Figure 2), while the methoxy group at δ 3.59 was positioned at C-7 as demonstrated by long range couplings observed in the same spectrum

with C-7 and C-8 [30]. These positions were confirmed by the correlations observed in the NOESY spectrum between MeO-C6 with H-5 and MeO-C7 with H-8 (Figure 2).

The couplings observed in the HSQC spectrum [21] (Table 1) allowed to assign all the protonated carbons. The couplings observed in the HMBC spectrum (Table 1, Figure 2) allowed to assign the six quaternary sp^2 carbons, three of which were oxygenated [31]. Thus, the chemical shifts were assigned to all the protons and corresponding carbons of **1** as reported in Table 1.

Table 1. ^{1}H, ^{13}C NMR and HMBC data of gigantelline and gigantellinine (**1** and **2**)[a,b].

1				**2**		
No.	δ_C[c]	δ_H	HMBC	δ_C[c]	δ_H	HMBC
1	54.9 t	3.81 d (14.3)		58.9 t	3.72 br d (14.5)	N-Me, H_2-3, H-8
		3.53 d (14.3)			3.47 br d (14.5)	
3	61.8 t	3.08 br dd (11.6, 5.9)	H-4, N-Me	63.4 t	3.06 br dd (11.6, 6.1)	H-4, H_2-1, N-Me
		2.44 dd (11.6, 10.7)[d]			2.44 dd (11.6, 10.1)[d]	
4	44.3 d	4.18 dd (10.7, 5.9)	H-8, H-3',5'	45.9 d	4.13 dd (10.1, 6.1)	H-2', H-6', H_2-3, H-5
4a	129.5 s		H-4, H-5, H-3A	129.5 s		H-8, H_2-3
5	109.2 d	6.76 s	H-8, MeO-C6, H-2',6'	113.2 d	6.36 s	H_2-1
6	147.9 s		H-5, MeO-C6	148.2 s		MeO-C6, H-8
7	147.8 s		H-8, MeO-C7	146.4 s		MeO-C6, H-5
8	112.0 d	6.37 s	H-5, H-4, MeO-C7	113.6 d	6.56 s	H-5, H_2-1
8a	126.7 s		H-8, H_2-1	128.2 s		H-5, H-4, H_2-1
1'	134.5 s		H-2',6', H-3',5'	138.6 s		H-3', H-4
2'	129.6 d[e]	6.73 d (8.5)[e]	H-4, H-3',5'	121.5 d	6.67 dd (8.2, 2.1)	H-6'
3'	114.9 d[f]	7.00 d (8.5)[f]	H-2',6'	112.9 d	6.88 d (8.2)	
4'	155.9 s		H-2',6'	147.7 s		H-3', H-6', MeO-C4'
5'	114.9 d[f]	7.00 d (8.5)[f]	H-2',6'	148.1 s		H-3'
6'	129.6 d[e]	6.73 d (8.5)[e]	H-4, H-3',5'	117.1 d	6.60 d (2.1)	H-2', H-4
MeO-C6	57.4 q	3.83 s	H-5	56.4 q	3.62 s	
MeO-C7	55.1 q	3.59 s				
MeO-C4'				56.6 q	3.85 s	
N-Me	44.4 q	2.44 s[d]		46.0 q	2.43 s[d]	H-1B

[a] 2D ^{1}H, ^{1}H (COSY) and ^{13}C, ^{1}H (HSQC) NMR experiments confirmed the correlations of all the protons and the corresponding carbons.
[b] Coupling constants (*J*) are given in parenthesis.
[c] Multiplicities were assigned with DEPT.
[d] These two signals are in part overlapped.
[e] These protons are magnetically equivalent.
[f] These protons are magnetically equivalent.

These results were consistent bands recorded in the IR and UV spectra [30, 32]. According to these findings, **1** was formulated as 4-(6,7-dimethoxy-2-methyl-1,2,3,4-tetrahydro-isoquinolin-4-yl)-phenol. The structure assigned to **1** was supported by the pseudomolecular ion $[M+H]^+$ observed in its HR ESIMS spectrum at *m/z* 300.1591.

The structure assigned to **1** was further confirmed by the preparation of its 4'-*O*-acetyl derivative (**10**, Figure 1) which showed the absence of the hydroxy group in the IR spectrum while its ^1H NMR spectrum differed from that of **1** for the downfield shifts of H-3',5' and H-2',6' and for the singlet of the acetyl group at δ 2.29. Its ESIMS spectrum showed the pseudomolecular ion $[M+H]^+$ at *m/z* 342 and the fragmentation peak at *m/z* 300 $[M+H - CH_2CO]^+$.

Gigantellinine (**2**, Figure 1) has a molecular formula of $C_{18}H_{21}NO_4$ consistent with 9 hydrogen deficiencies as in **1** but differing by one extra oxygen atom. The comparison between the ^1H and ^{13}C NMR spectra of **1** and **2** (Table 1) showed differences essentially in the signal system of the phenol ring. In fact, this latter appears to be a 2,5-disubstituted phenol always linked through the C-1'-C-4 bond to the almost unchanged tetrahydroisoquinoline moiety, as showed by the long range couplings observed in the HMBC spectrum (Table 1, Figure 2). Its ^1H and COSY NMR spectra (Table 1) showed again two singlets due to the methoxy groups at δ 3.62 and 3.85, with the first located at C-6 in agreement with the coupling observed in the HMBC of MeO-C6 with both C-6 and C-7 (Table 1, Figure 2). The other one was located at C-4' in agreement with the long-range coupling observed between MeO-C4' and C-4'. These assignments were also confirmed by the correlations observed in NOESY spectrum reported in Figure 2.

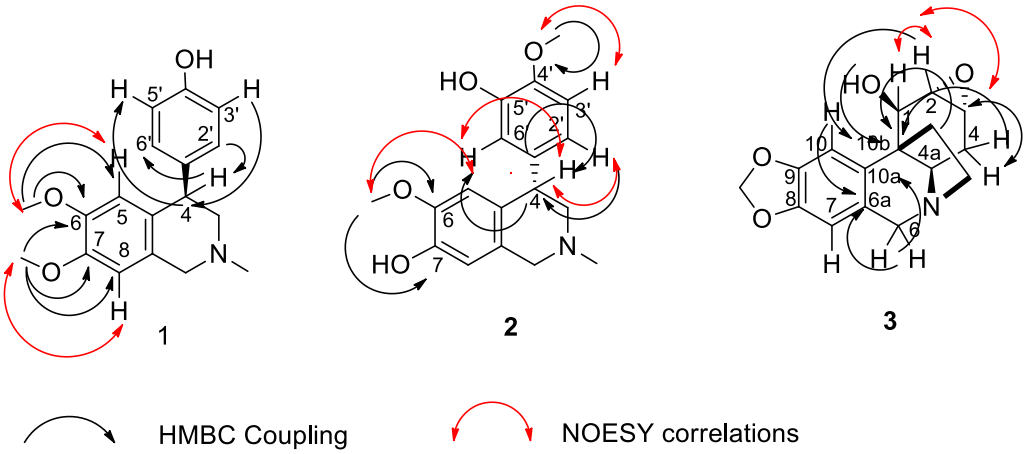

Figure 2 The key correlations observed in the HMBC and NOESY spectra of alkaloids **1**-**3**.

Thus, **1** and **2** differed only in the position of two methoxy groups, which were assigned as reported above, and for the hydroxy groups at C-7 and C-5'. Consequently, the ^{13}C NMR spectrum of **2** (Table 1) showed an extra oxygenated sp^2 quaternary carbon at δ 114.9 which was assigned to carbon C-5' due to its couplings in the HMBC spectrum with H-3' (Table 1). The other ^{13}C resonances remained unaltered and based on the couplings observed in the COSY, HSQC and HMBC spectra (Table 1), all the proton and carbon signals were assigned and reported in Table 1 [30, 31].

These findings agreed with the bands recorded in the IR and UV spectra. Thus, **2** was formulated as the 7-*O*-demethyl-5'-hydroxy-4'-methoxy derivative of **1**. Its structure was supported by the HR ESIMS spectrum which showed the pseudomolecular ion $[M+H]^+$ at *m/z* 316.1539.

The absolute configuration of **1** and **2** was determined by comparison of their ECD spectra with that of cherylline (**5**), as the three compounds have consistent chromophores and the same skeleton. The ECD spectra of the three alkaloids (**1**, **2** and **5**) are reported in Figure 3 and showed a quite perfect overlapping between the spectra of cherylline and gigantellinine, while that of **1** had a mirror image appearance with respect to the former ones. Thus, as the C-4 in **5** has *S* stereochemistry [25], the same was assigned to the C-4 of **2,** while the *R* absolute configuration was assigned to the same carbon of **1**.

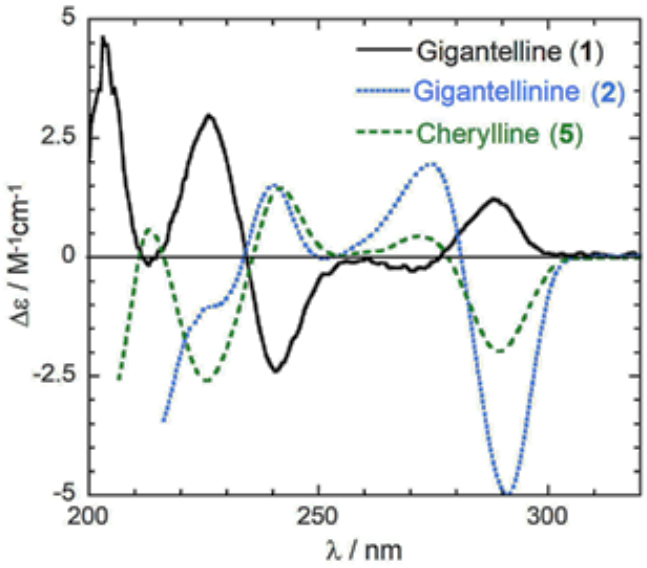

Figure 3 Experimental ECD spectra of gigantelline (**1**) (black solid line), gigantellinine (**2**) (blue dotted line) and cherylline (**5**) (green dashed line) measured in methanol (ca. 3 mM, 0.1 cm cell).

Thus, the same plant synthesizes two closely related alkaloids **1** and **2** with different stereochemistry at C-4. To explain this point, it is necessary to investigate the biosynthetic pathway of gigantelline and gigantellinine. Amigo Chan in his PhD thesis [33], "Biosynthesis of cherylline using doubly-labled norbelladine type precursor" reports some results on the biosynthesis of cherylline based on the incorporation of doubly labeled O-methyl [1'-^{3}H, 1-^{14}C] norbelladine into *Crinum powellii*. His results confirmed the previous ones obtained by Shaffer [34] and Miller [35], who already demonstrated that O-methyl [1'-3H]norbelladine was incorporated intact in cherylline, lycorine and ambelline. Thus, it is possible to hypothesize that gigantelline is biosynthesized from the same biosynthetic pathway and then that the intermediate cherylline is methylated at the hydroxyl group attached at C-7 by S-adenosylmethionine. Amigo Chan also postulated that montanine could be a biosynthetic precursor of a cherylline ring system but with an opposite configuration at C-4. Consequently, to clarify the origin of the different stereochemistry at C-4 in **2**, the biosynthetic pathway of gigantellinine should be investigated by incorporation a suitable label (with radioactive or heavy isotopic atoms depending from the fraction of incorporation into the precursor) in *C. jagus*. Then the

labeled gigantellinine should be isolated and the site(s) of label incorporation investigated. However, this challenging project is beyond the scope of the present manuscript.

Gigancrinine (**3**, Figure 1) has a molecular formula $C_{16}H_{17}NO_4$ with nine hydrogen deficiencies. The first investigation of its ^{1}H and ^{13}C NMR spectra (Table 4) showed that it is closely related to crinine-type alkaloids [6, 14]. These preliminary findings are consistent with the bands observed in the IR spectrum and UV spectra.

In particular, the ^{1}H NMR and COSY spectra of **3** (Table 2) showed the expected singlets of the two protons of a 2,3,5,6-tetrasubstituted benzene ring (ring A) and the singlet of the methylene of a dioxolane ring. The two doublets of a methylene (H_2C-6) linked to the tertiary nitrogen atom account for the presence of ring B. This latter, judging also from the couplings observed in HMBC spectrum (Table 2, Figure 2), was linked to the aromatic ring (ring A), and this latter to the dioxolane ring. Similarly, the two double doublets of H_2C-11, coupled with the multiplet and the double triplet of H_2C-12, which appeared linked to the nitrogen atom, accounted for the ethano bridge between C-10b and the nitrogen atom, which is characteristic of crinine-type alkaloids [6, 14]. In addition, the presence of ring D, joined to rings B and C, was confirmed on the basis of the couplings observed in the HMBC spectrum. The signal pattern of ring C consisted of a broad singlet (H-1) resonating at δ 4.47, which coupled with the adjacent proton (H-2), a doublet at δ 3.12 and this, in turn, with the multiplet of its adjacent proton (H-3) at δ 3.48. Both the chemical shifts of H-2 and H-3 are typical of an oxirane ring [30, 36]. H-3, in turn, coupled with the protons of the adjacent methylene group (H_2C-4), observed as two doublets of double doublets at δ 2.37 and 1.81, which coupled both with H-4a resonating as a double doublet at δ 3.21.

Table 2. ^{1}H, ^{13}C NMR and HMBC data of gigancrinine (**3**).

No.	δ_C[c]	δ_H (*J* in Hz)	HMBC
1	69.2 d	4.47 br s	H-3
2	54.9 d	3.12 d (3.8)	H-1, H-4A
3	53.5 d	3.48 m[d]	H-1, H_2-4
4	24.9 t	2.37 ddd (15.4, 6.6, 2.4)	H-4a
		1.81 ddd (15.4, 11.0, 1.5)	
4a	60.6 d	3.21 dd (11.0, 6.6)	H_2-4, H_2-11
6	59.7 t	4.36 d (16.0)	H-7, H-4a, H_2-12
		3,89 d (16.0)	
6a	122.6 s		H-10, H_2-6
7	105.4 d	6.53 s	H-10, H_2-6
8	146.6 s		H-10, H-7, H_2-6
9	147.2 s		H-10, H-7
10	104.9 d	7.27 s	H-7
10a	138.2 s		H-10, H-7, H_2-6
10b	47.0 s		H-10, H-2, H-1, H-4A, H_2-11
11	34.9 t	2.27 ddd (13.0, 10.3, 8.2)	H_2-12, H-4a
		2.08 ddd (13.0, 8.2, 2.6)	
12	48.2 t	3.48 m[d]	H_2-6, H-4a, H_2-11
		2.91 dt (12.8, 8.2)	
OCH_2O	100.9 t	5.92 s (2H)	

[a] With the GIAO method at ωB97X-D/6-31G(d) level, empirical corrections according to [37].
[b] Root-mean-square deviation between experimental and calculated values.
[c] Fermi contact term calculated at ωB97X-D/pcJ-0 level.
[d] Too small to be measured.

The ^{13}C NMR spectrum (Table 2) showed the signals of sixteen carbons which were all assigned by the coupling observed in the HSQC and HMBC spectra (Table 2, Figure 2).

Thus, the chemical shifts were assigned to all the protons and corresponding carbons and reported in Table 2 and gigancrinine (**3**) was formulated as 5,6a,7,7a,8a,9-hexahydro-6,9a-ethano [1,3] dioxolo[4,5-j]oxireno[2,3-b]phenanthridin-9-ol. Gigancrinine then appears

as a constitutional isomer of flexinine (**8**), obtained upon the shift of the hydroxy group and epoxy ring positions on ring C.

The structure assigned to **3** was supported by the data of its HR ESIMS spectrum which showed the protonated molecular ion $[M+H]^+$ at *m/z* 288.1228.

The relative stereochemistry of **3** was deduced from the correlations observed in the NOESY spectrum (Figure 2), from a detailed analysis of *J*-couplings and from NMR calculations. Compound **3** contains 6 different stereogenic centers (5 carbons and 1 nitrogen). However, the relative configuration of C-4a, C-10b and N is restricted by the ethano bridge, while that of C-2 and C-3 is dictated by the epoxy ring; thus, the set of possible stereoisomers is limited to 4 pairs of enantiomers. Still, the stereochemical assignment is complicated by the fact that ring C assumes a half-chair conformation, making some pieces of information not immediate. We started assuming the same configuration at C-4a, C-10b and N as for flexinine (**8**), thus with the ethano bridge in β-orientation (Figure 1). The NOE cross-peak observed between H-1 and H-2 and the small (undetectable) coupling constant suggested their *gauche* spatial relation. Furthermore, the significant cross peak between H-1 and H-10 together with the lack of cross-peaks between H-1 and H-11 allowed to assign H-1 as α-oriented and the hydroxyl group attached at C-1 as β-oriented. The lack of coupling between H-2 and especially H-3 and H-4a in the NOESY spectrum suggested that the former hydrogens were β-oriented, if H-4a is α-oriented as in flexinine. Finally, a set of diagnostic $^3J_{HH}$ coupling constants was detected (Table 3). To interpret the overall set of data by means of molecular modeling, we built 4 different isomers by keeping the configuration (4a*R*,10b*S*) fixed and varying the configuration at C-1, C-2 and C-3 as (1*R*,2*R*,3*R*), (1*S*,2*R*,3*R*), (1*R*,2*S*,3*S*) and (1*S*,2*S*,3*S*). Then, we applied a computational protocol to predict ^{13}C chemical shifts and ^{1}H-^{1}H couplings based on density functional theory (DFT) calculations [37]. The input structures were generated after a multi-step conformational search (see Computational Section) culminating in ωB97X-V/6-311+G(2df,2p)//ωB97X-D/6-31G(d) energy estimation and geometry optimization. Magnetic shielding and spin-spin coupling calculations were then run at ωB97X-D/6-31G(d) and ωB97X-D/pcJ-0 level, respectively.

The results for the four isomers are summarized in Table 6 and compared therein with the experiments; correlation graphs (Figure S2) are shown in the Supporting Information. The above computational protocol normally leads to overall RMSD (root-mean-square deviations) between experimental and calculated ^{13}C chemical shifts below 2 ppm [37]. In the current case, the significantly smallest RMSD of 1.8 ppm was obtained for the (1*R*,2*R*,3*R*) isomer, but an acceptable RMSD of 2.3 ppm was also obtained for the (1*R*,2*S*,3*S*) isomer. However, only the former one provided an excellent agreement between calculated and diagnostic $^{3}J_{HH}$ coupling constants (Table 3). Thus, the relative configuration 1*R**,2*R**,3*R**,4a*R**,10b*S** was assigned to **3**.

Table 3. Comparison between experimental and calculated NMR data of gigancrinine (**3***).*

Experimental ^{13}C		Calculated[a]			
No.	δ_C (ppm)	(1*R*,2*R*,3*R*)	(1*S*,2*R*,3*R*)	(1*R*,2*S*,3*S*)	(1*S*,2*S*,3*S*)
1	69.2	73	65.8	65.5	71.8
2	54.9	55.1	54.7	56	57.4
3	53.5	53	56.7	50.1	53.4
4	24.9	26.7	26.7	26.8	26.2
4a	60.6	61.3	59.5	60.4	65.6
6	59.7	61	60.9	60.9	61.1
6a	122.6	126.1	126.6	129.1	125.6
7	105.4	106.2	106	108.6	105.8
8	146.6	145.9	145.4	145.7	145.8
9	147.2	146.3	145.5	146.7	146.3
10	104.9	107	109.8	102.8	107.7
10a	138.2	139.2	135.7	137.5	140.2
10b	47.0	46.5	47.7	49.1	48.5
11	34.9	36.3	39.9	37.9	36.7
12	48.2	50.1	49.9	50.9	51
OCH_2O	100.9	103.5	103.6	104	103.6
RMSD (ppm)[b]		1.8	2.7	2.7	2.3
Expoerimental $^{3}J_{HH}$		Calculated[c]			
Protons	J (Hz)	(1*R*,2*R*,3*R*)	(1*S*,2*R*,3*R*)	(1*S*,2*S*,3*S*)	(1*S*,2*S*,3*S*)
H1-H2	n.d. [d]	0.0	5.6	2.3	3.3
H2-H3	3.8	3.1	3.5	3.7	3.7
H3-H4A	2.4	2.2	2.4	0.0	0.5
H3-H4B	1.5	1.8	1.9	6	6.1

[a] With the GIAO method at ωB97X-D/6-31G(d) level, empirical corrections according to [37].

[b] Root-mean-square deviation between experimental and calculated values.

[c] Fermi contact term calculated at ωB97X-D/pcJ-0 level.

[d] Too small to be measured.

The absolute configuration of **3** was inferred by its ECD spectrum (Figure 4), which was very similar to that flexinine (**8**), either reported in the literature [26] or measured on our sample of **8**. The ECD spectra of gigancrinine (**3**), crinine (**7**), flexinine (**8**) and related alkaloids are mainly determined by the configuration of the chirality centers on ring B, which is close to the aromatic chromophore [26, 38]. Therefore, we anticipated the configuration of **3** and **8** to be the same as for the corresponding chirality centers C-4a and C-10b. The final confirmation came from the comparison between the experimental ECD spectrum of **3** with that calculated by time-dependent DFT (TD-DFT) [39, 40]. Using input structures with (1*R*,2*R*,3*R*,4a*R*,10b*S*) configuration, the spectrum calculated at B3LYP/def2-TZVP/PCM level (solvent model for acetonitrile) fitted very well the experimental spectrum (Figure 4). Therefore, the absolute configuration of gigancrinine was ultimately assigned as (1*R*,2*R*,3*R*,4a*R*,10b*S*)-**3**.

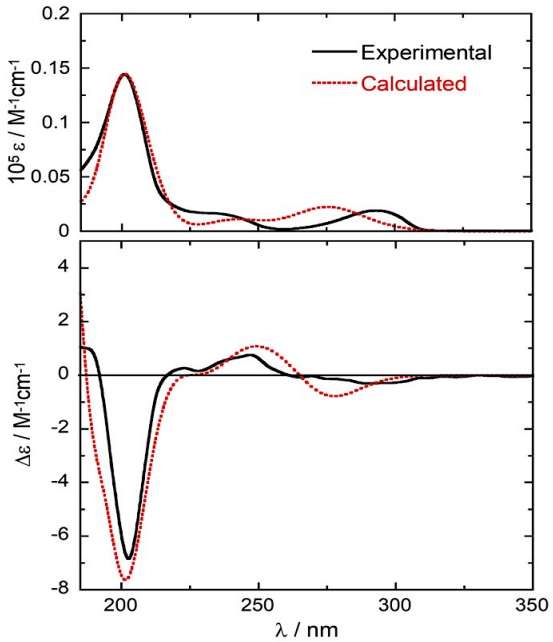

Figure 4 **UV−vis absorption (top) and ECD spectra (bottom) of gigancrinine (3).** The spectra were measured in acetonitrile (solid lines, 8.0 mM, 0.01 cm cell) compared with spectra calculated for (1*R*,2*R*,3*R*,4a*R*,10b*S*)-**3** at the B3LYP/def2-TZVP/PCM level as Boltzmann average of **3** conformers at 300K (dotted lines). Calculated spectra were obtained as sums of Gaussian bands with 0.25 eV exponential half-width, red-shifted by 5 nm, ECD spectrum scaled by a factor 3.

Few references are available on the alkaloids produced by *C. jagus* isolated in different parts of the world [16, 18, 20] but its aqueous and organic extracts, showed several biological activities [15-19]. Among them one the most promising resulted to be the inhibition of acetylcholinesterase (AChE) [8, 18].

AChE is a serine protease located at neuromuscular junctions, in cholinergic synapses of the central nervous system [41] and in red blood cells [42, 43]. Currently, AChE inhibitors have become the main target treatment for Alzheimer's disease and donepezil, rivastigmine, and galantamine are the major therapies approved for its treatment [44]. However, these drugs are not curatives, their benefit are short-term [45], and cause serious side effects [46]. Therefore, the discovery of new drugs for Alzheimer's disease with improved AChE inhibition and less side effects is required [47].

All isolated compounds, except for hippadine that was not obtained in sufficient amount, were assayed for their AChE inhibitory activity. Galanthamine hydrobromide was used as a positive control. Cherylline (**5**), gigantellinine (**2**), crinine (**7**), flexinine (**8**) and sanguinine (**4**) all inhibited the activity of AChE in a dose-dependent manner (Table 4, Figure S3) whereas gigantelline (**1**), lycorine (**6**) and gigancrinine (**3**) did not. The result obtained testing lycorine is in perfect agreement with the data previously reported [48, 49].

Table 4. Anti-cetylcholinesterase activity of alkaloids extracted from *C. jagus*, expressed in μM.

Compound	IC_{50} (μM)[a]
Gigantelline (**1**)	n.s.
Gigantellinine (**2**)	174.90 ± 2.30
Gigancrinine (**3**)	n.s.
Sanguinine (**4**)	1.83 ± 0.01
Cherylline (**5**)	154.70 ± 1.01
Lycorine (**6**)	n.s.
Crinine (**7**)	161.30 ± 0.80
Flexinine (**8**)	164.60 ± 1.12
Hippadine (**9**)	n.d.
Galanthamine[b]	7.50 ± 0.02

[a] not significant (n.s.) when the IC_{50} was not reached and not determined (n.d.) when the compound could not be assayed because of its polarity.
[b] It was used as hydrobromide.

Cherylline is a 4-arylisoquinoline derivative, a compound with a weak AChE inhibitory activity [50]. Therefore, the low AChE inhibitory activity observed for gigantelline is not surprising. Gigantellinine is less active than cherylline, according to our study probably for its opposite stereochemistry at C-4. Flexinine, tested for the first time, and crinine had weak AChE inhibitory activities. The result of crinine is in agreement with the data previously reported [48]. The most active AA in the AChE inhibition assay was sanguinine (**4**), a galantamine-type alkaloid, with an IC_{50} value of 1.83 ± 0.01 μM and was 4 times more active than our positive control galantamine (IC_{50} of 7.2 μM; Figure S3). This result, which not surprised because the two alkaloids differ only in the substituents on the benzene ring, is very similar to that recently reported by Ortiz et al. [49]. As regards the AAs belonging to crinine group (**3**, **7** and **8**), the results showed that the stereochemistry of the ethano bridge is not important for the activity while the substitution of C ring plays an important role.

Cytotoxic activity was measured on human breast cancer cell line MCF-7 using the XTT cell viability assay. Lycorine was used as a positive control and it was toxic at all concentrations tested (Figure S4). Sanguinine, flexinine, gigancrinine and crinine did not exhibit any detectable cytotoxic activity on MCF-7 cells. Cherylline, hippadine, gigantelline, gigantellinine and sanguinine had a significant cytotoxicity at 400 μM (Figure S4). At 100 μM, only hippadine and cherylline remained weakly but significantly cytotoxic, whereas all compounds lost any cytotoxic potential at lower concentrations (Figure S4). This is in agreement with the strong anticancer activity showed by the isocarbostyril narciclasine close to lycorine [7].

Thus, the undescribed compounds are not good candidate as anti-breast cancer drugs. However, other cell lines derived from different cancer types could be tested in the future. Further bioassays measuring other biological activities such as larvicidal, antimicrobial and anti-inflammatory will also be investigated in future studies.

Conclusions

In conclusion, eight Amaryllidaceae alkaloids and an isoquinolinone derivative were isolated from *C. jagus* collected in Senegal. Five alkaloids resulted to be known and identified as sanguinine, cherylline, lycorine, crinine and flexinine, while the isoquinolinone derivative was identified as hippadine. The other three resulted to be previously undescribed tetrahydroisoqionoline- and crinine-type alkaloids and were named gigantelline, gigantellinine and gigancrinine. Alkaloids belonging to tetrahydroisoquinoline subgroup are rarely isolated from Amamaryllidaceae plants. To the best of our knowledge this is the first report of alkaloids produced by *C. jagus* collected in Senegal with sanguinine, cherylline, crinine, flexinine, and isoquinolinone hippadine isolated for the first time from this species. The isolated compounds were evaluated for their acetylcholinesterase (AChE) inhibitory potential and cytotoxic activity on the breast cancer cell line MCF-7. Cherylline, gigantellinine, crinine, flexinine and sanguinine inhibited the activity of AChE in a dose-dependent manner and sanguinine inhibition was remarkably effective. Cherylline and hippadine showed a weak cytotoxicity

potential at 100 μM. This study can expand the chemical library of Amaryllidaceae alkaloids and their possible application in medicine.

Acknowledgements

The authors would like to thank professors Cèline Van Themsche and Carlos Reyes-Moreno and Maria-Grazia Martinoli (Université du Québec at Trois-Rivières, Canada) for kindly providing MCF-7 cells and cell cultures equipment. This work was supported by the Centre SEVE international scholarship to S.K. and by the Natural Sciences and Engineering Research Council of Canada (NSERC) award number RGPIN 05294-2014 (Discovery) to I.D-P. A.E. is associated to the Instituto di Chimica Biomolecolare del CNR, Pozzuoli, Italy. M.G. thanks the program Bekker of the Polish National Agency for Academic Exchange. G.P. acknowledges the CINECA award under the ISCRA initiative for the availability of high-performance computing resources and support.

References

1. Evidente, A.; Kornienko, A., Anticancer evaluation of structurally diverse Amaryllidaceae alkaloids and their synthetic derivatives. *Phytochemistry Reviews* **2009,** *8* (2), 449-59.

2. Nair, J. J.; van Staden, J., Pharmacological and toxicological insights to the South African Amaryllidaceae. *Food and Chemical Toxicology* **2013,** *62*, 262-75.

3. Jin, Z.; Yao, G., Amaryllidaceae and Sceletium alkaloids. *Natural product reports* **2019,** *36* (10), 1462-88.

4. Christenhusz, M. J.; Byng, J. W., The number of known plants species in the world and its annual increase. *Phytotaxa* **2016,** *261* (3), 201-17.

5. Meerow, A.; Snijman, D., Amaryllidaceae. In *Flowering plants· monocotyledons*, Springer: 1998; pp 83-110.

6. Kornienko, A.; Evidente, A., Chemistry, biology, and medicinal potential of narciclasine and its congeners. *Chemical reviews* **2008,** *108* (6), 1982-2014.

7. Cimmino, A.; Masi, M.; Evidente, M.; Superchi, S.; Evidente, A., Amaryllidaceae alkaloids: Absolute configuration and biological activity. *Chirality* **2017,** *29* (9), 486-99.

8. Houghton, P. J.; Ren, Y.; Howes, M.-J., Acetylcholinesterase inhibitors from plants and fungi. *Natural product reports* **2006,** *23* (2), 181-99.

9. Karakoyun, Ç.; Masi, M.; Cimmino, A.; Önür, M. A.; Somer, N. U.; Kornienko, A.; Evidente, A., A Brief Up-to-Date Overview of Amaryllidaceae Alkaloids: Phytochemical Studies of Narcissus tazetta subsp. tazetta L., Collected in Turkey. *Natural Product Communications* **2019,** *14* (8), 1934578X19872906.

10. Masi, M.; Cala, A.; Tabanca, N.; Cimmino, A.; Green, I. R.; Bloomquist, J. R.; Van Otterlo, W. A.; Macias, F. A.; Evidente, A., Alkaloids with activity against the Zika virus vector Aedes aegypti (L.)—Crinsarnine and sarniensinol, two new crinine and mesembrine type alkaloids isolated from the South African plant Nerine sarniensis. *Molecules* **2016,** *21* (11), 1432.

11. Masi, M.; van der Westhuyzen, A. E.; Tabanca, N.; Evidente, M.; Cimmino, A.; Green, I. R.; Bernier, U. R.; Becnel, J. J.; Bloomquist, J. R.; van Otterlo, W. A., Sarniensine, a mesembrine-type alkaloid isolated from Nerine sarniensis, an indigenous South African Amaryllidaceae, with larvicidal and adulticidal activities against Aedes aegypti. *Fitoterapia* **2017,** *116*, 34-8.

12. Masi, M.; Gunawardana, S.; van Rensburg, M.; James, P.; Mochel, J.; Heliso, P.; Albalawi, A.; Cimmino, A.; van Otterlo, W.; Kornienko, A., Alkaloids isolated from Haemanthus humilis Jacq., an indigenous South African Amaryllidaceae: Anticancer activity of coccinine and montanine. *South African Journal of Botany* **2019,** *126*, 277-81.

13. Masi, M.; Mubaiwa, B.; Mabank, T.; Karakoyun, C.; Cimmino, A.; Van Otterlo, W.; Green, I.; Evidente, A., Alkaloids isolated from indigenous South African Amaryllidaceae: Crinum buphanoides (Welw. ex Baker), Crinum graminicola (I. Verd.), Cyrtanthus mackenii (Hook. f) and Brunsvigia grandiflora (Lindl). *South African Journal of Botany* **2018,** *118*, 188-91.

14. Ghosal, S.; Saini, K. S.; Razdan, S., Crinum alkaloids: their chemistry and biology. *Phytochemistry* **1985,** *24* (10), 2141-56.

15. Kapu, S.; Ngwai, Y.; Kayode, O.; Akah, P.; Wambebe, C.; Gamaniel, K., Anti-inflammatory, analgesic and anti-lymphocytic activities of the aqueous extract of Crinum giganteum. *Journal of Ethnopharmacology* **2001,** *78* (1), 7-13.

16. Adesanya, S.; Olugbade, T.; Odebiyl, O.; Aladesanmi, J., Antibacterial alkaloids in Crinum jagus. *International Journal of Pharmacognosy* **1992,** *30* (4), 303-7.

17. Amos, S.; Binda, L.; Akah, P.; Wambebe, C.; Gamaniel, K., Central inhibitory activity of the aqueous extract of Crinum giganteum. *Fitoterapia* **2003,** *74* (1-2), 23-8.

18. Cortes, N.; Sierra, K.; Alzate, F.; Osorio, E. H.; Osorio, E., Alkaloids of Amaryllidaceae as inhibitors of cholinesterases (AChEs and BChEs): An integrated bioguided study. *Phytochemical Analysis* **2018,** *29* (2), 217-27.

19. Ogbole, O. O.; Akinleye, T. E.; Segun, P. A.; Faleye, T. C.; Adeniji, A. J., In vitro antiviral activity of twenty-seven medicinal plant extracts from Southwest Nigeria against three serotypes of echoviruses. *Virology journal* **2018,** *15* (1), 1-8.

20. Kintsurashvili, L.; Vachnadze, V., Plants of the Amaryllidaceae family grown and introduced in Georgia: a source of galanthamine. *Pharmaceutical Chemistry Journal* **2007,** *41* (9), 492-4.

21. Berger, S.; Braun, S., *200 and more NMR experiments*. Wiley-Vch Weinheim: 2004.

22. Kobayashi, S.; Satoh, K.; Numata, A.; Shingu, T.; Kihara, M., Alkaloid N-oxides from Lycoris sanguinea. *Phytochemistry* **1991,** *30* (2), 675-7.

23. Kobayashi, S.; Tokumoto, T.; Kihara, M.; Imakura, Y.; Shingu, T.; Taira, Z., Alkaloidal constituents of Crinum latifolium and Crinum bulbispermum (Amaryllidaceae). *Chemical and pharmaceutical bulletin* **1984,** *32* (8), 3015-22.

24. Lebrun, S.; Couture, A.; Deniau, E.; Grandclaudon, P., A new synthesis of (+)-and (−)-cherylline. *Organic & biomolecular chemistry* **2003,** *1* (10), 1701-6.

25. Brossi, A.; Teitel, S., Synthesis of cherylline. *The Journal of Organic Chemistry* **1970,** *35* (10), 3559-61.

26. Pham, L. H.; Döpke, W.; Wagner, J.; Mügge, C., Alkaloids from Crinum amabile. *Phytochemistry* **1998,** *48* (2), 371-6.

27. Lamoral-Theys, D.; Andolfi, A.; Van Goietsenoven, G.; Cimmino, A.; Le Calvé, B.; Wauthoz, N.; Mégalizzi, V.; Gras, T.; Bruyère, C.; Dubois, J., Lycorine, the main phenanthridine Amaryllidaceae alkaloid, exhibits significant antitumor activity in cancer cells that display resistance to proapoptotic stimuli: an investigation of structure− activity relationship and mechanistic insight. *Journal of medicinal chemistry* **2009,** *52* (20), 6244-56.

28. Viladomat, F.; Codina, C.; Bastida, J.; Mathee, S.; Campbell, W. E., Further alkaloids from Brunsvigia josephinae. *Phytochemistry* **1995,** *40* (3), 961-5.

29. Ghosal, S.; Rao, P. H.; Jaiswal, D. K.; Kumar, Y.; Frahm, A. W., Alkaloids of Crinum pratense. *Phytochemistry* **1981,** *20* (8), 2003-7.

30. Pretsch, E.; Bühlmann, P.; Affolter, C.; Pretsch, E.; Bhuhlmann, P.; Affolter, C., *Structure determination of organic compounds*. Springer: 2000.

31. Breitmaier, E.; Voelter, W., Carbon-13 NMR spectroscopy. **1987**.

32. Nakanishi, K.; Solomon, P. H., *Infrared absorption spectroscopy*. Holden-day: 1977.

33. Chan, J. L. A., Biosynthesis of cherylline using doubly-labled norbelladine-type precursors. **1973**.

34. Shaffer, R. D., Synthetic and biosynthetic approaches to cherylline and related compounds. **1972**.

35. Miller, J., Biosynthetic Studies on Tazettine and Ambelline. *Unpublished Ph D Thesis, Library, Iowa State University of Science and Technology, Ames, Iowa* **1966**.

36. Batterham, T. J., NMR spectra of simple heterocycles. **1973**.

37. Hehre, W.; Klunzinger, P.; Deppmeier, B.; Driessen, A.; Uchida, N.; Hashimoto, M.; Fukushi, E.; Takata, Y., Efficient Protocol for Accurately Calculating 13C Chemical Shifts of Conformationally Flexible Natural Products: Scope, Assessment, and Limitations. *Journal of natural products* **2019,** *82* (8), 2299-306.

38. Wagner, J.; Pham, H. L.; Döpke, W., Alkaloids from Hippeastrum equestre Herb.—5. Circular dichroism studies. *Tetrahedron* **1996,** *52* (19), 6591-600.

39. Superchi, S.; Scafato, P.; Gorecki, M.; Pescitelli, G., Absolute configuration determination by quantum mechanical calculation of chiroptical spectra: basics and applications to fungal metabolites. *Current medicinal chemistry* **2018,** *25* (2), 287-320.

40. Pescitelli, G.; Bruhn, T., Good computational practice in the assignment of absolute configurations by TDDFT calculations of ECD spectra. *Chirality* **2016,** *28* (6), 466-74.

41. Brimijoin, S., Molecular forms of acetylcholinesterase in brain, nerve and muscle: nature, localization and dynamics. *Progress in neurobiology* **1983,** *21* (4), 291-322.

42. Heller, M.; Hanahan, D. J., Human erythrocyte membrane bound enzyme acetylcholinesterase. *Biochimica et Biophysica Acta (BBA)-Biomembranes* **1972,** *255* (1), 251-72.

43. Szelényi, J. G.; Bartha, E.; Hollán, S. R., Acetylcholinesterase activity of lymphocytes: an enzyme characteristic of T-cells. *British journal of haematology* **1982,** *50* (2), 241-5.

44. Lahiri, D. K.; Farlow, M. R.; Greig, N. H.; Sambamurti, K., Current drug targets for Alzheimer's disease treatment. *Drug development research* **2002,** *56* (3), 267-81.

45. Giacobini, E., Cholinesterase inhibitors stabilize Alzheimer disease. *Neurochemical research* **2000,** *25* (9), 1185-90.

46. Moodie, L. W.; Sepčić, K.; Turk, T.; Frangež, R.; Svenson, J., Natural cholinesterase inhibitors from marine organisms. *Natural product reports* **2019,** *36* (8), 1053-92.

47. Kim, Y. J.; Lim, H.-S.; Kim, Y.; Lee, J.; Kim, B.-Y.; Jeong, S.-J., Phytochemical quantification and the in vitro acetylcholinesterase inhibitory activity of Phellodendron chinense and its components. *Molecules* **2017,** *22* (6), 925.

48. Elgorashi, E. E.; Stafford, G. I.; Van Staden, J., Acetylcholinesterase enzyme inhibitory effects of Amaryllidaceae alkaloids. *Planta medica* **2004,** *70* (03), 260-2.

49. Ortiz, J. E.; Garro, A.; Pigni, N. B.; Agüero, M. B.; Roitman, G.; Slanis, A.; Enriz, R. D.; Feresin, G. E.; Bastida, J.; Tapia, A., Cholinesterase-inhibitory effect and in silico analysis of alkaloids from bulbs of Hieronymiella species. *Phytomedicine* **2018,** *39*, 66-74.

50. Bastida, J.; Lavilla, R.; Viladomat, F., Chemical and biological aspects of Narcissus alkaloids. *The alkaloids: chemistry and biology* **2006,** *63*, 87-179.

Supplementary materials

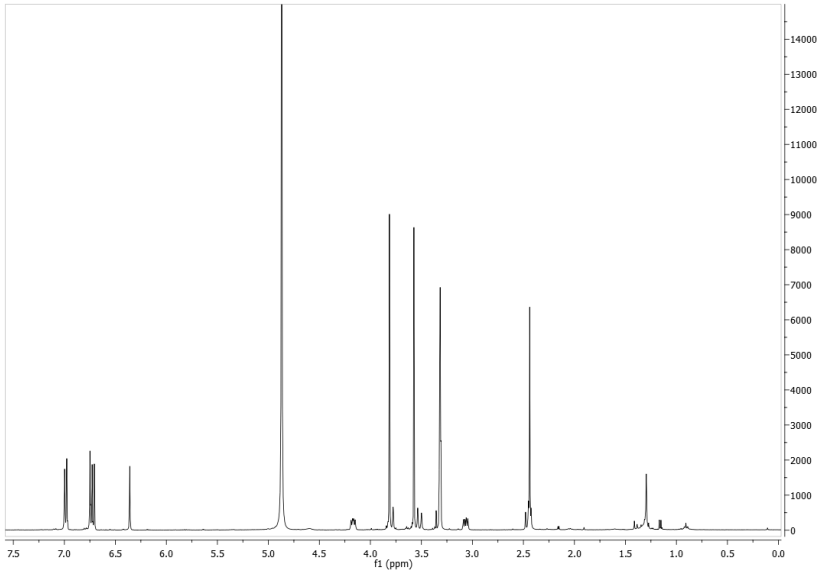

Spectra 1. ^{1}H NMR spectrum of gigantelline (1 (D_3COD, 500 MHz).

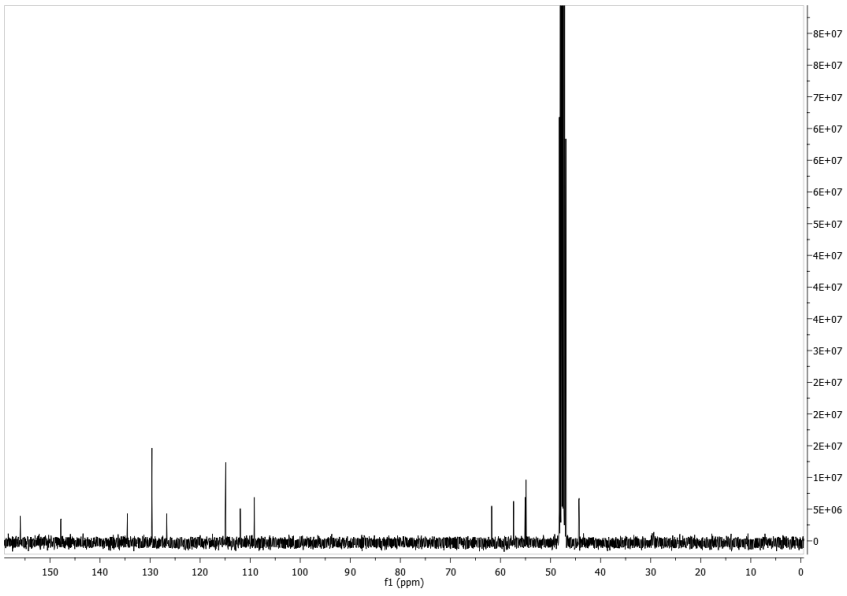

Spectra 2. ^{13}C NMR spectrum of gigantelline (**1**) (CD_3OD, 125 MHz).

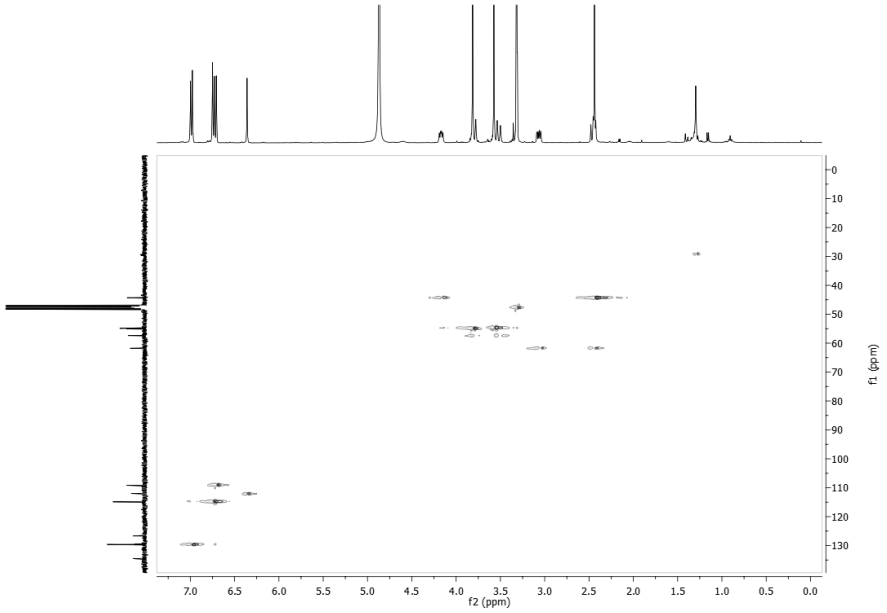

Spectra 3. HSQC spectrum of gigantelline (**1**) (CD_3OD, 500/125 MHz).

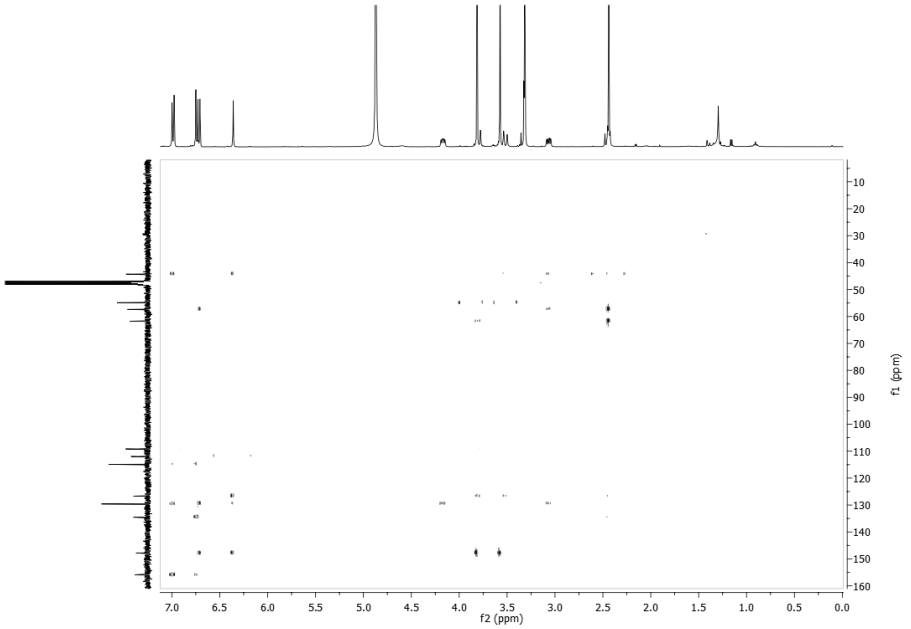

Spectra 4. HMBC spectrum of gigantelline (**1**) (CD_3OD, 500/125 MHz).

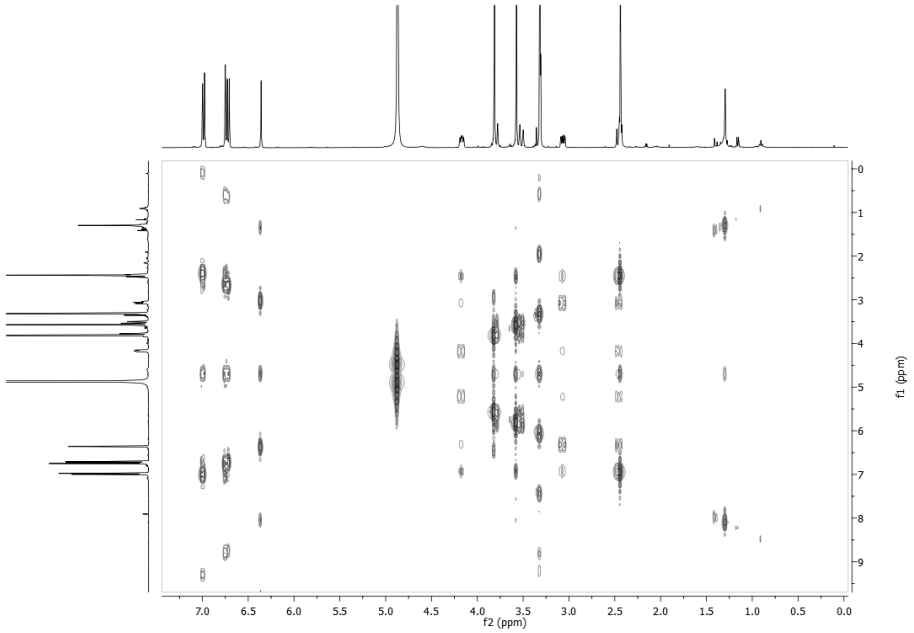

Spectra 5. COSY spectrum of gigantelline (**1**) (CD_3OD, 500 MHz).

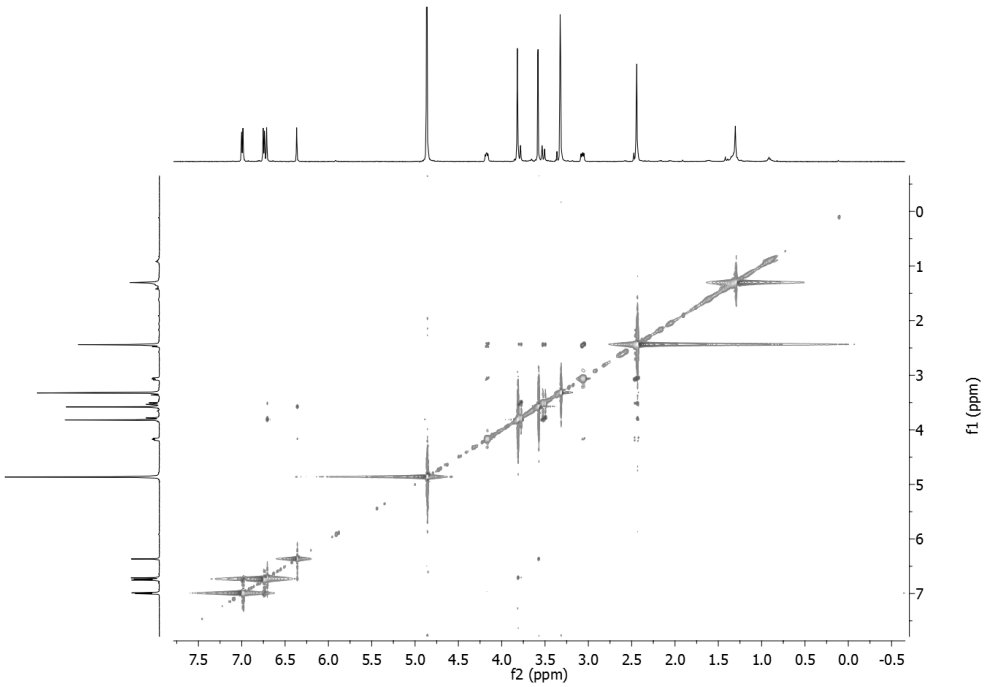

Spectra 6. NOESY spectrum of gigantelline (**1**) (CD_3OD, 500 MHz).

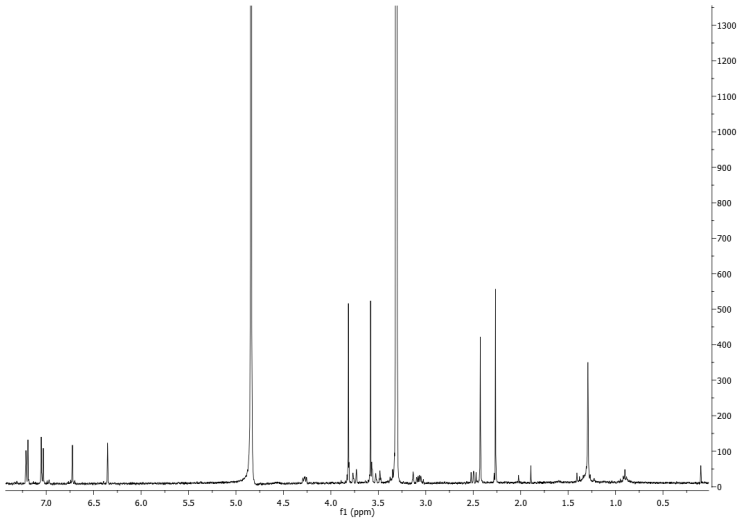

Spectra 7. ^{1}H NMR spectrum of 4'-*O*-Acetylgigantelline (**10**) (CD_3OD, 500 MHz).

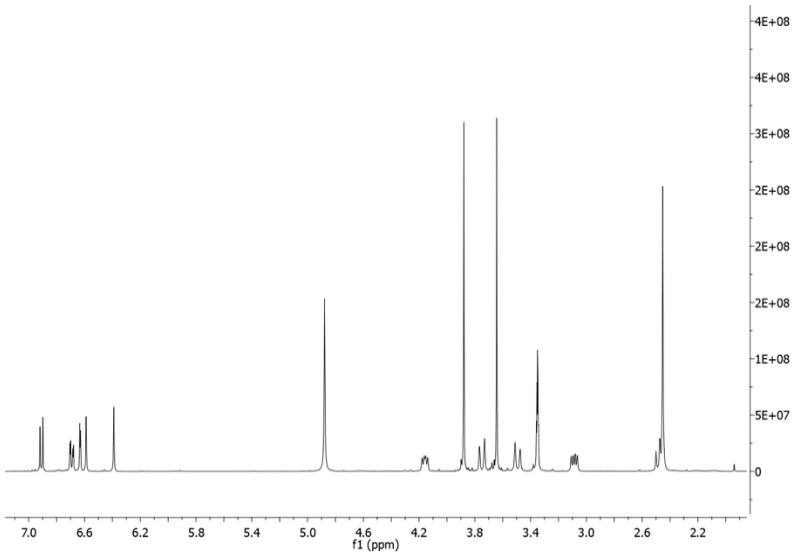

Spectra 8. ^{1}H NMR spectrum of gigantellinine (**2**) (CD_3OD, 500 MHz).

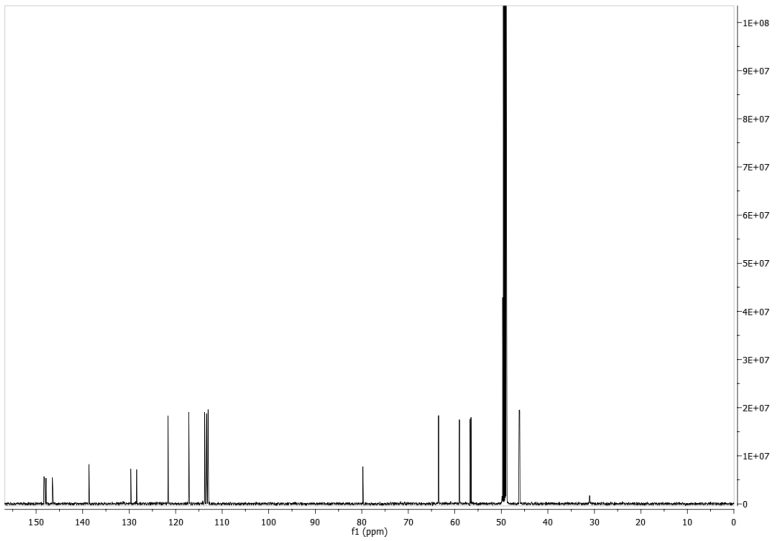

Spectra 9. ^{13}C NMR spectrum of gigantellinine (**2**) (CD_3OD, 125 MHz).

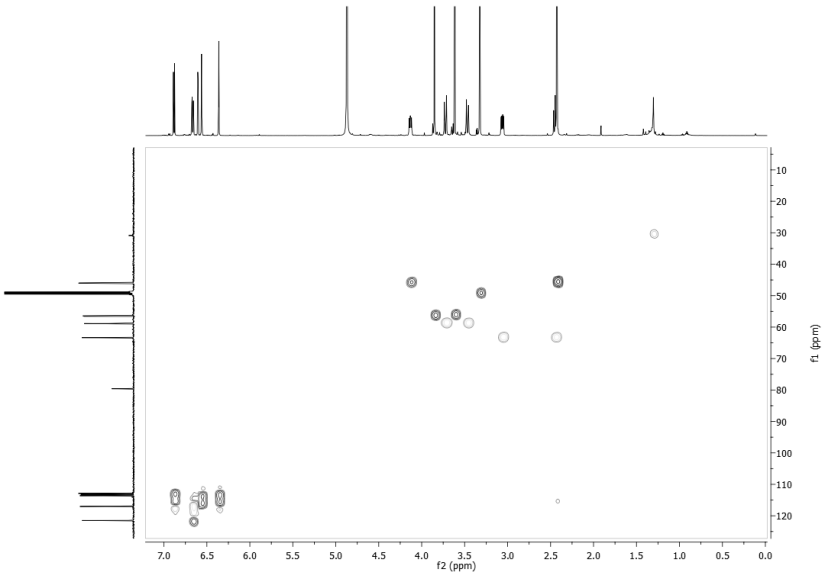

Spectra 10. HSQC spectrum of gigantellinine (**2**) (CD_3OD, 500/125 MHz).

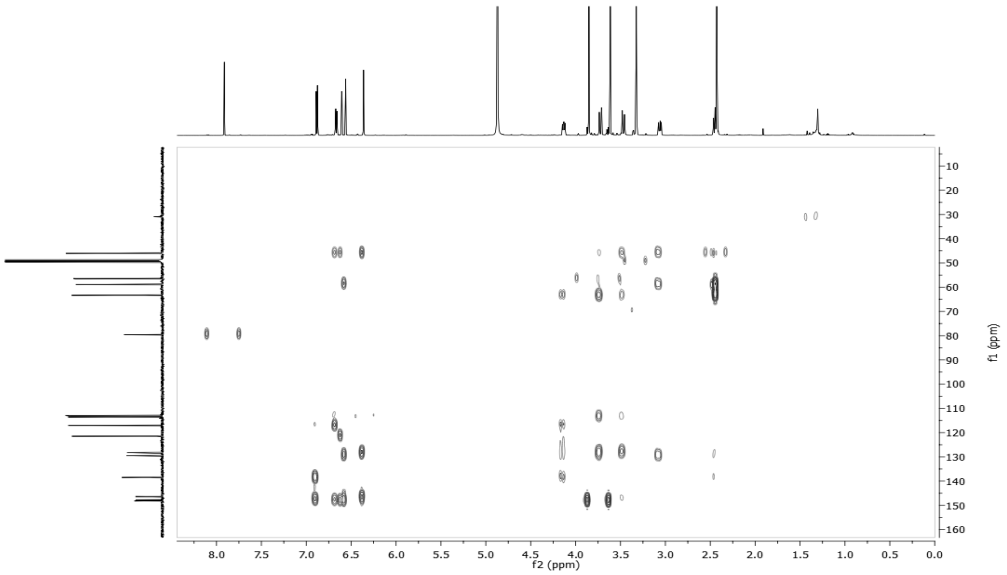

Spectra 11. HMBC spectrum of gigantellinine (**2**) (CD_3OD, 500/125 MHz).

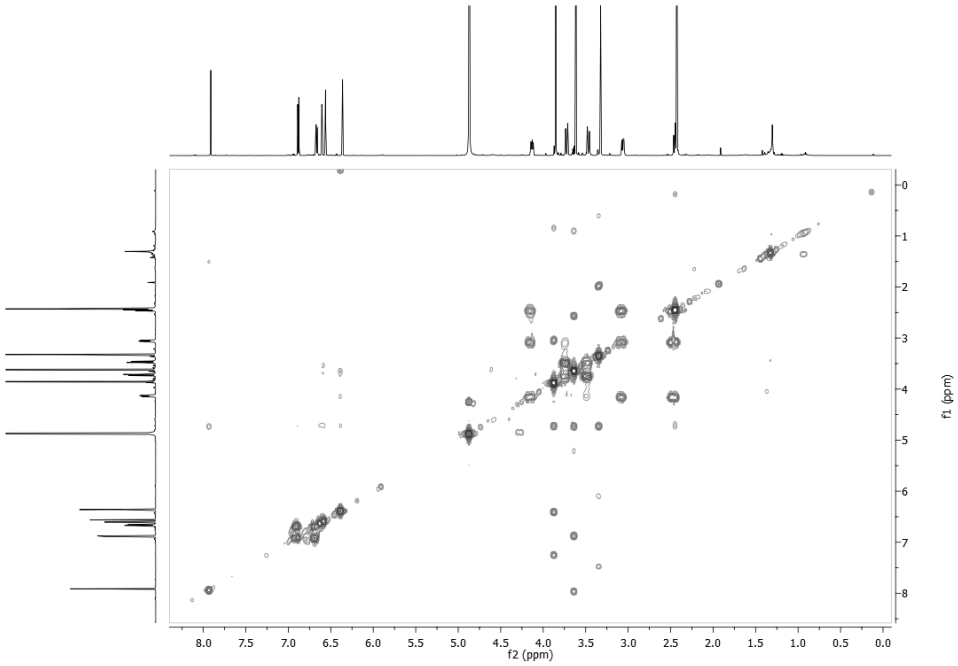

Spectra 12. COSY spectrum of gigantellinine (**2**) (CD_3OD, 500 MHz).

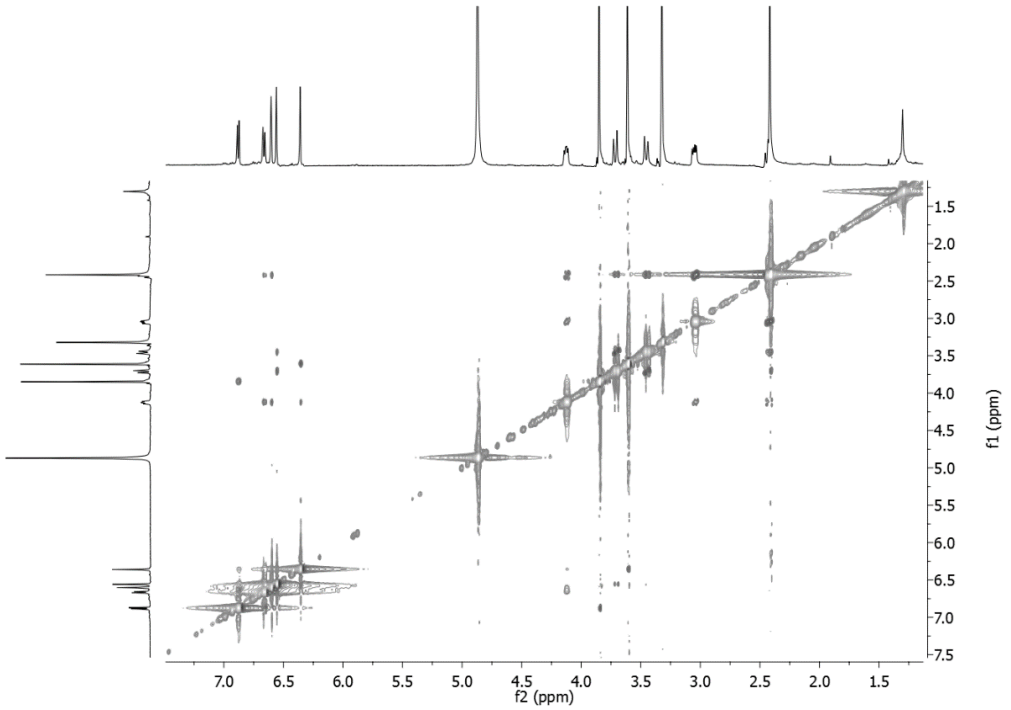

Spectra 13. NOESY spectrum of gigantellinine (**2**) (CD_3OD, 500 MHz)

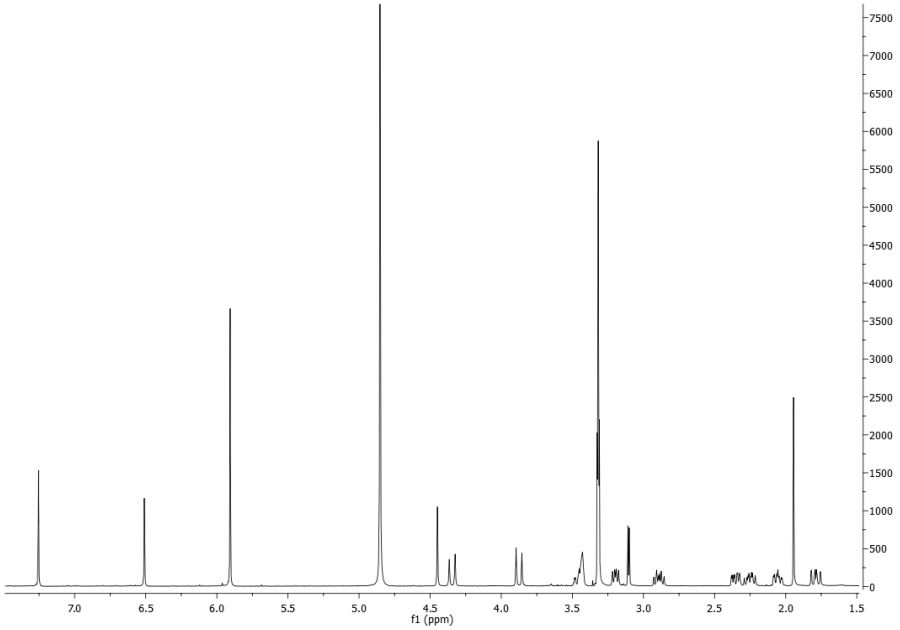

Spectra 14. ^1H NMR spectrum of gigancrinine (**3**) (CD_3OD, 500 MHz).

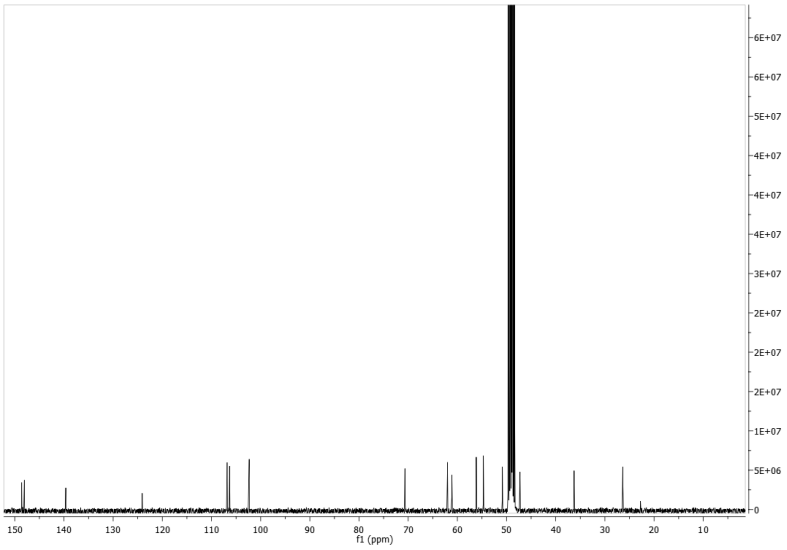

Spectra 15. ^{13}C NMR spectrum of gigancrinine (**3**) (CD_3OD, 125 MHz).

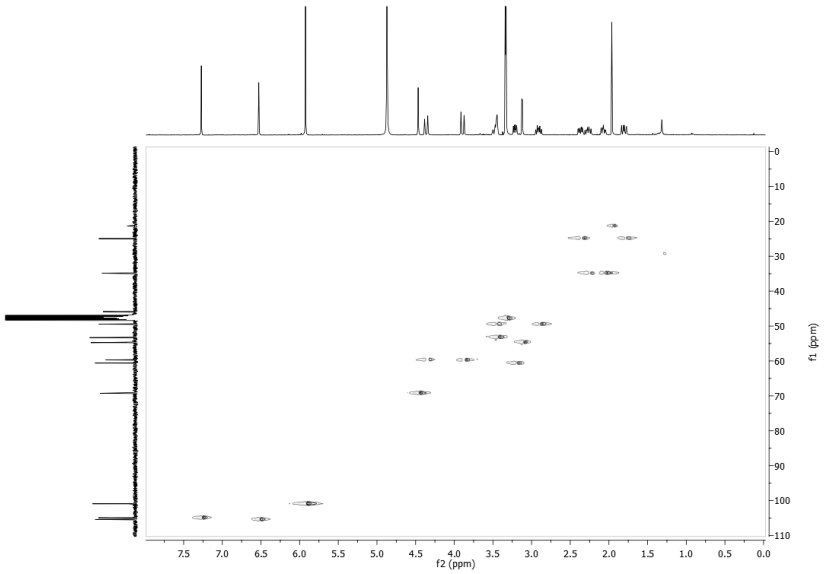

Spectra 16. HSQC spectrum of gigancrinine (**3**) (CD_3OD, 500/125 MHz).

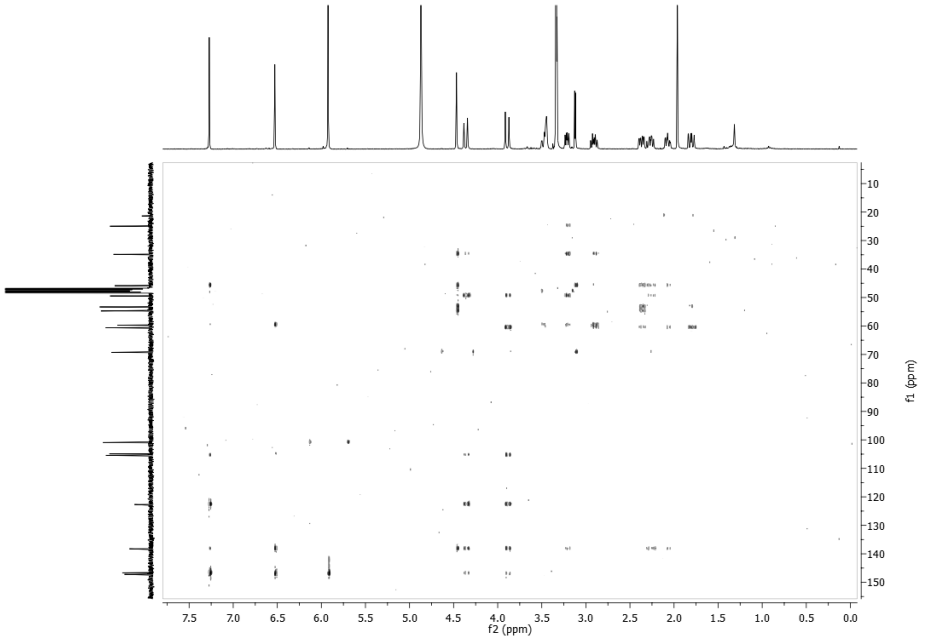

Spectra 17. HMBC spectrum of gigancrinine (**3**) (CD_3OD, 500/125 MHz).

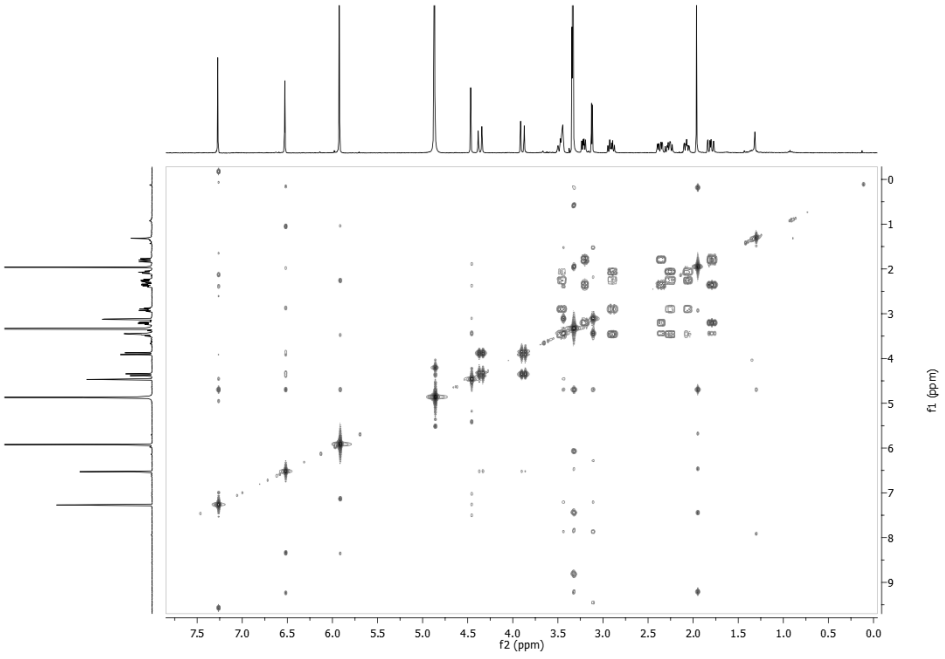

Spectra 18. COSY spectrum of gigancrinine (**3**) (CD_3OD, 500 MHz).

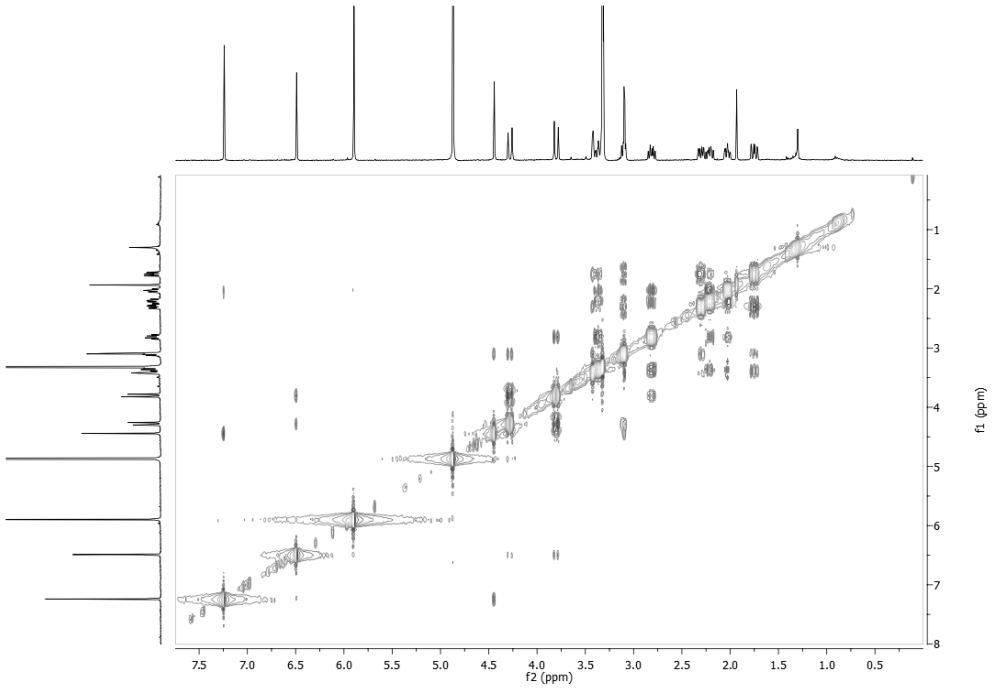

Spectra 19. NOESY spectrum of gigancrinine (**3**) (CD_3OD, 500 MHz).

Figure S1

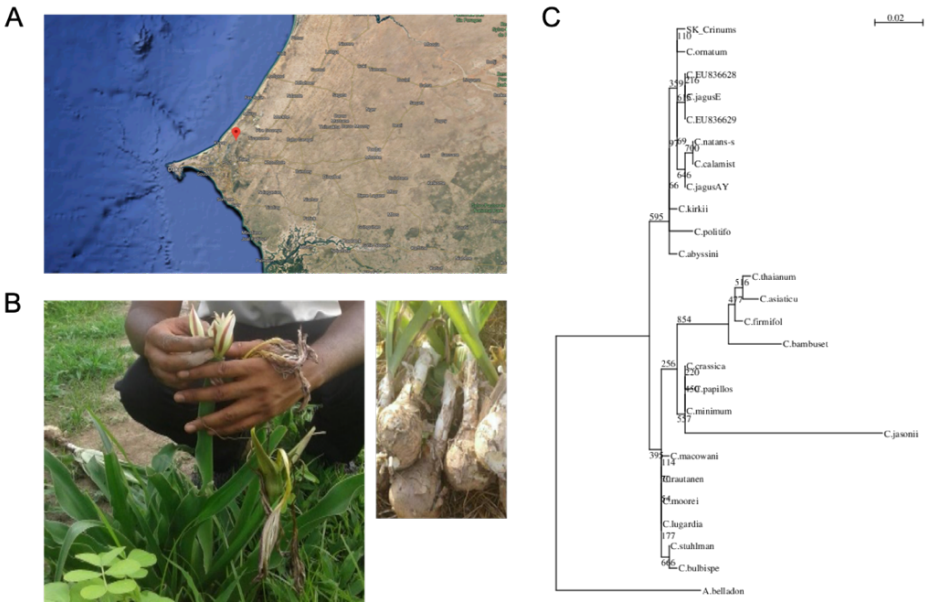

Figure S1. Localization and identification of the Amaryllidaceae species studied. Bulbs of *Crinum jagus* (syn. = *Crinum giganteum*) (SK_Crinum in C) were collected in Senegal, in Montrolland district (14°55'56,22''N and 16°59'38,62''W); in December 2018. (A) map of the localization where the plants were collected (https://www.google.com/intl/fr/help/terms_maps/). (B) Pictures of the plant and bulbs collected. A senior scientist from the Herbarium of IFAN of University Cheikh Anta Diop of Dakar taxonomically identified the plant materials. The voucher specimen is 239. (C) A phylogenetic tree was constructed using partial ITS2 sequences. *Amaryllis belladonna* was used as an outgroup, and non-parametric bootstrap analysis was performed on 1000 replicates using Phyml and ploted using NJplot.

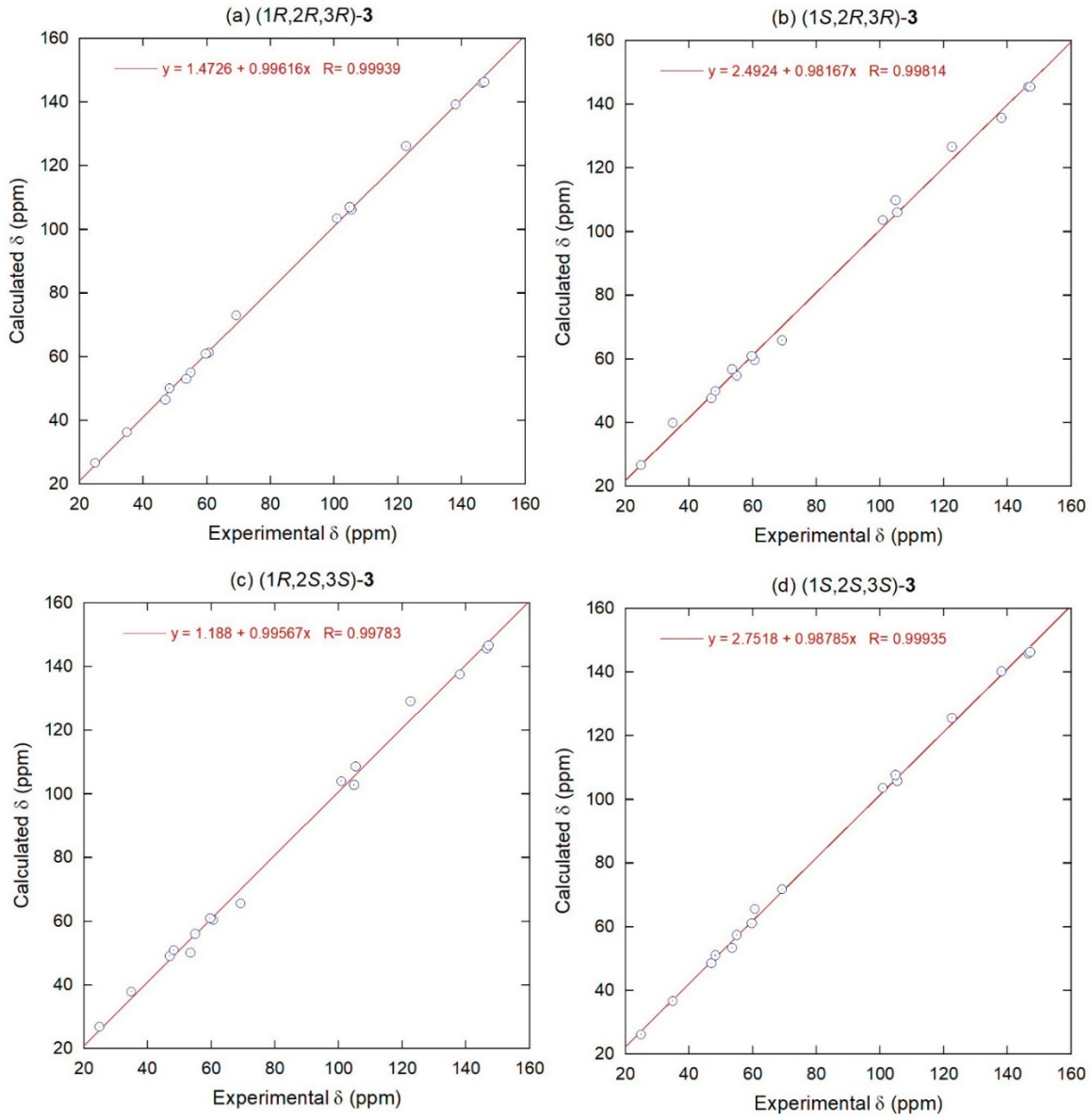

Figure S2. Correlation plots between ^{13}C-NMR chemical shifts measured for gigancrinine (**3**) and calculated with the GIAO method at ωB97X-D/6-31G(d) level, after empirical corrections according to Hehre et al. (J. Nat. Prod. 2019, 82, 2299-2306), for four possible isomers of **3**.

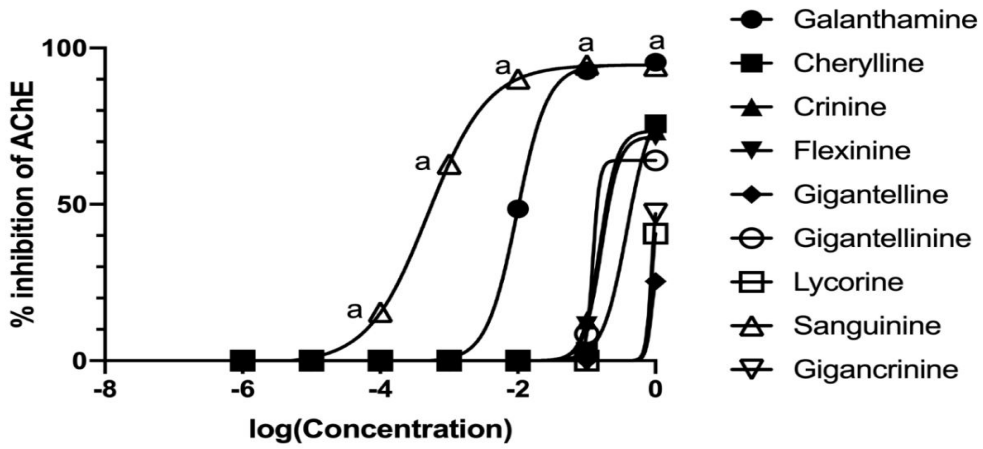

Figure S3. Anti-acetylcholinesterase activity of Amaryllidaceae alkaloids compounds. The percentage of inhibition of acetylcholinesterase activity was calculated as explained in the Method section. Log (Concentration) is expressed in mM. Galanthamine (in hydrobromide form) was used as a positive control. Sanguinine (**4**) was the most potent inhibitor. A two-way Anova and a Dunnet's multiple comparisons test were used to assess the activity of the compounds in comparison to DMSO, a = $p < 0.0001$.

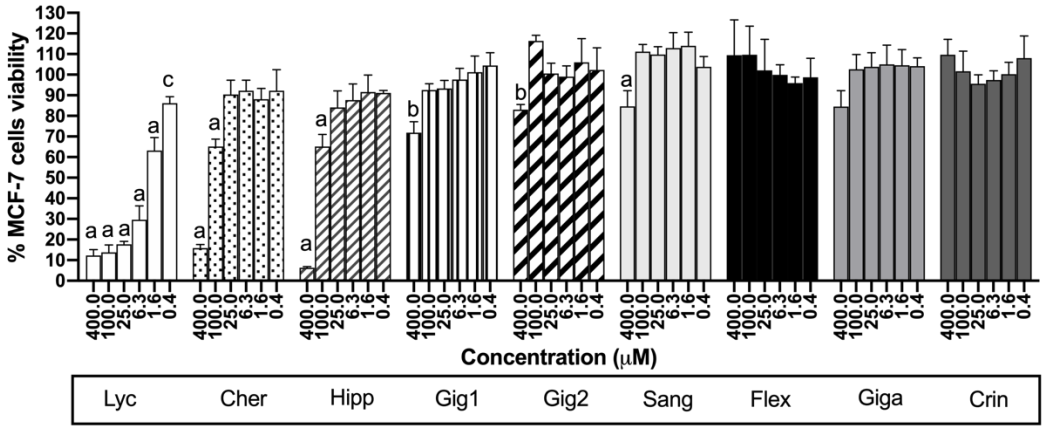

Figure S4. Viability of MCF-7 cells exposed to alkaloids extracted from *C. jagus*. The percentage of MCF-7 cells viability was calculated as explained in the Method section. Differences were measured using a two-way Anova and a Dunnet's multiple comparisons test in comparison to untreated cells (a = $p < 0.0001$; b = $p < 0.001$, c = $p < 0.05$). Lycorine (6), a known cytotoxic AA, was used as a positive control. Abbreviations: lycorine (Lyc), cherylline (Cher), hippadine (Hipp), gigantelline (Gig1), gigantellinine (Gig2), sanguinine (Sang), flexinine (Flex), gigancrinine (Giga) and crinine (Crin).

Le chapitre IV contient les activités anti-Dengue et Zika des alcaloïdes isolés à partir des bulbes de *C. jagus*.

CHAPITRE IV

AMARYLLIDACEAE ALKALOID CHERYLLINE INHIBITS THE REPLICATION OF DENGUE AND ZIKA VIRUSES

Seydou Ka, **Natacha Merindol, Aïssatou Aïcha Sow**, Amita Singh, Karima Landelouci, Mélodie B.Plourde, Geneviève Pépin, Marco Masi, Roberta Di Lecce, Antonio Evidente, Matar Seck, Lionel Berthoux, Laurent Chatel-Chaix, Isabel Desgagné-Penix.

Le contenu de ce chapitre est sous forme d'un article soumis dans la revue *Journal Antimicrobial Agents and Chemotherapy* (numéro de soumission AAC00398-21, accepté avec corrections majeures. Les expériences sont en cours)

4.1 Contribution des auteurs

SK, NM, AS et AAS ont planifié les expériences et écrit le manuscrit. SK, RDL, MM et AE ont isolé les alcaloïdes. GP et KL ont aidé SK à mener les expériences IFN. IDP, MS, LCC et LB ont édité et corrigé le manuscrit.

4.2 Résumé de l'article (français)

Transmise par un moustique, la Dengue est l'une des maladies les plus répandues dans les régions tropicales et subtropicales du monde. Elle est causée par le virus de la dengue (VDEN), apparenté au virus Zika (VZIK) appartenant tous deux au genre des *Flavivirus*. Le VZIK se transmet *in utero* provoquant ainsi le syndrome congénital de Zika et d'autres anomalies congénitales. Chez l'adulte, le VZIK est associé au syndrome de Guillain-Barré. Il n'existe pas de traitements antiviraux approuvés contre ces deux virus, et le vaccin anti-VDEN ne protège pas non plus les personnes n'ayant jamais été infectées

par le VDEN. Des composés antiviraux efficaces sont nécessaires de toute urgence. Les alcaloïdes des Amaryllidaceae (AAs) sont une classe spécifique de composés azotés produits par les plantes de la famille des Amaryllidaceae. Certains AAs, comme la lycorine, inhibent à la fois l'infection par le VDEN et le VZIK. Auparavant, nous avons démontré que les extraits alcaloïdes de *Crinum jagus* étaient efficaces pour bloquer la réplication du VDEN. Dans cette étude, nous évaluons l'activité anti-VDEN et anti-VZIK des AAs purifiés de cet Amaryllidaceae. Ainsi, plusieurs composés ont été capables d'inhiber les infections flavivirales, avec une large gamme d'efficacité. Parmi eux, la cherylline a bloqué le VDEN (EC_{50} = 8,8 μM ; CC_{50} = 64 μM) et l'infection par le VZIK (EC50 = 20.3μM), alors qu'elle n'a eu aucun effet sur l'infection par des vecteurs pseudo-VIH-1. Les expériences de temps d'ajout et d'élimination des composés ont identifié les premières étapes de réplication post-entrée comme cibles. À l'aide de réplications sous-génomiques, nous avons confirmé que ni l'entrée du virion, ni sa libération n'étaient influencées par la cherylline, et que la traduction virale n'était pas inhibée. Nous avons montré que la cherylline entrave spécifiquement l'étape de synthèse de l'ARN viral. En conclusion, les AAs sont une source sous-estimée de composés antiflavivirus. La cherylline est un inhibiteur efficace du VDEN et du VZIK qui pourrait être optimisé pour déboucher sur de nouvelles options thérapeutiques.

4.3 Article complet (anglais) : Amaryllidaceae alkaloid cherylline inhibits the replication of dengue and Zika viruses

Abstract

Dengue fever, caused by dengue virus (DENV) is the most prevalent arthropod-borne viral disease, and is endemic in many tropical and sub-tropical parts of the world with an increasing incidence in temperate regions. The closely related flavivirus Zika virus (ZIKV) can be transmitted vertically *in utero* and causes congenital Zika syndrome and other birth defects. In adults, ZIKV is associated with Guillain-Barré syndrome. There are no approved antiviral therapies against neither viruses. Effective antiviral compounds are urgently needed. Amaryllidaceae alkaloids (AAs) are a specific class of nitrogen-containing compounds produced by plants of the Amaryllidaceae family with numerous biological activities. Recently, the AA lycorine was shown to present strong antiflaviviral properties. Previously, we demonstrated that *Crinum jagus* contained lycorine and several alkaloids of cherylline, crinine and galanthamine-types with unknown antiviral potential. In this study, we explored their biological activities. We show that *C. jagus* crude alkaloid extract inhibited DENV infection. Among the purified AAs, cherylline inhibited efficiently both DENV (EC_{50} = 8.8 μM) and ZIKV replication (EC_{50} = 20.3 μM) but had no effect on HIV-1 infection. Time-of-drug-addition and -removal experiments identified a post-entry step as the one targeted by cherylline. Consistently, using subgenomic replicons and replication-defective genomes, we demonstrate that cherylline specifically hinders the viral RNA-synthesis step but not viral translation. In conclusion, AAs are an underestimated source of antiflavivirus compounds, including the effective inhibitor cherylline that could be optimized for new therapeutic approaches.

Keywords: Amaryllidaceae, alkaloids, flavivirus, cherylline, antivirals, dengue virus, Zika virus.

Introduction

Dengue fever is a viral disease caused by dengue virus (DENV), a flavivirus related to Zika virus (ZIKV) belonging to the *Flaviviridae* family. Both viruses are transmitted to humans through biting of female mosquitoes *Aedes aegypti* or *Aedes albopictus* [1]. DENV and ZIKV possess an ~11 kb-long positive-sense stranded RNA genome encoding capsid (C), membrane precursor (prM) and envelope (E) structural proteins, and NS1, NS2A, NS2B, NS3, NS4A, NS4B and NS5 non-structural proteins [2-4]. To date, four serotypes of DENV (DENV1-4) are described as the cause dengue hemorrhagic fever and dengue shock syndrome, both being potentially fatal [5, 6]. Nearly four billion of individuals are at risk of contracting dengue fever. An estimated 400 million people catch it every year. Between 50-100 millions of human symptomatic cases are reported annually in tropical and subtropical regions, with a yearly death toll of 20,000 individuals, most of them being children [7], posing a considerable threat for public health in over 100 countries [8]. The number of cases is constantly increasing. Between 2017 and 2018, two outbreaks associated with DENV-1 occurred in Senegal [9], and DENV is now present in more temperate regions such as southern Europe.

ZIKV infection is mostly asymptomatic or associated with mild symptoms in adults, but it can cause the Guillain-Barré syndrome [10, 11]. Fetal ZIKV infection causes more serious conditions, such as the congenital Zika syndrome and other severe birth defects. During the 2015 ZIKV outbreak in Brazil, 4,300 children were born with microcephaly [10].

To date, there are no approved antiviral therapies against DENV or ZIKV, and no vaccine for ZIKV [12]. In the case of DENV, the efficacy of the approved tetravalent vaccine Dengvaxia is not optimal for all serotypes and its use is not recommended for DENV-seronegative individuals [13, 14]. Therefore, effective compounds inhibiting ZIKV and DENV replication are urgently required and drugs with broad-spectrum activity against several pathogenic flaviviruses would definitely constitute an asset in the therapeutic arsenal.

Medicinal plants such as Amaryllidaceae contain alkaloids with various biological activities, including anti-mosquito activity against *Aedes aegypti* and antiviral properties [15-19]. The Amaryllidaceae *Crinum macawonii* methanolic extract inhibits *in vitro* infection of yellow fever virus (YFV) and Japanese encephalitis virus (JEV), two flaviviruses [20]. Aqueous and organic extracts from *C. jagus* contain molecules exhibiting anti-inflammatory [21], antibacterial [22] and anti-enterovirus activities [23], while their effect on flaviviruses replication remains unknown. We isolated Amaryllidaceae alkaloids (AAs) lycorine, sanguinine, crinine, gigancrinine, flexinine, cherylline, gigantelline, and gigantellinine and hippadine (an amide close to lycorine) from *C. jagus (giganteum)* and showed that some display cytotoxic activity and anti-acetylcholinesterase potential [24]. In preceding studies, lycorine was shown to inhibit *Flaviviridae* such as flaviviruses DENV, ZIKV, YFV, JEV and several viruses from other families including *Retroviridae* (HIV-1), *Coronaviridae*, as well as DNA viruses [25-32]. Except for lycorine, the antiviral potential of AAs has been poorly studied. Continuing our screening of biological activities of native and under-studied Amaryllidaceae from Senegal, we investigated *C. jagus'*s alkaloids potential. We hypothesized that *C. jagus* extract displays antiflaviviral properties, and that it contains alkaloids with antiflaviviral potential in addition to lycorine.

In this study, we assessed the *in cellulo* antiviral activity of AAs isolated from *C. jagus* and identified cherylline as a novel inhibitor of DENV and ZIKV life cycle. Using time-of-drug-addition and -removal assays, as well as modified DENV genomes, we further showed that the viral RNA replication step of DENV life cycle is the main target of cherylline. This comprehensive assessment uncovers cherylline as a new natural product candidate to be optimized for the development of therapeutics to fight flavivirus infections.

Materials and methods

Crinum jagus crude extract and GC-MS analyis

Bulbs of *C. jagus (giganteum)* were collected in Senegal, in Montrolland district (14°55'56,22''N and 16°59'38,62''W) in 2018 and taxonomically identified by a senior scientist from the Herbarium of IFAN of University Cheikh Anta Diop of Dakar. Alkaloids were extracted from dried bulbs of *C. jagus* using the method described in [33]. High-performance liquid chromatography with a diode-array detector (HPLC-DAD) and thin layer chromatography (TLC) confirmed the presence of alkaloids in the extract. Gas chromatography-mass spectrometry (GC-MS) analysis were performed using the method described in [34]. Alkaloids were identified by comparison with the National Institute of Standards and Technology (NIST 05) database based on matching mass spectra. Total ion current (TIC) percentage provided in Table 1 was connotated with the proportion of each compound in the extract. The area under the GC-MS peaks depends both on the concentration of the related compounds and on the intensity of their mass spectrum.

Table 1. Alkaloids identified by GC-MS in C. jagus bulb extract. Values are expressed as percentages of total ion current (TIC) for the relative quantitative (CJ).

Alkaloid	[M⁺]	B.P.	R.T. (min)	CJ (%)	Identification
Vittatine / Crinine	271	271	21.871	24.418	NIST 05 Database
Cherylline	285	242	23.173	9.413	NIST 05 Database
Lycorine	287	226	25.871	19.68	NIST 05 Database
Unidentified	299	225	23.531	31.422	n/a
Unidentified	315	241	25.030	15.68	n/a

BP: base peak, RT: retention time (in minute), CJ: *C. jagus*, n/a: not applicable.

Amaryllidaceae alkaloids

Lycorine, hippadine, sanguinine, crinine, gigancrinine, flexinine, cherylline, gigantelline, and gigantellinine were isolated from *C. jagus* as reported in [24]. Their purity >98%, was ascertained by ^{1}H NMR and LC/MS spectrometry. Each AA was dissolved in dimethylsulfoxide (DMSO) at 100 mM as a stock solution and stored at -20 °C until further usage. At the time of use, they were diluted in Dulbecco's Modified Eagle's Medium high glucose (DMEM) or Roswell Park Memorial Institute medium (RPMI) to the desired concentration. DMSO was used as a negative control, whereas guanosine analogue ribavirin and flaviviral NS5 inhibitor NITD008 (Tocris Bioscience) were used as positive antiviral control.

Cell culture

The human hepatocarcinoma Huh7 cell line was kindly provided by Hugo Soudeyns. Murine LL171 reporter cells [35], CRFK and Huh7 cells were maintained in DMEM, supplemented with 10% fetal bovine serum (FBS) and 1% penicillin-streptomycin (PS) solution (all from Wisent Inc, Canada). Hepatocarcinoma RIG-I-deficient Huh7.5 (a kind gift from Patrick Labonté), and Vero E6 (kindly shared by Tom Hobman) cells were cultured in DMEM (Life Technologies) containing 10% FBS, 1% PS and 1% non-essential amino acids (Thermo Fisher). Human embryonic kidney HEK293T and human monocytic cell line THP-1 were grown in RPMI (Wisent) with 10% FBS and 1% PS. Frozen human peripheral blood mononuclear cells (PBMCs) were obtained using Institutional Review Board (IRB)-approved consent forms and protocols (Stem Cell technologies). They were thawed in 20% FBS containing RPMI pre-warmed at 37 ºC, washed twice and incubated for 6 h. Medium was replaced by RPMI 10% FBS and 1% PS before cytotoxic and antiviral assays. All cells were maintained at 37 ºC and 5% CO_2.

Cytoxicity assay

Cytotoxicity properties were titrated through metabolism monitoring using the XTT (2,3-Bis-(2-Methoxy-4-Nitro-5-Sulfophenyl)-2*H*-Tetrazolium-5-Carboxanilide) assay kit (Roche, Millipore Sigma), as before [24]. Briefly, Huh7 were seeded at $10x10^3$ cells per well in 96-well plates. Concentrations of AAs and controls ranging from 0.4 to 400 µM were added the next day. After 72 h of incubation, medium was replaced by phenol-free DMEM (Wisent) containing 0.3 mg/mL XTT and cells were incubated for 4 h. Absorbance was measured at 450 nm using a microplate spectrophotometer (Synergy H1, Biotek). Control assays in which compounds were omitted (with 0.1% DMSO) were used to assess minimal cytotoxicity. The percentage of cell viability was calculated at each concentration for each AA. Experiments were performed in triplicates and CC_{50} values were calculated. Where indicated for Huh7.5, Vero E6 and PBMCs, cell viability was measured through monitoring of cellular ATP levels using the Cell-Titer GLO assay kit (Promega). Briefly, $10\text{-}20x10^3$ cells in 50-100 µL were seeded in 48-well or 96-well plates and cultured overnight. AAs were added at the designated concentrations for 24 or 48 h, as specified in the text. Then, 50-100 µL of room temperature Cell-Titer GLO reagent was added in each well to room temperature-equilibrated cell plates. Plates were rocked for 2 min, rested for 10 min and the luminescence signal was measured using a microplate spectrophotometer (Biotek Synergy H1 or Tecan Spark® multimode microplate reader). Viability was expressed as a fold change calculated using the value of DMSO-treated cells at each concentration, for each AA.

Preparation of flaviviral genomes

Plasmids for DENV or ZIKV vectors which encode GFP (pFK-DVs-G2A for $DENV_{GFP}$), Renilla luciferase (pFK-DVs-R2A, serotype 2, strain 16681 for $DENV_{R2A}$; pFL-ZIKV-R2A strain FSS13025 for $ZIKV_{R2A}$) reporter genomes, wildtype (WT) DENV (pFK-DVs; 16681), subgenomic (sg) replication-deficient NS5 mutant (sg-DVs-R2A-GND) and WT subgenomic replicon (sg-DVs-R2A-WT) were all obtained from Ralf Bartenschlager and Pei-Yong Shi. Plasmids were linearized with XbaI (DENV) or ClaI (ZIKV), purified and 1 µg was *in vitro* transcribed using mMESSAGE mMACHINE T7 or SP6

transcription kits (Invitrogen). Resulting RNAs quality and concentration were assessed by migration on a 0.8% agarose gel and Nanodrop spectrometry (Thermo Scientific), respectively.

Production of DENV and ZIKV stocks

Subconfluent trypsinized Vero E6 cells were washed once and resuspended in cytomix buffer (120 mM KCl, 0.15 mM $CaCl_2$, 10 mM potassium phosphate buffer, 25 mM HEPES, 2 mM EGTA, 5 mM $MgCl_2$ [pH 7.6], freshly supplemented with 2 mM ATP and 5 mM glutathione) at a density 1.5×10^7 cells/ml, as described in [36]. 10 µg of *in vitro*-transcribed viral RNA genomes (from pFK-DVs, pFK-DVs-R2A; pFK-DVs-GFP; pFL-ZIKV, pFL-ZIKV-R2A) were mixed with 400 µL of cells, transferred into an electroporation cuvette (Bio-Rad; 0.4-cm gap width), and pulsed once with a GenePulser Xcell (Bio-Rad) at 975 µF and 270 V. Cells were immediately transferred to prewarmed complete DMEM and seeded. Culture medium was changed 24 h after electroporation (p.e.). Virus-containing cell culture supernatants were harvested 4 to 8- days p.e., concomitantly with the appearance of cytopathic effect (CPE). Virus stocks were filtered through 0.45 µm syringe filters, supplemented with 10 mM HEPES (pH 7.5), and aliquots were stored at -80°C until use. ZIKV H/PF/2013 (French Polynesia) and ZIKV MR766 (Uganda) virus stock was obtained by the European Virus Archive Global (EVAg). ZIKV stocks (ZIKV H/PF/2013 and ZIKV MR766) were amplified and produced in Vero E6 cells. Plaque assays (described below) were used to determine the infectious titers of the virus stocks [37].

AAs anti-ZIKV and -DENV activity

Briefly, Huh7 cells were seeded at $15x10^3$ cells per well in 48-well plates and cultured for 16 h. Cells were pretreated with indicated concentrations of *C. jagus*' bulbs crude extract or AAs for 2 h and infected with $DENV_{GFP}$ at a MOI of 0.1 to 0.3, depending on the assay, and further incubated for 72 h at 37 ºC. PBMCs were infected with $DENV_{GFP}$ (MOI = 2) pre-incubated with the panflaviviral anti-envelope 4G2 antibody (clone D1-4G2-4-15,

Sigma-Aldrich) for 30 min at 4 ºC to enhance infection through antibody-dependent enhancement [38, 39]. Cells were washed 24 h p.i., and further incubated for 48 h. GFP signal of infected cells was visualized on an Axio Observer microscope (Carl Zeiss, Inc., Toronto, ON, Canada) or measured on a flow cytometer (FC500 MPL cytometer, or a BD FACSMelody, BD Lifesciences-Biosciences) and analyzed with FCS express 6 and FlowJo softwares (BD).

To determine half maximal effective concentration (EC_{50}), Huh7.5 cells were plated in 10-mm petri dishes and infected with $DENV_{R2A}$ and $ZIKV_{R2A}$ (MOI = 0.005). Virus inoculum was removed 2 h p.i., cells were washed with PBS, trypsinized and plated in 96-well plate with various concentrations of AAs. After 48 h, luciferase production was monitored as described below.

Subgenomes RNAs (sg-DVs-R2A-GND, sg-DVs-R2A-WT) were directly transfected into Huh7.5 by electroporation and luminescence was measured at indicated timepoints following the procedures described below.

Luciferase detection

Luminescence emitted from virus-encoded Renilla luciferase (Rluc) was measured to monitor replication (DENV-R2A, sg-DVs-R2A-WT and ZIKV-R2A) or viral protein translation (sgDVs-R2A-GND). Infected cells were lysed in 100 µL lysis buffer (0.1% Triton X-100, 25 mM glycylglycine [pH = 7.8], 15 mM MgSO4, 4 mM EGTA [pH = 8], 1 mM DTT). Rluc assays was performed by injecting 150 µL of assay buffer (25 mM glycylglycine [pH = 7.8], 15 mM MgSO4, 4 mM EGTA [pH = 8], 15 mM K2PO4 [pH = 7.8]) and coelenterazine (1.43 µM, Prolume) to 30 µL of the lysate, as described in [40]. Luminescence was measured in a Spark multimode microplate reader (Tecan).

DENV and ZIKV titration by plaque assay

Huh7.5 cells were infected with DENV 16881s, ZIKV H/PF/2013, ZIKV MR766 (MOI = 0.1) or left uninfected. Viral inoculum was removed 2 h p.i., and cells were treated with AAs, NITD008 or DMSO (vehicle). Supernatants were harvested 2 days p.i. and PFU were determined by plaque assay on VeroE6 cells. Cells incubated overnight (2×10^5 cells/well in 24-well plates) were infected with 10-fold serially diluted virus-containing supernatants for 2 h at 37 °C. Inoculum was then replaced with MEM (Life Technologies) containing 1.5% carboxymethylcellulose (Millipore-Sigma). ZIKV and DENV infected cells were incubated for 5 and 7 days, respectively. One volume of 10% formaldehyde was added to the cells for fixation. Two hours later, cells were washed with tap water and stained with a 1% crystal violet / 10% ethanol solution for 30 minutes. Wells were rinsed with tap water and the number of plaques were counted to calculate virus titers.

Time-of-drug-addition and -removal assays

$1.5x10^4$ Huh7 cells per well were seeded in 48-well plates and infected with $DENV_{GFP}$ at MOI = 0.15. For the time-of-drug addition, at time of infection, AAs were added in wells corresponding to 0 h. Two h p.i., viral inoculum was removed from every well, and AAs were added back at wells corresponding to 0 h and 2 h. At 4, 7, 12, and 24 h p.i., AAs or DMSO diluted in DMEM were added to the appropriate wells. After 72 h, cells were trypsinized and fixed in 4% formaldehyde to measure the percentage of infected cells on a FC500 MPL cytometer. Alternatively, pictures of Hoechst33342-stained cells were acquired on Axio Observer microscope. All assays were performed in triplicate.

For the time-of-drug-removal assay, Huh7 cells were seeded in 48-wells plates ($1.5x10^4$ cells per well), infected with $DENV_{GFP}$ at MOI = 0.15 and treated with medium containing AAs at indicated concentrations at time of infection. At 2 h p.i., plates were washed, and medium was replaced to remove remaining viruses in the supernatant. AAs were added back to all wells, except the ones corresponding to 2 h treatment, in which fresh medium exclusive of any AA was added. Accordingly, after 4, 7 and 12 h of

infection, the supernatant was replaced by fresh medium in corresponding wells. After 72 h of incubation, results were acquired as for time-of-drug-addition assay. All assays were performed in triplicate.

Production of VSV-G-pseudotyped Human immunodeficiency virus (HIV) -1 vectors

pNL4-$3_{GFP\Delta Env\Delta Nef}$ is replication-incompetent due to a deletion that produces a frameshift in *env,* and *nef* is replaced by *gfp* (green fluorescent protein) as described in [41]. pNL4-$3_{GFP\Delta Env\Delta Nef}$ and pMD.G (a plasmid encoding Vesicular Stomatitis Virus G glycoprotein., VSV-G) were prepared from bacterial stocks using the Qiagen MidiPrep kit. To produce HIV-1_{GFP} vectors, plasmids were co-transfected into 90% confluent HEK293T cells in 10-cm culture dishes using polyethylenimine (PEI; polysciences, Niles, II) as described in [42]. Medium was changed 6-16 h post-transfection. Supernatants containing HIV-1_{GFP} were harvested 24 h later, centrifuged for 10 min at 3000 rpm, 0.45 μm-filtered and stored at -80°C. The MOI was assessed by measuring infectivity of serially diluted vector preparation in CRFK cells.

HIV-1GFP infectivity assay

AAs antiretroviral activity was evaluated using HIV-1_{GFP} in THP-1 cells. Briefly, THP-1 cells were seeded at $1.5x10^4$ cells per well in 96 well-plates and incubated overnight. Cells were pretreated with two concentrations of AAs for 2 h and then infected with HIV_{GFP} at a MOI of 1. After 72 h, the percentage of infected cells was measured using a FC500 MPL cytometer (Beckman Coulter, Inc., CA) and analyzed using the FCS express 6 software (De novo software, CA). DMSO and Nevirapine (Sigma-Aldrich, Canada) were used as a negative and a positive control, respectively. All assays were performed in triplicate.

Type I IFN activation assay

In vitro type I IFN activation was measured in LL171 cells using the Luciferase Assay Systems kit (Promega). Briefly, 200 µL LL171 reporter cells (L929 cells expressing an IFN stimulated response element (ISRE)-Luciferase [43]), were seeded at $1.5x10^4$ cells/well in 96-well plates and cultured for 16 h. Medium was replaced with DMEM containing cherylline for 24 h. Supernatant was removed, cells were rinsed with PBS, and lysis buffer was added (Luciferase Assay Reagent, Promega). Then, cells were scraped and transferred into opaque 96 well plates. LAR (Luciferase Assay Reagent, Promega) was added to each well, and luminescence was measured at 480 nm using a microplate spectrophotometer (Synergy H1). 5,6-dimethylxanthenone-4-acetic acid (DMXAA, 20 µg/mL) was used as a positive control. All assays were performed in triplicate.

In silico characterization of cherylline

Tanimoto/Jacquard similarity index was used to compare the AAs structures on the basis of their isomeric SMILES (simplified molecular-input line-entry system) code with a script from RDKit (https://www.rdkit.org). SwissSimilarity was used to screen analogous compounds in the PDB database [44]. SwissTargetPrediction [45], ChemMapper [46] and PharmMapper [47] were used for the virtual reverse screening of cherylline's possible targets. SwissAdme was used to predict Admet properties [48].

Statistical analyses

Graphs and statistical analyses (EC_{50}, CC_{50}) were performed with the GraphPad Prism 7 software. Non-parametric Mann Whitney test was used, and p values ≤ 0.05 were considered significant.

Results

Crinum jagus alkaloid extract displays anti-DENV activity

First, we evaluated the effect of *C. jagus* extract on the replication of DENV. We used GFP-expressing reporter DENV particles for infection (Figure 1A, 1B, 1C). In this system, the GFP coding sequence is included in the unique open reading frame of the viral RNA genome, 103 nucleotides of DENV capsid gene are duplicated and cloned upstream of *gfp*, fused to the capsid gene with a 2A peptide. *Gfp* is translated in frame with the polyprotein. The 2A peptide allows GFP to be proteolytically released from DENV polyprotein during or shortly after translation [49]. Hence, GFP fluorescence is directly proportional to the extent of polyprotein production. This allows to detect viral replication in infected cells using microscopy or flow cytometry. The inhibitory properties of *C. jagus* crude extract were evaluated in Huh7 hepatocarcinoma cells, a classical model for flavivirus study. At concentrations ranging from 0.078 to 2.5 µg/mL, $DENV_{GFP}$ replication was significantly inhibited by the extract (Figure 1B, C). Viral inhibition followed a dose-dependent response with an EC_{50} of 0.25 µg/mL (Figure 1C). At 0.625 µg/mL, no infection could be detected by both flow cytometry and microscopy. We also verified the cytotoxicity of *C. jagus* crude extract antiviral concentrations in Huh7 cells. Extracts were weakly cytotoxic at all concentrations, with a minimum of 71% of viable cells at the highest concentration of 2.5 µg/mL. At 0.625 µg/mL, 100% of the cells were viable while 0% were infected (Figure 1D).

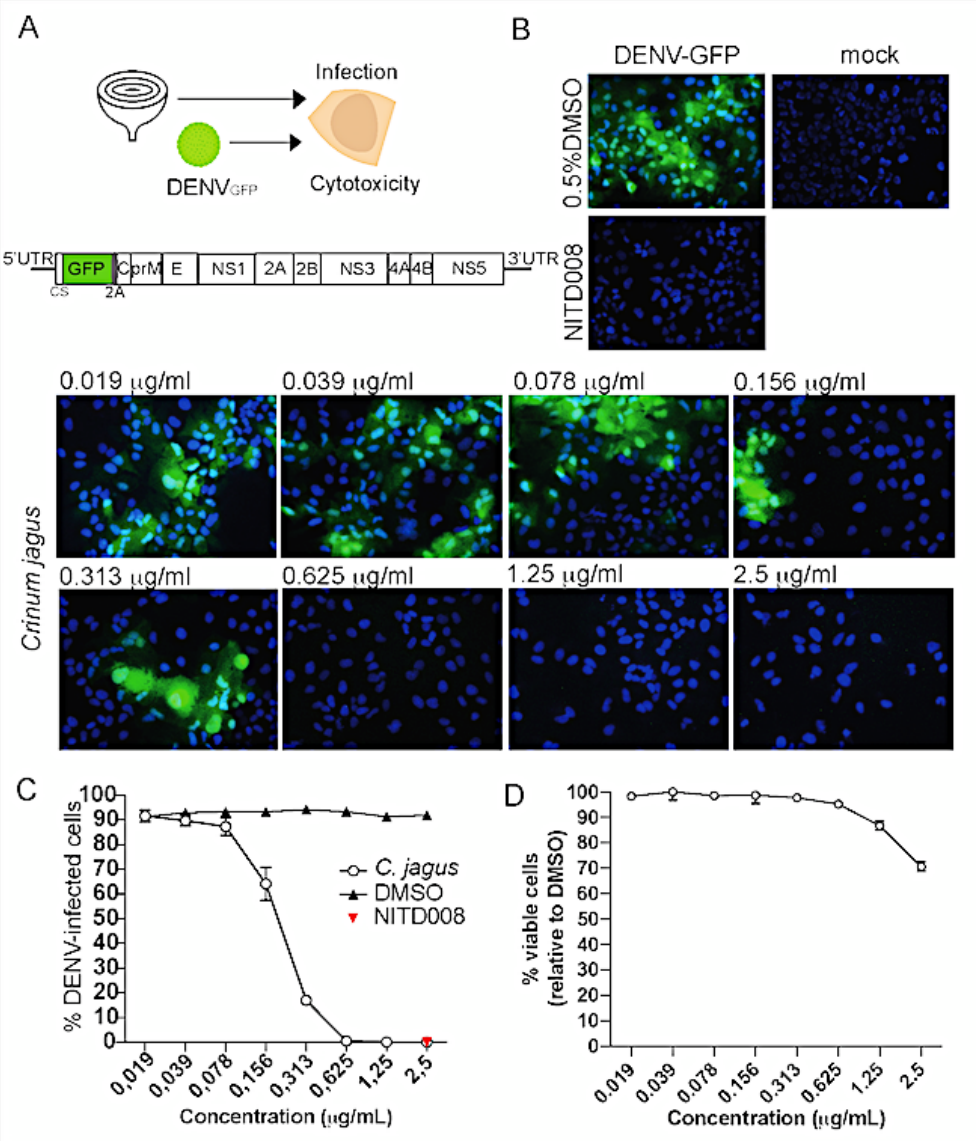

Figure 1 *C*rinum *jagus* alkaloid extract's anti-DENV activity.

We next wanted to gain further knowledge into which AA present in *C. jagus* extract was responsible for the anti-DENV activity. Thus, we studied the nine alkaloids isolated from *C. jagus, i.e.* three cherylline-type: cherylline, gigantelline, gigantellinine, three crinine-type: crinine, gigancrinine, flexinine; one galanthamine-type: sanguinine and lycorine, as sole representant of its own type, and hippadine (Figure 2A; Table S1). Excluding lycorine, the antiflaviviral abilities of these families of AAs are unknown. Huh7 cells were treated with AAs and infected with $DENV_{GFP}$ at a MOI = 0.15, 2 h later. Infection was visualized at 72 hpi by detecting GFP using microscopy (Figure 2B). Treatment with

lycorine caused a sharp decrease in DENV-GFP infected cells, confirming its strong anti-DENV activity. Interestingly, several other AAs were able to inhibit $DENV_{GFP}$ infection. A notably strong antiviral effect was observed in wells in which cells were treated with 50 µM of cherylline, with no detectable infection (Figure 2B and Figure S1). Other AAs displayed antiviral activity with an efficiency ranging from moderate (hippadine, flexinine, gigantellinine), weak (gigantelline) to very weak (sanguinine) at the chosen concentration. Interestingly, AAs of the same ring-type, with very similar structure such as cherylline, gigantelline and gigantellinine presented very distinct strength of inhibition on $DENV_{GFP}$ infectivity. Thus, differences in biological activity were not associated with a specific ring-type.

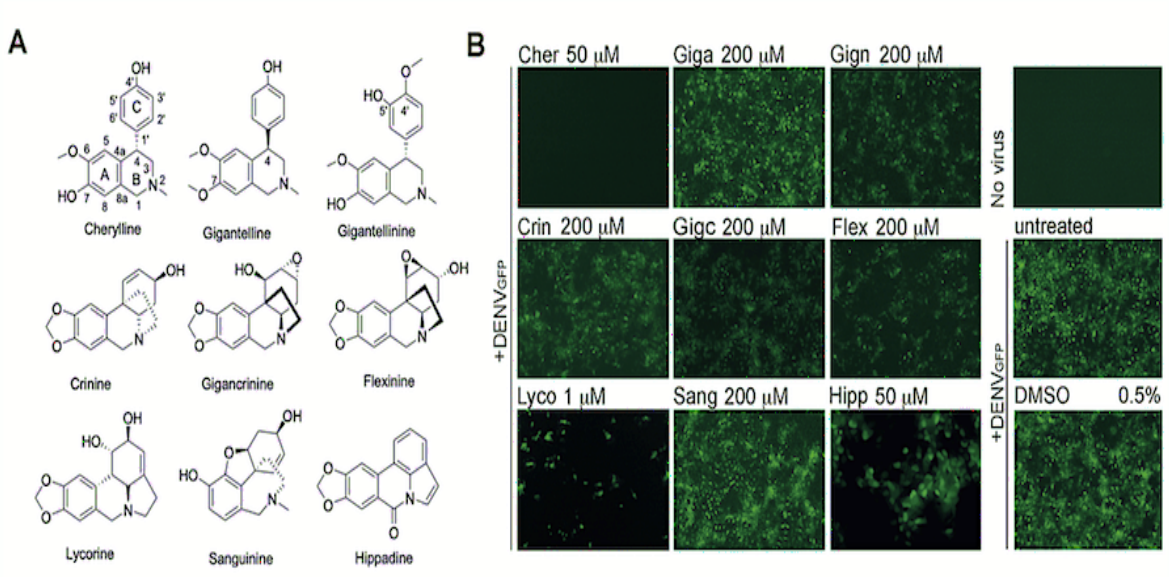

Figure 2 Screening of the anti-DENV activity of *C. jagus* isolated Amaryllidaceae alkaloids (AAs).

Cherylline is a potent inhibitor of DENV

Based on the antiviral activity screening from Figure 2, we pursued the characterization of the four alkaloids with the highest anti-DENV activity.

The antiviral activity of cherylline, hippadine, gigantellinine and flexinine was studied using $DENV_{R2A}$ constructs infection in Huh7.5 cells (Figure 3A, S2A). $DENV_{R2A}$ is

similar to $DENV_{GFP}$, but *Renilla luciferase* replaces *gfp* as reporter gene. NS5 RNA polymerase inhibitor NITD008 was used as a positive control [50, 51]. Infection levels were measured at 48 h p.i. Gigantellinine and flexinine anti-DENV activity required high concentrations (EC_{50} = 104.6 and 63.4 µM, respectively; Figure S2A). Hippadine antiviral activity on $DENV_{R2A}$ was difficult to distinguish from its cytopathic effect (EC_{50} = 73.8; CC_{50} = 175.9 µM; S I= 2.38) (Figure S3, Table 2). Cherylline inhibited $DENV_{R2A}$ replication at an EC_{50} of 8.8 µM (Figure 3A). Cherylline CC_{50} was not reached at the highest tested concentration (250 µM). Its therapeutic selectivity index can not be calculated but is predicted to be > 28 (Table 2). Furthermore, the inhibitory activity of cherylline, our best candidate, was assessed by infecting Huh7 cells with $DENV_{GFP}$ in presence of increasing concentrations (from 0.6 to 100 µM) of compound (Figure 3B and 3C). Interestingly, cherylline was more potent than the guanosine analogue ribavirin to counteract $DENV_{GFP}$ infection, with EC_{50} = 8 µM, similar to its effect on $DENV_{R2A}$, compared to EC_{50} = 100 µM for ribavirin. By microscopy, no infected cells were observed at 50 µM, confirming our first experiment. Several foci of infected cells became visible at 10 µM, whereas most of the cells were infected at 2 µM, and there was no apparent difference with control at 0.4 µM.

Table 2. $EC_{50,}$ CC_{50} and selectivity index of AAs were calculated with GraphPad Prism.

Alkaloids	**CC_{50} (µM)**	**EC_{50} (µM)**		**SI**	
		$DENV_{R2A}$	**$ZIKV_{R2A}$**	**$DENV_{R2A}$**	**$ZIKV_{R2A}$**
Lycorine	14.5	0.16	0.41	90.6	35.4
Cherylline	>250	8.8	20.33	>28	>12.3
Hippadine	175.9	73.8	114	2.38	1.54
Flexinine	>250	63.4	216.3	>3.9	>1.15
Gigantellinine	>250	104.6	>250	>2.3	nd

EC_{50} was determined using $DENV/ZIKV_{R2A}$ infection from 0.05 to 25 µM for lycorine and NITD008, from 0.5 to 250 µM for the others as in Figure 2A. CC_{50} was calculated using the same concentrations in the same cell type, Huh7.5 at 48 hrs post-treatment. CC = cytotoxic concentration, EC = Effective concentration, SI = therapeutic selectivity index.

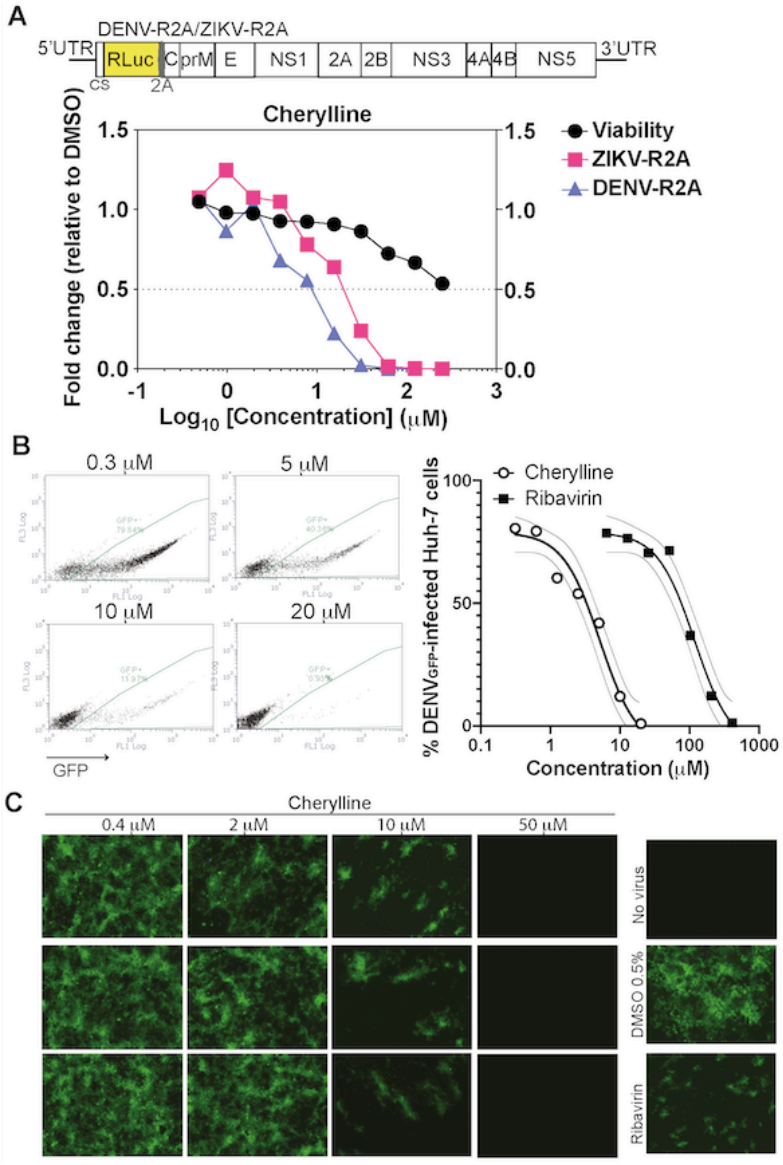

Figure 3 Cherylline displays anti-DENV activity.

To validate the antiviral properties of cherylline, we tested its ability to prevent the production of infectious particles using wild-type viruses instead of reporter infectious systems. We infected Huh7.5 cells with viral strain DENV2 16881s, and then treated with 50 μM of AAs 2 h p.i. (Figure 4A). Forty-eight hours later, cell supernatants were harvested, and extracellular infectious titers determined using plaque assays. In parallel, viability was monitored. As expected, NITD008 completely hindered the production of infectious particles (Figure 4A, S2B). Cherylline induced a 17-fold decrease in DENV 16881s viral titers (Figure 4A, S2B). In contrast, hippadine, gigantellinine and flexinine

treatments exhibited no effects on DENV production (Figure S2B). In conclusion, cherylline holds a notable anti-DENV potential.

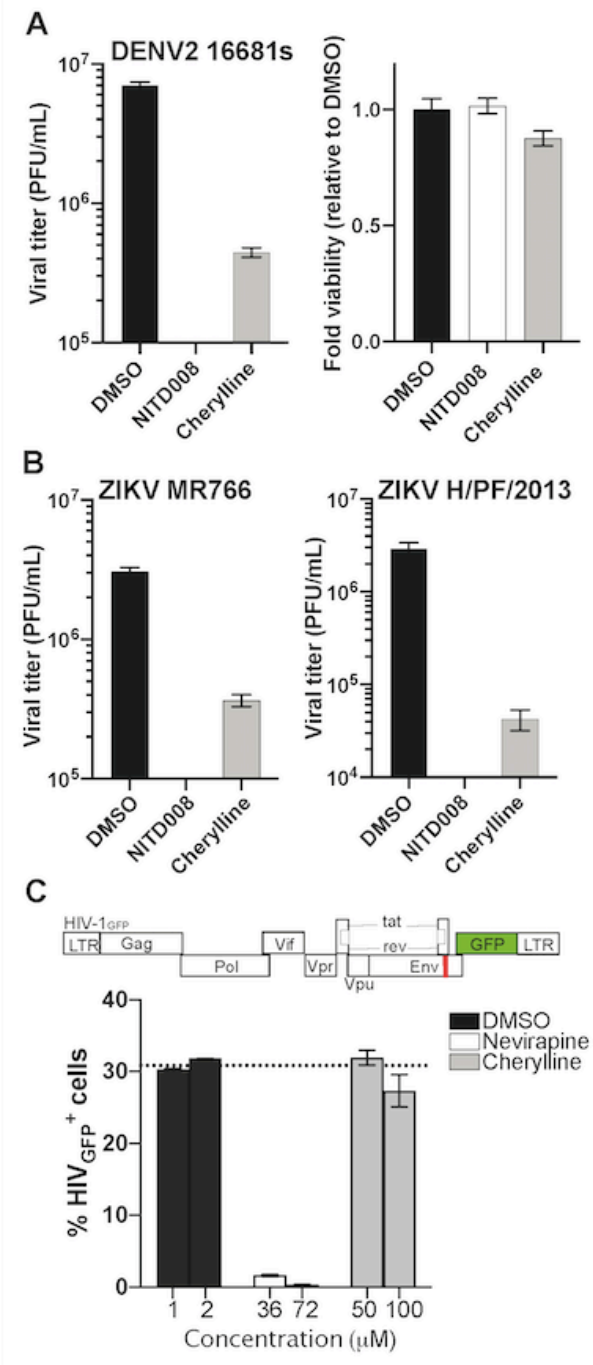

Figure 4 Cherylline displays antiviral activity against DENV and ZIKV.

Cherylline efficiently inhibits ZIKV

Next, we explored if the isolated AAs were also active on a closely related flavivirus. We examined the impact of cherylline, hippadine, gigantellinine and flexinine treatment on $ZIKV_{R2A}$ replication in Huh7.5 cells (Figure 3A, Figure S2A). Cherylline interfered with the replication of ZIKV at non-cytotoxic concentrations, with an EC_{50} = 20.3 µM and a selectivity index >12.3 (Figure 3A; Table 2). Hippadine, gigantellinine and flexinine did not impact significantly $ZIKV_{R2A}$ replication (Figure S2A).

To validate the anti-ZIKV properties of cherylline, we tested its ability to prevent the production of infectious particles using wild-type viral strains ZIKV H/PF/2013, ZIKV MR766 instead of reporter infectious systems, as previously described. NITD008 completely hindered the production of infectious particles for both ZIKV strains (Figure 4B, Figure S2B). Cherylline diminished the pathogenic ZIKV H/PF/2013 strain viral titer by 100-fold and ZIKV MR766 by 88% (Figure 4B and Figure S2B).

In contrast, hippadine treatment resulted in a moderate 3-fold (70%) decrease in ZIKV H/PF/2013 viral titers, while gigantellinine and flexinine treatments exhibited marginal effects on ZIKV production (Figure S2B). In conclusion, the plaque assay using WT viruses indicate that cherylline impedes the DENV2 and ZIKV life cycles.

Cherylline does not inhibit HIV-1 infection and the interferon response

Lycorine has been described as a broantiviral agent, inhibiting many viruses, including flaviviruses and retroviruses. To get insight into the specificity of cherylline antiviral spectrum, we examined its effect on VSV-G-pseudotyped-$HIV\text{-}1_{GFP}$ vector (Figure 4C). This vector does not enter through fusion into cytoplasm, but rather through endocytosis. It undergoes an incomplete single-cycle infection that include uncoating, reverse transcriptase, nuclear transport, provirus integration, virus genes transcription and mRNA translation. With the exception of Env and Nef, viral proteins are produced but do not assemble together to form new virions. Cherylline did not affect HIV-1 infection, nor did any of the AA tested (Figure S2C). We also assessed that cherylline did not trigger

significant amount of type I IFN through monitoring of ISRE-transcription compared to control treatments (Figure S3A). These results demonstrate that cherylline specifically targets several flaviviruses with less cytotoxicity than lycorine (Table 2).

Cherylline targets DENV RNA replication

We next investigated which step of DENV life cycle was inhibited by cherylline. DENV viral replication kinetics have been widely studied [52]. Timing of infection can be precisely associated with viral steps (Figure 5A, 5B). Binding and virus entry occur during the first 2 h of viral addition [53]. First, cells were treated with alkaloids 2 h prior to infection. We compared infection levels in cells with continuous treatment *vs.*, cells in which cherylline was removed 2 h p.i. (Figure 5A). DMSO was used as a negative control. Guanosine analogue ribavirin was added as a positive control. Its removal 2 h p.i. did not impact viral replication to levels comparable to DMSO treatment suggesting that cherylline targets a viral process occuring after that time point (Figure 5A). Similarly, cherylline removal 2 h p.i. restored virus replication completely (Figure 5A), as did hippadine, flexinine, gigantellinine, sanguinine and crinine (Figure S3B). Restoration of infection upon removal confirmed that cherylline is not virucidal and that it inhibits a step downstream viral entry. Following viral endocytosis, initiation of translation of viral RNA and protein maturation begins as early as 1 h p.i. RNA synthesis follows 6 h p.i., and virion assembly, maturation and exocytosis arise from 12 h p.i. We tested the impact cherylline addition at 0, 2, 4, 7, 12 and 24 h p.i. on the % of $DENV_{GFP}$ infected Huh7 cells 72 h p.i. As expected, the RNA synthesis inhibitor NITD008 abrogated GFP expression when added at 0, 2, 4, 7, or 12 h p.i., prior or during RNA synthesis (Figure 5C). Low levels of infection rose when NITD008 was added at 24 h p.i., confirming its activity at prior timing of DENV life cycle, during RNA replication. Cherylline entirely blocked viral replication when added between 0-7 h p.i. (Figure 5C), supporting that it acts at a post-entry step of the viral cycle that occurs from/after 7 h p.i. At 12 h p.i., some of cherylline antiviral activity was lost, suggesting that it optimally acts before that time of the life cycle. From our previous experiment (Figure 5B), we excluded an effect on virion infectivity

and viral entry, while these results suggest that cherylline possibly targets either translation, protein maturation, or RNA replication.

Next, cherylline was added to the cells at the time of infection and then removed at each indicated time point (Figure 5C, 5D). After removal of compounds, successfully produced DENV infectious particles replicate further until the time of analysis, amplifying overall infection levels. As expected, the effect of the NS5 inhibitor NITD008 was lost when the drug was removed at 2 and 4 h p.i., before RNA synthesis initiation. The continuing presence of the drug until 7 h p.i. was necessary to its the antiviral activity. Cherylline-dependent inhibition of viral replication was lost when the AA was removed at 2, 4 or 7 h p.i., while its presence for the first 12 h of the viral life cycle successfully impaired DENV replication. Similar kinetics of inhibition were observed for the other AAs tested (Figure S4A and B). Altogether, these results indicate that cherylline acts during the RNA synthesis of DENV life cycle. This is further supported by the fact the profile of cherylline inhibition kinetics closely mirrors the one of NITD008, a potent flaviviral polymerase inhibitor.

We next challenged this mode-of-action model in an experimental set-up in which the viral RNA genomes replicates without the entry and assembly steps. We took advantage of DENV subgenomic (sg) replicons (sgDVs-R2A WT), and RNA genomes that are defective in RNA replication (sg_DVs-R2A GND, mutated GDD motif in NS5 RdRp) (Figure 4. 5E). None of these genomes express structural proteins in transfected cells, hence, no viral particles are produced and neither virus release nor entry occur. sgDVs-R2A WT RNA replicates and is translated like the WT full length genome, luciferase emission is directly proportional to the efficacy of viral RNA replication and translation. *In vitro* transcribed sgDVs-R2A WT RNA was transfected into Huh7.5 cells and treated with DMSO, NITD008, or cherylline. At 48-72 h p.e., both compounds were efficient in blocking viral RNA replication (3 $\log_{10}$ reduction of RLU) during steps that occurred after entry and before release (Figure 5F and Figure S4C). In contrast, sgDVs-R2A GND does not replicate (Figure S4D), and hence luciferase activity 4 hours post-electroporation (p.e.) reflects the efficacy of DENV RNA translation (Figure 5E). Transfection using the RdRp-

deficient replicon led to a very different profile. In control DMSO-treated cells, luciferase luminescence was high at 4 h p.e., and waned significantly at 24 h, in accordance with the absence of replication of this system (Figure S4D). Cherylline, similarly to NITD008 had no effect on the luminescence of this genome at 4 h p.e., demonstrating that they do not interfere with protein synthesis (Figure 5G). Altogether, these results unambiguously demonstrate that cherylline disrupts the RNA synthesis step of DENV life cycle but not infectivity, entry and translation.

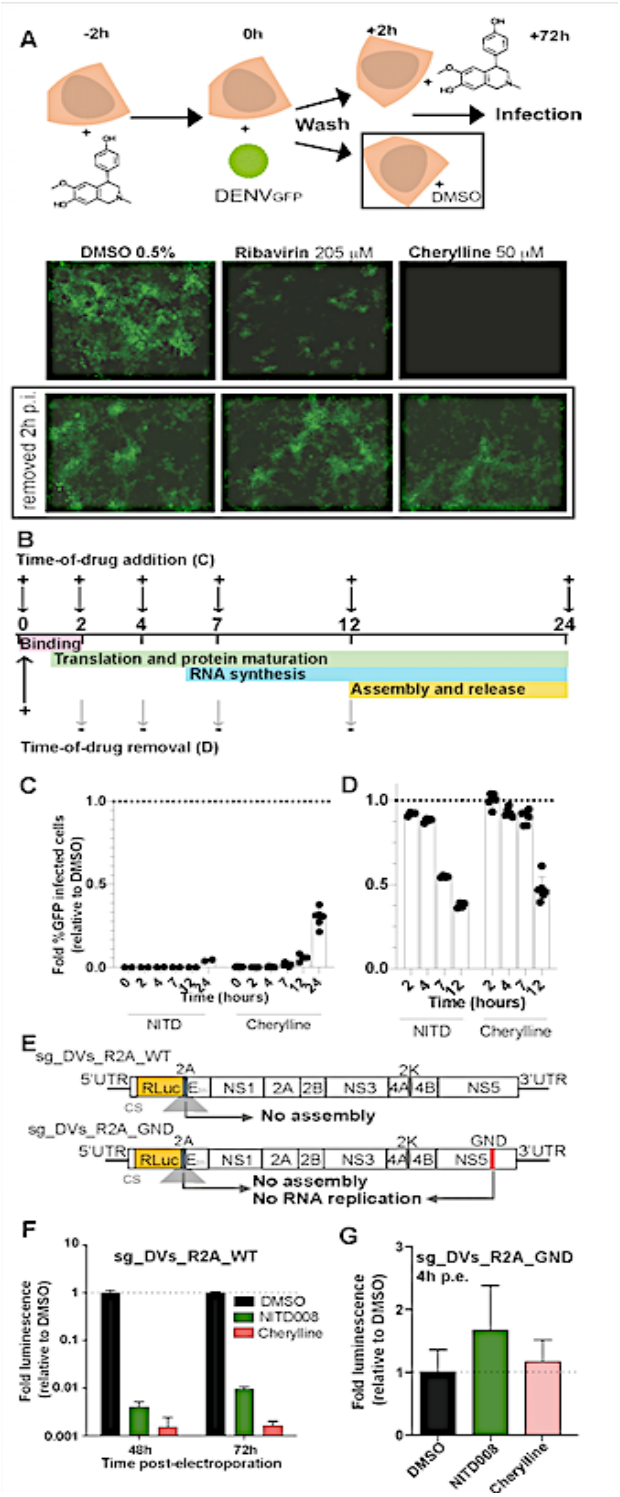

Figure 5 Cherylline blocks DENV replication during RNA synthesis.

In silico reverse screening of cherylline targets

Cherylline has been poorly studied and its cellular and viral targets are unknown. We used *in silico* algorithms to get more insight into cherylline's possible mode of action. Shape- and pharmacophore-based reverse screening with PharmMapper, ChemMapper, SwissSimilarity and Swisstarget did not uncover any viral protein as hits, indicating that cherylline is not homologous to any currently known viral inhibitors included in the databases that were screened. Several human proteins such as dopamine and estrogen receptors, as well as neurotransmitters transporters, and cell division protein kinase 5 were predicted to interact with cherylline (Table S2, S3), suggesting that it might target cellular proteins implicated in the viral life cycle. Interestingly, estrogen and neurotransmitters interacting proteins were most often uncovered as hits. Finally, we used SwissAdme to calculate ADME (absorption, distribution, metabolism, excretion) and Lipinski's parameters of cherylline (Table S4) and other AAs. Cherylline structure respects the five rules of Lipinski with a molecular weight <500 Da, a liposolubility (octanol/water) logP<4.15, less than 10 electron acceptors and less than 5 donors, and a biodisponibility score of 0.55. This prediction suggests that cherylline possesses the chemical properties that are compatible with a therapeutic usage in humans.

Cherylline inhibits DENV infection in peripheral blood mononuclear cells

Finally, we wanted to validate cherylline antiflaviviral potential in a human primary cell model relevant to dengue disease, namely peripheral blood mononuclear cells (PBMC) [54]. PBMCs were infected with $DENV_{GFP}$ particles which were pre-incubated with a panflaviviral anti-envelope antibody to increase infection levels in monocytes through antibody-dependent enhancement [55, 56]. Infected PBMCs were then treated during 72 hours with 30 µM cherylline, a concentration that was not toxic for these primary cells (Figure 6A). Of note, NITD008 was excluded from further analysis because it was cytotoxic in PBMCs. The percentage of infected cells (GFP-positive cells) was determined using flow cytometry (Figure 6B). In DMSO treated control cells, GFP intensity was low but readily detectable, and a median of 0.6% GFP^+ cells were productively infected with $DENV_{GFP}$. Cherylline treatment led to a 5.3-fold decrease in the % of GFP^+ cells

($p = 0.0011$, Mann-Whitney test), with a median of 0.1% GFP^+ cells, similar to background levels (Figure 6C). These results validate the anti-DENV potential of cherylline in human primary blood cells, a target of DENV during pathogenesis.

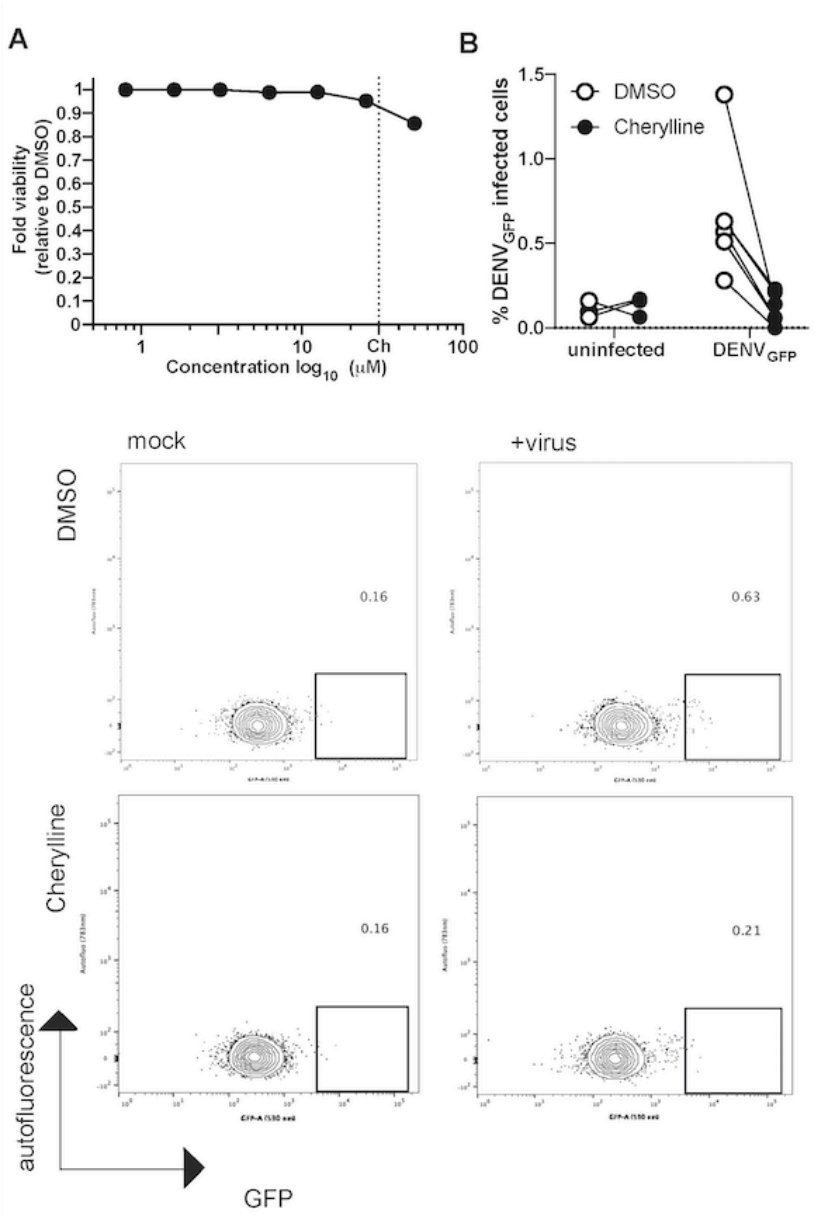

Figure 6 Cytotoxicity and antiviral effects of cherylline in PBMCs.

Discussion

In a previous study, we showed that several alkaloids from *C. jagus* display cytotoxicity and anticholinesterase activity [24]. Here, we uncovered that crude alkaloid extract from *Crinum jagus* inhibited DENV infection *in cellulo*. We further investigated the antiviral potential of the 9 alkaloids of crinine, lycorine, galanthamine and cherylline ring-types isolated from this plant. While lycorine's anti-viral activity is well-known, other AAs potential has not been previously characterized. Here, we investigated their activity on DENV and ZIKV and HIV-1 infection.

First, we discovered that in addition to lycorine, *C. jagus* extract contains another compound that efficiently blocks DENV, namely cherylline. Other AAs isolated from *C. jagus* displayed weak activity at high concentrations (gigantelline, gigantellinine and crinine- and galanthamine-type structures) or were highly cytotoxic (hippadine).

We confirmed the anti-DENV activity of cherylline measuring the inhibition of viral replication through modulation of the Rluc reporter gene expression. Because of the genetic proximity between DENV and ZIKV proteins, we tested cherylline anti-ZIKV activity and determined that it also efficiently blocked ZIKV replication. Then, to gain understanding about the specificity of cherylline's antiviral activity, we tested its effect on HIV-1 using a replication-deficient virus pseudotyped with a VSV-G envelope. Thus, if entry, assembly or release were targeted by tested compounds, this would be missed by the current assay. We did not detect any antiretroviral activity from cherylline, nor from any of the AAs tested against this virus. Lycorine was reported to inhibit HIV-1 infection in some studies [57, 58], while others have demonstrated that it was a very poor inhibitor of HIV-1 RT [59], or that it did not inhibit HIV-1 [26]. Its cytotoxicity could be responsible for these discrepancies, as even at antiviral concentrations (1-5 μM), lycorine treatment can non-specifically increase the detected antiviral activity because of the progressive depletion of viable permissive cells. Nonetheless, our results unequivocally show that HIV-1 life cycle steps between entry and release are not targeted by studied AAs in THP-1 cells. Interestingly, a study published in 1989 reported that cherylline derivatives had no significant effect against DNA virus herpes simplex virus [60].

Altogether, this suggests that cherylline antiviral activity exhibit some selectivity to flaviviruses.

Then, we assessed the effect of cherylline on the replication of WT strains of ZIKV and DENV2. Cherylline dampened viral titers from the pathogenic ZIKV H/PF/2013 strain of about a 100-fold. It diminished replication of WT ZIKV MR766 and WT DENV2 16881s 8- and 17-fold, to very low levels compared to control. Hippadine hindered French Polynesian ZIKV replication, albeit at concentrations that displayed cytotoxicity. It had little effect on propagation of other strains of ZIKV and on WT DENV-2. Gigantellinine and flexinine had little effect on all three viral strains.

Having established that cherylline inhibited flavivirus infection, we investigated the life cycle steps that could be targeted. We removed the drug 2 h p.i., which abolished its antiviral effect, showing that cherylline was not viricidal and that it did not prevent binding nor viral entry into cells. We pursued to identify the viral step that was targeted using time-of-drug-addition and -removal assays. Cherylline treatment did severely impede viral replication when added between 0-7 h p.i., whereas its antiviral potency was lost when removed at 2, 4 or 7 h p.i. and recovered at 12 h p.i. Thus, its presence between 7 to 12 h p.i. is required to successfully impair infection, suggesting that it acts at a post-entry step, possibly during RNA synthesis. By using subgenomic replicons and replication-deficient genomes, we confirmed that cherylline did inhibit the RNA replication step of DENV life cycle but did not target infectivity, entry, or translation.

The replication complex of DENV virus in the endoplasmic reticulum is comprised of its non-structural proteins in interaction with several cellular proteins, all playing a key role in viral replication [36, 61-63]. Lycorine also inhibits the RNA replication step, but the exact mechanism is not known. Chen *et al.* have shown that high concentrations of lycorine (100 μM) inhibited 80% of ZIKV NS5 RdRp activity *in vitro* [28], but this concentration is a 100-fold higher than what is tolerated by cells. Others reported that lycorine had no effect on West Nile virus NS5, but rather that its activity was dependent on the valine at the 9th position of the 2K peptide [27]. The 2K peptide is part of the

replication complex, playing a key role in polyprotein maturation and topology as well as in replication organelle biogenesis [64-67]. Lycorine and cherylline structures contain distinct ring types. Although AAs are known for their pleiotropic effects, cherylline does not display the same broad antiviral spectrum as lycorine. Cherylline could target multiple proteins to achieve its antiviral activity. It could interact with human proteins rather than viral proteins, such as dopamine and estrogen receptors, as predicted by *in silico* reverse screening. Indeed, dopamine receptor D1 and D4 antagonists prochlorperazine and dihydrobenzothiepines have been described to inhibit DENV replication [68, 69], but they target early steps of DENV replication, *i.e.* viral binding and entry, in contrast to cherylline. Recently, estrogen receptor modulators have also been identified as flavivirus inhibitors independently of the estrogen receptor itself. Cyclofenil which interacts with NS1, and raloxifene both target RNA replication and polyprotein translation by an unknown mechanism [70, 71]. Cyclofenil also impacted on viral assembly/maturation [71]. Although these inhibitors do not share the same mode of action as cherylline, this emphasizes that many cellular or viral proteins could be targeted by the AA. In any case, further investigations are required to uncover the target, which will enable interaction studies, potentially optimization and identification of resistance mechanism.

Despite their strong similitude in structure with cherylline (Figure 2A), gigantelline and gigantellinine effects were much poorer. These disparities are probably due to distinct functionalization or stereochemistry of their shared carbon skeleton. As cherylline and gigantellinine hold the same stereochemistry, the distinction between the two compounds associated with the reduction of antiviral potential rather lies on the presence of a further hydroxyl group at C-5' and/or methyoxylation of the hydroxyl group at C-4' in the C-ring of gigantellinine. In the case of gigantelline, the further loss of activity is associated with a singular stereochemistry of the junction between B/C rings and/or to the methoxylation of the hydroxyl group at C-7 of its A ring. Palmatine, another isoquinoline alkaloid, was shown to display anti-flaviviral potential, albeit higher concentrations were required to inhibit DENV with higher cytotoxicity (EC_{50} = 26,4 µM and CC_{50} = 1,031 µM) [72]. Plamatine' structure is distinct from cherylline's in several aspects, highlighting that the *para*-substituted phenol ring could play a role in the observed differences in antiviral

activity. Thus, our study provides some insight into cherylline structural determinants required for its antiflaviviral activity, which will have to be taken into consideration for chemical optimization in future structure-activity relationship studies.

Finally, we validated cherylline antiviral activity in human primary blood cells that are targeted by DENV in the natural course of infection *in vivo*. This cell population includes monocytes, which are believed to be main targets of DENV and to contribute to viral dissemination. Cherylline was not cytotoxic to PBMCs and efficiently inhibited $DENV_{GFP}$ infection in these cells. Importantly, lycorine has been successfully used in mice to fight ZIKV [73], highlighting that AAs may provide therapeutic gain. Although cherylline can be extracted from several Amaryllidaceae species, mostly from *Crinum* genus [74-76], it is considered as a rare alkaloid. Fortunately, cherylline chemical synthesis has been successfully performed through several methods [77-79], as reviewed in [80], providing an alternative way of production. AAs biosynthesis pathway is beginning to be uncovered [15], once the enzymes responsible for cherylline synthesis are confirmed, exogenous introduction of encoding genes into yeasts or microalgae will be an interesting strategy to produce AAs.

Conclusion

Until now, cherylline was mostly known for its moderate anti-acetylcholinesterase activity and has never been associated with antiflaviviral activity before, nor have any derivatives. We show that most AAs from *Crinum jagus* display a low to moderate effect against DENV. Our study shows that cherylline inhibits replication of both DENV and ZIKV. Although the EC_{50} obtained for cherylline was quite high, its low cytotoxicity in PBMCs places it an interesting lead compound to fight DENV and ZIKV and could pave the way to new therapeutic strategies.

Acknowledgements

The authors wish to thank Professors Celine Van Themsche, Maria-Grazia Martinoli and Carlos Reyes Moreno for generously sharing their laboratory equipment and material. We are grateful to Dr. Pei-Yong Shi and the World Reference Center for Emerging Viruses and Arboviruses (WRCEVA) for providing the ZIKV reporter system, and Dr. Ralf Bartenschlager (University of Heidelberg) for all DENV reporter constructs. We thank the European Virus Archive goes Global (EVAg) and Dr. Xavier de Lamballerie (Emergence des Pathologies Virales, Aix-Marseille University) for providing ZIKV MR766 and H/PF/2013 original stocks. We are grateful to Dr Patrick Labonté (Institut National de la Recherche Scientifique), Dr Tom Hobman (University of Alberta) and Dr. Anil Kumar (University of Saskatchewan) for generously providing Huh7.5 and Vero E6. cells. We would like to thank the Government of Senegal for awarding a scholarship to S.K. This work was funded by the Canada Research Chair on plant specialized metabolism Award No 950-232164 to I.D-P. Thanks are extended to the Canadian taxpayers and to the Canadian government for supporting the Canada Research Chairs Program.

Figure Legends

Figure 1. A. Schematic experimental design of the antiviral assay using *Crinum jagus* bulbs and DENV, with $DENV_{GFP}$ construct genome representation. In this system produced by Fishl et al, 103 nucleotides of DENV capsid gene were duplicated and cloned upstream of *gfp*, which was then fused to the capsid gene with a 2A peptide (47). *Gfp* is replicated as part of the viral genome and translated as a component of the polyprotein. The 2A peptide allows GFP to be released from DENV polyprotein during or following the translation process. B. Inhibition of DENVGFP infection with *C. jagus* alkaloid extract observed by inverted microscopy in Huh7 cells. Representative images are shown with cell nuclei stained with Hoechst33342 (blue) and DENV infection (green). C. Anti-DENV activity of *C. jagus* crude extracts. The inhibition of DENVGFP infection in Huh7 cells by *C. jagus* alkaloid extract dilutions was measured by flow cytometry. D. Cytotoxicity of *C. jagus* bulbs crude alkaloid extract in Huh7 cells as measured by the XTT assay.

Figure 2. A. Structures of the nine AAs isolated from bulbs of *C. jagus*. Cherylline-type alkaloids included cherylline, gigantelline and gigantellinine, while crinine-type included crinine, gigancrinine and flexinine. Lycorine, sanguinine and hippadine were also isolated. B. Anti-DENV activity of AAs. Huh7 cells were treated with compounds (AAs or DMSO vehicle) for 2 h and then infected with $DENV_{GFP}$ at MOI = 0.15 for 72 h. Infectivity was visualized as GFP+ cells on an inverted microscope system with 5X and 20X (hippadine) objectives. Experiment was performed in triplicates at two dilutions. At least 3 pictures were taken from each well. One representative picture of the lowest dilution is displayed. Cher: cherylline, Giga: gigantelline, Gign: gigantellinine, Crin: crinine, Gigc: gigancrinine, Flex: flexinine: Lyco: lycorine, Sang: sanguinine, Hipp: hippadine.

Figure 3. A. Impact of cherylline treatment on $DENV_{R2A}$ (purple) and $ZIKV_{R2A}$ (pink) replication was tested in Huh7.5 cells (MOI = 0.001), and viral-dependent luciferase luminescence was measured at 48 h p.i. Cell viablity (ATP) was assessed at 48 h. Results are displayed as fold changes in viability and replication, 1 meaning no change compared to matched concentrations of DMSO treated cells. B. Treatment of Huh7 with cherylline dampened infectivity of $DENV_{GFP}$ replication (MOI = 0.15) in a dose-

dependent manner, as measured by flow cytometry 72h p.i. Left, representative dot plots, right, % of Huh7 infected cells using 0.6 to 100 mM of cherylline and 10 to 500 mM of ribavirin as a positive control. The non-linear regression curve fit is shown with the 95% of confidence interval in finer lines. C. Representative pictures of Huh7 treated with different concentrations of cherylline and infected with $DENV_{GFP}$ at MOI = 0.15. Ribavirin was used as a positive control, DMSO as a negative control. Infected cells were visualized on an inverted microscope system at 72 h p.i.

Figure 4. A. Viral titers were measured by plaque assay on Vero E6 cells using cytopathic WT DENV2 16881s strains. Huh7.5 cells were infected and treated 2 h p.i. with compounds. 48 h later, supernatants were harvested and plated on Vero E6 cells (left). Fold changes in viability (ATP) were calculated at 48 h p.i. in Huh7.5 cells (righy). B. Viral titers were measured as in (A) on Vero E6 cells using cytopathic WT Uganda MR766 ZIKV strains (left) and French Polynesia H/PF/2013 (right). C. THP-1 cells were treated with two concentrations of each compound in triplicates for 2 h and infected with VSV-G pseudotyped HIV-1GFP at MOI = 1. The antiretroviral nevirapine was used as a positive control, and DMSO (vehicle) as negative control. Results were analyzed by flow cytometry 72 h p.i.

Figure 5. A. Infectivity of DENV in Huh7 cells continuously treated with cherylline compared to cells treated only for 2 h p.i. DMSO was used as a negative control, ribavirin, as positive antiviral control. Representative pictures taken at 5X with an inverted microscope system are shown. B. Schematic explanation of time-of-drug-addition and -removal rationale. + means addition of compound; - means removal. C. Time-of-drug-addition. D. Time-of-drug-removal. For C. and D., $DENV_{GFP}$ was used at MOI = 0.1; DMSO was used as a negative control and fold infectivity relative to control was calculated. A 1-fold means that the level of infection is the same as control. NITD008 (NITD) was used at 10 μM as a positive antiviral control targeting RNA synthesis. Cherylline was used at 50 μM. The impact of addition and removal of NITD and cherylline at 0, 2, 4, 7, 12 and 24 h p.i. on the % of $DENV_{GFP}$ infected Huh7 cells was monitored by flow cytometry at 72 h p.i. Experiments was performed in triplicates twice. Means with

SEM are shown. E. Schematic representation of subgenomic replicon sg_DVs_R2A_WT and subgenome sgDVs_R2A_GND used in F and G. Sgs were transfected into Huh7.5 cells, which were then treated with DMSO, NITD (5 μM), or cherylline (50 μM) at the indicated time. F. Luciferase levels were quantified at 48 and 72 h post-electroporation (p.e.) with sg_DVs_R2A_WT and normalized over levels detected in DMSO-treated. F. Luciferase levels were quantified at 4 h p.e. with RdRp deficient sg_DVs_R2A_GND and normalized over levels in cells treated with DMSO**.**

Figure 6. A. Cytotoxicity of antiviral concentrations of cherylline in PBMCs was measured by ATP production and normalized over DMSO at 48 h post-treatment. Means with SEM are shown. Dotted lines represent the concentration used in the antiviral assay. Ch: cherylline. B. Antiviral activity of cherylline in PBMCs. PBMCs were infected with $DENV_{GFP}$ pre-incubated with anti-Enveloppe antibody 4G2 at MOI = 2, treated with cherylline (30 μM), or DMSO (0.05%) and analyzed 72 hours p.i. by flow cytometry. Experiment was performed in triplicates (uninfected) and six-plicates (infected). Representative plots are shown.

References

1. Lambrechts, L.; Scott, T. W.; Gubler, D. J., Consequences of the expanding global distribution of Aedes albopictus for dengue virus transmission. *PLOS Neglected Tropical Diseasis* **2010,** *4* (5), e646.

2. Dwivedi, V. D.; Tripathi, I. P.; Tripathi, R. C.; Bharadwaj, S.; Mishra, S. K., Genomics, proteomics and evolution of dengue virus. *Briefings in Functional Genomic* **2017,** *16* (4), 217-27.

3. Rossmann, M.; Kuhn, R.; Zhang, W.; Pletnev, S.; Corver, J.; Lenches, E.; Jones, C.; Mukhopadhyay, S.; Chipman, P.; Strauss, E. In *Structure of dengue virus: implications for flavivirus organization, maturation, and fusion*, Acta Crystallographica a-Foundation and Advances, Int Union Crystallography 2 Abbey SQ, Chester, CH1 2HU, England: 2002; pp C6-C.

4. Rodenhuis-Zybert, I. A.; Wilschut, J.; Smit, J. M., Dengue virus life cycle: viral and host factors modulating infectivity. *CMLS* **2010,** *67* (16), 2773-86.

5. Quintana, V.; Selisko, B.; Brunetti, J.; Eydoux, C.; Guillemot, J.; Canard, B.; Damonte, E.; Julander, J.; Castilla, V., Antiviral activity of the natural alkaloid anisomycin against dengue and Zika viruses. *Antiviral Research* **2020,** *176*, 104749.

6. Gubler, D. J., Dengue and dengue hemorrhagic fever. *Clinical microbiology Reviews* **1998,** *11* (3), 480-96.

7. Factsheets, W. W. H. O.-. Dengue and Severe Dengue. **2017**.

8. Indu, P.; Arunagirinathan, N.; Rameshkumar, M. R.; Sangeetha, K.; Divyadarshini, A.; Rajarajan, S., Antiviral activity of astragaloside II, astragaloside III and astragaloside IV compounds against dengue virus: Computational docking and in vitro studies. *Microbial Pathogenesis* **2020**, 104563.

9. Dieng, I.; Cunha, M.; Diagne, M. M.; Sembène, P. M.; Zanotto, P. M. d. A.; Faye, O.; Faye, O., Origin and Spread of the Dengue Virus Type 1, Genotype V in Senegal, 2015–2019. *Viruses* **2021,** *13* (1), 57.

10. Petersen, L. R.; Jamieson, D. J.; Powers, A. M.; Honein, M. A., Zika virus. *New England Journal of Medicine* **2016,** *374* (16), 1552-63.

11. Plourde, A. R.; Bloch, E. M., A literature review of Zika virus. *Emerging infectious diseases* **2016,** *22* (7), 1185.

12. Check Hayden, E., Zika highlights role of controversial fetal-tissue research. *Nature News* **2016,** *532* (7597), 16.

13. Khetarpal, N.; Khanna, I., Dengue fever: causes, complications, and vaccine strategies. *Journal of Immunology Research* **2016,** *2016*.

14. Dong, H.; Zhang, B.; Shi, P.-Y., Flavivirus methyltransferase: a novel antiviral target. *Antiviral Research* **2008,** *80* (1), 1-10.

15. Desgagné-Penix, I., Biosynthesis of alkaloids in Amaryllidaceae plants: a review. *Phytochemistry Reviews* **2020**.

16. Hotchandani, T.; Desgagne-Penix, I., Heterocyclic Amaryllidaceae Alkaloids: Biosynthesis and Pharmacological Applications. *Current Topics in Medicinal Chemistry* **2017,** *17* (4), 418-27.

17. Ka, S.; Koirala, M.; Mérindol, N.; Desgagné-Penix, I., Biosynthesis and biological activities of newly discovered Amaryllidaceae alkaloids. *Molecules* **2020,** *25* (21), 4901.

18. Cimmino, A.; Masi, M.; Evidente, M.; Superchi, S.; Evidente, A., Amaryllidaceae alkaloids: Absolute configuration and biological activity. *Chirality* **2017,** *29* (9), 486-99.

19. Ding, Y.; Qu, D.; Zhang, K.-M.; Cang, X.-X.; Kou, Z.-N.; Xiao, W.; Zhu, J.-B., Phytochemical and biological investigations of Amaryllidaceae alkaloids: a review. *Journal of Asian Natural Products Research* **2017,** *19* (1), 53-100.

20. Duri, Z. J.; Scovill, J. P.; Huggins, J. W., Activity of a methanolic extract of Zimbabwean Crinum macowanii against exotic RNA viruses in vitro. *Phytotherapy Research* **1994,** *8* (2), 121-2.

21. Kapu, S.; Ngwai, Y.; Kayode, O.; Akah, P.; Wambebe, C.; Gamaniel, K., Anti-inflammatory, analgesic and anti-lymphocytic activities of the aqueous extract of Crinum giganteum. *Journal of Ethnopharmacology* **2001,** *78* (1), 7-13.

22. Adesanya, S.; Olugbade, T.; Odebiyl, O.; Aladesanmi, J., Antibacterial alkaloids in Crinum jagus. *International Journal of Pharmacognosy* **1992,** *30* (4), 303-7.

23. Ogbole, O. O.; Akinleye, T. E.; Segun, P. A.; Faleye, T. C.; Adeniji, A. J., In vitro antiviral activity of twenty-seven medicinal plant extracts from Southwest Nigeria against three serotypes of echoviruses. *Journal of Virolpgy* **2018,** *15* (1), 110.

24. Ka, S.; Masi, M.; Merindol, N.; Di Lecce, R.; Plourde, M. B.; Seck, M.; Gorecki, M.; Pescitelli, G.; Desgagne-Penix, I.; Evidente, A., Gigantelline, gigantellinine and gigancrinine, cherylline- and crinine-type alkaloids isolated from Crinum jagus with anti-acetylcholinesterase activity. *Phytochemistry* **2020,** *175*, 112390.

25. Wang, P.; Li, L. F.; Wang, Q. Y.; Shang, L. Q.; Shi, P. Y.; Yin, Z., Anti-dengue-virus activity and structure-activity relationship studies of lycorine derivatives. *ChemMedChem* **2014,** *9* (7), 1522-33.

26. Gabrielsen, B.; Monath, T. P.; Huggins, J. W.; Kefauver, D. F.; Pettit, G. R.; Groszek, G.; Hollingshead, M.; Kirsi, J. J.; Shannon, W. M.; Schubert, E. M.; et al., Antiviral (RNA) activity of selected Amaryllidaceae isoquinoline constituents and synthesis of related substances. *Journal of Natural Products* **1992,** *55* (11), 1569-81.

27. Zou, G.; Puig-Basagoiti, F.; Zhang, B.; Qing, M.; Chen, L.; Pankiewicz, K. W.; Felczak, K.; Yuan, Z.; Shi, P.-Y., A single-amino acid substitution in West Nile virus 2K peptide between NS4A and NS4B confers resistance to lycorine, a flavivirus inhibitor. *Journal of Virology* **2009,** *384* (1), 242-52.

28. Chen, H.; Lao, Z.; Xu, J.; Li, Z.; Long, H.; Li, D.; Lin, L.; Liu, X.; Yu, L.; Liu, W.; Li, G.; Wu, J., Antiviral activity of lycorine against Zika virus in vivo and in vitro. *Journal of Virology* **2020,** *546*, 88-97.

29. Li, S.-y.; Chen, C.; Zhang, H.-q.; Guo, H.-y.; Wang, H.; Wang, L.; Zhang, X.; Hua, S.-n.; Yu, J.; Xiao, P.-g., Identification of natural compounds with antiviral activities against SARS-associated coronavirus. *Antiviral Research* **2005,** *67* (1), 18-23.

30. Zhang, Y.-N.; Zhang, Q.-Y.; Li, X.-D.; Xiong, J.; Xiao, S.-Q.; Wang, Z.; Zhang, Z.-R.; Deng, C.-L.; Yang, X.-L.; Wei, H.-P., Gemcitabine, lycorine and oxysophoridine inhibit novel coronavirus (SARS-CoV-2) in cell culture. *Emerging Microbes & Infections* **2020,** (just-accepted), 1-10.

31. Jin, Y.-H.; Min, J. S.; Jeon, S.; Lee, J.; Kim, S.; Park, T.; Park, D.; Jang, M. S.; Park, C. M.; Song, J. H., Lycorine, a non-nucleoside RNA dependent RNA polymerase inhibitor, as potential treatment for emerging coronavirus infections. *Phytomedicine* **2020**, 153440.

32. Shen, L.; Niu, J.; Wang, C.; Huang, B.; Wang, W.; Zhu, N.; Deng, Y.; Wang, H.; Ye, F.; Cen, S., High-throughput screening and identification of potent broad-spectrum inhibitors of coronaviruses. *Journal of Virology* **2019,** *93* (12), e00023-19.

33. de Andrade, J. P.; Guo, Y.; Font-Bardia, M.; Calvet, T.; Dutilh, J.; Viladomat, F.; Codina, C.; Nair, J. J.; Zuanazzi, J. A. S.; Bastida, J., Crinine-type alkaloids from Hippeastrum aulicum and H. calyptratum. *Phytochemistry* **2014,** *103*, 188-95.

34. Tallini, L. R.; Torras-Claveria, L.; Borges, W. D. S.; Kaiser, M.; Viladomat, F.; Zuanazzi, J. A. S.; Bastida, J., N-oxide alkaloids from Crinum amabile (Amaryllidaceae). *Molecules* **2018,** *23* (6), 1277.

35. Pépin, G.; Nejad, C.; Thomas, B. J.; Ferrand, J.; McArthur, K.; Bardin, P. G.; Williams, B. R.; Gantier, M. P., Activation of cGAS-dependent antiviral responses by DNA intercalating agents. *Nucleic Acids Research* **2017,** *45* (1), 198-205.

36. Chatel-Chaix, L.; Fischl, W.; Scaturro, P.; Cortese, M.; Kallis, S.; Bartenschlager, M.; Fischer, B.; Bartenschlager, R., A Combined Genetic-Proteomic Approach Identifies Residues within Dengue Virus NS4B Critical for Interaction with NS3 and Viral Replication. *Journal of Virology* **2015,** *89* (14), 7170-86.

37. Anton, A.; Mazeaud, C.; Freppel, W.; Gilbert, C.; Tremblay, N.; Sow, A. A.; Roy, M.; Rodrigue-Gervais, I. G.; Chatel-Chaix, L., Valosin-containing protein ATPase activity regulates the morphogenesis of Zika virus replication organelles and virus-induced cell death. *Cellular Microbiology*, e13302.

38. Flipse, J.; Diosa-Toro, M. A.; Hoornweg, T. E.; van de Pol, D. P.; Urcuqui-Inchima, S.; Smit, J. M., Antibody-Dependent Enhancement of Dengue Virus Infection in Primary Human Macrophages; Balancing Higher Fusion against Antiviral Responses. *Scitific Reports* **2016,** *6*, 29201.

39. Boonnak, K.; Slike, B. M.; Burgess, T. H.; Mason, R. M.; Wu, S. J.; Sun, P.; Porter, K.; Rudiman, I. F.; Yuwono, D.; Puthavathana, P.; Marovich, M. A., Role of dendritic cells in antibody-dependent enhancement of dengue virus infection. *Journal of Virology* **2008,** *82* (8), 3939-51.

40. Kumar, A.; Buhler, S.; Selisko, B.; Davidson, A.; Mulder, K.; Canard, B.; Miller, S.; Bartenschlager, R., Nuclear localization of dengue virus nonstructural protein 5 does not strictly correlate with efficient viral RNA replication and inhibition of type I interferon signaling. *Journal of Virology* **2013,** *87* (8), 4545-57.

41. He, J.; Chen, Y.; Farzan, M.; Choe, H.; Ohagen, A.; Gartner, S.; Busciglio, J.; Yang, X.; Hofmann, W.; Newman, W.; Mackay, C. R.; Sodroski, J.; Gabuzda, D., CCR3 and CCR5 are co-receptors for HIV-1 infection of microglia. *Nature* **1997,** *385* (6617), 645-9.

42. Merindol, N.; El-Far, M.; Sylla, M.; Masroori, N.; Dufour, C.; Li, J. X.; Cherry, P.; Plourde, M. B.; Tremblay, C.; Berthoux, L., HIV-1 capsids from B27/B57+ elite controllers escape Mx2 but are targeted by TRIM5alpha, leading to the induction of an antiviral state. *PLOS Pathogens* **2018,** *14* (11), e1007398.

43. Uzé, G.; Di Marco, S.; Mouchel-Vielh, E.; Monneron, D.; Bandu, M.-T.; Horisberger, M. A.; Dorques, A.; Lutfalla, G.; Mogensen, K. E., Domains of interaction between alpha interferon and its receptor components. *Journal of molecular biology* **1994,** *243* (2), 245-57.

44. Zoete, V.; Daina, A.; Bovigny, C.; Michielin, O., SwissSimilarity: A Web Tool for Low to Ultra High Throughput Ligand-Based Virtual Screening. *Journal of Chemical Information and Modeling* **2016,** *56* (8), 1399-404.

45. Gfeller, D.; Grosdidier, A.; Wirth, M.; Daina, A.; Michielin, O.; Zoete, V., SwissTargetPrediction: a web server for target prediction of bioactive small molecules. *Nucleic Acids Research* **2014,** *42* (Web Server issue), W32-8.

46. Gong, J.; Cai, C.; Liu, X.; Ku, X.; Jiang, H.; Gao, D.; Li, H., ChemMapper: a versatile web server for exploring pharmacology and chemical structure association based on molecular 3D similarity method. *Bioinformatics* **2013,** *29* (14), 1827-9.

47. Wang, X.; Shen, Y.; Wang, S.; Li, S.; Zhang, W.; Liu, X.; Lai, L.; Pei, J.; Li, H., PharmMapper 2017 update: a web server for potential drug target identification with a comprehensive target pharmacophore database. *Nucleic Acids Research* **2017,** *45* (W1), W356-W60.

48. Daina, A.; Michielin, O.; Zoete, V., SwissADME: a free web tool to evaluate pharmacokinetics, drug-likeness and medicinal chemistry friendliness of small molecules. *Scitific Reports* **2017,** *7*, 42717.

49. Fischl, W.; Bartenschlager, R., High-throughput screening using dengue virus reporter genomes. *Methods in Molecula Biology* **2013,** *1030*, 205-19.

50. Deng, Y. Q.; Zhang, N. N.; Li, C. F.; Tian, M.; Hao, J. N.; Xie, X. P.; Shi, P. Y.; Qin, C. F., Adenosine Analog NITD008 Is a Potent Inhibitor of Zika Virus. *Open Forum Infectious Diseasis* **2016,** *3* (4), ofw175.

51. Yin, Z.; Chen, Y. L.; Schul, W.; Wang, Q. Y.; Gu, F.; Duraiswamy, J.; Kondreddi, R. R.; Niyomrattanakit, P.; Lakshminarayana, S. B.; Goh, A.; Xu, H. Y.; Liu, W.; Liu, B.; Lim, J. Y.; Ng, C. Y.; Qing, M.; Lim, C. C.; Yip, A.; Wang, G.; Chan, W. L.; Tan, H. P.; Lin, K.; Zhang, B.; Zou, G.; Bernard, K. A.; Garrett, C.; Beltz, K.; Dong, M.; Weaver, M.; He, H.; Pichota, A.; Dartois, V.; Keller, T. H.; Shi, P. Y., An adenosine nucleoside inhibitor of dengue virus. *Proceedings of the National Academy of Sciences* **2009,** *106* (48), 20435-9.

52. McCracken, M. K.; Gromowski, G. D.; Garver, L. S.; Goupil, B. A.; Walker, K. D.; Friberg, H.; Currier, J. R.; Rutvisuttinunt, W.; Hinton, K. L.; Christofferson, R. C., Route of inoculation and mosquito vector exposure modulate dengue virus replication kinetics and immune responses in rhesus macaques. *PLoS Neglected Tropical Diseasis* **2020,** *14* (4), e0008191.

53. Kang, J.; Zhang, Y.; Cao, X.; Fan, J.; Li, G.; Wang, Q.; Diao, Y.; Zhao, Z.; Luo, L.; Yin, Z., Lycorine inhibits lipopolysaccharide-induced iNOS and COX-2 up-regulation in RAW264.7 cells through suppressing P38 and STATs activation and increases the survival rate of mice after LPS challenge. *Int Immunopharmacol* **2012,** *12* (1), 249-56.

54. Chen, Y. L.; Abdul Ghafar, N.; Karuna, R.; Fu, Y.; Lim, S. P.; Schul, W.; Gu, F.; Herve, M.; Yokohama, F.; Wang, G.; Cerny, D.; Fink, K.; Blasco, F.; Shi, P. Y., Activation of peripheral blood mononuclear cells by dengue virus infection depotentiates balapiravir. *Journal of Virology* **2014,** *88* (3), 1740-7.

55. Alhoot, M. A.; Wang, S. M.; Sekaran, S. D., Inhibition of dengue virus entry and multiplication into monocytes using RNA interference. *PLoS Neglected Tropical Diseasis* **2011,** *5* (11), e1410.

56. Kwissa, M.; Nakaya, H. I.; Onlamoon, N.; Wrammert, J.; Villinger, F.; Perng, G. C.; Yoksan, S.; Pattanapanyasat, K.; Chokephaibulkit, K.; Ahmed, R.; Pulendran, B., Dengue virus infection induces expansion of a CD14(+)CD16(+) monocyte population that stimulates plasmablast differentiation. *Cell Host Microbe* **2014,** *16* (1), 115-27.

57. Peng, X.; Sova, P.; Green, R. R.; Thomas, M. J.; Korth, M. J.; Proll, S.; Xu, J.; Cheng, Y.; Yi, K.; Chen, L.; Peng, Z.; Wang, J.; Palermo, R. E.; Katze, M. G., Deep sequencing of HIV-infected cells: insights into nascent transcription and host-directed therapy. *Journal of Virology* **2014,** *88* (16), 8768-82.

58. Szlavik, L.; Gyuris, A.; Minarovits, J.; Forgo, P.; Molnar, J.; Hohmann, J., Alkaloids from Leucojum vernum and antiretroviral activity of Amaryllidaceae alkaloids. *Planta Medica* **2004,** *70* (9), 871-3.

59. Lin, L. Z.; Hu, S. F.; Chai, H. B.; Pengsuparp, T.; Pezzuto, J. M.; Cordell, G. A.; Ruangrungsi, N., Lycorine alkaloids from Hymenocallis littoralis. *Phytochemistry* **1995,** *40* (4), 1295-8.

60. Renard-Nozaki, J.; Kim, T.; Imakura, Y.; Kihara, M.; Kobayashi, S., Effect of alkaloids isolated from Amaryllidaceae on herpes simplex virus. *Research in Virology* **1989,** *140*, 115-28.

61. Nagy, P. D.; Pogany, J., The dependence of viral RNA replication on co-opted host factors. *Natural Review Microbiology* **2011,** *10* (2), 137-49.

62. Chatel-Chaix, L.; Bartenschlager, R., Dengue virus- and hepatitis C virus-induced replication and assembly compartments: the enemy inside--caught in the web. *Journal of Virol* **2014,** *88* (11), 5907-11.

63. Neufeldt, C. J.; Cortese, M.; Acosta, E. G.; Bartenschlager, R., Rewiring cellular networks by members of the Flaviviridae family. *Natural Review Microbiology* **2018,** *16* (3), 125-42.

64. Miller, S.; Sparacio, S.; Bartenschlager, R., Subcellular localization and membrane topology of the Dengue virus type 2 Non-structural protein 4B. *Journal of Biological Chemistry* **2006,** *281* (13), 8854-63.

65. Ambrose, R. L.; Mackenzie, J. M., A conserved peptide in West Nile virus NS4A protein contributes to proteolytic processing and is essential for replication. *Journal of Virology* **2011,** *85* (21), 11274-82.

66. Roosendaal, J.; Westaway, E. G.; Khromykh, A.; Mackenzie, J. M., Regulated cleavages at the West Nile virus NS4A-2K-NS4B junctions play a major role in rearranging cytoplasmic membranes and Golgi trafficking of the NS4A protein. *Journal of virology* **2006,** *80* (9), 4623-32.

67. Miller, S.; Kastner, S.; Krijnse-Locker, J.; Bühler, S.; Bartenschlager, R., The non-structural protein 4A of dengue virus is an integral membrane protein inducing membrane alterations in a 2K-regulated manner. *Journal of Biological Chemistry* **2007,** *282* (12), 8873-82.

68. Simanjuntak, Y.; Liang, J. J.; Lee, Y. L.; Lin, Y. L., Repurposing of prochlorperazine for use against dengue virus infection. *J Infectious Diseasis* **2015,** *211* (3), 394-404.

69. Smith, J. L.; Stein, D. A.; Shum, D.; Fischer, M. A.; Radu, C.; Bhinder, B.; Djaballah, H.; Nelson, J. A.; Fruh, K.; Hirsch, A. J., Inhibition of dengue virus replication by a class of small-molecule compounds that antagonize dopamine receptor d4 and downstream mitogen-activated protein kinase signaling. *Journal of Virology* **2014,** *88* (10), 5533-42.

70. Eyre, N. S.; Kirby, E. N.; Anfiteatro, D. R.; Bracho, G.; Russo, A. G.; White, P. A.; Aloia, A. L.; Beard, M. R., Identification of Estrogen Receptor Modulators as Inhibitors of Flavivirus Infection. *Antimicrobial Agents Chemotherapy* **2020,** *64* (8).

71. Tohma, D.; Tajima, S.; Kato, F.; Sato, H.; Kakisaka, M.; Hishiki, T.; Kataoka, M.; Takeyama, H.; Lim, C. K.; Aida, Y.; Saijo, M., An estrogen antagonist, cyclofenil, has anti-dengue-virus activity. *Archives of Virology* **2019,** *164* (1), 225-34.

72. Jia, F.; Zou, G.; Fan, J.; Yuan, Z., Identification of palmatine as an inhibitor of West Nile virus. *Archives of virology* **2010,** *155* (8), 1325-9.

73. Chen, H.; Lao, Z.; Xu, J.; Li, Z.; Long, H.; Li, D.; Lin, L.; Liu, X.; Yu, L.; Liu, W.; Li, G.; Wu, J., Antiviral activity of lycorine against Zika virus in vivo and in vitro. *Virology* **2020,** *546*, 88-97.

74. Kobayashi, S.; Tokumoto, T.; Kihara, M.; Imakura, Y.; Shingu, T.; Taira, Z., Alkaloidal constituents of Crinum latifolium and Crinum bulbispermum (Amaryllidaceae). *Chemical and pharmaceutical bulletin* **1984,** *32* (8), 3015-22.

75. Nair, J.; Machocho, A.; Campbell, W.; Brun, R.; Viladomat, F.; Codina, C.; Bastida, J., Alkaloids from Crinum macowanii. *Phytochemistry* **2000,** *54* (8), 945-50.

76. Tram, N. T. N.; Titorenkova, T. V.; Bankova, V. S.; Handjieva, N.; Popov, S., Crinum L.(Amaryllidaceae). *Fitoterapia* **2002,** *73* (3), 183-208.

77. Lebrun, S.; Couture, A.; Deniau, E.; Grandclaudon, P., A new synthesis of (+)- and (-)-cherylline. *Org Biomol Chem* **2003,** *1* (10), 1701-6.

78. Kale, B. Y.; Shinde, A. D.; Sonar, S. S.; Shingate, B. B.; Kumar, S.; Ghosh, S.; Venugopal, S.; Shingare, M. S., A short synthesis of +/--cherylline dimethyl ether. *Beilstein Journal of Organic Chemistry* **2009,** *5*, 80.

79. Couture, A.; Deniau, E.; Woisel, P.; Grandclaudon, P.; Carpentier, J. F., Base-induced cyclization of trimethoxy-o-aroyldiphenylphosphoryl methylbenzamide: A formal synthesis of (+/-)cherylline and (+/-)cherylline dimethylether. *Tetrahedron Letters* **1996,** *37* (21), 3697-700.

80. Manolov, S. P.; Atanasova, S. N.; Ghate, M.; Ivanov, I. I., A brief review of Cherylline synthesis. **2015**.

Supplementary materials

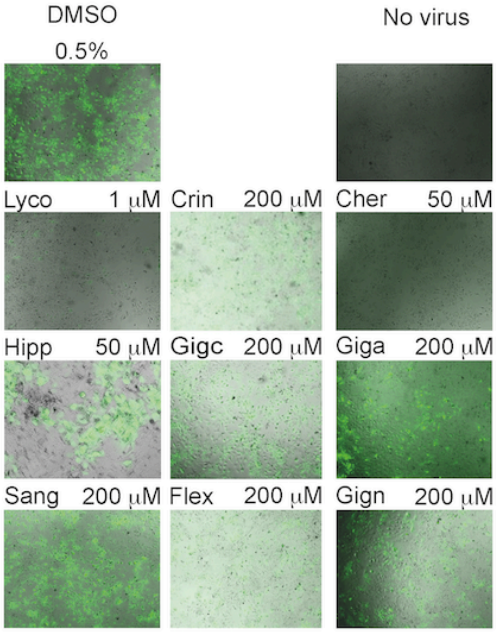

Figure S1. Merged pictures of brightfield and GFP channels of Huh7 cells treated with alkaloids and infected with $DENV_{GFP}$, corresponding to pictures of Figure 2B.

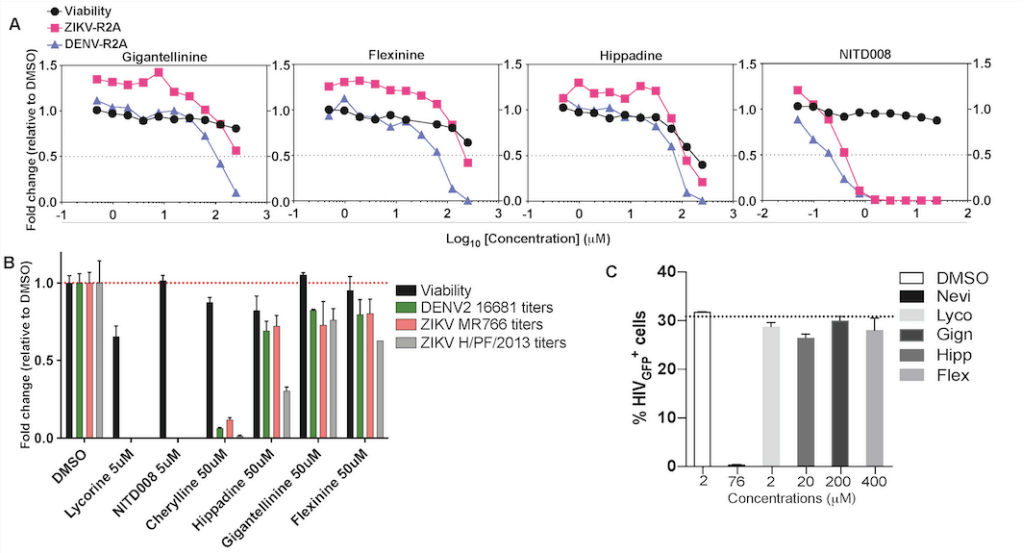

Figure S2. Screening of hippadine, gigantellinine and flexinine activity against DENV and ZIKV replication. A. Antiviral activity of hippadine, gigantellinine and flexinine was studied by measuring the levels of $DENV_{R2A}$ (purple) and $ZIKV_{R2A}$ (pink) replication in Huh7.5 cells through luciferase luminescence at 72 h p.i. Cell viablity (ATP) was assessed at 24 h. NITD008 was used as a positive control. Results are displayed as fold changes in viability and replication, 1 meaning no change compared to DMSO-treated cells. B. Viral titers were measured by plaque assay on Vero E6 cells using cytopathic WT

French Polynesia H/PF/2013 and Uganda MR766 ZIKV and DENV2 16881s strains. Huh7.5 cells were infected and treated 2 h p.i. with compounds. 48 h later, supernatants were harvested and plated on Vero E6 cells. Fold replication was calculated from viral titers values. Viability (ATP) was calculated at 48 h p.i. C. THP-1 cells were pre-treated with lycorine (lyco), hippadine (hipp), gigantellinine (gign) and flexinine (flex) in triplicates for 2 h, and infected with VSV-G pseudotyped HIV-1_{GFP} at MOI = 1. The antiretroviral nevirapine (nevi) was used as a positive control, while 2% DMSO was used as a negative control. Results were analyzed by flow cytometry 72 h p.i. Experiment was performed in triplicates with two concentrations, the highest being shown.

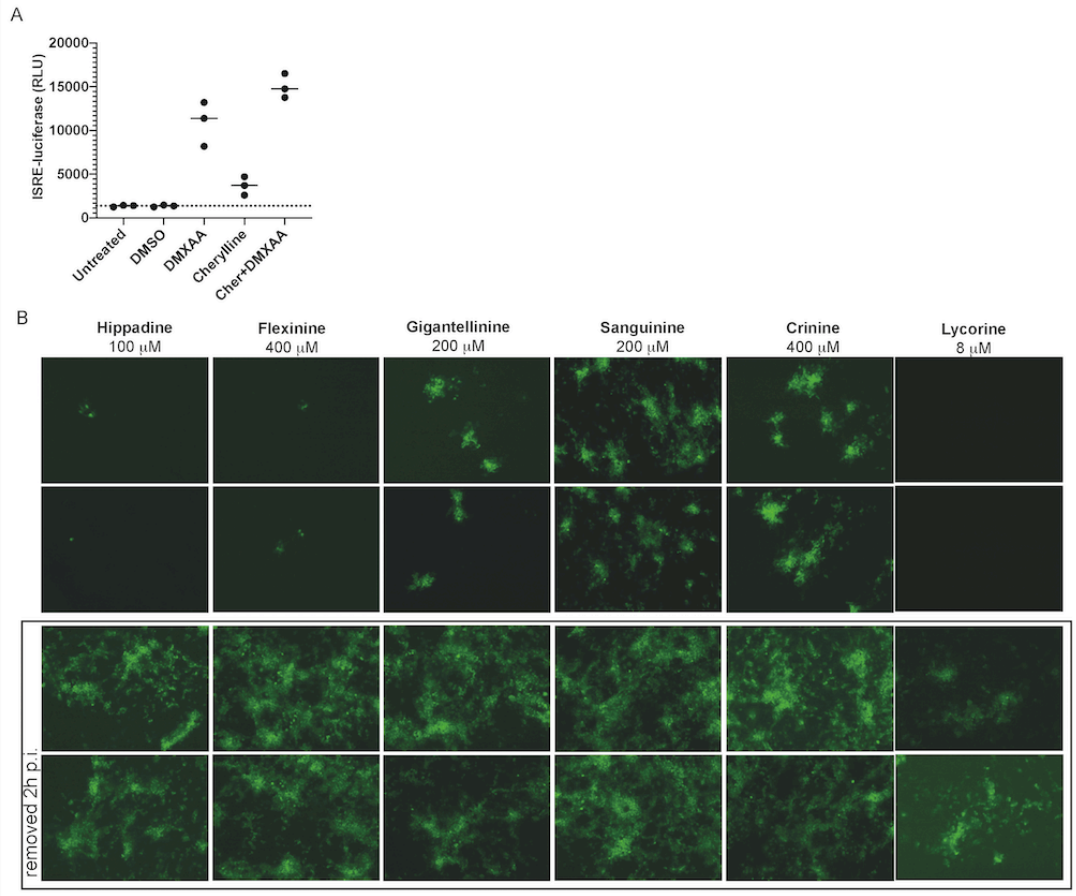

Figure S3. Screening of AAs activity on virions and on viral entry. A. LL71 cells were treated with 50 µM of cherylline (cher), matched concentrations of DMSO, medium only or with DMXAA (a STING activator) as positive control. Luciferase activity under the promoter of IFN-sensitive response element (ISRE) was measured 24 hours after treatment by luminescence. B. Infectivity of $DENV_{GFP}$ in Huh7 cells continuously treated with AAs compared to cells treated only for 2h p.i. Two representative pictures of each condition taken with a 5X objective on an inverted microscope system are shown.

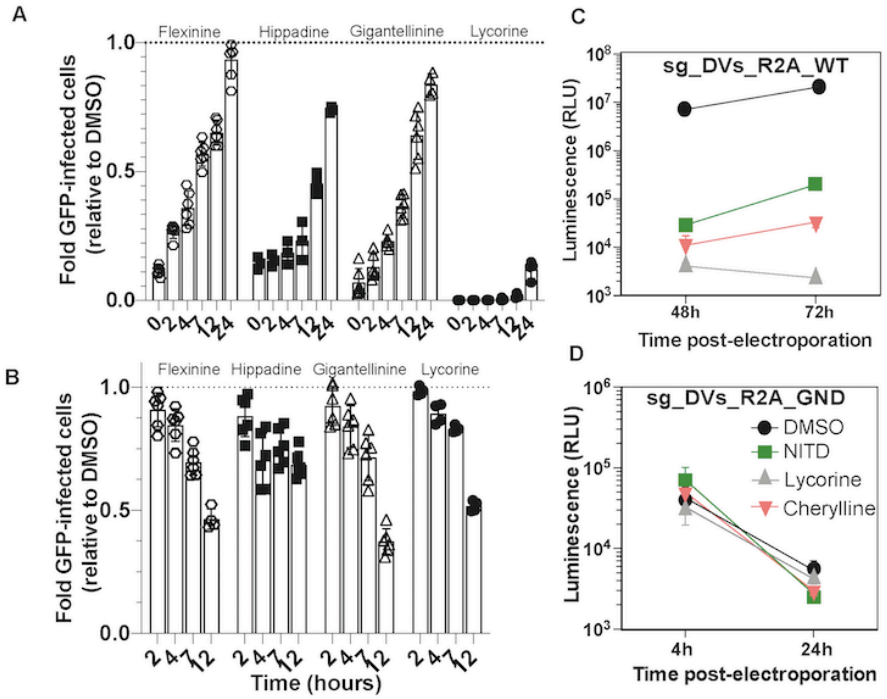

Figure S4. Viral life cycle steps targeted by AAs. A. Time-of-drug addition of lycorine, hippadine, gigantellinine and flexinine. B. Time-of-drug removal. C. Luciferase levels were quantified at 48 and 72 h post-electroporation (p.e.) with sg_DVs_R2A_WT and normalized over levels detected in DMSO-treated. D. Luciferase levels were quantified at 4 h and 24 h p.e. with RdRp deficient sg_DVs_R2A_GND and normalized over levels in cells treated with DMSO.

Table S1. Structural homology of AAs isolagted in *Crinum jagus* (*giganteum*) calculated with the Jacquard/Tanimoto similarity index. A score of 1 means that structures are identical.

	Cherylline	**Gigantelline**	**Gigantellinine**	**Crinine**	**Gigancrinine**	**Flexinine**	**Lycorine**	**Hippadine**	**Sanguinine**
Cherylline	1	0,9942	0,9786	0,4157	0,4111	0,4055	0,4067	0,2418	0,3750
Gigantelline		1	0,9815	0,4225	0,4175	0,4109	0,4121	0,2466	0,3796
Gigantellinine			1	0,4166	0,4129	0,4063	0,4078	0,2409	0,3759
Crinine				1	0,7349	0,7355	0,7089	0,2983	0,6720
Gigancrinine					1	0,9453	0,7410	0,2979	0,6455
Flexinine						1	0,7405	0,3042	0,6226
Lycorine							1	0,3086	0,6366
Hippadine								1	0,2819
Sanguinine									1

Table S2. Ligands from the PDB (Protein Data Bank) database uncovered as similar to cherylline with the SwissSimilarity tool.

		SwissSimilarity (PDB)	
	PDB	Name	Score
hit1	Ren	S-reticuline	0,93
hit2	MS5	7-methoxy-2-(3-methoxybenzyl)-1,2,3,4-tetrahydroisoquinolin-6-yl sulfamate	0,71
hit3	B2Q	(2S,3R,11bR)-3-butyl-9,10-dimethoxy-1,3,4,6,7,11b-hexahydro-2H-pyrido[2,1-a]isoquinolin-2-amine	0,59
hit4	3K8	14aR)-2,3,6-trimethoxy-11,12,13,14,14a,15-hexahydro-9H-dibenzo[f,h]pyrido[1,2-b]isoquinoline	0,413

Table S3. Cherylline's *in silico* predicted targets using shape or pharmacophore screening.

	Shape screening (SwissTargetPrediction)			**Shape screening (ChemMapper)**			**Pharmacophore screening (PharmMapper)**		
	Uniprot	Name	Score	Uniprot	name	Score	PDB	Name	z'- score
hit1	**Q01959**	Dopamine transporter	0,49	**Q00535**	Cell division protein kinase 5	1	**2ZKC**	Estrogen-related receptor gamma	3,87
hit2	**P31645**	Serotonine transporter	0,34	**P03372**	Estrogen receptor	0,95	**1QUG**	Lyzozyme	1,68
hit3	**P23975**	Norepinephrine transporter	0,31	**Q04828**	aldo-keto reductase family 1 member C1	0.92	**1OKL**	Carbonic anhydrase 2	1,57
hit4	**P21728**	Dopamine D1 receptor	0,26	**P21918**	D(1B) dopamine receptor	0	**1JV4**	Major urinary protein 2	1,52

Table S4. Admet properties of Cherylline calculated by the SwissAdme tool.

		Physicochemical properties								**Druglikeness**	
	Formul	**molecular weight (g/mol)**	**Heavy atoms**	**Aromatic heavy atoms**	**Rotating bounds**	**H bonds acceptors**	**H bond donor**	**Solubility logS**	**Ipophilicity logP $_{o/w}$**	**Lipinski – violation**	**Biodisponibility score**
Cherylline	$C_{17}H_{19}NO_3$	285,34	21	12	2	4	2	-3,48	2,70	Y ; 0	0,55
Gigantelline	$C_{18}H_{21}NO_3$	299,36	22	12	3	4	1	-3.68	2,89	Y ; 0	0,55
Gigantellinine	$C_{18}H_{21}NO_4$	315,36	23	12	3	5	2	-3,55	3,03	Y ; 0	0,55
Crinine	$C_{16}H_{17}NO_3$	271,31	20	6	0	4	1	-2,82	2,57	Y ; 0	0,55
Gigancrinine	$C_{16}H_{17}NO_4$	287,31	21	6	0	5	1	-2,39	2,57	Y ; 0	0,55
Flexinine	$C_{16}H_{17}NO_4$	287,31	21	6	0	5	1	-2,39	2,64	Y ; 0	0,55
Lycorine	$C_{16}H_{17}NO_4$	287,31	21	6	0	5	2	-1,82	2,24	Y ; 0	0,55
Hippadine	$C_{16}H_{19}NO_3$	263,25	20	16	0	3	0	-3,99	2,58	Y ; 0	0,55
Sanguinine	$C_{16}H_{19}NO_3$	273,33	20	6	0	4	2	-2,71	2,12	Y ; 0	0,55

Y : yes ; N : no. Cherylline isomeric smiles code:
CN1C[C@H](C2=CC(=C(C=C2C1)O)OC)C3=CC=C(C=C3)O was used as entry.

Le chapitre V contient les conclusions et perspectives
tirées des résultats des chapitres ci-avant.

CHAPITRE V

CONCLUSIONS ET PERSPECTIVES

Les travaux présentés dans cette thèse visent d'une part à valoriser les plantes médicinales (Amaryllidaceae) de la flore sénégalaise et les connaissances empiriques sur les composés associés à cette flore. Globalement, ils consistent à découvrir des molécules bioactives telles que alcaloïdes des Amaryllidaceae (AAs).

Nos travaux ont eu comme objectifs spécifiques de :

- réaliser une évaluation des potentiels biologiques notamment anti-AChE, cytotoxiques, antibactériennes et anti-virus de la Dengue de l'extrait alcaloïdique de *P. trianthum* utilisé dans la médecine traditionnelle sénégalaise. Nous cherchions à corréler son utilisation traditionnelle avec une activité biologique et découvrir d'autres activités biologiques.
- cribler et purifier l'extrait alcaloïdique de *C. jagus* afin de trouver des AAs biologiquement actifs notamment possédant des activités anti-AChE et cytotoxiques.
- et enfin évaluer les activités antiflavivirales des AAs notamment contre les virus de la Dengue et du Zika, deux virus touchant toutes les zones tropicales du monde contre lesquels il n'existe pas de thérapie.

Dans la première partie de cette thèse, nous avons utilisé une méthode acide base pour l'extraction des alcaloïdes. Les usages de *P. trianthum* en médecine traditionnelle ont permis d'évaluer le potentiel pharmacologique de l'extrait en mesurant son activité anti-AChE, antibactérienne, cytotoxicité et anti-Dengue. Les résultats obtenus ont montré une faible activité anti-AChE et une activité antibactérienne modérée. Cependant, plusieurs bactéries pathogènes sont isolées des plaies. Parmi ces bactéries,

on note le *Staphylococcus aureus, l'Escherichia coli* et le *Pseudomonas aeruginosa* [131]. Dans notre étude, des essais menés sur ces souches ont montré que l'extrait inhibait leur croissance par la méthode de diffusion sur gélose et par la méthode de microdilution. Donc l'extrait alcaloïdique de *P. trianthum* pourrait être un agent de cicatrisation grâce à ses propriétés antibactériennes démontrées. Ainsi, les résultats observés au niveau des tests antibactériens ont confirmé la valeur scientifique des connaissances empiriques de la médecine traditionnelle sénégalaise. Cependant, l'extrait est plus actif sur le Cocci à Gram+ (*Staphylococcus aureus*) que sur les souches à Gram- (*Escherichia coli* et *Pseudomonas aeruginosa*). L'extrait pourrait être aussi utilisé dans le traitement des infections liées aux Cocci à Gram+ telle que la pneumonie [132]. L'évaluation toxicologique d'extraits de plantes médicinales et des composés thérapeutiques serait essentielle afin de vérifier leur sécurité. Dans notre étude, la faible libération d'ATP par les cellules traitées avec l'extrait a montré que l'extrait était très cytotoxique avec des CC_{50} de 0,45 et 0,23 µg/mL pour les cellules Huh7 et THP-1 respectivement. Ainsi, cette forte cytotoxicité favorise un usage externe et confirme la dangerosité d'ingérer cette plante. Ainsi, la capacité de l'extrait alcaloïdique issu des bulbes de *P. trianthum* à cicatriser les plaies ou traiter les infections devrait être démontrée chez les souris afin de calculer leur pleine puissance. Une fois cette capacité vérifiée, une voie de valorisation possible pourrait être envisagée pour le développement d'un phytomédicament ayant pour vocation le traitement des plaies et des infections.

Le profilage des alcaloïdes a montré que l'extrait contenait majoritairement 58,34 % d'AAs de type crinine et 14,9 % de type lycorine. Or les alcaloïdes de type crinine ne sont pas décrits comme étant cytotoxiques à l'exception de l'haemanthamine et la crinamine [133]. Ces derniers ne sont pas identifiés dans l'extrait. Donc, une purification de l'extrait pourrait conduire à des AAs cytotoxiques potentiellement anticancéreuses dans la mesure où 21 % de l'extrait n'était pas identifié. L'extrait brut d'alcaloïde issu des bulbes de *P. trianthum* a inhibé complétement l'infection des cellules Huh7 par le virus de la Dengue à des concentrations non cytotoxiques. Cette étude est la première portant sur l'extrait brut d'alcaloïde d'Amaryllidaceae contre le virus de la Dengue. Il est probable que cette forte activité mesurée soit liée à la présence de la lycorine dans l'extrait ou bien

l'effet synergique de plusieurs molécules. Par ailleurs, des études antérieures ont démontré que la lycorine (5,909 % de TIC) inhibait fortement la réplication des flavivirus notamment le virus de la Dengue et du Zika à de faibles concentrations non cytotoxiques [134-136]. Compte tenu de la quantité de lycorine, l'extrait pourrait contenir d'autres inhibiteurs de flavivirus. Fort de ce constat, des études sur des souches sauvages pathogènes et chez les souris pourraient être envisagées pour confirmer le plein potentiel de l'extrait brut d'alcaloïde de *P. trianthum* contre les flavivirus notamment les virus de la Dengue et du Zika. De plus, l'extrait pourrait inhiber d'autres flavivirus dont les génomes sont similaires à celui du virus de la Dengue. Cependant, outre la lycorine la purification de l'extrait brut d'alcaloïde de *P. trianthum* conduirait probablement à des inhibiteurs puissants des flavivirus comme le virus de la Dengue et du Zika. Toutefois, face aux résultats prometteurs des alcaloïdes issus des bulbes de *P. trianthum*, des tests de toxicité chronique et aiguë devront être réalisés sur des souris pour confirmer la sécurité d'emploi de l'extrait.

À la deuxième partie de notre étude, nous nous sommes particulièrement intéressés à l'étude de l'espèce *Crinum jagus*. Pour les investigations chimiques et biologiques de l'extrait brut alcaloïdique issu des bulbes de *C. jagus*, nous avons adopté une combinaison de deux approches notamment : l'approche chimio-guidée et l'approche bio-guidée. L'analyse GC-MS de l'extrait brut a permis de détecter cinq AAs dont trois sont connus (cherylline, lycorine et vittatine/crinine) et les pics non identifiés représentaient environ 47 % de l'extrait. Ainsi, l'extrait brut d'alcaloïdes issu des bulbes de *C. jagus* a complètement inhibé l'infection des cellules Huh7 par le virus de la Dengue à des concentrations non cytotoxiques. La purification de l'extrait *C. jagus* a conduit à l'isolement de neuf AAs à savoir la cherylline, la gigantelline, la gigantellinine, la crinine la gigancrinine, la flexinine, la lycorine, la sanguinine et l'hippadine. Parmi ces composés, la gigantelline, la gigantellinine, et la gigancrinine ont été décrites pour la première fois. La gigantelline et la gigantellinine appartiennent à la famille de la cherylline alors que gigancrinine appartient à la famille de la crinine. La découverte de gigantelline et gigantellinine est importante et novatrice étant donné que ces types de composés sont extrêmement rares chez les Amaryllidacées et leurs effets biologiques sont peu connus.

La mesure de la cytotoxité sur des cellules MCF7 de ces AAs isolées nous a permis de conclure qu'à l'exception de la lycorine et l'hippadine, ces AAs sont peu cytotoxiques à de fortes concentrations. Cependant, la mesure de l'inhibition de l'activité de l'AChE nous a permis de conclure qu'à l'exception de la sanguinine (IC_{50} = 1.83 ± 0.01µM), les autres AAs sont faiblement actifs voir même inactifs. Antérieurement, il a été démontré que la cherylline, lycorine et crinine ont de faibles activités anti-AChE [54, 137-139]. En revanche, la sanguine est presque quatre fois plus active que le control positif, la galanthamine qui est d'ailleurs utilisée pour le traitement des symptômes de la maladie d'Alzheimer. Cette activité a été antérieurement démontrée par d'autres études. La rareté de la sanguinine dans les espèces d'Amaryllidaceae et l'impossibilité actuelle de sa synthèse à cause de sa structure complexe, compromettent son utilisation dans la prise en charge des personnes atteintes de la maladie d'Alzheimer. Dans ce contexte, le *C. jagus* pourrait constituer une source de production de la sanguinine.

Dans la troisième partie de cette thèse, nous nous sommes intéressés à l'activité antivirale des alcaloïdes purifiés de *C. jagus*. Les capacités de tous les composés isolés ont été évaluées individuellement contre l'infection des cellules Huh7 par le virus de la Dengue. Les résultats ont montré qu'en plus de la lycorine, la cherylline bloque efficacement l'infection des cellules Huh7 par le virus de la Dengue. Les autres AAs à savoir la gigantellinine, la flexinine et l'hippadine ont des effets modérés, tandis que la gigantelline, la crinine, gigancrinine et la sangunine ont des effets très faibles à fortes concentrations. La relation structure-activité de la cherylline et de ses dérivés à savoir la gigantelline et la gigantellinine a permis de mettre en évidence des critères qui pourraient affecter l'activité antivirale. Ainsi, le fait que la gigantelline soit moins active que la cherylline et la gigantellinine, nous révèle l'importance de la configuration absolue du carbone C-4 de la jonction des cycles B et C (Figure 2 – Chapitre IV). Il semble que la configuration absolue *R* pour le cas de la gigantelline diminue significativement l'activité, tandis que la configuration absolue *S* pour le cas de la cherylline et la gigantellinine augmente l'activité antivirale. Comme la cherylline et la gigantellinine ont la même configuration absolue, la différence entre ces deux composés associés à la réduction du potentiel antiviral repose plutôt sur la présence d'un groupe hydroxyle supplémentaire en

C-5' et/ou la méthyoxylation du groupe hydroxyle en C-4' dans le cycle C de la gigantellinine. La capacité de la cherylline à inhiber la réplication du virus de la Dengue a été confirmée sur une souche exprimant la luciférase. Nous avons ensuite démontré que la cherylline bloquait efficacement la réplication du virus Zika qui a des protéines similaires (capside (C), enveloppe (E), membranaire (prM), NS1, NS2A, NS2B, NS3, NS4A, NS4B et NS5) au virus de la Dengue, mais n'avait aucun effet sur le VIH-1. Ainsi, ces résultats suggèrent que la cherylline pourrait être un inhibiteur spécifique des flavivirus. La cherylline a par la suite atténué les titres viraux des souches sauvages pathogènes notamment virus humain Zika de Polynésie francaise (HVZIK/PF/2013), le virus africain Zika (MR766) et le sérotype-2 du virus de la Dengue (VDEN-2) à des niveaux significatifs par rapport au contrôle. Au regard de ces résultats sur les souches sauvages, nous avons conclu que la cherylline était un inhibiteur de la réplication du virus de la Dengue et du Zika. Pour connaître le cycle viral de la cherylline, dans un premier temps nous avons fait une comparaison de l'infectivité traitée en continu par la cherylline par rapport aux cellules traitées pendant 2 h après infection. Nos résultats ont montré qu'il n y'avait pas d'infection dans le traitement continu, alors que pour le traitement de 2 h, toutes les cellules étaient presque infectées. Nous avons ainsi conclu que la cherylline ne ciblait pas l'entrée du virus et elle n'est pas virucide non plus. Nous avons en outre combiné des expériences de temps d'ajout et d'élimination et utilisé des réplicons sous-génomiques pour connaître à quel moment après son entrée la cherylline agissait. Ces combinaisons de résultats nous ont permis de conclure que la cherylline pourrait cibler toutes les protéines nécessaires à la réplication de l'ARN du virus de la Dengue. Des études postérieures sont envisagées pour déterminer la cible protéique spécifique de la cherylline. Cependant, il serait intéressant de tester si la cherylline ciblerait les protéines non structurales notamment NS3 et NS5 car ces protéines sont plus conservées chez les 4 sérotypes du VDEN [140]. Dans ce cas, la cherylline pourrait être active sur tous les 4 sérotypes. Le traitement par la cherylline des cellules mononuclées du sang périphérique (PBMC) infectées par le virus de la Dengue nous a permis de conclure que la cherylline était un inhibiteur efficace et non cytotoxique du virus de la Dengue. Or, entre 2017 et 2018, le Sénégal a connu deux épidémies de la Dengue principalement VDEN-1. Dans ce

contexte, les extraits bruts de *P. trianthum*, *C. jagus* et la cherylline présentés dans ce travail apparaissent comme des solutions pour lutter contre la maladie de la Dengue.

Les résultats obtenus dans ce travail ont permis de caractériser la capacité pharmacologique de deux plantes à savoir *P. trianthum* et *C. jagus* qui pourraient être proposées dans l'intégration de la pharmacopée sénégalaise. Pour toutes les deux, il s'agit d'une première étude contre le virus de la Dengue. Cependant, l'extrait alcaloïdique issu des bulbes de *P. trianthum* est environ 10 fois plus actif contre la réplication du virus de la Dengue et 5 fois plus cytotoxique que l'extrait alcaloïdique issu des bulbes de *C.jagus*. Néanmoins, face aux résultats concluants de ces deux extraits alcaloïdiques, des tests de cytotoxicités aigues et chroniques devront être envisagés chez des souris avant leur potentielle intégration dans la pharmacopée sénégalaise.

Nos résultats ont confirmé l'intérêt scientifique des résultats ethno-pharmacologiques pour traiter des plaies et des infections.

En sommes, nos résultats de recherche concluants laissent entrevoir de nombreuses voies de valorisations des extraits alcaloïdiques suivant :

Concernant celui *P. trianthum* : le développement de phytomédicaments à moindre coût contre les infections bactériennes et la maladie de la Dengue.

Pour celui de *C. jagus* : le développement d'un phytomédicament riche en sanguinine à moindre coût pour une meilleure prise en charge des personnes souffrantes de la maladie d'Alzheimer ainsi qu'un phytomédicament contre la maladie de la Dengue.

Enfin, la cherylline isolée des bulbes de *C. jagus* a démontré une activité prometteuse contre les virus de la Dengue et du Zika avec une EC_{50} assez élevée et une faible cytotoxicité sur toutes les lignées cellulaires utilisées. Au regard de ces résultats, elle semble être une stratégie pour lutter contre ces flavivirus.

En guise de perspectives, il serait intéressant :

- d'évaluer la capacité cytotoxique des extraits bruts alcaloïdiques de *P. trianthum* et de *C. jagus* chez les souris ainsi que la cherylline;
- de purifier l'extrait brut alcaloïdique de *P. trianthum* par la chromatographie sur colonne et évaluer l'activité anti-flavivirale notamment le virus de la Dengue et du Zika des alcaloïdes isolés;
- de cultiver le *P. trianthum* et le *C. jagus* dans les champs en vue de développer des phytomédicament à moindre coût pour la prise en charges des personnes atteintes de la Dengue et du Zika;
- de faire une étude transcriptomique de *C. jagus* pour identifier les gènes impliqués dans la biosynthèse de la sangunine et la cherylline;
- et enfin de produire ces molécules rares à savoir la sanguinine et la cherylline par la biologie synthétique à partir des microalgues.

BIBLIOGRAPHIE

1. Organization, W. H. Stratégie de l'OMS pour la médecine traditionnelle pour 2002-2005; Genève : Organisation mondiale de la Santé : 2002.

2. Fabricant, D. S.; Farnsworth, N. R., The value of plants used in traditional medicine for drug discovery. *Environmental Health Perspectives* **2001,** *109* (suppl 1), 69-75.

3. Alves, R. R.; Rosa, I. M., Biodiversity, traditional medicine and public health: where do they meet? *Journal of Ethnobiology and Ethnomedicine* **2007,** *3* (1), 1-9.

4. Boakye, M. K.; Pietersen, D. W.; Kotzé, A.; Dalton, D.-L.; Jansen, R., Knowledge and uses of African pangolins as a source of traditional medicine in Ghana. *PLoS One* **2015,** *10* (1), e0117199.

5. Chukwuma, E. C.; Soladoye, M. O.; Feyisola, R. T., Traditional medicine and the future of medicinal Plants in Nigeria. *Journal of Medicinal Plants Studies* **2015,** *3* (4), 23-9.

6. Faye, P. M., *Plantes médicinales et savoirs locaux: un patrimoine économique, social et culturel menacé de disparition*. Editions L'Harmattan: 2018.

7. Kerharo, J.; Adam, J.-G., La pharmacopée sénégalaise traditionnelle : plantes médicinales et toxiques. **1974**.

8. Sy, F. Phytomédicaments : Une aubaine pour populations pauvres. http://www.santetropicale.com/Actualites/0903/0903_1.htm

9. Cisse, A.; Gueye, M.; Ka, A.; Ndiaye, F.; Koma, S.; Akpo, L. E., Ethnobotanique des plantes médicinales chez les bergers peuls de Widou Thiengoly de la commune de Téssékéré (Ferlo-Nord Sénégal). *Journal of Applied Biosciences* **2016,** *98*, 9301-8.

10. Diatta, C.; Gueye, M.; Akpo, L., Les plantes médicinales utilisées contre les dermatoses dans la pharmacopée Baïnounk de Djibonker, région de Ziguinchor (Sénégal). *Journal of Applied Biosciences* **2013,** *70*, 5599-607.

11. Kerharo, J.; Adam, J. G., Les plantes médicinales, toxiques et magiques des Niominka et des Socé des Iles du Saloum (Sénégal). *Acta Tropica* **1964,** *8*, 279-334.

12. Ka, S.; Koirala, M.; Mérindol, N.; Desgagné-Penix, I., Biosynthesis and Biological Activities of Newly Discovered Amaryllidaceae Alkaloids. *Molecules* **2020,** *25* (21), 4901.

13. Bastida Armengol, J.; Berkov, S.; Torras Claveria, L.; Pigni, N. B.; Andrade, J. P. d.; Martínez, V.; Codina Mahrer, C.; Viladomat Meya, F., Chemical and biological aspects of Amaryllidaceae alkaloids. *Recent Advances in Pharmaceutical Sciences, 2011, Chapter 3, p 65-100 Editor: Diego Muñoz-Torrero* **2011**.

14. Kornienko, A.; Evidente, A., Chemistry, biology, and medicinal potential of narciclasine and its congeners. *Chemical Reviews* **2008,** *108* (6), 1982-2014.

15. Chopra, R. N.; Nayar, S. L.; Chopra, I. C., *Glossary of Indian medicinal plants*. Council of Scientific & Industrial Research New Delhi: 1956; Vol. 1.

16. Breyer-Brandwijk, M. G., The Medicinal and Poisonous Plants of Southern and Eastern Africa being an Account of their Medicinal and other Uses, Chemical Composition, Pharmacological Effects and Toxicology in Man and Animal. *The Medicinal and Poisonous Plants of Southern and Eastern Africa being an Account of their Medicinal and other Uses, Chemical Composition, Pharmacological Effects and Toxicology in Man and Animal* **1962,** (Edn 2).

17. Noumi, E.; Zollo, A.; Lontsi, D., Aphrodisiac plants used in Cameroon. *Fitoterapia (Milano)* **1998,** *69* (2), 125-34.

18. Sür-Altiner, D.; Gürkan, E.; Mutlu, G.; Tuzlaci, E.; Ang, Ö., The antifungal activity of Pancratium maritimum. *Fitoterapia* **1999,** *70* (2), 187-9.

19. Kerharo, J.; Adam, J., The Medicinal, Poisonous, and Magical Plants of the Niominka and Socé People of the Islands of Saloum, Senegal. *Acta Tropica* **1964,** (Suppl. 8), 279-334.

20. Ba, D. Le pancraium trianthum. http://seyilaabe-htkm.blogspot.com/2015/10/ (accessed 25 Novembre 2020).

21. Cedrón, J. C.; Del Arco-Aguilar, M.; Estévez-Braun, A.; Ravelo, Á. G., Chemistry and biology of Pancratium alkaloids. In *The Alkaloids: Chemistry and Biology*, Elsevier: 2010; Vol. 68, pp 1-37.

22. Mugnier, J., Nouvelle Flore illustrée du Sénégal et des régions voisines. *Agroservices fr, France* **2008**.

23. Struwe, L., Field identification of the 50 most common plant families in temperate regions. The State University of New Jersey.< http. www. rci. rutger. edu: 2009.

24. Daly, D. C.; Cameron, K. M.; Stevenson, D. W., Plant systematics in the age of genomics. *Plant Physiology* **2001,** *127* (4), 1328-33.

25. APG, I., An update of the Angiosperm Phylogeny Group classification for the orders and families of flowering plants: APG IV. *Botanical Journal of the Linnean Society* **2016,** *181*, 1-20.

26. Ekici, N.; Dane, F., Cytological and histological studies on female gametophyte of Leucojum aestivum (Amaryllidaceae). *Biologia* **2008,** *63* (1), 67-72.

27. Saliba, S. Nouvelles approches biotechnologiques pour l'obtention d'alcaloïdes: culture in vitro de Leucojum aestivum L. et isolement d'endophytes bactériens d'Amaryllidaceae. Université de Lorraine, 2015.

28. Adesanya, S.; Olugbade, T.; Odebiyl, O.; Aladesanmi, J., Antibacterial alkaloids in Crinum jagus. *International Journal of Pharmacognosy* **1992,** *30* (4), 303-7.

29. lanata Tuss, A., chapter I occurrence of alkaloids in plant species. *Chemistry of Natural Compounds* **1996,** *32* (1).

30. Bruneton, J.; Barton, D. H. R., *Eléments de Phytochimie et de Pharmacognosie*. Technique et documentation: 1987.

31. Farnsworth, N. R.; Akerele, O.; Bingel, A. S.; Soejarto, D. D.; Guo, Z., Medicinal plants in therapy. *Bulletin of the world health organization* **1985,** *63* (6), 965.

32. Le Marec, C., Histoire de l'opium médicinal: Du pavot aux alcaloïdes de l'opium. *Douleurs: Evaluation-Diagnostic-Traitement* **2004,** *5* (2), 83-98.

33. Cardinali, G.; Cardinali, G.; ENEIN, M. A., Studies on the antimitotic activity of leurocristine (vincristine). *Blood* **1963,** *21* (1), 102-10.

34. Singh, A.; Desgagné-Penix, I., Biosynthesis of the Amaryllidaceae alkaloids. *Plant Science Today* **2014,** *1* (3), 114-20.

35. Gerrard, A., The proximate principles of the Narcissus pseudonarcissus. *Pharm J* **1877,** *8*, 214-5.

36. Asahina, Y.; Sugii, Y., Ueber die Identität des Lycorins und Narcissins. *Archiv der Pharmazie* **1913,** *251* (5), 357-60.

37. Morishima, K., Chemische und pharmakologische Untersuchungen über die Alkaloide der Lycoris radiata Herb. *Archiv für experimentelle Pathologie und Pharmakologie* **1897,** *40* (3-4), 221-40.

38. Desgagné-Penix, I., Biosynthesis of alkaloids in Amaryllidaceae plants: a review. *Phytochemistry Reviews* **2020**.

39. Kilgore, M. B.; Kutchan, T. M., The Amaryllidaceae alkaloids: biosynthesis and methods for enzyme discovery. *Phytochemistry Reviews* **2016,** *15* (3), 317-37.

40. El Tahchy, A.; Ptak, A.; Boisbrun, M.; Barre, E.; Guillou, C.; Dupire, F. o.; Chrétien, F. o.; Henry, M.; Chapleur, Y.; Laurain-Mattar, D., Kinetic study of the rearrangement of deuterium-labeled 4′-O-methylnorbelladine in Leucojum aestivum shoot cultures by mass spectrometry. Influence of precursor feeding on Amaryllidaceae alkaloid accumulation. *Journal of Natural Products* **2011,** *74* (11), 2356-61.

41. Saliba, S.; Ptak, A.; Laurain-Mattar, D., 4′-O-Methylnorbelladine feeding enhances galanthamine and lycorine production by Leucojum aestivum L. shoot cultures. *Engineering in Life Sciences* **2015,** *15* (6), 640-5.

42. Barton, D.; Kirby, A.; Kirby, G., Phenol oxidation and biosynthesis. Part XVII. Investigations on the biosynthesis of sinomenine. *Journal of the Chemical Society C: Organic* **1968**, 929-36.

43. El Tahchy, A.; Boisbrun, M.; Ptak, A.; Dupire, F.; Chrétien, F.; Henry, M.; Chapleur, Y.; Laurain-Mattar, D., New method for the study of Amaryllidaceae alkaloid biosynthesis using biotransformation of deuterium-labeled precursor in tissue cultures. *Acta Biochimica Polonica* **2010,** *57* (1).

44. Suhadolnik, R.; Fischer, A.; Zulalian, J., Biogenesis of the Amaryllidaceae alkaloids. II. Studies with whole plants, floral primordia and cell free extracts. *Biochemical and Biophysical Research Communications* **1963,** *11* (3), 208-12.

45. Wildman, W.; Battersby, A.; Breuer, S., Biosynthesis in the Amaryllidaceae. Incorporation of 3-C14-Tyrosine and Phenylalanine in Nerine Bowdenii W. Wats. *Journal of the American Chemical Society* **1962,** *84* (23), 4599-600.

46. He, M.; Qu, C.; Gao, O.; Hu, X.; Hong, X., Biological and pharmacological activities of amaryllidaceae alkaloids. *RSC Advances* **2015,** *5* (21), 16562-74.

47. Hotchandani, T.; Desgagne-Penix, I., Heterocyclic Amaryllidaceae alkaloids: biosynthesis and pharmacological applications. *Current Topics in Medicinal chemistry* **2017,** *17* (4), 418-27.

48. Ghavre, M.; Froese, J.; Pour, M.; Hudlicky, T., Synthesis of Amaryllidaceae constituents and unnatural derivatives. *Angewandte Chemie International Edition* **2016,** *55* (19), 5642-91.

49. McNulty, J.; Zepeda-Velázquez, C., Enantioselective Organocatalytic Michael/Aldol Sequence: Anticancer Natural Product (+)-trans-Dihydrolycoricidine. *Angewandte Chemie* **2014,** *126* (32), 8590-4.

50. Santos, A. S.; Martins, M. M.; Marques, M. M. B., Recent Developments in the Chemical Synthesis of Amaryllidaceae Alkaloids. *Synthetic Approaches to Nonaromatic Nitrogen Heterocycles* **2020**, 549-93.

51. Kim, H. K.; Choi, Y. H.; Verpoorte, R., NMR-based metabolomic analysis of plants. *Nature protocols* **2010,** *5* (3), 536-49.

52. Lubbe, A.; Pomahačová, B.; Choi, Y. H.; Verpoorte, R., Analysis of metabolic variation and galanthamine content in Narcissus bulbs by 1H NMR. *Phytochemical Analysis: An International Journal of Plant Chemical and Biochemical Techniques* **2010,** *21* (1), 66-72.

53. Silverstein, R.; Webster, F.; Kiemle, D., Identification spectrométrique de composés organiques, de Boeck. *de Boeck Universite: Bruxelles* **2007**, 27.

54. Bastida, J.; Lavilla, R.; Viladomat, F., Chemical and biological aspects of Narcissus alkaloids. *The Alkaloids: Chemistry and Biology* **2006,** *63*, 87-179.

55. Torras-Claveria, L.; Berkov, S.; Jáuregui, O.; Caujapé, J.; Viladomat, F.; Codina, C.; Bastida, J., Metabolic profiling of bioactive Pancratium canariense extracts by GC-MS. *Phytochemical Analysis: An International Journal of Plant Chemical and Biochemical Techniques* **2010,** *21* (1), 80-8.

56. Nair, J. J.; Wilhelm, A.; Bonnet, S. L.; van Staden, J., Antibacterial constituents of the plant family Amaryllidaceae. *Bioorganic & Medicinal Chemistry Letters* **2017,** *27* (22), 4943-51.

57. Brossi, A.; Grethe, G.; Teitel, S.; Wildman, W. C.; Bailey, D. T., Cherylline, a 4-phenyl-1, 2, 3, 4-tetrahydroisoquinoline alkaloid. *The Journal of Organic Chemistry* **1970,** *35* (4), 1100-4.

58. Jin, Z.; Yao, G., Amaryllidaceae and Sceletium alkaloids. *Natural Product Reports* **2019,** *36* (10), 1462-88.

59. Chabrier, P.-E. In *Stratégies thérapeutiques et maladie d'Alzheimer : que peuvent apporter les modèles animaux?*, Annales pharmaceutiques françaises, Elsevier: 2009; pp 97-103.

60. mondiale de la Santé, A. *Projet de plan mondial d'action de santé publique contre la démence: rapport du Directeur général*; Organisation mondiale de la Santé: 2017.

61. Coumé, M.; Touré, K.; Thiam, M. H.; Zunzunegui, M. V.; Bacher, Y.; Diop, T. M.; Ndiaye, M. M., Estimation de la prévalence du déficit cognitif dans une population de personnes âgées sénégalaises du Centre médico-social et universitaire de l'Institution de prévoyance retraite du Sénégal. *Gériatrie et Psychologie Neuropsychiatrie du Vieillissement* **2012,** *10* (1), 39-46.

62. Berkov, S.; Codina, C.; Viladomat, F.; Bastida, J., N-Alkylated galanthamine derivatives: Potent acetylcholinesterase inhibitors from Leucojum aestivum. *Bioorganic & Medicinal Chemistry Letters* **2008,** *18* (7), 2263-6.

63. Heinrich, M., Galanthamine from Galanthus and other Amaryllidaceae–chemistry and biology based on traditional use. In *The Alkaloids: Chemistry and Biology*, Elsevier: 2010; Vol. 68, pp 157-65.

64. Gnoula, c. Etudes des proprietes cytotoxiques et antiradicalaires d'extraits de feuilles et de galles. Universite de Ouagadougou, 2009.

65. Gondhowiardjo, S.; Christina, N.; Ganapati, N. P.; Hawariy, S.; Radityamurti, F.; Jayalie, V. F.; Octavianus, S.; Prawira Putra, A.; Sekarutami, S. M.; Prajogi, G. B., Five-Year Cancer Epidemiology at the National Referral Hospital: Hospital-Based Cancer Registry Data in Indonesia. *JCO Global Oncology* **2021,** *5* (1), 190-203.

66. Organization, W. H., International Agency for Research on Cancer Latest world cancer statistics: global cancer burden rises to 14.1 million new cases in 2012: marked increase in breast cancers must be addressed. 2014.

67. Bray, F.; Ferlay, J.; Soerjomataram, I.; Siegel, R. L.; Torre, L. A.; Jemal, A., Global cancer statistics 2018: GLOBOCAN estimates of incidence and mortality worldwide for 36 cancers in 185 countries. *CA: A Cancer Journal for Clinicians* **2018,** *68* (6), 394-424.

68. Bouri, N.-V.; Ba, O.; Dieme, J.-L.; Mbengue, M.; Boye, A.; Fall, T.; Dia, D.; Diouf, G.; Guèye, M.-N., État des lieux du registre des tumeurs au Sénégal: bilan à 6 ans d'enregistrement en ligne. *Revue des Maladies Respiratoires* **2017,** *34*, A75.

69. Mbaye, E. H. S.; Gheit, T.; Dem, A.; McKay-Chopin, S.; Toure-Kane, N. C.; Mboup, S.; Tommasino, M.; Sylla, B. S.; Boye, C. S. B., Human papillomavirus infection in women in four regions of Senegal. *Journal of Medical Virology* **2014,** *86* (2), 248-56.

70. Hu, H.; Wang, S.; Shi, D.; Zhong, B.; Huang, X.; Shi, C.; Shao, Z., Lycorine exerts antitumor activity against osteosarcoma cells in vitro and in vivo xenograft model through the JAK2/STAT3 pathway. *OncoTargets and Therapy* **2019,** *12*, 5377.

71. Sun, Y.; Wu, P.; Sun, Y.; Sharopov, F. S.; Yang, Q.; Chen, F.; Wang, P.; Liang, Z., Lycorine possesses notable anticancer potentials in on-small cell lung carcinoma cells via blocking Wnt/β-catenin signaling and epithelial-mesenchymal transition (EMT). *Biochemical and Biophysical Research Communications* **2018,** *495* (1), 911-21.

72. Berkov, S.; Osorio, E.; Viladomat, F.; Bastida, J., Chemodiversity, chemotaxonomy and chemoecology of Amaryllidaceae alkaloids. *The Alkaloids: Chemistry and Biology* **2020,** *83*, 113-85.

73. Lambrechts, L.; Scott, T. W.; Gubler, D. J., Consequences of the expanding global distribution of Aedes albopictus for dengue virus transmission. *PloS Neglected Tropical Disseasis* **2010,** *4* (5), e646.

74. Dwivedi, V. D.; Tripathi, I. P.; Tripathi, R. C.; Bharadwaj, S.; Mishra, S. K., Genomics, proteomics and evolution of dengue virus. *Briefings in Functional Genomics* **2017,** *16* (4), 217-27.

75. Rossmann, M.; Kuhn, R.; Zhang, W.; Pletnev, S.; Corver, J.; Lenches, E.; Jones, C.; Mukhopadhyay, S.; Chipman, P.; Strauss, E. In *Structure of dengue virus: implications for flavivirus organization, maturation, and fusion*, Acta Crystallographica a-Foundation and Advances, Int union Crystallography 2 Abbey sq, Chester, ch1 2hu, England: 2002; pp C6-C.

76. Rodenhuis-Zybert, I. A.; Wilschut, J.; Smit, J. M., Dengue virus life cycle: viral and host factors modulating infectivity. *CMLS* **2010,** *67* (16), 2773-86.

77. Quintana, V.; Selisko, B.; Brunetti, J.; Eydoux, C.; Guillemot, J.; Canard, B.; Damonte, E.; Julander, J.; Castilla, V., Antiviral activity of the natural alkaloid anisomycin against dengue and Zika viruses. *Antiviral Research* **2020,** *176*, 104749.

78. Gubler, D. J., Dengue and dengue hemorrhagic fever. *Clinical Microbiology Reviews* **1998,** *11* (3), 480-96.

79. Petersen, L. R.; Jamieson, D. J.; Powers, A. M.; Honein, M. A., Zika virus. *New England Journal of Medicine* **2016,** *374* (16), 1552-63.

80. Plourde, A. R.; Bloch, E. M., A literature review of Zika virus. *Emerging infectious diseases* **2016,** *22* (7), 1185.

81. Aubry, P.; Gaüzère, B.-A.; Vanhecke, C. Dengue. http://medecinetropicale.free.fr/cours/dengue.pdf (accessed 18/02/2021).

82. Dieng, I.; Cunha, M.; Diagne, M. M.; Sembène, P. M.; Zanotto, P. M. d. A.; Faye, O.; Faye, O., Origin and Spread of the Dengue Virus Type 1, Genotype V in Senegal, 2015–2019. *Viruses* **2021,** *13* (1), 57.

83. Check Hayden, E., Zika highlights role of controversial fetal-tissue research. *Nature News* **2016,** *532* (7597), 16.

84. Khetarpal, N.; Khanna, I., Dengue fever: causes, complications, and vaccine strategies. *Journal of Immunology Research* **2016,** *2016*.

85. Dong, H.; Zhang, B.; Shi, P.-Y., Flavivirus methyltransferase: a novel antiviral target. *Antiviral research* **2008,** *80* (1), 1-10.

86. Hotchandani, T.; Desgagne-Penix, I., Heterocyclic Amaryllidaceae Alkaloids: Biosynthesis and Pharmacological Applications. *Current Topics in Medicinal Chemistry* **2017,** *17* (4), 418-27.

87. Ka, S.; Koirala, M.; Mérindol, N.; Desgagné-Penix, I., Biosynthesis and biological activities of newly discovered Amaryllidaceae alkaloids. *Molecules* **2020,** *25* (21), 4901.

88. Cimmino, A.; Masi, M.; Evidente, M.; Superchi, S.; Evidente, A., Amaryllidaceae alkaloids: Absolute configuration and biological activity. *Chirality* **2017,** *29* (9), 486-99.

89. Ding, Y.; Qu, D.; Zhang, K.-M.; Cang, X.-X.; Kou, Z.-N.; Xiao, W.; Zhu, J.-B., Phytochemical and biological investigations of Amaryllidaceae alkaloids: a review. *Journal of Asian Natural Products Research* **2017,** *19* (1), 53-100.

90. Duri, Z. J.; Scovill, J. P.; Huggins, J. W., Activity of a methanolic extract of Zimbabwean Crinum macowanii against exotic RNA viruses in vitro. *Phytotherapy Research* **1994,** *8* (2), 121-2.

91. Wang, P.; Li, L. F.; Wang, Q. Y.; Shang, L. Q.; Shi, P. Y.; Yin, Z., Anti-dengue-virus activity and structure-activity relationship studies of lycorine derivatives. *ChemMedChem* **2014,** *9* (7), 1522-33.

92. Gabrielsen, B.; Monath, T. P.; Huggins, J. W.; Kefauver, D. F.; Pettit, G. R.; Groszek, G.; Hollingshead, M.; Kirsi, J. J.; Shannon, W. M.; Schubert, E. M.; et al., Antiviral (RNA) activity of selected Amaryllidaceae isoquinoline constituents and synthesis of related substances. *Journal of Natural Products* **1992,** *55* (11), 1569-81.

93. Zou, G.; Puig-Basagoiti, F.; Zhang, B.; Qing, M.; Chen, L.; Pankiewicz, K. W.; Felczak, K.; Yuan, Z.; Shi, P.-Y., A single-amino acid substitution in West Nile virus 2K peptide between NS4A and NS4B confers resistance to lycorine, a flavivirus inhibitor. *Journal of Virology* **2009,** *384* (1), 242-52.

94. Chen, H.; Lao, Z.; Xu, J.; Li, Z.; Long, H.; Li, D.; Lin, L.; Liu, X.; Yu, L.; Liu, W.; Li, G.; Wu, J., Antiviral activity of lycorine against Zika virus in vivo and in vitro. *Journal of Virology* **2020,** *546*, 88-97.

95. Li, S.-y.; Chen, C.; Zhang, H.-q.; Guo, H.-y.; Wang, H.; Wang, L.; Zhang, X.; Hua, S.-n.; Yu, J.; Xiao, P.-g., Identification of natural compounds with antiviral activities against SARS-associated coronavirus. *Antiviral research* **2005,** *67* (1), 18-23.

96. Zhang, Y.-N.; Zhang, Q.-Y.; Li, X.-D.; Xiong, J.; Xiao, S.-Q.; Wang, Z.; Zhang, Z.-R.; Deng, C.-L.; Yang, X.-L.; Wei, H.-P., Gemcitabine, lycorine and oxysophoridine inhibit novel coronavirus (SARS-CoV-2) in cell culture. *Emerging Microbes & Infections* **2020,** (just-accepted), 1-10.

97. Jin, Y.-H.; Min, J. S.; Jeon, S.; Lee, J.; Kim, S.; Park, T.; Park, D.; Jang, M. S.; Park, C. M.; Song, J. H., Lycorine, a non-nucleoside RNA dependent RNA polymerase inhibitor, as potential treatment for emerging coronavirus infections. *Phytomedicine* **2020**, 153440.

98. Shen, L.; Niu, J.; Wang, C.; Huang, B.; Wang, W.; Zhu, N.; Deng, Y.; Wang, H.; Ye, F.; Cen, S., High-throughput screening and identification of potent broad-

spectrum inhibitors of coronaviruses. *Journal of Virology* **2019,** *93* (12), e00023-19.

99. Vaneckova, N.; Host'alkova, A.; Safratova, M.; Kunes, J.; Hulcova, D.; Hrabinova, M.; Doskocil, I.; Stepankova, S.; Opletal, L.; Novakova, L.; Jun, D.; Chlebek, J.; Cahlikova, L., Isolation of Amaryllidaceae alkaloids from *Nerine bowdenii* W. Watson and their biological activities. *Rsc Advances* **2016,** *6* (83), 80114-20.

100. N'Tamon, A. D.; Okpekon, A. T.; Bony, N. F.; Bernadat, G.; Gallard, J.-F.; Kouamé, T.; Séon-Méniel, B.; Leblanc, K.; Rharrabti, S.; Mouray, E., Streamlined targeting of Amaryllidaceae alkaloids from the bulbs of Crinum scillifolium using spectrometric and taxonomically-informed scoring metabolite annotations. *Phytochemistry* **2020,** *179*, 112485.

101. Al Mamun, A.; Maříková, J.; Hulcová, D.; Janoušek, J.; Šafratová, M.; Nováková, L.; Kučera, T.; Hrabinová, M.; Kuneš, J.; Korábečný, J., Amaryllidaceae Alkaloids of Belladine-Type from Narcissus pseudonarcissus cv. Carlton as New Selective Inhibitors of Butyrylcholinesterase. *Biomolecules* **2020,** *10* (5), 800.

102. Ka, S.; Masi, M.; Merindol, N.; Di Lecce, R.; Plourde, M. B.; Seck, M.; Gorecki, M.; Pescitelli, G.; Desgagne-Penix, I.; Evidente, A., Gigantelline, gigantellinine and gigancrinine, cherylline- and crinine-type alkaloids isolated from Crinum jagus with anti-acetylcholinesterase activity. *Phytochemistry* **2020,** *175*, 112390.

103. Ang, S.; Liu, X. M.; Huang, X. J.; Zhang, D. M.; Zhang, W.; Wang, L.; Ye, W. C., Four New Amaryllidaceae Alkaloids from Lycoris radiata and Their Cytotoxicity. *Planta Med* **2015,** *81* (18), 1712-8.

104. Endo, Y.; Sugiura, Y.; Funasaki, M.; Kagechika, H.; Ishibashi, M.; Ohsaki, A., Two new alkaloids from Crinum asiaticum var. japonicum. *Journal of Natural Medecine* **2019,** *73* (3), 648-52.

105. Zhan, G.; Zhou, J.; Liu, R.; Liu, T.; Guo, G.; Wang, J.; Xiang, M.; Xue, Y.; Luo, Z.; Zhang, Y.; Yao, G., Galanthamine, Plicamine, and Secoplicamine Alkaloids from Zephyranthes candida and Their Anti-acetylcholinesterase and Anti-inflammatory Activities. *Journal of Natural Products* **2016,** *79* (4), 760-6.

106. Liu, Z. M.; Huang, X. Y.; Cui, M. R.; Zhang, X. D.; Chen, Z.; Yang, B. S.; Zhao, X. K., Amaryllidaceae alkaloids from the bulbs of Lycoris radiata with cytotoxic and anti-inflammatory activities. *Fitoterapia* **2015,** *101*, 188-93.

107. Tallini, L. R.; Osorio, E. H.; Santos, V. D. D.; Borges, W. S.; Kaiser, M.; Viladomat, F.; Zuanazzi, J. A. S.; Bastida, J., Hippeastrum reticulatum (Amaryllidaceae): Alkaloid Profiling, Biological Activities and Molecular Docking. *Molecules* **2017,** *22* (12), 2191.

108. Zhan, G.; Zhou, J.; Liu, J.; Huang, J.; Zhang, H.; Liu, R.; Yao, G., Acetylcholinesterase Inhibitory Alkaloids from the Whole Plants of Zephyranthes carinata. *Journal Natural Products* **2017,** *80* (9), 2462-71.

109. Emir, A.; Emir, C.; Bozkurt, B.; Onur, M. A.; Bastida, J.; Somer, N. U., Alkaloids from Galanthus fosteri. *Phytochem Lett* **2016,** *17*, 167-72.

110. Breiterova, K.; Koutova, D.; Marikova, J.; Havelek, R.; Kunes, J.; Majorosova, M.; Opletal, L.; Hostalkova, A.; Jenco, J.; Rezacova, M.; Cahlikova, L., Amaryllidaceae Alkaloids of Different Structural Types from Narcissus L. cv. Professor Einstein and Their Cytotoxic Activity. *Plants (Basel)* **2020,** *9* (2), 137.

111. Katoch, D.; Kumar, D.; Padwad, Y. S.; Singh, B.; Sharma, U., Pseudolycorine N-oxide, a new N-oxide from Narcissus tazetta. *Natural Product Reports* **2020,** *34* (14), 2051-8.

112. Carvalho, K. R.; Silva, A. B.; Torres, M. C. M.; Pinto, F. C. L.; Guimaraes, L. A.; Rocha, D. D.; Silveira, E. R.; Costa-Lotufo, L. V.; Braz, R.; Pessoa, O. D. L., Cytotoxic Alkaloids from Hippeastrum solandriflorum Lindl. *Journal of the Brazilian Chemical Society* **2015,** *26* (10), 1976-80.

113. Ortiz, J. E.; Pigni, N. B.; Andujar, S. A.; Roitman, G.; Suvire, F. D.; Enriz, R. D.; Tapia, A.; Bastida, J.; Feresin, G. E., Alkaloids from Hippeastrum argentinum and Their Cholinesterase-Inhibitory Activities: An in Vitro and in Silico Study. *Journal of Natural Products* **2016,** *79* (5), 1241-8.

114. Hanh, T. T. H.; Huong, P. T. T.; Van Thanh, N.; Trung, N. Q.; Van Cuong, T.; Mai, N. T.; Cuong, N. T.; Cuong, N. X.; Nam, N. H.; Van Minh, C., Crinane, augustamine, and β-carboline alkaloids from Crinum latifolium. *Phytochemistry Letter* **2018,** *24*, 27-30.

115. Cho, N.; Du, Y.; Valenciano, A. L.; Fernandez-Murga, M. L.; Goetz, M.; Clement, J.; Cassera, M. B.; Kingston, D. G. I., Antiplasmodial alkaloids from bulbs of Amaryllis belladonna Steud. *Bioorg Med Chem Lett* **2018,** *28* (1), 40-2.

116. Tallini, L. R.; Torras-Claveria, L.; Borges, W. S.; Kaiser, M.; Viladomat, F.; Zuanazzi, J. A. S.; Bastida, J., N-oxide alkaloids from Crinum amabile (Amaryllidaceae). *Molecules* **2018,** *23* (6), 1277.

117. Masi, M.; Cala, A.; Tabanca, N.; Cimmino, A.; Green, I. R.; Bloomquist, J. R.; van Otterlo, W. A.; Macias, F. A.; Evidente, A., Alkaloids with Activity against the Zika Virus Vector Aedes aegypti (L.)-Crinsarnine and Sarniensinol, Two New Crinine and Mesembrine Type Alkaloids Isolated from the South African Plant Nerine sarniensis. *Molecules* **2016,** *21* (11), 1432.

118. Bessa, C. D. P. B.; de Andrade, J. P.; de Oliveira, R. S.; Domingos, E.; Santos, H.; Romao, W.; Bastida, J.; Borges, W. S., Identification of Alkaloids from Hippeastrum aulicum (Ker Gawl.) Herb. (Amaryllidaceae) Using CGC-MS and Ambient Ionization

Mass Spectrometry (PS-MS and LS-MS). *Journal of the Brazilian Chemical Society* **2017,** *28* (5), 819-30.

119. Chaichompoo, W.; Chokchaisiri, R.; Sangkaew, A.; Pabuprapap, W.; Yompakdee, C.; Suksamrarn, A., Alkaloids with anti-human carbonic anhydrase isozyme II activity from the bulbs of Crinum asiaticum L. var. asiaticum. *Phytochemistry Letter* **2020,** *37*, 101-5.

120. Moodley, N.; Crouch, N.; Bastida, J.; Mulholland, D., Novel alkaloids and a ceramide from Brunsvigia natalensis (Amaryllidaceae) and their anti-neoplastic activity. *South African Journal of Botanyt* **2020**.

121. Katoch, D.; Kumar, D.; Padwad, Y. S.; Singh, B.; Sharma, U., Narciclasine-4-O-beta-D-xylopyranoside, a new narciclasine glycoside from Zephyranthes minuta. *Natural Product Research* **2020,** *34* (2), 233-20.

122. Masi, M.; Frolova, L. V.; Yu, X.; Mathieu, V.; Cimmino, A.; De Carvalho, A.; Kiss, R.; Rogelj, S.; Pertsemlidis, A.; Kornienko, A.; Evidente, A., Jonquailine, a new pretazettine-type alkaloid isolated from Narcissus jonquilla quail, with activity against drug-resistant cancer. *Fitoterapia* **2015,** *102*, 41-8.

123. Chen, M. X.; Huo, J. M.; Hu, J.; Xu, Z. P.; Zhang, X., Amaryllidaceae alkaloids from Crinum latifolium with cytotoxic, antimicrobial, antioxidant, and anti-inflammatory activities. *Fitoterapia* **2018,** *130*, 48-53.

124. Presley, C. C.; Krai, P.; Dalal, S.; Su, Q.; Cassera, M.; Goetz, M.; Kingston, D. G. I., New potently bioactive alkaloids from Crinum erubescens. *Bioorganic and Medicinal Chemistry* **2016,** *24* (21), 5418-22.

125. Masi, M.; van der Westhuyzen, A. E.; Tabanca, N.; Evidente, M.; Cimmino, A.; Green, I. R.; Bernier, U. R.; Becnel, J. J.; Bloomquist, J. R.; van Otterlo, W. A.; Evidente, A., Sarniensine, a mesembrine-type alkaloid isolated from Nerine sarniensis, an indigenous South African Amaryllidaceae, with larvicidal and adulticidal activities against Aedes aegypti. *Fitoterapia* **2017,** *116*, 34-8.

126. Zhan, G.; Qu, X.; Liu, J.; Tong, Q.; Zhou, J.; Sun, B.; Yao, G., Zephycandidine A, the First Naturally Occurring Imidazo[1,2-f]phenanthridine Alkaloid from Zephyranthes candida, Exhibits Significant Anti-tumor and Anti-acetylcholinesterase Activities. *Scientific Reports* **2016,** *6*, 33990.

127. Chen, N.; Ji, Y. B.; Zhang, W. G.; Xu, Y.; Yan, X. J.; Sun, Y. F.; Song, H.; Xu, C. R.; Cai, L. P.; Zheng, H. X.; Xiang, Z., Chemical Constituents from Hymenocallis littoralis. *Letters in Organic Chemistry* **2016,** *13* (7), 536-9.

128. Zhan, G.; Liu, J.; Zhou, J.; Sun, B.; Aisa, H. A.; Yao, G., Amaryllidaceae alkaloids with new framework types from Zephyranthes candida as potent acetylcholinesterase inhibitors. *European Journal of Medicinal Chemistry* **2017,** *127*, 771-80.

129. Safratova, M.; Hostalkova, A.; Hulcova, D.; Breiterova, K.; Hrabcova, V.; Machado, M.; Fontinha, D.; Prudencio, M.; Kunes, J.; Chlebek, J.; Jun, D.; Hrabinova, M.; Novakova, L.; Havelek, R.; Seifrtova, M.; Opletal, L.; Cahlikova, L., Alkaloids from Narcissus poeticus cv. Pink Parasol of various structural types and their biological activity. *Archives of Pharmacal Research* **2018,** *41* (2), 208-18.

130. Hulcova, D.; Marikova, J.; Korabecny, J.; Hostalkova, A.; Jun, D.; Kunes, J.; Chlebek, J.; Opletal, L.; De Simone, A.; Novakova, L.; Andrisano, V.; Ruzicka, A.; Cahlikova, L., Amaryllidaceae alkaloids from Narcissus pseudonarcissus L. cv. Dutch Master as potential drugs in treatment of Alzheimer's disease. *Phytochemistry* **2019,** *165*, 112055.

131. Mummed, B.; Abraha, A.; Feyera, T.; Nigusse, A.; Assefa, S., In vitro antibacterial activity of selected medicinal plants in the traditional treatment of skin and wound infections in eastern Ethiopia. *BioMed research international* **2018,** *2018*.

132. Woodford, N.; Livermore, D. M., Infections caused by Gram-positive bacteria: a review of the global challenge. *Journal of Infection* **2009,** *59*, S4-S16.

133. Nair, J. J.; Bastida, J.; Viladomat, F.; van Staden, J., Cytotoxic agents of the crinane series of Amaryllidaceae alkaloids. *Natural product communications* **2012,** *7* (12), 1934578X1200701234.

134. Wang, P.; Li, L. F.; Wang, Q. Y.; Shang, L. Q.; Shi, P. Y.; Yin, Z., Anti-dengue-virus activity and structure–activity relationship studies of lycorine derivatives. *ChemMedChem* **2014,** *9* (7), 1522-33.

135. Zou, G.; Puig-Basagoiti, F.; Zhang, B.; Qing, M.; Chen, L.; Pankiewicz, K. W.; Felczak, K.; Yuan, Z.; Shi, P.-Y., A single-amino acid substitution in West Nile virus 2K peptide between NS4A and NS4B confers resistance to lycorine, a flavivirus inhibitor. *Virology* **2009,** *384* (1), 242-52.

136. Chen, H.; Lao, Z.; Xu, J.; Li, Z.; Long, H.; Li, D.; Lin, L.; Liu, X.; Yu, L.; Liu, W., Antiviral activity of lycorine against Zika virus in vivo and in vitro. *Virology* **2020,** *546*, 88-97.

137. Elgorashi, E. E.; Stafford, G. I.; Van Staden, J., Acetylcholinesterase enzyme inhibitory effects of Amaryllidaceae alkaloids. *Planta medica* **2004,** *70* (03), 260-2.

138. Ortiz, J. E.; Garro, A.; Pigni, N. B.; Agüero, M. B.; Roitman, G.; Slanis, A.; Enriz, R. D.; Feresin, G. E.; Bastida, J.; Tapia, A., Cholinesterase-inhibitory effect and in silico analysis of alkaloids from bulbs of Hieronymiella species. *Phytomedicine* **2018,** *39*, 66-74.

139. Tallini, L. R.; Torras-Claveria, L.; Borges, W. D. S.; Kaiser, M.; Viladomat, F.; Zuanazzi, J. A. S.; Bastida, J., N-oxide alkaloids from Crinum amabile (Amaryllidaceae). *Molecules* **2018,** *23* (6), 1277.

140. Massé, N.; Selisko, B.; Malet, H.; Peyrane, F.; Debarnot, C.; Decroly, E.; Benarroch, D.; Egloff, M.; Guillemot, J.; Alvarez, K., Le virus de la dengue: cibles virales et antiviraux. *Virologie* **2007,** *11* (2), 121-33.

141. http://www.ansaarudine.org/confislam2015/?page_id=134 (consulté 29 Mai 2021).

ANNEXE A

BIOSYNTHESIS AND BIOLOGICAL ACTIVITIES OF NEWLY DISCOVERED AMARYLLIDACEAE ALKALOIDS

Seydou Ka, Manoj Koirala, Natacha Mérindol and Isabel Desgagné-Penix

Publiée le 23 octobre 2020 dans le journal *Molecules.*

Abstract

Alkaloids are an important group of specialized nitrogen metabolites with a wide range of biochemical and pharmacological effects. Since the first publication on lycorine in 1877, more than 650 alkaloids have been extracted from Amaryllidaceae bulbous plants and clustered together as the Amaryllidaceae alkaloids (AAs) family. AAs are specifically remarkable for their diverse pharmaceutical properties, as exemplified by the success of galantamine used to treat the symptoms of Alzheimer's disease. This review addresses the isolation, biological, and structure activity of AAs discovered from January 2015 to August 2020, supporting their therapeutic interest.

Keywords: Amaryllidaceae alkaloids; specialized metabolism; biosynthesis; antitumor; anti-cholinesterase; antiviral; antiparasitic

Introduction

The Amaryllidaceae species, belonging to the Asparagales monocot order, are a class of herbaceous, perennial, and bulbous flowering plants. The Amaryllidaceae plant family contains 85 genera and 1100 species that are widely distributed in the tropic and warm temperate regions of the globe [1]. In addition, the Amaryllidaceae plants are cultivated and exploited as ornamental plants for their beautiful flowers [2]. For centuries,

Amaryllidaceae have been used in traditional medicine, such as the oil extracted from the daffodil *Narcissus poeticus,* used to treat uterine tumors [3]. Since the isolation of lycorine in 1877 (initially named narcissia) from *Narcissus pseudonarcissus* and in 1897 from *Lycoris radiata* [4-6], the structures of hundreds of Amaryllidaceae alkaloids (AAs) have been elucidated [1,3,7]. They are exploited for their wide range of biological potentials including antitumor, antiviral, antibacterial, antifungal, antimalarial, anti-acetylcholinesterase (anti-AChE), analgesic, and cytotoxic activities [8,9]. Currently, in terms of commercial success, galantamine, widely occurring in the Amaryllidaceae plants, has been approved as an AChE inhibitor by the United States Food and Drug Administration to treat the symptoms of Alzheimer's disease (AD) [10]. Moreover, several other AAs, including lycorine, haemanthamine, and narciclasine have been used as lead molecules for anticancer research [11]. Thus, AAs represent an important resource for drug discovery.

This review addresses the isolation, biosynthesis, biological activities and structure activity of AAs discovered from January 2015 to August 2020.

Classification of Amaryllidaceae Alkaloids

To date, more than 650 AAs have been reported, and their chemical library is still expanding [1,12-24]. Although diverse in structure, this plethora of AAs are categorized together as they share a common initial synthesis pathway. In previous literature, large numbers of AAs have been classified into different groups according to chemical characteristics, e.g., molecular skeleton and ring structure [1,3,8,25]. For this review, AAs were classified into 10 main groups instead, following a biochemical classification based on biogenetic lineage and ring type, to easily track the biosynthetic pathways [26] (Table 1, Figure 1). For example, haemanthamine and crinine were grouped together with respect to their biosynthetic origin and ring type even if they were previously categorized separately [11]. Some AAs with ring types different than those of group I to IX were classified in group X (or other-types) because they follow distinct biogenetic pathway, or because we cannot clearly indicate their biosynthetic origin (Table 1). Galanthindole

contains a non-fused indole ring and might represent an artifact of homolycorine- or of pretazettine-type derivatives [27]. Ismine is considered to be a catabolic product from the haemanthamine-type skeleton, thus not a specific type of AA [28]. The latter examples demand further investigation on biogenetic origin and are not yet included on any particular type of AA.

Table 1. Main types of Amaryllidaceae alkaloids grouped according to their ring type and biosynthetic origin.

Number	Type Name	Ring-Type
I	Norbelladine	*N*-(3,4-Dioxybenzyl) -4-oxyphenethylamine
II	Cherylline	Tetrahydroisoquinoline
III	Galantamine	6H-Benzof,f]-2-benzazepine
IV	Lycorine	Pyrrolo[d,e]phenanthridine
V	Homolycorine	2-Benzopyrano-[3,4-g]indole
VI	Crinine	5,10b-Ethanophenanthridine
VII	Narciclasine	Lycoricidine
VIII	Pretazettine	2-Benzopyrano[3,4-c]indole
IX	Montanine	5,11-Methanomorphanthridine
X	Other	Different ring types and biogenetic origin

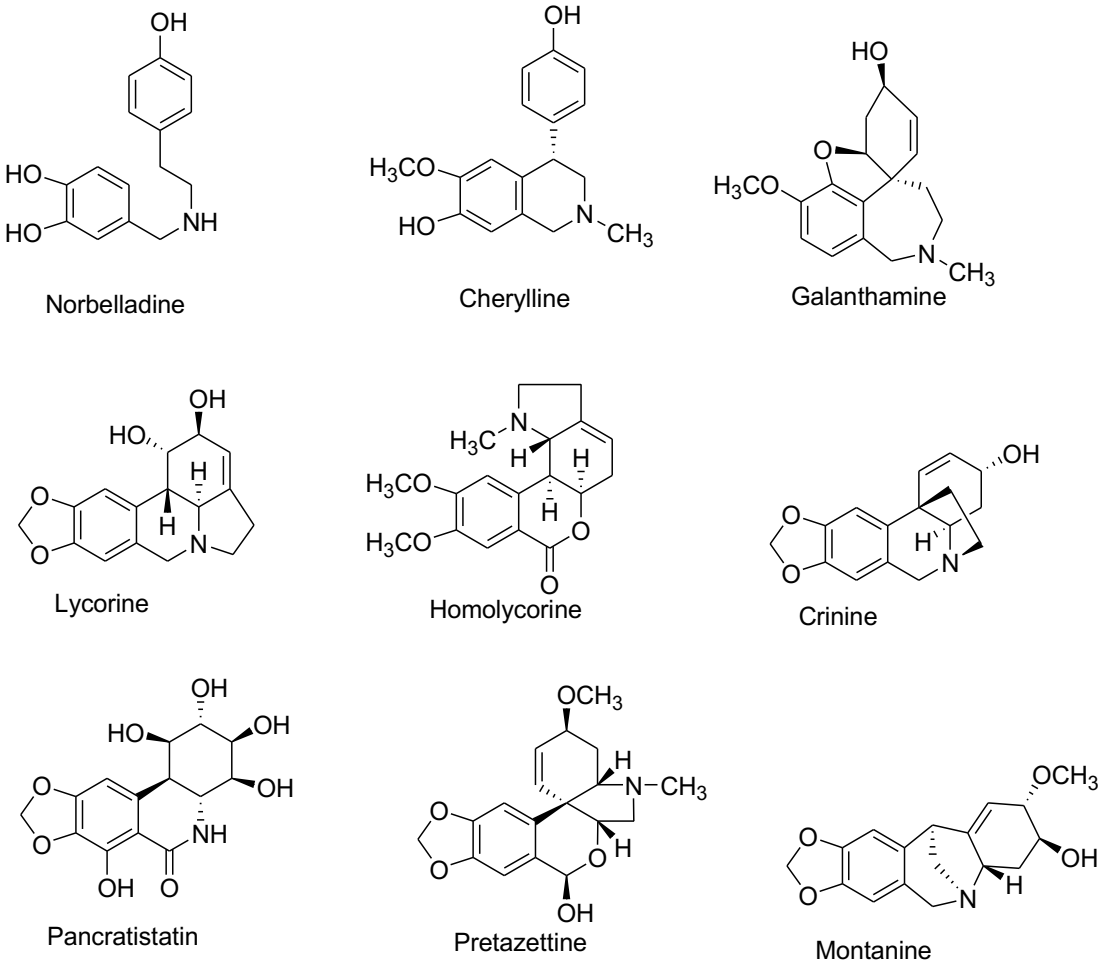

Figure 1 Representative Amaryllidaceae alkaloid structure for the main Amaryllidaceae alkaloid (AA)-types.

Some types of AA, such as plicamine and secoplicamine, are extracted in trace amounts exclusively from specific Amaryllidaceae species, such as Zephyranthes, but are classified in type X as they are rare, dinitrogenous members of AA, with a distinct biosynthetic linage [28-31]. Mesembrine alkaloids (also known as sceletium) have a distinct biosynthetic pathway, without norbelladine as key intermediate, they are usually extracted from Aizoaceae, but can be collected from several species of Amaryllidaceae [20]. Here, we concentrated exclusively on AAs that were discovered since 2015; hence, some alkaloids families are not represented.

Biosynthesis of Amaryllidaceae Alkaloids

Biosynthesis of AAs with their diverse and complex carbon skeleton involves a sequence of biochemical reactions such as oxidation, reduction, hydroxylation, methylation, phenol-phenol coupling, and oxide bridge formation. Although the complete AA biosynthetic pathway has not yet been elucidated, several steps with catalyzing enzymes can be predicted on the basis of the reaction types and enzyme families [2,26,32,33]. Here, we briefly discuss the AAs biosynthesis pathway and the enzymes involved.

Although novel AAs are still being discovered, radiolabeling experiments demonstrated that they all share a common biochemical pathway with a key intermediate; norbelladine, which is subsequently *O*-methylated, and then undergoes cyclization to give diverse basic skeletons of AAs (Figure 1; Figure 2) [34-40]. Norbelladine originates from the condensation of tyramine and 3,4-dihydroxybenzaldehyde (3,4-DHBA), molecules derived from the aromatic amino acids L-tyrosine and L-phenylalanine, respectively (Figure 2). The enzyme responsible for tyramine biosynthesis is the tyrosine decarboxylase (TYDC) (Figure 2). Two gene transcript variants of TYDC*,* named *TYDC1* and *TYDC2,* were identified from the transcriptome of different Amaryllidaceae species including *N. pseudonarcissus* [41], *Narcissus papyraceus* [42], *Lycoris radiata* [43], and *L. aureus* [44].

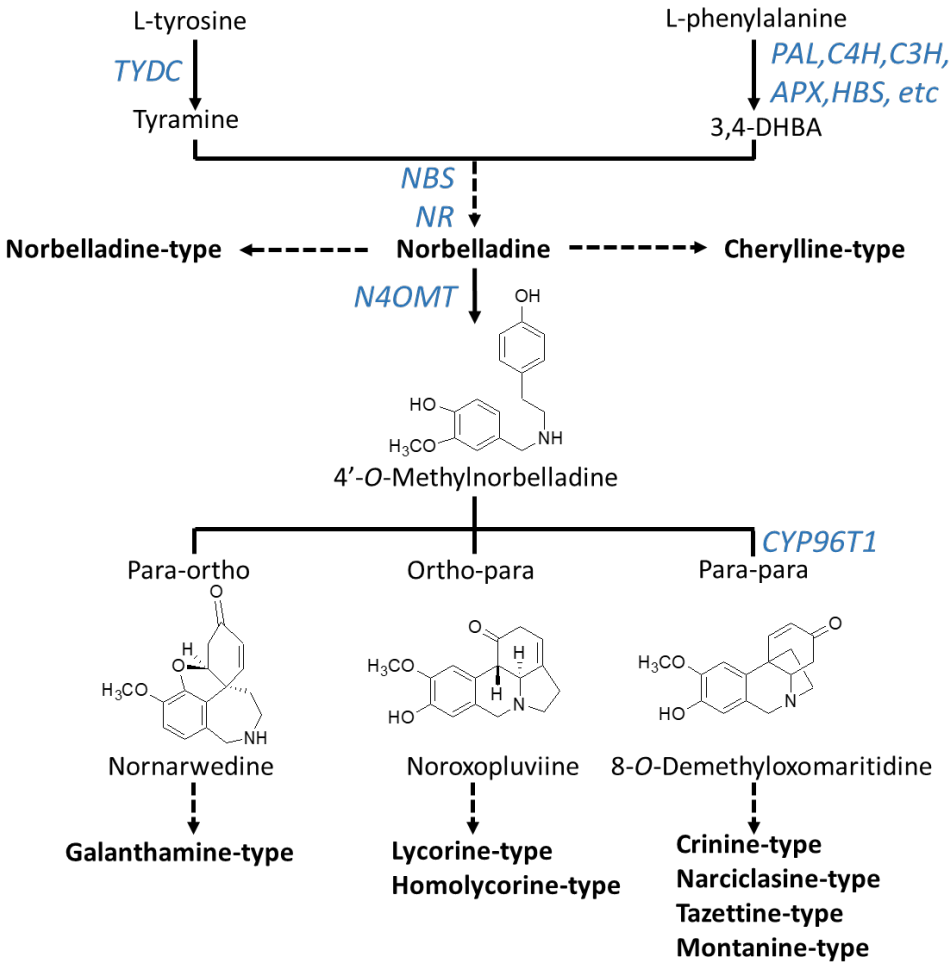

Figure 2 Biosynthesis pathway to major types of Amaryllidaceae alkaloids. Arrows without labeling reflect chemical reactions that have not been enzymatically characterized. Enzymes that have been identified are labeled in blue. A solid arrow symbolizes one enzymatic step whereas a broken arrow shows multiple enzymatic reactions. Chemical structures of precursors were added to clarify the regioselective phenol-phenol' coupling reaction. Enzyme abbreviations: PAL, phenylalanine ammonia-lyase; C4H, cinnamate 4-hydroxylase; C3H, coumarate 3-hydroxylase; APX, ascorbate peroxidase; HBS, 4-hydroxybenzaldehyde synthase; TYDC, tyrosine decarboxylase; NBS, norbelladine synthase; NR, noroxomaritidine reductase; CYP96T1, cytochrome P450 monooxygenase 96T1.

The pathway leading to 3,4-DHBA from L-phenylalanine involves a series of reactions known as the phenylpropanoid pathway which is phylogenetically spread in most plant species. In Amaryllidaceae, using precursor feeding experiments, it was reported that *trans*-cinnamic acid, *p*-coumaric acid, and caffeic acid were intermediate products that

ultimately led to 3,4-DHBA [45,46]. Specifically, L-phenylalanine is converted to *trans*-cinnamic acid by the phenylalanine ammonia-lyase (PAL) (Figure 2). Several *PAL* gene transcripts were identified and characterized from different species of Amaryllidaceae [41–43,47–49]. Interestingly, two main phylogenetic *PAL* clusters were identified; the first one contained *PAL* transcripts ubiquitously expressed in Amaryllidaceae whereas the second cluster contained *PAL* transcripts with expression highest and correlating with organs where AAs accumulated [26]. This indicates that different *PAL* transcripts encode enzymes with distinct functions in the phenylpropanoid pathway and it suggests the role of the latter cluster in AA biosynthesis. Next, *trans*-cinnamic acid is hydroxylated to form *p*-coumaric acid by the cinnamate 4-hydroxylase (C4H), a cytochrome P450 of the CYP73 subfamily (cinnamate 4-hydroxylase, C4H) [50,51]. Transcripts encoding C4H were reported from several Amaryllidaceae species [41–43,49] including *C4H* from *L. radiate*, which was characterized as producing a region-specific 4-hydroxylation of *trans*-cinnamic acid [49]. The reactions catalyzed by PAL and C4H are also crucial steps in the biosynthesis of many phenylpropanoids such as flavonoids, linins, coumarins and stilbenes. From there, the enzymes and order of reactions leading to 3,4-DHBA are not known however it is hypothesized that it may involve the CYP98A3 named coumarate 3-hydroxylase (C3H) and/or the ascorbate peroxidase (APX) and/or the 4-hydroxybenzaldehyde synthase (HBS) [26] (Figure 2). A few studies have reported on the presence of phenolic acids such as caffeic, *p*-coumaric, and ferulic acids in *N. pseudonarcissus, N. poeticus and Galanthus nivalis* [52–54]. In addition, 3,4-DHBA was detected in plants outside the Amaryllidaceae family [55]. Collectively, this suggest that the initial reactions and enzymes of the phenylpropanoid pathway participate in the synthesis of the AA precursor 3,4-DHBA.

The condensation of tyramine and 3,4-DHBA leads to the formation of norbelladine catalyzed by the norbelladine synthase (NBS) and/or the noroxomaritidine reductase (NR) or a combination of these enzymes [56,57]. Norbelladine is the precursor to all AAs. For example, norbelladine can undergo different biochemical reactions such as methylation, hydroxylation, dehydration, cyclization and tautomerization to form cherylline-type AAs (Figure 2). Alternatively, norbelladine can be methylated by the

norbelladine 4′-*O*-methyltransferase (N4OMT) to form 4′-*O*-methylnorbelladine [58]. 4′-*O*-methylnorbelladine cyclization in a regioselective phenol-phenol oxidative coupling forms the ortho-para', para-para' or para-ortho' C-C coupled producing the various structural types of AAs (Figure 2). The para-ortho' C-C coupling leads to galantamine-type AAs whereas the ortho-para' phenol coupling elaborates lycorine- and homolycorine-types of AAs (Figure 2). The para-para phenol-phenol' coupling reaction produces the crinine-, narciclasine-, tazettine- and montanine-types of AAs. A cytochrome P450 sequence was identified through comparative transcriptomics of *N.* sp. *aff. pseudonarcissus*, *Galanthus* sp., and *Galanthus elwesii*. Through heterologous expression and characterization, CYP96T1 formed the products (10b*R*,4a*S*)-noroxomaritidine and (10b*S*,4a*R*)-noroxomaritidine from 4′-*O*-methylnorbelladine supporting its involvement as a para-para' C-C phenol coupling cytochrome P450 [59].

The core skeletons obtained from norbelladine, methylnorbelladine, and the phenol coupling steps form the basis of AA diversity. A complex network of enzyme catalyzing various types of reactions, such as C-C and C-O bond formations, *O*- and *N*-methylations, demethylations, hydroxylations, oxidations and reductions, yield the several hundred of structurally related AAs. Only a few of these enzymes are known to date and they are reported in Figure 2.

Occurrence of Amaryllidaceae Alkaloids

From January 2015 to August 2020, a total of 91 new AAs were isolated and identified from different plant species of the genus *Crinum*, *Zephyranthes*, *Narcissus*, *Galanthus*, *Hymenocallis*, *Nerine*, *Lycoris*, *Brunsvigia,* and *Hippeastrum* (Table 2).

Several of these novel AAs belong to known structural types, while others harbor new structures. The 91 AAs were classified in this manuscript as I) norbelladine-type (**1-6**), II) cherylline-type (**7**, **8**), III) galantamine-type (**9-16**), IV) lycorine-type (**17-25**), V) homolycorine-type (**26-30**), VI) crinine-type (**31-50**), VII) narciclasine-type (**51**), VIII) pretazettine-type (**52-54**), IX) montanine-type (**55**), and X) other types including

AAs related to plicamine (**56-67**), *seco*-plicamine (**68-70**), cripowellin (**71-76**), mesembrine (**77**, **78**), and various others AAs (**79-91**). Structures of novel AAs belonging to the I to III scaffold types (norbelladine-, cherylline-, and galantamine-type) are depicted in Figure 3, whereas types IV and V (lycorine- and homolycorine-type) are represented in Figure 4. Figure 5 displays the structures of the para-para phenol coupled AAs of the VI to IX types including crinine-, narciclasine-, tazettine-, and montanine-type. AA of the type X including plicamine-, *seco*-plicamine, cripowellin, and mesembrine-types are represented in Figure 6, whereas all other types with different chemical structures are shown in Figure 7.

Table 2. Novel Amaryllidaceae alkaloids. Name, activity, chemical formula, and anatomic origin are displayed. The bold number in the first column corresponds to the assigned number of its corresponding chemical structure shown in Figures 3-7.

No	Alkaloid	Activity	Formula	Organ	Ref.
	I–NORBELLADINE-TYPE				
1	6-*O*-Demethylbelladine	CNS	$C_{18}H_{23}NO_3$	B	[60]
2	4′-*O*-Demethylbelladine	CNS	$C_{18}H_{23}NO_3$	B	[60]
3	4′-*O,N*-dimethylnorbelladine *N*-oxide	Tum	$C_{17}H_{22}NO_4$	B	[61]
4	Carltonine A	CNS	$C_{27}H_{32}N_2O_3$	B	[62]
5	Carltonine B	CNS	$C_{26}H_{28}N_2O_3$	B	[62]
6	Carltonine C	CNS	$C_{44}H_{49}N_3O_5$	B	[62]
	II–CHERYLLINE-TYPE				
7	Gigantelline	CNS, Tum	$C_{18}H_{21}NO_3$	B	[63]
8	Gigantellinine	CNS, Tum	$C_{18}H_{21}NO_4$	B	[63]
	III–GALANTAMINE-TYPE				
9	Lycoranine C	Tum	$C_{16}H_{21}NO_3$	B	[64]
10	Crijaponine B	CNS, Tum	$C_{19}H_{23}NO_5$	R, F	[65]
11	11β-Hydroxylycoramine	Inf	$C_{17}H_{23}NO_4$	B, L, F	[66]
12	9-De-*O*-methyl-11β-hydroxylycoramine	Inf	$C_{16}H_{21}NO_4$	B, L, F	[66]
13	9-De-*O*-methyl-11β-hydroxygalantamine	CNS, Inf	$C_{16}H_{19}NO_4$	B, L, F	[66]
14	11β-Hydroxylycoramine *N*-oxide	Inf	$C_{17}H_{23}NO_5$	B, L, F	[66]
15	11β-Hydroxygalantamine *N*-oxide	Inf	$C_{17}H_{21}NO_5$	B, L, F	[66]
16	2β,11β-Dihydroxygalantamine	Inf	$C_{17}H_{21}NO_5$	B, L, F	[66]

No	Alkaloid	Activity	Formula	Organ	Ref.
		IV–LYCORINE-TYPE			
17	(+)-1-Hydroxy-ungeremine	Inf, Tum	$C_{16}H_{12}NO_4^+$	B	[67]
18	Reticulinine	CNS	$C_{17}H_{21}NO_4$	B, L	[68]
19	Isoreticulinine	CNS	$C_{17}H_{21}NO_4$	B, L	[68]
20	Galanthine *N*-β-oxide	CNS	$C_{18}H_{23}NO_5$	B, L, F	[69]
21	Carinatine *N*-α-oxide	CNS	$C_{17}H_{21}NO_5$	B, L, F	[69]
22	Zephycarinatine I	CNS	$C_{17}H_{15}NO_3$	B, L, F	[69]
23	Oxoincartine	CNS	$C_{18}H_{21}NO_6$	B, L, F	[70]
24	7-Oxonorpluviine	nm	$C_{16}H_{17}NO_4$	B	[71]
25	pseudolycorine *N*-oxide	Tum	$C_{16}H_{19}NO_5$	B, L, F	[72]
		V–HOMOLYCORINE-TYPE			
26	(+)-2-Hydroxy-8-demethyl-homolycorine-α-*N*-oxide	Inf, Tum	$C_{17}H_{19}NO_6$	B	[67]
27	Lycoranine E	Tum	$C_{17}H_{19}NO_6$	B	[64]
28	Lycoranine F	Tum	$C_{17}H_{19}NO_4$	B	[64]
29	2α-10bα-Dihydroxy-9-*O*-demethylhomolycorine	Tum	$C_{17}H_{19}NO_6$	B	[73]
30	7-Hydroxyclivonine	CNS	$C_{17}H_{19}NO_6$	B	[74]
		VI–CRININE-TYPE			
31	(+)-6β-Acetyl-8-hydroxy-9-methoxy-crinamine	Inf, Tum	$C_{19}H_{23}NO_6$	B	[67]
32	Crijaponine A	CNS, Tum	$C_{16}H_{19}NO_4$	R, F	[65]
33	6α-Methoxyundulatine	Tum	$C_{19}H_{23}NO_6$	L	[75]
34	6α-Methoxycrinamidine	Tum	$C_{18}H_{21}NO_6$	L	[75]
35	Undulatine *N*-oxide	Tum	$C_{18}H_{21}NO_6$	L	[75]
36	1,4-Dihydroxy-3-methoxy powellan	Par, Tum	$C_{18}H_{23}NO_6$	B	[76]
37	Augustine *N*-oxide	CNS, Par	$C_{17}H_{19}NO_5$	B, L	[77]
38	Buphanisine *N*-oxide	CNS, Par	$C_{17}H_{19}NO_4$	B, L	[77]
39	6α-Hydroxymaritidine	CNS, Par	$C_{17}H_{21}NO_4$	B, L	[68]
40	6β-Hydroxymaritidine	CNS, Par	$C_{17}H_{21}NO_4$	B, L	[68]
41	3,11-*O*-Diacetyl-9-*O*-demethylmaritidine	CNS	$C_{20}H_{22}NO_6$	B, L, F	[70]
42	11-*O*-Acetyl-9-*O*-demethylmaritidine	CNS	$C_{18}H_{20}NO_5$	B, L, F	[70]
43	Crinsarnine	Ins, Lar	$C_{20}H_{25}NO_6$	B	[78]
44	Gigancrinine	CNS, Tum	$C_{16}H_{17}NO_4$	B	[63]
45	Haemanthamine *N*-oxide	nm	$C_{17}H_{19}NO_5$	B, L	[79]
46	Crinasiaticine A	hCAII	$C_{18}H_{19}NO_5$	B	[80]
47	Crinasiaticine B	hCAII	$C_{18}H_{21}NO_5$	B	[80]
48	3-*O*-Acetylvittatine	Tum	$C_{18}H_{19}NO_4$	B	[61]
49	3-*O*-Methyl-*epi*-vittatine	Tum	$C_{17}H_{19}NO_3$	B	[81]
50	Crouchinine	nm	$C_{19}H_{23}NO_6$	B	[81]

No	Alkaloid	Activity	Formula	Organ	Ref.
	VIII–NARCICLASINE-TYPE				
51	Narciclasine-4-*O*-β-D-xylopyranoside	Tum	$C_{19}H_{21}NO_{11}$	B, L, F	[82]
	VIII–TAZETTINE-TYPE				
52	Jonquailine	Tum	$C_{19}H_{23}NO_5$	B	[83]
53	Scillitazettine	Par, Tum	$C_{19}H_{21}NO_6$	B	[61]
54	Scilli-*N*-desmethylpretazettine	Par, Tum	$C_{18}H_{19}NO_5$	B	[61]
	IX–MONTANINE-TYPE				
55	4-*O*-Methylnangustine	CNS	$C_{17}H_{19}NO_4$	B	[74]
	X–OTHER-TYPES				
	PLICAMINE				
56	*N*-Isopentyl-5,6-dihydroplicane	Inf	$C_{23}H_{30}N_2O_4$	B, L, F	[66]
57	*N*-(*S*)-*s*-Pentyl-5,6-dihydroplicane	Inf	$C_{23}H_{30}N_2O_4$	B, L, F	[66]
58	*N*-Hexyl-5,6-dihydroplicane	Inf	$C_{24}H_{32}N_2O_4$	B, L, F	[66]
59	*N*-Hydroxycarbonylpropyl-5,6-dihydroplicane	Inf	$C_{22}H_{26}N_2O_6$	B, L, F	[66]
60	*N*-Phenethyl-5,6-dihydroplicane	Inf	$C_{26}H_{28}N_2O_4$	B, L, F	[66]
61	*N*-3-Indolylethyl-5,6-dihydroplicane	CNS, Inf	$C_{28}H_{29}N_3O_4$	B, L, F	[66]
62	*N*-Isopentyl-5,6-dihydroplicane *N*-oxide	Inf	$C_{23}H_{30}N_2O_5$	B, L, F	[66]
63	Bliquine *N*-oxide	CNS	$C_{26}H_{28}N_2O_6$	B, L, F	[66]
64	Zephycarinatine C	Inf	$C_{23}H_{28}N_2O_5$	B, L, F	[69]
65	Zephycarinatine D	Inf	$C_{19}H_{20}N_2O_5$	B, L, F	[69]
66	Zephycarinatine E	Inf	$C_{23}H_{28}N_2O_5$	B, L, F	[69]
67	Zephycarinatine F	CNS, Inf	$C_{20}H_{24}N_2O_6$	B, L, F	[69]
	SECO-PLICAMINE				
68	*N*-Methyl-11,12-*seco*-5,6-dihydroplicane	Inf	$C_{19}H_{22}N_2O_5$	B, L, F	[66]
69	*N*-Isopentyl-11,12-*seco*-5,6-dihydroplicane	Inf	$C_{23}H_{30}N_2O_5$	B, L, F	[66]
70	Zephycarinatine H	CNS	$C_{23}H_{32}N_2O_4$	B, L, F	[69]
	CRIPOWELLIN				
71	4,8-Dimethoxy-cripowellin C	Inf, Mic, Oxi, Tum	$C_{26}H_{35}NO_{11}$	B	[84]
72	4,8-Dimethoxy-cripowellin D	Inf, Mic, Oxi, Tum	$C_{26}H_{37}NO_{10}$	B	[84]
73	9-Methoxy-cripowellin B	Inf, Mic, Oxi, Tum	$C_{26}H_{35}NO_{12}$	B	[84]
74	4-Methoxy-8-hydroxy-cripowellin B	Inf, Mic, Oxi, Tum	$C_{25}H_{35}NO_{11}$	B	[84]
75	Cripowellin C	Tum	$C_{25}H_{31}NO_{11}$	L	[85]
76	Cripowellin D	Tum	$C_{25}H_{33}NO_{10}$	L	[85]

No	Alkaloid	Activity	Formula	Organ	Ref.
		MESEMBRINE			
77	Sarniensinol	Ins, Lar	$C_{18}H_{23}NO_4$	B	[78]
78	Sarniensine	Ins, Lar	$C_{19}H_{25}NO_4$	B	[86]
		OTHERS			
79	(+)-*N*-Methoxylcarbonyl-2-demethyl-isocorydione	Inf, Tum	$C_{20}H_{17}NO_7$	B	[67]
80	Lycoranine D	Tum	$C_{15}H_{15}NO_3$	B	[64]
81	Zephycandidine A	Tum	$C_{16}H_{10}N_2O_2$	B, L, F	[87]
82	Hymenolitatine	Tum	$C_{17}H_{15}NO_4$	B	[88]
83	Zephycandidine I	CNS	$C_{18}H_{25}NO_4$	B, L, F	[30]
84	Zephycandidine II	CNS	$C_{15}H_{19}NO_2$	B, L, F	[30]
85	Zephycandidine III	CNS	$C_{17}H_{19}NO_4$	B, L, F	[30]
86	Narcipavline	CNS	$C_{33}H_{34}N_2O_5$	B	[29]
87	Narcikachnine	nm	$C_{33}H_{36}N_2O_5$	B	[29]
88	Narcimatuline	CNS	$C_{33}H_{34}N_2O_5$	B	[89]
89	Zephycarinatine A	CNS	$C_{25}H_{32}N_2O_5$	B, L, F	[69]
90	Zephycarinatine B	CNS	$C_{22}H_{30}N_2O_4$	B, L, F	[69]
91	Zephycarinatine G	CNS	$C_{23}H_{32}N_2O_3$	B, L, F	[69]

Abbreviation for biological activities are CNS: central nervous system, hCAII: human carbonic isozyme II, Inf: anti-inflammatory, Ins: insecticidal, Lar: larvicidal, Mic: antimicrobial, Oxi: antioxidant, Par: antiparasitic, Tum: antitumoral, and nm: not measured. Abbreviation for organs are L: leaves, B: bulbs, F: flowers, and R: rhizomes.

Lycoris genus encompasses 20 species originating from south and east Asia [90]. From the ethanol extract of the bulbs of *L. radiata*, two known alkaloids, (+)-*6*β-acetyl-crinamine and 8-demethyl-homolycorine-α-*N*-oxide, and four new alkaloids, namely (+)-1-hydroxy-ungeremine (**17)**, (+)-6β-acetyl-8-hydroxy-9-methoxy-crinamine (**31)**, (+)-2-hydroxy-8-demethyl-homolycorine-α-*N*-oxide (**26)** and (+)-*N*-methoxylcarbonyl-2-demethyl-isocorydione (**79)**, belonging to the lycorine-, crinine-, homolycorine- and other-types respectively, were isolated. Their structural elucidation was performed by spectroscopic methods, such as 1D and 2D (^{1}H–^{1}H, COrrelation SpectroscopY (COSY), Heteronuclear Multiple Quantum Coherence (HMQC), and Heteronuclear Multiple Bond Correlation (HMBC)) Nuclear Magnetic Resonance (NMR) spectroscopy, in addition to high resolution mass spectrometry [67]. From the bulb of *L. radiata,* were also isolated

four new AAs, lycoranines C-F (**9**, **27**, **28**, **80)**, respectively belonging to galantamine- (**9**), homolycorine- (**27**, **28**) and other-types (**80**), with known alkaloids homolycorine, haemanthidine, haemanthamine, α-dihydrolycorine, galanthine, lycorine, and pseudolycorine. Their structure was determined using extensively NMR and high-resolution electrospray ionization mass spectrometry (HR-ESIMS) data. Their absolute and relative configuration were assigned by Electronic Circular Dichroism (ECD) and Rotating-frame Overhauser Spectroscopy (ROESY) NMR experiments [64].

The *Narcissus* genus is composed of approximately 50 species that originate from the area of the Iberian Peninsula. Jonquailine (**52**), a pretazettine-type AA, was isolated from the dried bulbs of *N. jonquilla quail* and characterized for structural elucidation and absolute configuration using various spectroscopic techniques [83]. Narcipavline (**6**) and narcikachnine (**87**), two new alkaloids, were isolated, together with thirteen known alkaloids, from fresh bulbs of *N. poeticus* cv. Pink Parasol, their chemical structure was elucidated by MS, together with 1D and 2D NMR spectroscopic analyses, and by comparison with literature data [29]. From the fresh bulbs of *N. pseudonarcissus* L. cv. Dutch Master, a new AA, named narcimatuline (**88**), was isolated, together with twenty-one known AAs of various structural types. Their chemical structure was elucidated by a combination of MS, HR-MS, 1D and 2D NMR spectroscopic techniques and also by comparison with existing data [89].

The phytochemical investigation of fresh bulbs of *Narcissus pseudonarcissus* cv. Carlton led to the isolation of thirteen known AAs, and three new norbelladine-type AAs: carltonine A–C (**4-6**). Their structure was determined using spectroscopic methods including 1D NMR, 2D NMR, and HR-MS [62]. 7-Oxonorpluviine (**24**), a lycorine-type alkaloid was isolated from fresh bulbs of *Narcissus* L. cv. Professor Einstein, together with twenty three known AAs, and their structures were identified by using various spectroscopic methods like (GC-MS, LC-MS, 1D, and 2D NMR spectroscopy) [71]. Pseudolycorine *N*-oxide (**25**) was isolated from *Narcissus tazetta* whole plant, and the structural elucidation was determined by spectroscopic data analysis [72].

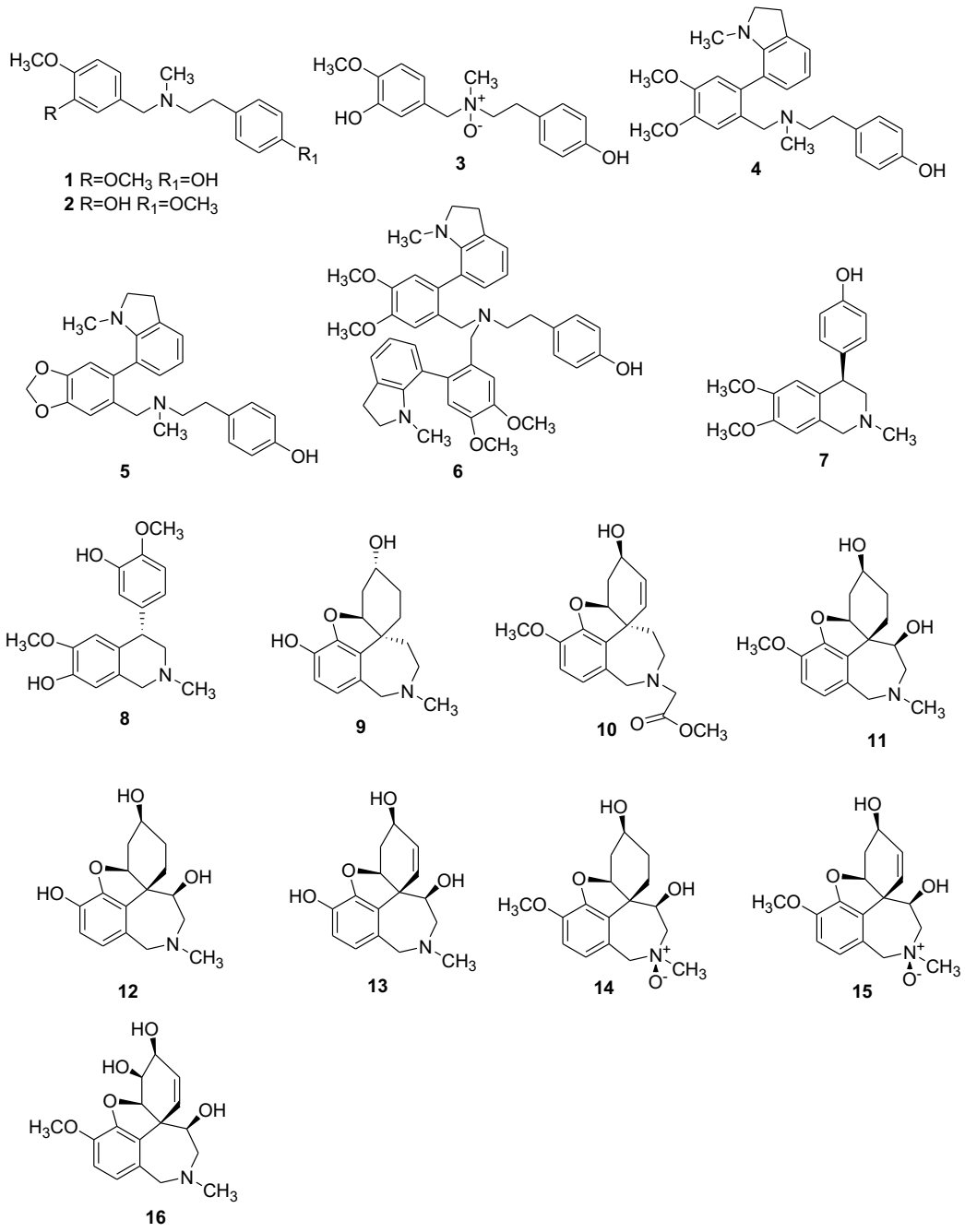

Figure 3 Chemical structure of novel Amaryllidaceae alkaloids of the norbelladine- (**1-6**), cherylline (**7-8**) and galantamine-type (**9-16**). Numbers in bold refer to the compounds depicted in Table 2.

Twenty species are included in the genus *Galanthus* native of Europe and of Middle East [91]. From whole plants of *Galanthus fosteri* Baker, three new AAs, namely oxoincartine (**23**), 3,11-*O*-diacetyl-9-*O*-demethylmaritidine (**41**) and 11-*O*-acetyl-9-*O*-demethylmaritidine (**42**) belonging to the lycorine and crinine-type, were isolated together

with seven known compounds. Their structure was elucidated by spectroscopic analyses (UV, IR, MS, ECD, and 1D/2D NMR) [70].

Hymenocallis plants are native of Central and South America and include more than 60 species. Novel AA hymenolitatine (**82**) was isolated together with trispheridine and tazettine from the dichloromethane extract of the bulbs of *Hymenocallis littoralis* (Jacq.) Salisb. Chemical characterization of these compounds was performed by spectroscopic methods including 1D NMR, 2D NMR, and HR-MS [88].

The *Hippeastrum* genus contains approximately 94 species native of tropical and subtropical regions of the America [92]. One new alkaloid named 2α-10bα-dihydroxy-9-*O*-demethylhomolycorine (**29**), belonging to homolycorine-type and seven known alkaloids were isolated from the bulbs of *Hippeastrum solandriflorum*. Structural elucidation was performed by spectroscopic methods NMR (^{1}H–^{1}H, COSY, HMQC, HMBC, and Nuclear Overhauser Effect SpectroscopY (NOESY)) and mass spectrometry (HR-ESIMS) [73]. From a phytochemical study of the fresh bulbs and leaves of *Hippeastrum reticulatum*, eight known alkaloids and four new alkaloids named 6α-hydroxymaritidine (**39**), 6β-hydroxymaritidine (**40**), reticulinine (**18**) and isoreticulinine (**19)** were identified. The epimers (6α-hydroxymaritidine (**39**) and 6β-hydroxymaritidine (**0**)) were isolated as a mixture. Chemical characterization was performed by NMR, they belong to the crinine and lycorine-types [68]. Two novel AAs, 4-*O*-methylnangustine (**55**) and 7-hydroxyclivonine (**30**), of montanine and homolycorine types, respectively, and four known alkaloids were isolated from the bulbs of *H. argentinum* [74]. Phytochemical investigation of fresh bulbs and leaves of *Hippeastrum aulicum* (Ker Gawl.) Herb. enabled the characterization of the new alkaloid haemanthamine *N*-oxide (**45**), chemically characterized by NMR technics [79].

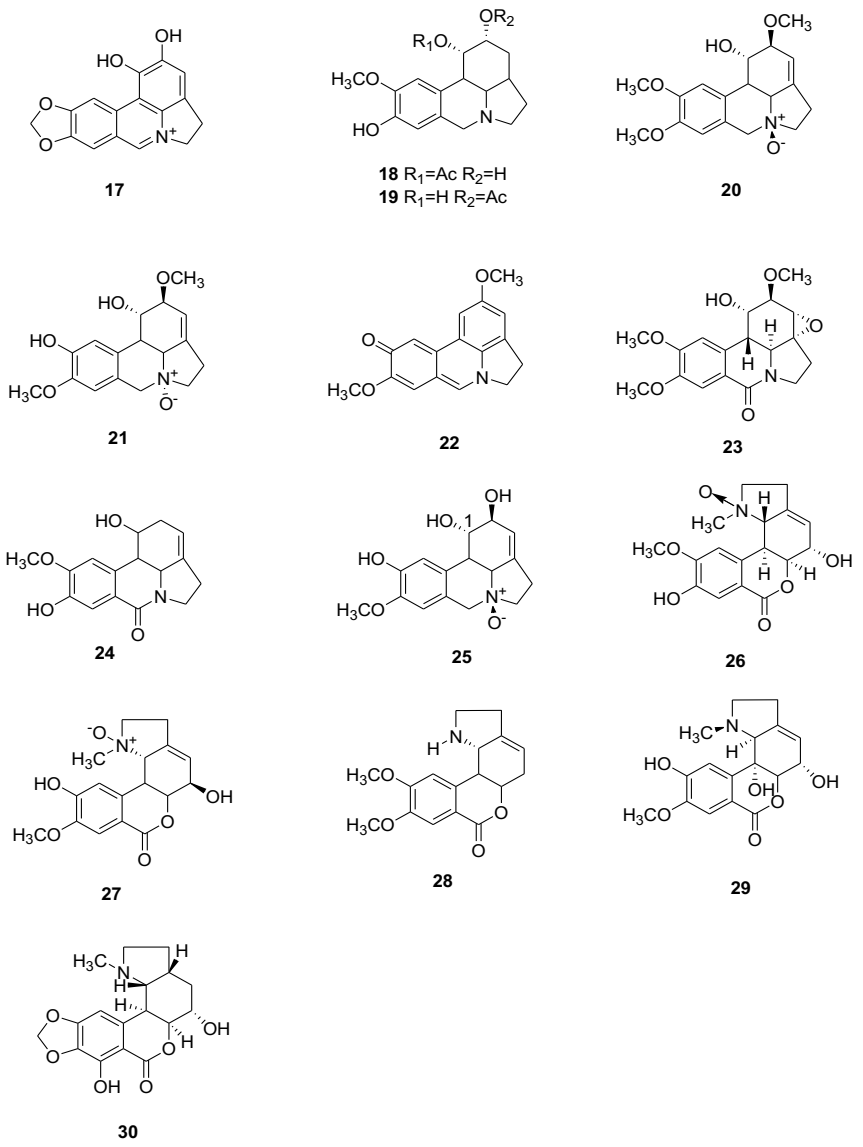

Figure 4 Chemical structure of new alkaloids of the lycorine- (**17-25**) and homolycorine-type (**26**–**30**). Numbers in bold refer to the compounds depicted in Table 2.

The *Nerine* genus contains 30 species that originate from South Africa and several may go extinct due to loss of habitat [93]. Two new AAs, 6-*O*-demethylbelladine (**1**) and 4′-*O*-demethylbelladine (**2**), belonging to the norbelladine-type, together with twenty known alkaloids, were isolated from fresh bulbs of *Nerine bowdenii* by standard chromatographic methods [60]. From the organic extract of *N. sarniensis*, an indigenous South African Amaryllidaceae, were isolated two new alkaloids named sarniensinol **(77)** and sarniensine (**78)** belonging to the mesembrine group, and a new crinine-type alkaloid

named crinsarnine (**43**), together with bowdensine, tazettine, 3-epimacronine, lycorine, 1-*O*-acetyl-lycorine, and hippadine. Sarniensinol (**77**), sarniensine (**78**), and crinsarnine (**43**) were characterized by extensive spectroscopic and chiroptical methods [78,86].

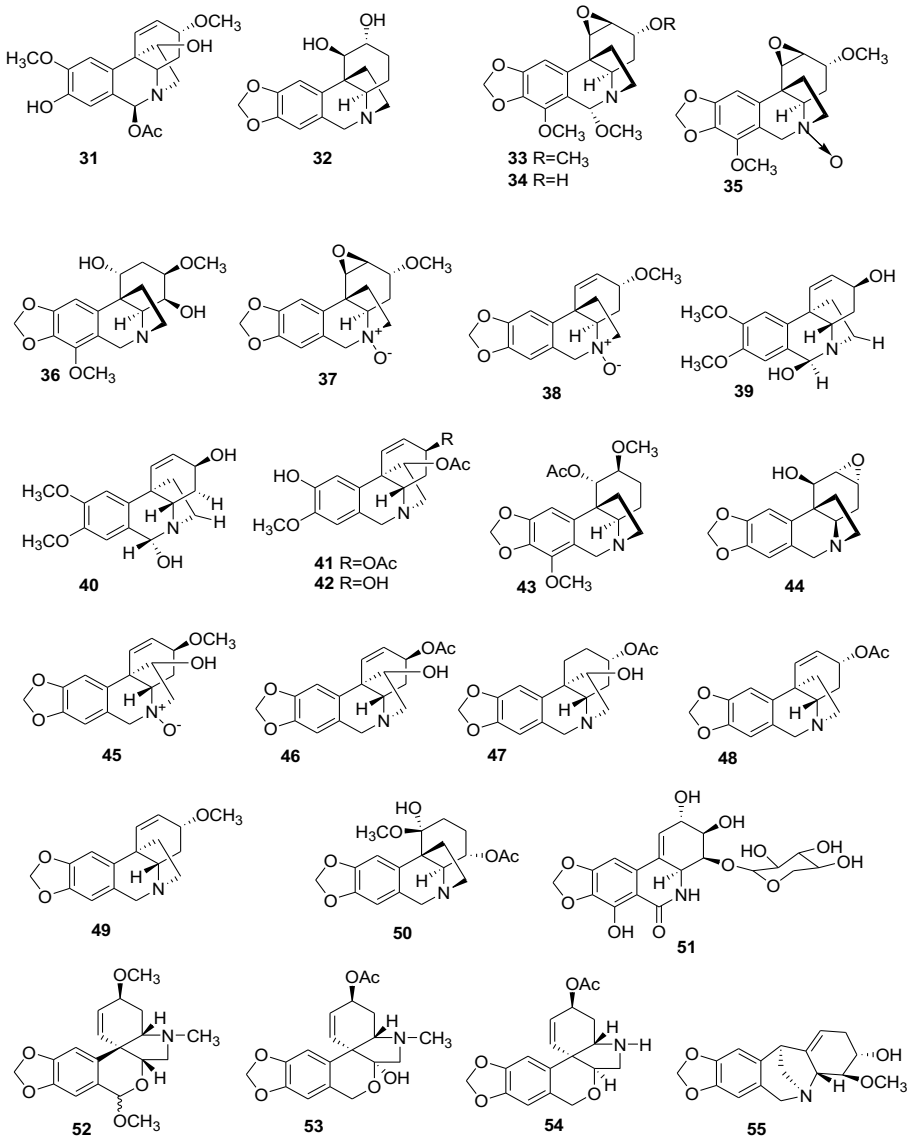

Figure 5 Chemical structure of new alkaloids crinine-, narciclasine-, tazettine-, and montanine-type (**31**–**55**). Numbers in bold refer to the compounds depicted in Table 2.

The *Zephyranthes* genus encompasses more than 70 species native to the Americas. From the whole dried plants of *Zephyranthes candida*, Zephycandidine A (**81**), a first naturally occurring imidazol[1,2-f] phenanthridine alkaloid was isolated and characterized

by spectroscopic analyses and NMR calculations [87]. From the 95% EtOH extract of the whole dried plant of *Z. candida*, three new alkaloids, zephycandidines I-III (**83**–**85**) were isolated, and their structures were elucidated by spectroscopic methods (HR-ESIMS, ^{1}H NMR, ^{13}C NMR, DEPT, ^{1}H-^{1}H COSY, HSQC, HMBC, ROESY). The absolute configuration of zephycandidines II and III (**84-85**) was estimated by ECD calculation, while the absolute configuration of zephycandidine I (**83**) was determined by single crystal X-ray diffraction using Cu Kα radiation [30]. Sixteen new alkaloids belonging to the galantamine (**11-16**), plicamine (**56-63**), and *seco*-plicamine (**68** and **69**) types, together with eight known compounds, were isolated from the whole plant of *Z. candida*. The chemical structures of these alkaloids were determined by extensive spectroscopic analyses, and absolute configurations of **11**, **12**, **56** and **57** were confirmed by single crystal X-ray diffraction analysis [66]. Further study on whole plants of *Z. carinata* led to the isolation of eleven new AAs, classified as 12-acetylplicamine (**89**), *N*-deformyl-*seco*-plicamine (**90**), plicamine (**64**−**67**), 4a-*epi*-plicamine (**1**), *seco*-plicamine (**70**), and lycorine (**20**−**22**) framework types, together with fifteen known alkaloids. The chemical structure of these alkaloids was determined by extensive spectroscopic analyses, and absolute configuration of **20** and **21** was confirmed by single crystal X-ray diffraction analysis. Zephycarinatines A (**74**), B (**75**), and G (**76**) represent the first examples of 12-acetylplicamine, *N*-deformyl-*seco*-plicamine, and 4a-*epi*-plicamine alkaloids, respectively [69]. Narciclasine-4-*O*-β-D-xylopyranoside (**51**), a new narciclasine glycoside, was isolated from the whole plant of *Zephyranthes minuta*. The structure of this new alkaloid was resolved using spectroscopic data analysis.

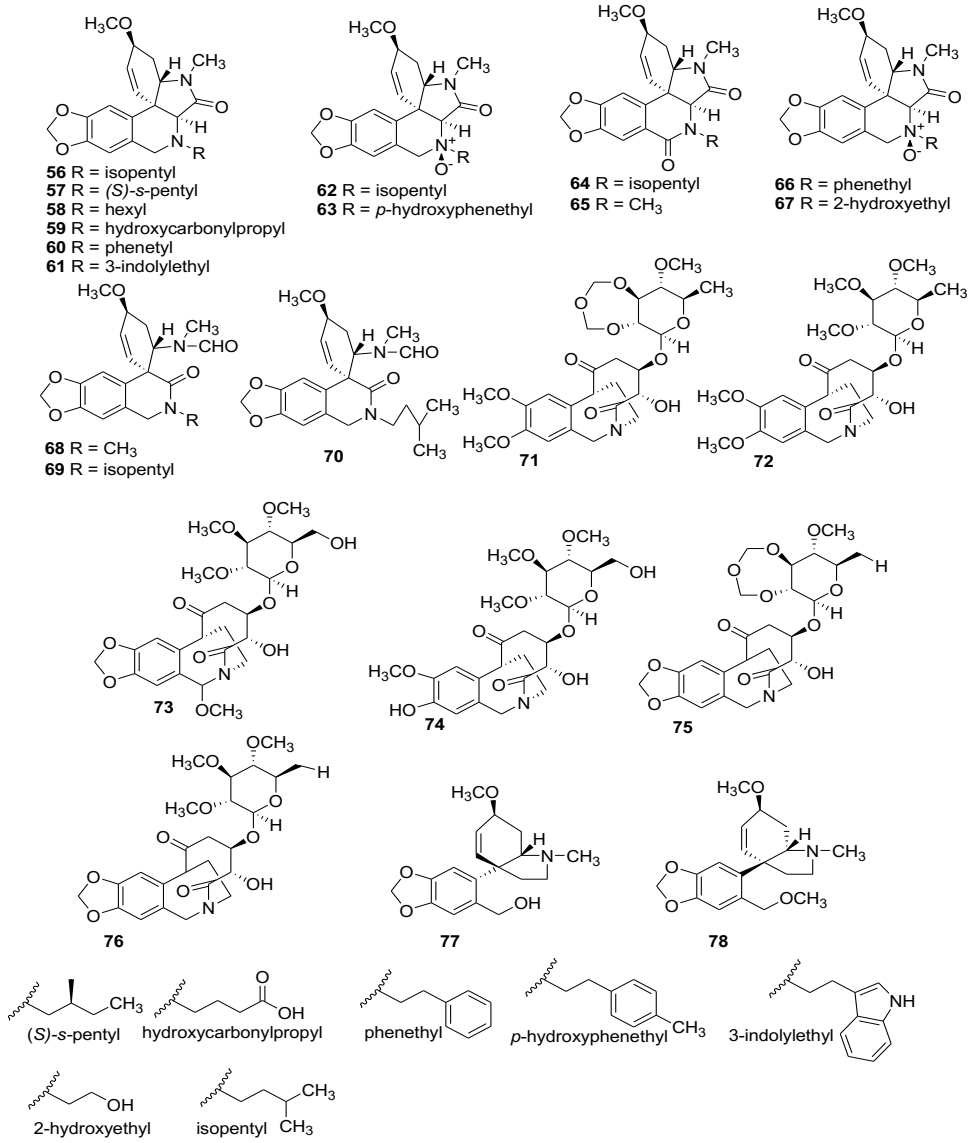

Figure 6 Chemical structure of new alkaloids plcamine-, *seco*-plicamine-, cripowellin-, and mesembrine-type. Numbers in bold refer to the compounds depicted in Table 2.

Crinum genus contains 180 species native of sub-Saharan and pantropical region. Four new potently bioactive cripowellin derivatives. 4,8-Dimethoxy-cripowellin C (**71**), 4,8-dimethoxy-cripowellin D (**72**), 9-methoxy-cripowellin B (**73**), and 4-methoxy-8-hydroxy-cripowellin B (**74)**, together with one known alkaloid, cripowellin C were isolated from 95% EtOH extract of the bulbs of *Crinum latifolium*. Structural elucidation was performed by spectroscopic methods like NMR (^{1}H–^{1}H, COSY, HMQC, and HMBC) and mass spectrometry (HR-ESIMS) [84]. From the rhizome and fruits of

Crinum asiaticum var. japonicum, two new AAs, crijaponine A (**32**) and crijaponine B (**10**) belonging to the crinine and galantamine-class, were isolated, together with eleven known alkaloids, ungeremine, lycorine, 2-*O*-acetyllycorine, 1, 2-*O*-diacetyllycorine, (−)crinine, 11-hydroxyvittatine, hamayne, (+)-epibuphanisine, crinamine, yemenine A, and epinorgalantamine. Structural elucidation was performed by spectroscopic methods including 1D and 2D NMR [65]. From the leaves of *C. latifolium*, three new crinine-category alkaloids, named 6-methoxyundulatine (33), 6-methoxycrinamidine (**34**), and undulatine *N*-oxide (**35**), were isolated, together with eight known alkaloids, 6-hydroxyundulatine, 6-hydroxybuphanidrine, undulatine, crinamidine, ambelline, filifoline, augustamine, and perlolyrine. Structural elucidation and absolute configuration were performed by various spectroscopic techniques such as NMR, ECD, and HR-Q-TOF-MS [75]. Antimalarial bioassay-guided fractionation MeOH extracts from dried powder of above-ground parts of *Crinum erubescens*, led to the isolation of two new alkaloids, cripowellin C (**75**) and cripowellin D (**76**), all together with two known alkaloids, cripowellin A and cripowellin B. Structural elucidation was performed using 1D and 2D-NMR techniques [85]. Phytochemical investigation of fresh bulbs and leaves of *Crinum amabile*, led to the identification of twenty-three alkaloids by GC-MS, and the isolation of two new crinine-kind alkaloids named augustine *N*-oxide (**37**) and buphanisine *N*-oxide (**38**). Their chemical structure was elucidated by NMR [77]. Three new cherylline- and crinine-type of AAs, named gigantelline **(7)**, gigantellinine (**8**) and gigancrinine (**44**), were isolated from *Crinum jagus* (*Crinum giganteum*) collected in Senegal, together with the already known sanguinine, cherylline, lycorine, crinine, flexinine and the isoquinolinone derivative hippadine. All of the new isolated alkaloids were characterized by using spectroscopic (1D and 2D ^{1}H and ^{13}C NMR and HR-ESIMS) and chemical methods. Their relative configuration was assigned by NOESY NMR spectra and NMR calculations, while the absolute configuration was assigned using ECD experiments and calculations [63]. From bulbs of *Crinum asiaticum* L., two new alkaloids, crinasiaticine A (**46**) and crinasiaticine B (**47**), and fifteen known alkaloids were isolated. Their structural elucidation and absolute configuration were performed by spectroscopic methods (HR-TOF-MS, ^{1}H NMR, ^{13}C NMR, ^{1}H-^{1}H COSY, HMBC, NOESY, ECD) [80]. Four new alkaloids named, scillitazettine (**53**), scilli-*N*-desmethylpre*tazettine* (**54**),

3-*O*-acetylvittatine (**48**), and 4′-*O,N*-dimethylmethylnorbelladine *N*-oxide (**3**) were isolated from bulbs of *Crinum scillifolium*. Their structure was elucidated using various spectroscopic methods (1D and 2D ^{1}H and ^{13}C NMR and HR-ESIMS). Their relatives and absolute configurations were determined by DFT-NMR and ECD calculations [61].

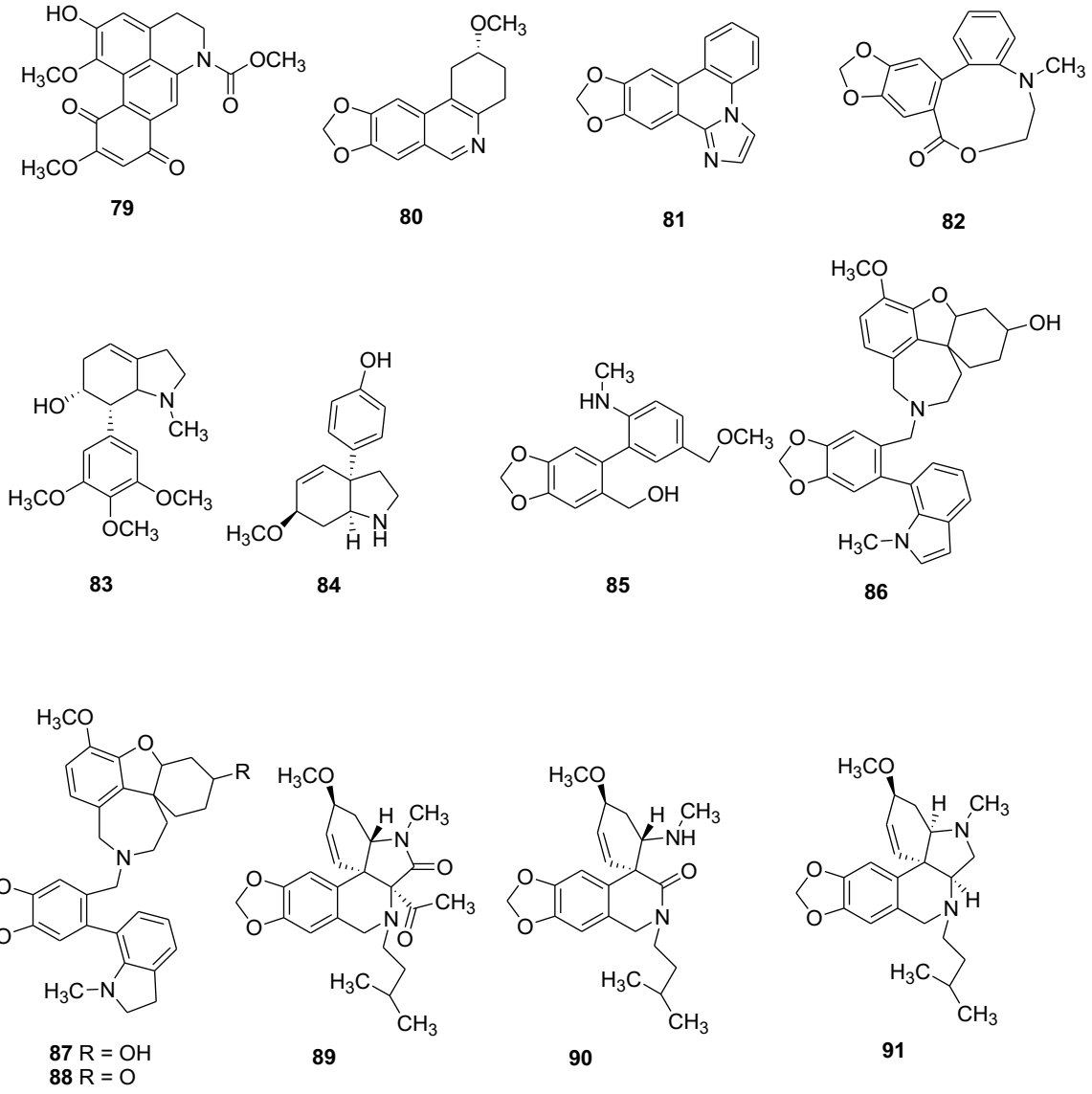

Figure 7 Chemical structure of new alkaloids of other types. Numbers in bold refer to the compounds depicted in Table 2.

Amaryllis is a small genus comprised of two species (*A. belladonna* L. and *A. paradisicola* Snijman). In particular *A. belladonna* is native of South Africa [94]. A new crinine alkaloid 1,4-dihydroxy-3-methoxy powellan (**36**), together with five known alkaloids,

were isolated from the bulbs of *A. belladonna* Steud. by bioassay-guided isolation. Structures were elucidated by interpretation of combined HR-ESIMS, CD, and 2D NMR spectroscopic data [76].

Brunsvigia genus contains seventeen species endemic to Southern Africa [95]. Two new AAs named 3-*O*-methyl-*epi*-vittatine (**49**) and crouchinine (**50**) were isolated from bulbs of *Brunsvigia natalensis*. The AAs structures were determined by spectroscopic analyses (UV, FT-IR, MS, ECD, and 1D/2D NMR) [81].

Pharmacological Properties of Novel Amaryllidaceae Alkaloids

The pharmacological properties of the newly discovered AAs (**1-91**) were assessed when isolated in sufficient amount. AAs display a wide range of biological activities, including cytotoxicity, effects on the central nervous systems (CNS), anti-inflammatory, anti-microbial, anti-parasitic, larvicidal, and antioxidant activities.

Antitumoral Cytotoxic Activity

Lycorine is the most abundantly found AA, it belongs to the pyrrolo[*de*]phenanthridine subgroup. The biological effects of lycorine have been known for many years, and lycorine is still being investigated for a variety of therapeutic application, in particular as anticancer agent showing promising activity against tumors with dismal prognoses [96,97]. The structure–activity relationship (SAR) of lycorine and its derivatives has been evaluated using human leukemia T cells (Jurkat). The results showed that the free 1,2-diol functionality in the C-ring is required to induce apoptosis [98]. Furthermore, it has been demonstrated that the presence of the unaltered diol functionality in the C-ring in its original configuration in lycorine series, the stereochemistry of the C/D ring junction and the conformational freedom of the C-ring were required for the anticancer activity [96]. 4′-*O,N*-dimethylnorbelladine *N*-oxide (**3**) displayed a weak cytotoxicity activity against the human colon cancer cell line HCT116 at concentration ranging from 10^{-5} M and 10^{-6} M [61].

Among the new lycorine-type alkaloids, (+)-1-hydroxy-ungeremine (**17)** was evaluated for its cytotoxic potential against BEN-MEN-1 (meningioma), CCF-STTG1 (astrocytoma), CHG-5 (glioma), SHG-44 (glioma), U251 (glioma), HL-60 (human myeloid leukemia), SMMC-7721 (hepatocellular carcinoma), and W480 (colon cancer) cell lines and exhibited the most potent cytotoxicity against all tested tumor cell lines except BEN-MEN-1, with IC_{50} values ranging from 9.4 to 11.8 μM [67]. Pseudolycorine *N*-oxide (**25**) was inactive against human cervical cancer (SiHa) and human epidermoid carcinoma (KB) cells [72].

Among the homolycorine-type alkaloids, (+)-2-hydroxy-8-demethyl-homolycorine-α-*N*-oxide (**26)** had no significant cytotoxic activity (IC_{50} > 80 μM) against BEN-MEN-1 (meningioma), CCF-STTG1 (astrocytoma), CHG-5 (glioma), SHG-44 (glioma), U251 (glioma), HL-60 (human myeloid leukemia), SMMC-7721 (hepatocellular carcinoma), and W480 (colon cancer) cell lines [67]. Lycoranines E and F (**27** and **28)** showed moderate cytotoxicity against A549 (human lung carcinoma) and LoVo (human colon carcinoma) cells lines with IC_{50} > 20 μM [64]. 2α-10bα-Dihydroxy-9-*O*-demethylhomolycorine (**29**) showed significant cytotoxicity against the HCT-116 (colon adenocarcinoma), OVCAR-8 (ovarian carcinoma) and SF-295 (glioblastoma) cell lines with IC_{50} values 11.69, 15.11, and 16.31 μM respectively [73].

Numerous additional types of AAs displayed interesting anti-cancer activity. Of the cherylline-type, gigantellinine **(8)** had a weak but significant cytotoxicity at 400 μM against breast cancer cell line MCF-7, while gigantelline **(7)** showed no cytotoxicity at the same concentration [63]. Crinine-derivatives (+)-6β-acetyl-8-hydroxy-9-methoxy-crinamine (**31)** showed significant cytotoxicity against HL-60 (IC_{50} < 10 μM), and moderate cytotoxicity against astrocytoma and glioma cell lines, CCF-STTG1, CHG-5, SHG- 44 and U251 (10 μM < IC_{50} ≤ 30 μM) [67]. The cleavage between C-1 and C-13 and the hydroxyl at C-6′ in crinine alkaloid skeleton might be essential to their bioactivity [84]. Crijaponine A (**32**) was inactive towards both human epithelial carcinoma HeLa and HL-60 cell lines (IC_{50} > 60 μM) [65]. 6α-Methoxyundulatine (**33**), 6α-methoxycrinamidine (**34**), and undulatine *N*-oxide (**35**) did not show significant

cytotoxicity against the KB (derived from a human carcinoma of the naropharynx), HepG2 (human liver cancer), MCF7 (breast cancer), SK-Mel2 (melanoma), and LNCaP (human prostate) cancer cell lines with IC_{50} > 100 μM [75]. 1,4-Dihydroxy-3-methoxy powellan (**36**) displayed an IC_{50} > 60 μM against the A2780 human ovarian cancer cell line [76]. Gigancrinine **(44)** showed no cytotoxicity at 400 μM against breast cancer cell line MCF-7 [63]. 3-*O*-Methyl-*epi*-vittatine (**49**) did not shown any cytotoxicity against MCF7, TK10 and UACC62 cancer cell lines [81]. Narciclasine-4-*O*-β-D-xylopyranoside (**51**), a narciclasine-type was inactive against KB and SiHa cell lines at all the concentrations [82]. Jonquailine (**52**), a pretazettine-tye, showed significant antiproliferative activities against cells derived from glioblastoma (U87, U373, and Hs683), melanoma (SKMEL-28), uterine sarcoma (MES-SA and MES-SA/Dx5), and lung carcinoma (A549, H1993 and H2073) with IC_{50} values ranging from 1 to 85 μM [83]. Moreover, (**52**) showed synergic effects with paclitaxel in its anti-proliferative action against lung carcimoma drug-resistant H1993 and H2073 cells in a dose-dependent manner with IC_{50} values between 0.39 and 100 μM. The SAR of (**52)** suggested that hydroxylation of C-8 was required for its anticancer activity [83].

Among cripowellin-type AAs, 4,8-dimethoxy-cripowellin C (**71**), 4,8-dimethoxy-cripowellin D (**72**), 9-methoxy-cripowellin B (**73**), and 4-methoxy-8-hydroxy-cripowellin B (**74**) showed impressive cytotoxicity against seven lung cancer cell lines (A549, H446, H460, H292, 95-D, and SPCA-1) with IC_{50} < 30 nM, with (**73**) and (**74**) being more active than (**71**) and (**72**). Cripowellin C (**75**) and cripowellin D (**76**) were efficiently cytotoxic against the A2780 human ovarian cancer cell line with IC_{50} values of 25 ± 2, and 28 ± 1 nM, respectively [85].

Other-type of AA (+)-*N*-methoxylcarbonyl-2-demethyl-isocorydione (**79)** exhibited strong cytotoxic against all tested tumor cell lines (astrocytoma, glioma, human myeloid leukemia, hepatocellular carcinoma, colon cancer) except meningioma (BEN-MEN-1), with IC_{50} values of 9.2-12.8 μM [67]. Zephycandidine A (**81**) was cytotoxic for five cancer cell lines, HL-60, A549, MCF-7, colon cancer SW480 (colon cancer), and hepatocellular carcinoma SMMC- 7721 (hepatocellular carcinoma), with IC_{50} values of 1.98, 6.49, 3.44,

6.27, and 7.03 μM, respectively. Moreover, zephycandidine A (**81**) showed weak cytotoxicity against the normal Beas-2B cell line (IC_{50} = 20.08 μM) with selectivity index as high as 10 when compared normal Beas-2B cell line, via activation of caspase-3, upregulation of Bax, down-regulation of Bcl-2, and degradation of PARP expression [87]. Hymenolitatine (**82**) showed weak cytotoxic activity against four cancer cell lines, HepG-2, LoVo, Hela, and A549, with IC_{50} values of 75.19, 69.81, 96.37, and 102.53 μM, respectively [88]. Cripowellin-form (**71**–**76**) and Zephycandidine A (**81**) belonging to the other-type of AA may be potential targets for further anticancer investigations.

Effects on the Central Nervous System (CNS)

Several enzymes of the CNS are interesting drug targets. AChE is a serine protease located at neuromuscular junctions, in cholinergic synapses of the central nervous system and in red blood cells [99-101]. The enzyme catalyzes the rapid hydrolysis and inactivation of the neurotransmitter acetylcholine into acetate and choline to enable cholinergic neurons to return to their resting state. Butyrylcholinesterase (BChE) can also hydrolyze acetylcholinesterase into acetate and choline. BChE is produced by the liver and detected in the plasma. Changes in its plasmatic levels can indicate of liver dysfunction. BChE is also expressed in neurons of the CNS [102].

In Alzheimer's disease (AD), AChE is overly active, and the consequential lower level of acetylcholine in the brain cause weakened neurotransmission [103]. Similarly, BChE deregulation is measured in the brain of individuals suffering from AD. Malfunction of the cholinergic system may be pharmacologically tackled via AChE inhibitors that ameliorate the cholinergic deficit at early stages of the disease and reduce progression. In addition, glycogen synthase kinase-3 (GSK-3) is a ubiquitous serine/threonine kinase, implicated in AD, which can trigger abnormal hyperphosphorylation of tau protein, which is believed to be a critical event in neurofibrilary tangle formation. Thus, GSK-3 inhibition represents an attractive drug target for AD and other neurodegenerative disorders [104]. Finally, prolyloligopeptidase (POP) is a cytosolic serine peptidase widely distributed in the organs of the body, including the brain, which cleaves peptide bonds at the carboxyl

end of proline [105,106]. Previous studies have shown that POP inhibitors are efficient anti-dementia drugs [107,108].

The AA galantamine, donepezil and rivastigmine are potent reversible inhibitors of AChE approved for the symptomatic treatment of AD [109,110]. Since cholinesterase enzyme inhibitors are first generation drugs for AD, AChE and BChE are the most targeted enzymes at the moment.

Galantamine derivative sanguinine is ten times more active than galantamine whereas 11-hydroxygalantamine exhibits inhibitory activity similar to that of galantamine. The extra or protected hydroxyl group in its allylic position in (R_1) may be required for the activities [111]. SAR of galantamine and its derivatives was comprehensively reviewed elsewhere [8].

Among the six new galantamine-type alkaloids only 9-de-*O*-methyl-*11*β-hydroxygalantamine (**13**) showed a weak AChE inhibitory activity with IC_{50} value 168.7 μM. The SAR of new galantamine derivatives alkaloids (**11-16)** and known alkaloids isolated from the same plant species revealed that the 4,4a double bond and 9-OH are required for the AChE inhibitory activity, while the presence of the 11-OH group dramatically decreases AChE inhibitory activity [66].

Norbelladine-type alkaloids 6-*O*-demethylbelladine (**1**) and 4′-*O*-demethylbelladine (**2**) were identified as weak inhibitors of AChE with IC_{50} values of 223.2 ± 23.6 and 606.8 ± 74.2 μM, respectively, for (**1)** and (**2**) [60]. They were more potent against BChE, (**2**) (IC_{50} = 30.7 ± 4.0 μM) being more active than (**1**) (IC_{50} = 115.7 ± 10.1μM). 4′-*O*-Demethylbelladine (**2**) exhibited weak POP inhibition with IC_{50} value of 370 ± 30 μM), but more potently than 6-*O*-demethylbelladine (**1**) (IC_{50} = 660 ± 90 μM) [60]. Carltonine A–C (**4-6**) were evaluated for their potential activity against AChE, BChE and POP. Carltonine A–B (**4** and **5**) inhibited BChE with IC_{50} values of 0.91 ± 0.02 and 0.031 ± 0.001 μM. Computational studies detected a plausible binding site on BChE while

SAR suggested that the 1,3-dioxolane ring of carltonine B of (**5**) may be responsible of the BChE activity compared to the opening dimethoxybenzene analogue of (**4**) [62].

As for the cherylline-type, gigantellinine **(8)** inhibited the activity of AChE in a dose-dependent manner with IC_{50} value of 174.90 ± 2.30 μM, while gigantelline **(7)** did not [63].

The lycorine-type, galanthine *N*-β-oxide (20) did not exhibit significantly AChE inhibitory activity (IC_{50} > 200 μM) compared to galanthine. The *N*-oxide fragment seems to be deactivating the inhibitory activity of AChE. New lycorine derivatives (**22)** displayed moderate AChE inhibition (IC_{50} = 35.61 ± 1.90 μM) compared to carinatine (IC_{50} > 200 μM). The aromatic C-ring in lycorine-sort alkaloids may be essential for their activity against AChE [69]. Oxoincartine (**23**) was inactive against both cholinesterases (AChE and BChE) [70].

7-Hydroxyclivonine (**30**), a homolycorine-type exhibited weak AChE inhibition with IC_{50} value 114.07 μM and moderate effect against BChE with IC_{50} = 67.3 μM. Molecular docking with BChE revealed that (**30)** and galantamine both interact with similar amino acids in the same binding pocket [74].

In the crinine subgroup, augustine *N*-oxide (**37**) showed moderate inhibition of AChE at 79.64 μg. mL^{-1} (250,44 μM), while buphanisine *N*-oxide (**38**) did not inhibit the enzyme activity [77]. A mixture of 6α-hydroxymaritidine (**39**) and 6β-hydroxymaritidine (**40**) showed weak AChE inhibitory activity with IC_{50} = 90.43 μM, and was inactive of for BChE inhibitory activity (IC_{50} > 600 μM). Molecular docking studies of 6α-hydroxymaritidine (**39**), 6β-hydroxymaritidine (**40**), lycorine-type reticulinine (**18**), and isoreticulinine (**19**) at the active sites of AChE and BChE identified (19) as a potential inhibitory molecule, since it was stabilized in the active site through hydrogen bonds, π-π stacking and hydrophobic interactions [68]. Crijaponine A (**32**) showed anti-AChE activity with IC_{50} > 10 μM [65]. Moreover, 11-*O*-Acetyl-9-*O*-demethylmaritidine (**42)** inhibited both cholinesterases (AChE and BChE) with IC_{50} values 6.04 and 29.72 μM,

respectively. Furthermore, 3,11-*O*-Diacetyl-9-*O*-demethylmaritidine (**41**) showed weaker AChE inhibition with IC_{50} value 67.4 μM and was inactive against BChE. The SAR of some haemanthamine-derivatives revealed that two free hydroxyl groups present at C-3 and C-11 may be essential for the anti-cholinesterase activity [70]. Gigancrinine **(44)** did not show any anti-AChE activity [63].

The 4-*O*-Methylnangustine (**55**), a montanine-type AA was inactive (IC_{50} > 200 μM) against both AChE and BChE [74].

Among plicamine- and *seco*-plicamine subgroups of alkaloids, (**61-63)** exhibited weak AChE inhibition, with IC_{50} values of 110.6, 57.26, and 75.3 μM [66]. Moreover, (**67**) showed weak AChE inhibitory activity with IC_{50} value 126.16 μM, whereas the others new plicamine- and *seco*-plicamine-types were almost inactive (IC_{50} > 200 μM). The *N*-2-hydroxyethyl group in plicamine-form alkaloids may be essential for this activity [69].

Other types of alkaloids, zephycandidine III (**85**) significantly inhibited AChE with IC_{50} value of 8.82 μM, while (**83**) and (**84**) were inactive at 200 μM. Narcipavline (**86**) exhibited weak AChE inhibitory activity with IC_{50} value 208 ± 37 μM and a significant BChE inhibitory activity IC_{50} = 24.4 ± 1.2 μM. Zephycandidine A (**81**) displayed anti-AChE activity in a dose-dependent manner with IC_{50} = 127.99 μM. Molecular docking studies of zephycandidines (**81**), **(83**–**85**) and galantamine with AChE revealed that interactions with W286 and Y337 are necessary for inhibitory activity [30] [87]. Narcimatuline (**88**) was evaluated for its AChE, BChE, POP, and GSK-3β inhibitory activities and significant inhibited BChE, POP and GSK-3 activities, with IC_{50} values of 5.9 ± 0.2, 29.2 ± 1.0 and 20.7 ± 2.4 μM, respectively, but only a weak activity against AChE with IC_{50} value 489 ± 60 μM [89].

Of all the candidates investigated recently, crinine-derivative 11-*O*-acetyl-9-*O*-demethylmaritidine (**42**) and other-type Zephycandidine III (**85**) are interesting targets for further anti-AChE investigation for Alzheimer's disease.

Anti-Inflammatory and Antioxidant Activity

Unfortunately, the anti-inflammatory activity of AAs is rarely reported. In vitro anti-inflammatory studies of fifteen AAs isolated from different *Crinum* species was comprehensively reviewed in 2003 and their activity was very low [112]. More recently, the anti-inflammatory activity of lycorine-type AAs, such as (+)-1-hydroxy-ungeremine (**17**), homolycorine-type, such as (+)-2-hydroxy-8-demethyl-homolycorine-α-*N*-oxide (**26**), crinine-type (+)-6β-acetyl-8-hydroxy-9-methoxy-crinamine (**31**), and other-type (+)-*N*-methoxylcarbonyl-2-demethyl-isocorydione (**79**) against cyclooxygenase-1 (COX,-1), and cyclooxygenase-2 (COX-2) was evaluated in vitro, and AA (**17**) and (**79**) displayed selective inhibition of COX-2 (> 90%) [67].

Cripowellin derivatives, 4,8-dimethoxy-cripowellin C (**71**), 4,8-dimethoxy-cripowellin D (**72**), 9-methoxy-cripowellin B (**73**) and 4-methoxy-8-hydroxy-cripowellin B (**74**) displayed significant inhibition of COX-1 (> 64%) and of COX-2 (> 90%), respectively [84]. They were also evaluated for their antioxidant potential activities using $ABTS^{\cdot+}$ (2,2′-azino-bis(3-ethylbenzo-thiazoline-6-sulphonic acid) and DPPH (1,1-diphenyl-2-picrylhydrazyl) methods. AAs (**72**), (**73**), and (**74**) showed significant antiradical activity with IC_{50} values of from 52.2 to 80.1μM.

The anti-inflammatory activity of galantamine-, plicamin- and *seco*-plicamin-type (**11-16**, **56-67** and **68-69)** was evaluated in vitro by studying the inhibition of lipopolysaccharide (LPS)-induced nitric oxide (NO) production in RAW 264.7 mouse macrophages. Among the tested compounds, two plicamine-type alkaloids (**59)** and (**60)** showed significant inhibitory activities with IC_{50} values of 18.77 and 10.21 μM, respectively, while other alkaloids were inactive at 200 μM [66].

Anti-Parasitic and Antibacterial Activity

The 4,8-Dimethoxy-cripowellin C (**71**), 4,8-dimethoxy-cripowellin D (**72**), 9-methoxy-cripowellin B (**73**), and 4-methoxy-8-hydroxy-cripowellin B (**74)** were evaluated for their antimicrobial against eight species of bacteria (*Streptococcus pneumoniae,*

Staphylococcus aureus, Staphylococcus epidermidis, Klebsiella pneumoniae, Pseudomonas aeruginosa, Haemophilus influenzae, Enterobacter cloacae, and *Shigella dysenteriae*). Moreover, (**73**) and (**74)** displayed highest antibacterial activity with IC_{50} values < 0.50 mM, while (**71**) and (**72**) had weak activity [84].

Malaria (*Plasmodium sp*.), leishmaniasis (*Leishmania sp*.), and trypanosomiasis (*Trypanosoma brucei* and *Trypanosoma cruzi*) are the most common chronic protozoan diseases and occur mainly in poor rural and urban areas in tropical and subtropical regions of the world. Previously, several AAs were reported for their potent in vitro antiprotozoal activity [113]. The anti-plasmodial activity was recently reviewed elsewhere [114,115]. Newly isolated alkaloids such as cripowellin C (**75**) and D (**76**) were evaluated against the chloroquine/mefloquine-resistant Dd2 strain of *Plasmodium falciparum* and were found to have potent antiplasmodial activity, with IC_{50} values of 180 ± 20, 26 ± 2, and 260 ± 20 nM, respectively [85].

Crinine-type 1,4-dihydroxy-3-methoxy powellan (**36**) had a weak activity, with IC_{50} = 37 ± 3 μM against the same pathogen [76]. The two epimers (6α-hydroxymaritidine (**39**) and 6β-hydroxymaritidine (**40**)) were evaluated for their antiprotozoal activity against *T. brucei rhodesiense* (trypomastigotes forms, STIB 900 strain), *T. cruzi* (amastigotes forms, Tulahuen C4 strain), *L. donovani* (amastigotes forms, MHOM-ET-67/L82 strain), and *P. falciparum* (intraerythrocytic forms, IEF, NF54 strain). They displayed low toxicity against all protozoans tested with IC_{50} values of 30.68, 66.11, > 100 and 32.86 μg. mL^{-1} respectively [68]. Augustine *N*-oxide (**37**) and buphanisine *N*-oxide (**38**) were also evaluated against the same strains mentioned above and displayed low activity with IC_{50} values ranging from 32 to > 100 μg. mL^{-1}. The presence of an *N*-oxide group in (**37**) and (**38**) appears to decrease their activity against *T. brucei* and *P. falciparum* compared to the previously characterized anti-protozoal compounds belonging to the same subgroup [77].

Scillitazettine (**53**) and scilli-*N*-desmethylpre*tazettine* (**54**) were evaluated against the chloroquine-resistant strain *P. falciparum* FcB1 and displayed antiparasitic activity with IC_{50} values of 77.0 ± 2.0 and 46.5 ± 2.0 μM, respectively [61].

Larvicidal and Insecticidal

Insects are important vectors of many diseases, controlling their proliferation is an efficient way of preventing disease spread. *Aedes aegypti* is the main vector for dengue, yellow fever and Zika infection. In an earlier study, organic extracts of the bulbs of *Nerine sarniensis*, demonstrated strong larvicidal and insecticidal activity with LC_{50} of 0.008 μg.μL^{-1} against *A. aegypti* larvae and against grown-up females with LD_{50} of 4.6 μg/mosquito. Sarniensine (**78**) was less efficient against larvae at the most minimal concentration of 0.1 μg/μL but displayed strong adulticidal activity with an LD_{50} of 1.38 ± 0.056 μg/mosquito [86]. Mesembrine-class sarniensinol (**77**), sarniensine (**78**) and crinine-type crinsarnine (**43**) had no effect against *A. aegypti* larvae at all concentrations tested. In adult topical bioassays, only (**43**) displayed adulticidal activity, with an LD_{50} = 2.29 ± 0.049 μg per mosquito. SAR studies revealed that the scaffold of pretazettine alkaloids in (**77**) and (**78**) and (**43**) and in bowdensine were important for their activity. Among the mesembrine group, the opening of the B-ring or the presence of a B-ring lactone as well as the trans-stereochemistry of the A/B-ring junction seem to be important for their activity, while in crinine-type alkaloids, the substituent at C-2 appears to be important [78,86,116].

Others Activities

The carbonic anhydrases (CAs) are metalloenzymes that catalyze the reversible hydration of carbon dioxide with water into a bicarbonate ion and a proton. In humans, sixteen isozymes have been identified including human cabonic isozyme II (hCAII) reported to be involved many diseases like glaucoma, epilepsy and cancer. Thus, hCAII is a target for therapeutic interventions [80]. Crinasiaticine A (**46**) and crinasiaticine B (**47**) were evaluated for their inhibitory potential against hCAII and they were inactive [80].

Production of Amaryllidaceae Alkaloids

Chemical Extraction from Amaryllidaceae Plants

The acid-base extraction is the classical method used to extract alkaloids from Amaryllidaceae. The acid extraction usually uses 0.1% to 2% sulfuric acid (H_2SO_4) or hydrochloric acid (HCl) as solvent by maceration. For example, in a recent study by our group, fresh bulbs of *C. jagus* were dried at room temperature and then finely powdered [63]. The resultant powder (1.35 kg) was extracted with 1% H_2SO_4, (2 × 2 L) overnight at room temperature. The suspension was filtered through a cloth and successively centrifuged at 10 °C at 7000 rpm for 30 min. The acid extract was alkalinized to pH 9-10 with 12 N NaOH. The aqueous solution was extracted with EtOAc (3 × 1.2 L), and the organic extracts were combined, dried (Na_2SO_4) and evaporated under reduced pressure to give a brown oil residue (3.0 g) [63].

Alcoholic solvent such as methanol or ethanol can also be used to extract both free and salt of alkaloids. For example, fresh bulbs (1.5 kg) and leaves (400 g) of *H. reticulatum* were collected, crushed and extracted with MeOH (2 × 1.0 L) at room temperature for 4 days, and the combined macerate was filtered and evaporated under reduced pressure. The crude extracts of the bulbs and leaves (117.3 and 53.5 g, respectively) were acidified with H_2SO_4 (2%, *v/v*) to pH 3 and extracted with Et_2O (10 × 150 mL) and EtOAc (3 × 150 mL) to remove the neutral material. The aqueous solutions were basified with ammonia (25%, *v/v*) up to pH 9–10 and extracted with n-Hex (16 × 150 mL) to give the n-Hex extracts (0.14 and 0.02 g, respectively. This was followed by extraction with EtOAc (15 × 150 mL) to give the EtOAc extracts (1.6 and 0.3 g, respectively) and finally extracted with EtOAc:MeOH (3:1, *v/v*) (4 × 150 mL) to provide the EtOAc:MeOH extracts (2.10 and 1.56 g, respectively) [68].

Biotechnological Production of Amaryllidaceae Alkaloids

Usually, extraction of bioactive compound from its natural source is low, time-consuming and costly, which hinders further research and application. With the commercialization of

galantamine as a drug, its demand from generic pharmaceutical companies increased, and production from native source became challenging to fulfill [117]. The diversity and quantity of AAs in plants also vary with plant species, developmental stage and types of tissue/cell. Plants growth can be affected by seasonal changes and environmental factors [25,42,118]. Therefore, mass production of AAs by cultivation of plants is not always sustainable.

Alternatively, several studies have depicted other approaches to produce specialized metabolites such as alkaloids by using in vitro culture of plant parts/tissues. Results from in vitro culture of *Narcissus confusus* and *Leucojum aestivum* show that alkaloids' amounts are low in undifferentiated cells as compared to differentiated cells, indicating that undifferentiated cells are unsuitable for such biotechnological process [119-121]. Growth and production of alkaloids and biomass in in vitro system often vary with source and concentration of carbohydrate (sucrose, fructose, glucose *etc*.), phosphorous and nitrogen. Optimization of these basal requirements in growth medium is crucial and can be achieved by using mathematical analysis to enhance production of target metabolites, increase biomass, or both. Another important factor that can regulate phytochemical profile of culture cells are phytohormones, i.e., auxins and cytokinins. Optimal ratio of phytohormones is essential and specific to maintain different stages of cultured cells, which ultimately can result in variation of phytochemicals [54,122,123]. Biosynthesis of galantamine was not detected in the in vitro culture of *N. pseudonarcissus* cv. Carlton in absence of phytohormone, whereas high amounts of galantamine were detected in differentiated tissues cultured in low auxin (4 mg/L of NAA) as compared to undifferentiated tissue cultured in high auxin (20 mg/L of NAA) [54]. Furthermore, in nature it was observed that plants synthesize alkaloids in response to different biotic and abiotic factors [124]. Therefore, these factors, or the associated signaling compounds produced in response to these factors, can be used as elicitors to enhance the biosynthesis of specialized metabolites in in vitro techniques [125,126]. For example, using methyl jasmonate as an elicitor in Leucojum shoot culture can enhance production of galantamine by two-fold [127]. Physical parameters further modulate production in in vitro system. Light, temperature and bioreactor types can greatly enhance the production of AAs in in

vitro system. Finally, with a better understanding of the effect of the environment, and of microorganism–plant interactions, applying this knowledge to artificial culture system could boost the production of AAs and should be considered as a promising approach.

Like other specialized metabolites, AAs can be produced by heterologous expression of genes cluster that express the enzymes required for their biosynthesis. Precise and reliable construction of DNA fragments can be rapidly achieved by using modern recombination and DNA assembly techniques. Several strategies have been developed to engineer microbial hosts, such as bacteria, or yeast, for the heterologous production of alkaloids and their precursors [128–134]. Synthetic biology approaches for production of plant-derived specialized metabolites by metabolic engineering have been carried out primarily in yeast (*Saccharomyces cerevisiae*) so far and to a lesser extent in *Escherichia coli*; whereas tobacco species *Nicotiana tabacum* and *Nicotiana benthamiana* have emerged as hosts for the heterologous expression of biosynthetic genes and production of specialized metabolites in plants [135-138]. However, the lack of knowledge in biosynthetic pathway hinders this approach as of yet. Elucidation of the reactions will be achieved by using modern sequencing technology interrelated with metabolite studies, systems biology, and bioinformatic analysis. This will not only provide techniques to produce AAs but also help with biosynthesis of novel AAs derivatives.

Conclusions

A total of 91 new AAs has been isolated in the last 5 years, and some of their biological activities have been uncovered. AAs are a rich group of specialized metabolites with pleiotropic effects that represent an important resource for new drugs discovery. They should be deeper exploited, at the image of galantamine used to treat the symptoms of AD. Recent years of AAs research have been marked by the discovery of compounds with potent anticancer (e.g., **17**, **52**, **72-74**, **75**, **76**, and **79**), anticholinesterase (**42** and **85**), anti-inflammatory (**59**, **60**, and **71-74**), antiparasitic (**75** and **76**), larvicidal and insecticidal (**43** and **77**), antibacterial and antioxidant (**73** and **74**) biological activities. This review helps expand the chemical library of AAs and their possible application in medicine.

References

1. Jin, Z.; Yao, G. Amaryllidaceae and Sceletium alkaloids. *Nat. Prod. Rep.* **2019**, *36*, 1462-1488.

2. Singh, A.; Desgagné-Penix, I. Biosynthesis of the Amaryllidaceae alkaloids. *Plant. Sci. Today* **2014**, *1* (3), 114-120.

3. Kornienko, A.; Evidente, A., Chemistry, biology, and medicinal potential of narciclasine and its congeners. *Chem. Rev.* **2008**, *108*, 1982-2014.

4. Gerrard, A.W. The proximate principles of the Narcissus pseudonarcissus. *Pharm. J.* **1877**, *8*, 214.

5. Asahina, Y.; Sugii, Y. Ueber die Identitaet des Lycorins und Narcissins. *Arch. Pharm.* **1913**, *251*, 357.

6. Morishima, K. Chemische und pharmakologische Untersuchungen über die Alkaloide der *Lycoris radiata* Herb. *Arch. Exptl. Path. Pharmakol.* **1897**, *40*, 221-240.

7. Hartwell, J. Plants used against cancer. A survey. *Lloydia* **1971**, *30*, 379-463.

8. He, M.M.; Qu, C.R.; Gao, O.D.; Hu, X.M.; Hong, X.C. Biological and pharmacological activities of amaryllidaceae alkaloids. *Rsc. Adv.* **2015**, *5*, 16562-16574.

9. Hotchandani, T.; Desgagne-Penix, I., Heterocyclic Amaryllidaceae Alkaloids: Biosynthesis and Pharmacological Applications. *Curr. Top. Med. Chem.* **2017**, *17*, 418-427.

10. Heinrich, M. Galantamine from Galanthus and other Amaryllidaceae-chemistry and biology based on traditional use. *Alkaloids Chem. Biol.* **2010**, *68*, 157-165.

11. Berkov, S.; Osorio, E.; Viladomat, F.; Bastida, J. Chemodiversity, chemotaxonomy and chemoecology of Amaryllidaceae alkaloids. *Alkaloids Chem. Biol.* **2020**, *83*, 113-185.

12. Lewis, J.R. Amaryllidaceae and Sceletium Alkaloids. *Nat. Prod. Rep.* **1992**, *9*, 183-191.

13. Lewis, J.R. Amaryllidaceae and Sceletium Alkaloids. *Nat. Prod. Rep.* **1993**, *10*, 291-299.

14. Lewis, J.R. Amaryllidaceae and Sceletium Alkaloids. *Nat. Prod. Rep.* **1995**, *12*, 339-345.

15. Lewis, J.R. Amaryllidaceae and Sceletium alkaloids. *Nat. Prod. Rep.* **1996**, *13*, 171-176.

16. Lewis, J.R. Amaryllidaceae, sceletium, imidazole, oxazole, thiazole, peptide and miscellaneous alkaloids. *Nat. Prod. Rep.* **2002**, *19*, 223-258.

17. Jin, Z.; Li, Z.; Huang, R. Muscarine, imidazole, oxazole, thiazole, Amaryllidaceae and Sceletium alkaloids. *Nat. Prod. Rep.* **2002**, *19*, 454-476.

18. Jin, Z. Amaryllidaceae and Sceletium alkaloids. *Nat. Prod. Rep.* **2003**, *20*, 606-614.

19. Jin, Z. Amaryllidaceae and Sceletium alkaloids. *Nat. Prod. Rep.* **2005**, *22*, 111-126.

20. Jin, Z. Amaryllidaceae and Sceletium alkaloids. *Nat. Prod. Rep.* **2007**, *24*, 886-905.

21. Jin, Z. Amaryllidaceae and Sceletium alkaloids. *Nat. Prod. Rep.* **2009**, *26*, 363–381.

22. Jin, Z., Amaryllidaceae and Sceletium alkaloids. *Nat. Prod. Rep.* **2011**, *28*, 1126-1142.

23. Jin, Z. Amaryllidaceae and Sceletium alkaloids. *Nat. Prod. Rep.* **2013**, *30*, 849-868.

24. Jin, Z. Amaryllidaceae and Sceletium alkaloids. *Nat. Prod. Rep.* **2016**, *33*, 1318-1343.

25. Ding, Y.; Qu, D.; Zhang, K.M.; Cang, X.X.; Kou, Z.N.; Xiao, W.; Zhu, J.B. Phytochemical and biological investigations of Amaryllidaceae alkaloids: A review. *J. Asian Nat. Prod. Res.* **2017**, *19*, 53-100.

26. Desgagné-Penix, I. Biosynthesis of alkaloids in Amaryllidaceae plants: A review. *Phytochem. Rev.* **2020**.

27. Unver, N.; Kaya, G.I.; Werner, C.; Verpoorte, R. Galanthindole: A new indole alkaloid from Galanthus plicatus ssp. byzantinus. *Planta. Med.* **2003**, *69*, 869-871.

28. Bastida, J., Berkov, S., Torras, L., Pigni, N.B., de Andrade, J.P., Martinez, V., Codina, C., Viladomat, F. Chemical and biological aspects of Amaryllidaceae alkaloids. *Rec. Adv. Pharm. Sci.* **2011**, 65-100.

29. Safratova, M.; Hostalkova, A.; Hulcova, D.; Breiterova, K.; Hrabcova, V.; Machado, M.; Fontinha, D.; Prudencio, M.; Kunes, J.; Chlebek, J.; etal. Alkaloids from Narcissus poeticus cv. Pink Parasol of various structural types and their biological activity. *Arch. Pharm. Res.* **2018**, *41*, 208-218.

30. Zhan, G.; Liu, J.; Zhou, J.; Sun, B.; Aisa, H.A.; Yao, G. Amaryllidaceae alkaloids with new framework types from Zephyranthes candida as potent acetylcholinesterase inhibitors. *Eur. J. Med. Chem.* **2017**, *127*, 771-780.

31. Wang, H.Y.; Qu, S.M.; Wang, Y.; Wang, H.T. Cytotoxic and anti-inflammatory active plicamine alkaloids from Zephyranthes grandiflora. *Fitoterapia* **2018**, *130*, 163-168.

32. Singh, A.; Desgagné-Penix, I., *Chapter 3: Biosynthesis of Amaryllidaceae alkaloids: A biochemical outlook.* In*: Alkaloids: Biosynthesis, Biological Roles and Health benefits.* Eduardo Sobarzo-Sanchez, Eds; Nova Science Publishers: Hauppauge, NY, USA, 2015.

33. Kilgore, M.B.; Kutchan, T.M. The Amaryllidaceae alkaloids: Biosynthesis and methods for enzyme discovery. *Phytochem. Rev.* **2016**, *15*, 317-337.

34. El Tahchy, A.; Ptak, A.; Boisbrun, M.; Barre, E.; Guillou, C.; Dupire, F.; Chretien, F.; Henry, M.; Chapleur, Y.; Laurain-Mattar, D. Kinetic study of the rearrangement of deuterium-labeled 4′-O-methylnorbelladine in Leucojum aestivum shoot cultures by mass spectrometry. Influence of precursor feeding on amaryllidaceae alkaloid accumulation. *J. Nat. Prod.* **2011**, *74*, 2356-2361.

35. Saliba, S.; Ptak, A.; Laurain-Mattar, D. 4′-O-Methylnorbelladine feeding enhances galantamine and lycorine production by Leucojum aestivum L. shoot cultures. *Eng. Life Sci.* **2015**, *15*, 640-645.

36. Barton, D.H.R.; Kirby, G.W. 153. Phenol oxidation and biosynthesis. Part V. The synthesis of galantamine. *J. Chem. Soc. (Resumed)* **1962**, *153*, 806-817.

37. Barton, D.H.R.; Kirby, G.W.; Taylor, J.B.; Thomas, G.M. 866. Phenol oxidation and biosynthesis. Part VI. The biogenesis of amaryllidaceae alkaloids. *J. Chem. Soc. (Resumed)* **1963**, *866*, 4545-4558.

38. Eichhorn, J.; Takada, T.; Kita, Y.; Zenk, M.H. Biosynthesis of the Amaryllidaceae alkaloid galantamine. *Phytochemistry* **1998**, *49* (4), 1037-1047.

39. El Tahchy, A. Étude de la voie de biosynthèse de la galantamine chez Leucojum aestivum L. – Criblage phytochimique de quelques Amaryllidaceae. Doctorate thesis. Nancy Université Henri Poincaré, Nancy, France, 2010.

40. El Tahchy, A.; Boisbrun, M.; Ptak, A.; Dupire, F.; Chretien, F.; Henry, M.; Chapleur, Y.; Laurain-Mattar, D. New method for the study of Amaryllidaceae alkaloid biosynthesis using biotransformation of deuterium-labeled precursor in tissue cultures. *Acta. Biochim. Pol.* **2010**, *57*, 75-82.

41. Singh, A.; Desgagne-Penix, I. Transcriptome and metabolome profiling of Narcissus pseudonarcissus ‘King Alfred’ reveal components of Amaryllidaceae alkaloid metabolism. *Sci. Rep.* **2017**, *7*, 17356.

42. Hotchandani, T.; de Villers, J.; Desgagne-Penix, I. Developmental Regulation of the Expression of Amaryllidaceae Alkaloid Biosynthetic Genes in Narcissus papyraceus. *Genes* **2019**, *10*, 594.

43. Park, C.H.; Yeo, H.J.; Park, Y.E.; Baek, S.A.; Kim, J.K.; Park, S.U. Transcriptome Analysis and Metabolic Profiling of Lycoris Radiata. *Biology* **2019**, *8*, 63.

44. Wang, R.; Han, X.; Xu, S.; Xia, B.; Jiang, Y.; Xue, Y.; Wang, R. Cloning and characterization of a tyrosine decarboxylase involved in the biosynthesis of galantamine in Lycoris aurea. *PeerJ* **2019**, *7*, e6729.

45. Suhadolnik, R.J.; Fischer, A.G.; Zulalian, J. Biogenesis of the Amaryllidaceae alkaloids. II. Studies with whole plants, floral primordia and cell free extracts. *Biochem. Biophys. Res. Commun.* **1963**, *11*, 208-212.

46. Wildman, W.; Battersby, A.; Breuer, S. Biosynthesis in the Amaryllidaceae. Incorporation of 3-C14-Tyrosine and Phenylalanine in Nerine Bowdenii, W. Wats. *J. Am. Chem. Soc.* **1962**, *84*, 4599-4600.

47. Jiang, Y.; Xia, N.; Li, X.; Shen, W.; Liang, L.; Wang, C.; Wang, R.; Peng, F.; Xia, B. Molecular cloning and characterization of a phenylalanine ammonia-lyase gene (LrPAL) from Lycoris radiata. *Mol. Biol. Rep.* **2011**, *38*, 1935-1940.

48. Jiang, Y.; Xia, B.; Liang, L.; Li, X.; Xu, S.; Peng, F.; Wang, R. Molecular and analysis of a phenylalanine ammonia-lyase gene (LrPAL2) from Lycoris radiata. *Mol. Biol. Rep.* **2013**, *40*, 2293-2300.

49. Li, W.; Yang, Y.; Qiao, C.; Zhang, G.; Luo, Y. Functional characterization of phenylalanine ammonia-lyase- and cinnamate 4-hydroxylase-encoding genes from Lycoris radiata, a galantamine-producing plant. *Int. J. Biol. Macromol.* **2018**, *117*, 1264-1279.

50. Fahrendorf, T.; Dixon, R.A. Stress responses in alfalfa (Medicago sativa L.). XVIII: Molecular cloning and expression of the elicitor-inducible cinnamic acid 4-hydroxylase cytochrome P450. *Arch. Biochem. Biophys.* **1993**, *305*, 509-515.

51. Teutsch, H.G.; Hasenfratz, M.P.; Lesot, A.; Stoltz, C.; Garnier, J.M.; Jeltsch, J.M.; Durst, F.; Werck-Reichhart, D. Isolation and sequence of a cDNA encoding the Jerusalem artichoke cinnamate 4-hydroxylase, a major plant cytochrome P450 involved in the general phenylpropanoid pathway. *Proc. Natl. Acad. Sci. USA* **1993**, *90*, 4102-4106.

52. Nikolova, M.; Gevrenova, R. Determination of phenolic acids in amaryllidaceae species by high performance liquid chromatography. *Pharm. Biol.* **2005**, *43*, 289-291.

53. Benedec, D.; Oniga, I.; Hanganu, D.; Gheldiu, A.M.; Puscas, C.; Silaghi-Dumitrescu, R.; Duma, M.; Tiperciuc, B.; Varban, R.; Vlase, L. Sources for developing new medicinal products: Biochemical investigations on alcoholic extracts obtained from aerial parts of some Romanian Amaryllidaceae species. *BMC Complement. Altern Med.* **2018**, *18*, 226.

54. Ferdausi, A.; Chang, X.M.; Hall, A.; Jones, M. Galantamine production in tissue culture and metabolomic study on Amaryllidaceae alkaloids in Narcissus pseudonarcissus cv. Carlton. *Ind Crops Prod.* **2020**, *144*, 112058.

55. Prachayasittikul, S.; Buraparuangsang, P.; Worachartcheewan, A.; Isarankura-Na-Ayudhya, C.; Ruchirawat, S.; Prachayasittikul, V. Antimicrobial and antioxidative activities of bioactive constituents from Hydnophytum formicarum Jack. *Molecules* **2008**, *13*, 904-921.

56. Singh, A.; Massicotte, M.A.; Garand, A.; Tousignant, L.; Ouellette, V.; Berube, G.; Desgagne-Penix, I. Cloning and characterization of norbelladine synthase catalyzing the first committed reaction in Amaryllidaceae alkaloid biosynthesis. *BMC Plant. Biol.* **2018**, *18*, 338.

57. Kilgore, M.B.; Holland, C.K.; Jez, J.M.; Kutchan, T.M. Identification of a Noroxomaritidine Reductase with Amaryllidaceae Alkaloid Biosynthesis Related Activities. *J. Biol. Chem.* **2016**, *291*, 16740-16752.

58. Kilgore, M.B.; Augustin, M.M.; Starks, C.M.; O'Neil-Johnson, M.; May, G.D.; Crow, J.A.; Kutchan, T.M. Cloning and characterization of a norbelladine 4′-O-methyltransferase involved in the biosynthesis of the Alzheimer's drug galantamine in Narcissus sp. aff. pseudonarcissus. *PLoS ONE* **2014**, *9*, e103223.

59. Kilgore, M.B.; Augustin, M.M.; May, G.D.; Crow, J.A.; Kutchan, T.M. CYP96T1 of Narcissus sp. aff. pseudonarcissus Catalyzes Formation of the Para-Para' C-C Phenol Couple in the Amaryllidaceae Alkaloids. *Front. Plant. Sci.* **2016**, *7*, 225.

60. Vaneckova, N.; Host'alkova, A.; Safratova, M.; Kunes, J.; Hulcova, D.; Hrabinova, M.; Doskocil, I.; Stepankova, S.; Opletal, L.; Novakova, L.; et al. Isolation of Amaryllidaceae alkaloids from *Nerine bowdenii* W. Watson and their biological activities. *Rsc. Adv.* **2016**, *6*, 80114-80120.

61. N'Tamon, A.D.; Okpekon, A.T.; Bony, N.F.; Bernadat, G.; Gallard, J.-F.; Kouamé, T.; Séon-Méniel, B.; Leblanc, K.; Rharrabti, S.; Mouray, E. Streamlined targeting of Amaryllidaceae alkaloids from the bulbs of Crinum scillifolium using spectrometric and taxonomically-informed scoring metabolite annotations. *Phytochemistry* **2020**, *179*, 112485.

62. Al Mamun, A.; Maříková, J.; Hulcová, D.; Janoušek, J.; Šafratová, M.; Nováková, L.; Kučera, T.; Hrabinová, M.; Kuneš, J.; Korábečný, J. Amaryllidaceae Alkaloids of Belladine-Type from Narcissus pseudonarcissus cv. Carlton as New Selective Inhibitors of Butyrylcholinesterase. *Biomolecules* **2020**, *10*, 800.

63. Ka, S.; Masi, M.; Merindol, N.; Di Lecce, R.; Plourde, M.B.; Seck, M.; Gorecki, M.; Pescitelli, G.; Desgagne-Penix, I.; Evidente, A. Gigantelline, gigantellinine and gigancrinine, cherylline- and crinine-type alkaloids isolated from Crinum jagus with anti-acetylcholinesterase activity. *Phytochemistry* **2020**, *175*, 112390.

64. Ang, S.; Liu, X.M.; Huang, X.J.; Zhang, D.M.; Zhang, W.; Wang, L.; Ye, W.C. Four New Amaryllidaceae Alkaloids from Lycoris radiata and Their Cytotoxicity. *Planta Med.* **2015**, *81*, 1712-1718.

65. Endo, Y.; Sugiura, Y.; Funasaki, M.; Kagechika, H.; Ishibashi, M.; Ohsaki, A. Two new alkaloids from Crinum asiaticum var. japonicum. *J. Nat. Med.* **2019**, *73*, 648-652.

66. Zhan, G.; Zhou, J.; Liu, R.; Liu, T.; Guo, G.; Wang, J.; Xiang, M.; Xue, Y.; Luo, Z.; Zhang, Y.; et al. Galantamine, Plicamine, and Secoplicamine Alkaloids from Zephyranthes candida and Their Anti-acetylcholinesterase and Anti-inflammatory Activities. *J. Nat. Prod.* **2016**, *79*, 760-766.

67. Liu, Z.M.; Huang, X.Y.; Cui, M.R.; Zhang, X.D.; Chen, Z.; Yang, B.S.; Zhao, X.K. Amaryllidaceae alkaloids from the bulbs of Lycoris radiata with cytotoxic and anti-inflammatory activities. *Fitoterapia* **2015**, *101*, 188-193.

68. Tallini, L.R.; Osorio, E.H.; Santos, V.D.D.; Borges, W.S.; Kaiser, M.; Viladomat, F.; Zuanazzi, J.A.S.; Bastida, J. Hippeastrum reticulatum (Amaryllidaceae): Alkaloid Profiling, Biological Activities and Molecular Docking. *Molecules* **2017**, *22*, 2191.

69. Zhan, G.; Zhou, J.; Liu, J.; Huang, J.; Zhang, H.; Liu, R.; Yao, G. Acetylcholinesterase Inhibitory Alkaloids from the Whole Plants of Zephyranthes carinata. *J. Nat. Prod.* **2017**, *80*, 2462-2471.

70. Emir, A.; Emir, C.; Bozkurt, B.; Onur, M.A.; Bastida, J.; Somer, N.U. Alkaloids from Galanthus fosteri. *Phytochem Lett* **2016**, *17*, 167-172.

71. Breiterova, K.; Koutova, D.; Marikova, J.; Havelek, R.; Kunes, J.; Majorosova, M.; Opletal, L.; Hostalkova, A.; Jenco, J.; Rezacova, M.; et al. Amaryllidaceae Alkaloids of Different Structural Types from Narcissus, L. cv. Professor Einstein and Their Cytotoxic Activity. *Plants* **2020**, *9*, 137.

72. Katoch, D.; Kumar, D.; Padwad, Y.S.; Singh, B.; Sharma, U. Pseudolycorine N-oxide, a new N-oxide from Narcissus tazetta. *Nat. Prod. Res.* **2020**, *34*, 2051-2058.

73. Carvalho, K.R.; Silva, A.B.; Torres, M.C.M.; Pinto, F.C.L.; Guimaraes, L.A.; Rocha, D.D.; Silveira, E.R.; Costa-Lotufo, L.V.; Braz, R.; Pessoa, O.D.L. Cytotoxic Alkaloids from Hippeastrum solandriflorum Lindl. *J. Braz. Chem. Soc.* **2015**, *26*, 1976-1980.

74. Ortiz, J.E.; Pigni, N.B.; Andujar, S.A.; Roitman, G.; Suvire, F.D.; Enriz, R.D.; Tapia, A.; Bastida, J.; Feresin, G.E. Alkaloids from Hippeastrum argentinum and Their Cholinesterase-Inhibitory Activities: An in Vitro and in Silico Study. *J. Nat. Prod.* **2016**, *79*, 1241-1248.

75. Hanh, T.T.H.; Huong, P.T.T.; Van Thanh, N.; Trung, N.Q.; Van Cuong, T.; Mai, N.T.; Cuong, N.T.; Cuong, N.X.; Nam, N.H.; Van Minh, C. Crinane, augustamine, and β-carboline alkaloids from Crinum latifolium. *Phytochem. Lett.* **2018**, *24*, 27-30.

76. Cho, N.; Du, Y.; Valenciano, A.L.; Fernandez-Murga, M.L.; Goetz, M.; Clement, J.; Cassera, M.B.; Kingston, D.G.I. Antiplasmodial alkaloids from bulbs of Amaryllis belladonna Steud. *Bioorg. Med. Chem. Lett.* **2018**, *28*, 40-42.

77. Tallini, L.R.; Torras-Claveria, L.; Borges, W.S.; Kaiser, M.; Viladomat, F.; Zuanazzi, J.A.S.; Bastida, J. N-oxide alkaloids from Crinum amabile (Amaryllidaceae). *Molecules* **2018**, *23*, 1277.

78. Masi, M.; Cala, A.; Tabanca, N.; Cimmino, A.; Green, I.R.; Bloomquist, J.R.; van Otterlo, W.A.; Macias, F.A.; Evidente, A. Alkaloids with Activity against the Zika Virus Vector Aedes aegypti (L.)-Crinsarnine and Sarniensinol, Two New Crinine and Mesembrine Type Alkaloids Isolated from the South African Plant Nerine sarniensis. *Molecules* **2016**, *21*, 1432.

79. Bessa, C.D.P.B.; de Andrade, J.P.; de Oliveira, R.S.; Domingos, E.; Santos, H.; Romao, W.; Bastida, J.; Borges, W.S. Identification of Alkaloids from Hippeastrum aulicum (Ker Gawl.) Herb. (Amaryllidaceae) Using CGC-MS and Ambient Ionization Mass Spectrometry (PS-MS and LS-MS). *J. Braz. Chem. Soc.* **2017**, *28*, 819-830.

80. Chaichompoo, W.; Chokchaisiri, R.; Sangkaew, A.; Pabuprapap, W.; Yompakdee, C.; Suksamrarn, A. Alkaloids with anti-human carbonic anhydrase isozyme II activity from the bulbs of Crinum asiaticum L. var. asiaticum. *Phytochem. Lett.* **2020**, *37*, 101-105.

81. Moodley, N.; Crouch, N.; Bastida, J.; Mulholland, D. Novel alkaloids and a ceramide from Brunsvigia natalensis (Amaryllidaceae) and their anti-neoplastic activity. *S. Af.r J. Bot.* **2020**.

82. Katoch, D.; Kumar, D.; Padwad, Y.S.; Singh, B.; Sharma, U. Narciclasine-4-O-beta-D-xylopyranoside, a new narciclasine glycoside from Zephyranthes minuta. *Nat. Prod. Res.* **2020**, *34*, 233-20.

83. Masi, M.; Frolova, L.V.; Yu, X.; Mathieu, V.; Cimmino, A.; De Carvalho, A.; Kiss, R.; Rogelj, S.; Pertsemlidis, A.; Kornienko, A.; et al. Jonquailine, a new pretazettine-type alkaloid isolated from Narcissus jonquilla quail, with activity against drug-resistant cancer. *Fitoterapia* **2015**, *102*, 41-48.

84. Chen, M.X.; Huo, J.M.; Hu, J.; Xu, Z.P.; Zhang, X. Amaryllidaceae alkaloids from Crinum latifolium with cytotoxic, antimicrobial, antioxidant, and anti-inflammatory activities. *Fitoterapia* **2018**, *130*, 48-53.

85. Presley, C.C.; Krai, P.; Dalal, S.; Su, Q.; Cassera, M.; Goetz, M.; Kingston, D.G.I. New potently bioactive alkaloids from Crinum erubescens. *Bioorg. Med. Chem.* **2016**, *24*, 5418-5422.

86. Masi, M.; van der Westhuyzen, A.E.; Tabanca, N.; Evidente, M.; Cimmino, A.; Green, I.R.; Bernier, U.R.; Becnel, J.J.; Bloomquist, J.R.; van Otterlo, W.A.; et al. Sarniensine, a mesembrine-type alkaloid isolated from Nerine sarniensis, an indigenous South African Amaryllidaceae, with larvicidal and adulticidal activities against Aedes aegypti. *Fitoterapia* **2017**, *116*, 34-38.

87. Zhan, G.; Qu, X.; Liu, J.; Tong, Q.; Zhou, J.; Sun, B.; Yao, G. Zephycandidine A, the First Naturally Occurring Imidazo [1,2-f]phenanthridine Alkaloid from Zephyranthes candida, Exhibits Significant Anti-tumor and Anti-acetylcholinesterase Activities. *Sci. Rep.* **2016**, *6*, 33990.

88. Chen, N.; Ji, Y.B.; Zhang, W.G.; Xu, Y.; Yan, X.J.; Sun, Y.F.; Song, H.; Xu, C.R.; Cai, L.P.; Zheng, H.X.; et al. Chemical Constituents from Hymenocallis littoralis. *Lett. Org. Chem.* **2016**, *13*, 536-539.

89. Hulcova, D.; Marikova, J.; Korabecny, J.; Hostalkova, A.; Jun, D.; Kunes, J.; Chlebek, J.; Opletal, L.; De Simone, A.; Novakova, L.; et al. Amaryllidaceae alkaloids from Narcissus pseudonarcissus L. cv. Dutch Master as potential drugs in treatment of Alzheimer's disease. *Phytochemistry* **2019**, *165*, 112055.

90. Zhang, F.J.; Shu, X.C.; Wang, T.; Zhuang, W.B.; Wang, Z. The complete chloroplast genome sequence of Lycoris radiata. *Mitochondrial DNA Part. B-Resour.* **2019**, *4*, 2886-2887.

91. Erenler, R.; Nusret, G.; Elmastaş, M.; Eminağaoğlu, Ö. Evaluation of antioxidant capacity with total phenolic content of Galanthus krasnovii (Amaryllidaceae). *Turk. J. Biod.* **2019**, *2*, 13-17.

92. Costa, G.G.P. d.; Silva, C.A.G.; Gomes, J.V.D.; Torres, A.G.; Santos, I.R.I.; Almeida, F.T.C. d.; Fagg, C.W.; Simeoni, L.A.; Silveira, D.; Gomes-Copeland, K.K.P. Influence of in vitro micropropagation on lycorine biosynthesis and anticholinesterase activity in Hippeastrum goianum. *Rev. Bras. de Farm.* **2019**, *29*, 262-265.

93. Cahlikova, L.; Vaneckova, N.; Safratova, M.; Breiterova, K.; Blunden, G.; Hulcova, D.; Opletal, L. The Genus Nerine Herb. (Amaryllidaceae): Ethnobotany, Phytochemistry, and Biological Activity. *Molecules* **2019**, *24*, 4238.

94. El Mokni, R.; Pasta, S.; Pacifico, D. Amaryllis belladonna L. (Amaryllidaceae; Amaryllidoideae), first record as naturalised geophyte in Tunisia and North Africa. *Hacquetia* **2020**, *19*, 331-336.

95. Balmford, B.; Balmford, J.; Balmford, A.; Blakeman, S.; Manica, A.; Cowling, R.M. Diurnal versus nocturnal pollination of Brunsvigia gregaria RA Dyer (Amaryllidaceae) at a coastal site. *S. Afr. J. Bot.* **2006**, *72*, 291-294.

96. Lamoral-Theys, D.; Andolfi, A.; Van Goietsenoven, G.; Cimmino, A.; Le Calve, B.; Wauthoz, N.; Megalizzi, V.; Gras, T.; Bruyere, C.; Dubois, J.; et al. Lycorine, the main phenanthridine Amaryllidaceae alkaloid, exhibits significant antitumor activity in cancer cells that display resistance to proapoptotic stimuli: An investigation of structure-activity relationship and mechanistic insight. *J. Med. Chem.* **2009**, *52*, 6244-6256.

97. Lamoral-Theys, D.; Decaestecker, C.; Mathieu, V.; Dubois, J.; Kornienko, A.; Kiss, R.; Evidente, A.; Pottier, L. Lycorine and its derivatives for anticancer drug design. *Mini. Rev. Med. Chem* **2010**, *10*, 41-50.

98. McNulty, J.; Nair, J.J.; Bastida, J.; Pandey, S.; Griffin, C. Structure-activity studies on the lycorine pharmacophore: A potent inducer of apoptosis in human leukemia cells. *Phytochemistry* **2009**, *70*, 913-919.

99. Brimijoin, S. Molecular forms of acetylcholinesterase in brain, nerve and muscle: Nature, localization and dynamics. *Prog. Neurobiol.* **1983**, *21*, 291-322.

100. Heller, M.; Hanahan, D.J. Human erythrocyte membrane bound enzyme acetylcholinesterase. *Biochim. Biophys. Acta.* **1972**, *255*, 251-272.

101. Szelenyi, J.G.; Bartha, E.; Hollan, S.R. Acetylcholinesterase activity of lymphocytes: An enzyme characteristic of T-cells. *Br. J. Haematol.* **1982**, *50*, 241-245.

102. Darvesh, S.; Hopkins, D.A.; Geula, C. Neurobiology of butyrylcholinesterase. *Nat. Rev. Neurosci.* **2003**, *4*, 131-138.

103. Lane, R.M.; Potkin, S.G.; Enz, A. Targeting acetylcholinesterase and butyrylcholinesterase in dementia. *Int J. Neuropsychopharmacol* **2006**, *9*, 101-124.

104. Sereno, L.; Coma, M.; Rodriguez, M.; Sanchez-Ferrer, P.; Sanchez, M.B.; Gich, I.; Agullo, J.M.; Perez, M.; Avila, J.; Guardia-Laguarta, C.; et al. A novel GSK-3beta inhibitor reduces Alzheimer's pathology and rescues neuronal loss in vivo. *Neurobiol Dis.* **2009**, *35*, 359-367.

105. Garcia-Horsman, J.A.; Mannisto, P.T.; Venalainen, J.I. On the role of prolyl oligopeptidase in health and disease. *Neuropeptides* **2007**, *41*, 1-24.

106. Polgar, L. The prolyl oligopeptidase family. *Cell Mol. Life Sci.* **2002**, *59*, 349-362.

107. Orhan, I.E. Current concepts on selected plant secondary metabolites with promising inhibitory effects against enzymes linked to Alzheimer's disease. *Curr. Med. Chem.* **2012**, *19*, 2252-2261.

108. Babkova, K.; Korabecny, J.; Soukup, O.; Nepovimova, E.; Jun, D.; Kuca, K. Prolyl oligopeptidase and its role in the organism: Attention to the most promising and clinically relevant inhibitors. *Future Med. Chem.* **2017**, *9*, 1015-1038.

109. Lahiri, D.K.; Farlow, M.R.; Greig, N.H.; Sambamurti, K. Current drug targets for Alzheimer's disease treatment. *Drug Dev. Res.* **2002**, *56*, 267-281.

110. Galimberti, D.; Scarpini, E. Old and new acetylcholinesterase inhibitors for Alzheimer's disease. *Expert Opin. Investig. Drugs* **2016**, *25*, 1181-1187.

111. López, S.; Bastida, J.; Viladomat, F.; Codina, C. Acetylcholinesterase inhibitory activity of some Amaryllidaceae alkaloids and Narcissus extracts. *Life Sci.* **2002**, *71*, 2521-2529.

112. Elgorashi, E.E.; Zschocke, S.; van Staden, J. The anti-inflammatory and antibacterial activities of Amaryllidaceae alkaloids. *S. Afr. J. Bot.* **2003**, *69*, 448-449.

113. Osorio, E.J.; Robledo, S.M.; Bastida, J. Alkaloids with antiprotozoal activity. *Alkaloids Chem. Biol.* **2008**, *66*, 113-190.

114. Nair, J.J.; van Staden, J. The Amaryllidaceae as a source of antiplasmodial crinane alkaloid constituents. *Fitoterapia* **2019**, *134*, 305-313.

115. Nair, J.J.; van Staden, J. Antiplasmodial constituents in the minor alkaloid groups of the Amaryllidaceae. *S. Afr. J. Bot* **2019**, *126*, 362-370.

116. Cimmino, A.; Masi, M.; Evidente, M.; Superchi, S.; Evidente, A. Amaryllidaceae alkaloids: Absolute configuration and biological activity. *Chirality* **2017**, *29*, 486-499.

117. Takos, A.M.; Rook, F. Towards a molecular understanding of the biosynthesis of amaryllidaceae alkaloids in support of their expanding medical use. *Int. J. Mol. Sci.* **2013**, *14*, 11713-11741.

118. Emir, A.; Onur, M.A. Simultaneous Quantification of Galantamine and Lycorine in Galanthus fosteri by HPLC-DAD. *Marmara Pharm. J.* **2016**, *20*, 320-324.

119. Pavlov, A.; Berkov, S.; Courot, E.; Gocheva, T.; Tuneva, D.; Pandova, B.; Georgiev, M.; Georgiev, V.; Yanev, S.; Burrus, M.; et al. Galantamine production by Leucojum aestivum in vitro systems. *Process. Biochem.* **2007**, *42*, 734-739.

120. Diop, M.; Hehn, A.; Ptak, A.; Chrétien, F.; Doerper, S.; Gontier, E.; Bourgaud, F.; Henry, M.; Chapleur, Y.; Laurain-Mattar, D. Hairy root and tissue cultures of *Leucojum aestivum* L.—relationships to galantamine content. *Phytochem. Rev.* **2007**, *6*, 137-141.

121. Berkov, S.; Pavlov, A.; Georgiev, V.; Bastida, J.; Burrus, M.; Ilieva, M.; Codina, C. Alkaloid synthesis and accumulation in Leucojum aestivum in vitro cultures. *Nat. Prod. Commun* **2009**, *4*, 359-364.

122. Ikeuchi, M.; Sugimoto, K.; Iwase, A., Plant callus: Mechanisms of induction and repression. *Plant. Cell* **2013**, *25*, 3159-3173.

123. Diop, M.F.; Ptak, A.; Chretien, F.; Henry, M.; Chapleur, Y.; Laurain-Mattar, D. Galantamine content of bulbs and in vitro cultures of Leucojum aestivum L. *Nat. Prod. Commun* **2006**, *1*, 475-479.

124. Zhou, J.; Liu, Z.; Wang, S.; Li, J.; Li, Y.; Chen, W.K.; Wang, R. Fungal endophytes promote the accumulation of Amaryllidaceae alkaloids in Lycoris radiata. *Environ. Microbiol.* **2020**, *22*, 1421-1434.

125. Singh, S.; Pandey, S.S.; Shanker, K.; Kalra, A. Endophytes enhance the production of root alkaloids ajmalicine and serpentine by modulating the terpenoid indole alkaloid pathway in Catharanthus roseus roots. *J. Appl. Microbiol.* **2020**, *128*, 1128-1142.

126. Ho, T.T.; Murthy, H.N.; Park, S.Y. Methyl Jasmonate Induced Oxidative Stress and Accumulation of Secondary Metabolites in Plant Cell and Organ Cultures. *Int. J. Mol. Sci.* **2020**, *21*, 716.

127. Ivanov, I.; Georgiev, V.; Pavlov, A. Elicitation of galantamine biosynthesis by Leucojum aestivum liquid shoot cultures. *J. Plant. Physiol.* **2013**, *170*, 1122-1129.

128. Diamond, A.; Desgagne-Penix, I. Metabolic engineering for the production of plant isoquinoline alkaloids. *Plant. Biotechnol. J.* **2016**, *14*, 1319-1328.

129. Facchini, P.J.; Bohlmann, J.; Covello, P.S.; De Luca, V.; Mahadevan, R.; Page, J.E.; Ro, D.K.; Sensen, C.W.; Storms, R.; Martin, V.J. Synthetic biosystems for the production of high-value plant metabolites. *Trends Biotechnol.* **2012**, *30*, 127-131.

130. Fossati, E.; Narcross, L.; Ekins, A.; Falgueyret, J.P.; Martin, V.J. Synthesis of Morphinan Alkaloids in Saccharomyces cerevisiae. *PLoS ONE* **2015**, *10*, e0124459.

131. Hawkins, K.M.; Smolke, C.D. Production of benzylisoquinoline alkaloids in Saccharomyces cerevisiae. *Nat. Chem. Biol.* **2008**, *4*, 564-573.

132. Matsumura, E.; Nakagawa, A.; Tomabechi, Y.; Ikushiro, S.; Sakaki, T.; Katayama, T.; Yamamoto, K.; Kumagai, H.; Sato, F.; Minami, H. Microbial production of novel sulphated alkaloids for drug discovery. *Sci Rep.* **2018**, *8*, 7980.

133. Narcross, L.; Fossati, E.; Bourgeois, L.; Dueber, J.E.; Martin, V.J.J. Microbial Factories for the Production of Benzylisoquinoline Alkaloids. *Trends Biotechnol* **2016**, *34*, 228-241.

134. Slattery, S.S.; Diamond, A.; Wang, H.; Therrien, J.A.; Lant, J.T.; Jazey, T.; Lee, K.; Klassen, Z.; Desgagne-Penix, I.; Karas, B.J.; et al. An Expanded Plasmid-Based Genetic Toolbox Enables Cas9 Genome Editing and Stable Maintenance of Synthetic Pathways in Phaeodactylum tricornutum. *ACS Synth. Biol.* **2018**, *7*, 328-338.

135. Liu, Q.; Majdi, M.; Cankar, K.; Goedbloed, M.; Charnikhova, T.; Verstappen, F.W.; de Vos, R.C.; Beekwilder, J.; van der Krol, S.; Bouwmeester, H.J. Reconstitution of the costunolide biosynthetic pathway in yeast and Nicotiana benthamiana. *PLoS ONE* **2011**, *6*, e23255.

136. Farhi, M.; Marhevka, E.; Ben-Ari, J.; Algamas-Dimantov, A.; Liang, Z.; Zeevi, V.; Edelbaum, O.; Spitzer-Rimon, B.; Abeliovich, H.; Schwartz, B.; et al. Generation of the potent anti-malarial drug artemisinin in tobacco. *Nat. Biotechnol* **2011**, *29*, 1072-1074.

137. Kumar, S.; Hahn, F.M.; Baidoo, E.; Kahlon, T.S.; Wood, D.F.; McMahan, C.M.; Cornish, K.; Keasling, J.D.; Daniell, H.; Whalen, M.C. Remodeling the isoprenoid pathway in tobacco by expressing the cytoplasmic mevalonate pathway in chloroplasts. *Metab. Eng.* **2012**, *14*, 19-28.

138. Wu, S.; Jiang, Z.; Kempinski, C.; Eric Nybo, S.; Husodo, S.; Williams, R.; Chappell, J. Engineering triterpene metabolism in tobacco. *Planta* **2012**, *236*, 867-877.